STUDY OF HYDROGENATED AMORPHOUS SILICON FILMS GROWN BY A NOVEL PULSED PLASMA DISCHARGE

THESIS

Submitted in partial fulfilment of the requirements for the degree of DOCTOR OF PHILOSOPHY

By

CHANDRACHUR MUKHERJEE

Under the Supervision of

Dr. R. Bhattacharyya

BIRLA INSTITUTE OF TECHNOLOGY AND SCIENCE
PILANI (RAJASTHAN) INDIA

1997

Acknowledgements

Words do not suffice to express my gratitude to Dr. R. Bhattacharyya, Scientist In-charge, Thin Film Technology Group, National Physical Laboratory, New Delhi for his guidance, sharing his deep experimental understanding and insight of the amorphous materials, providing experimental facilities of the highest international standards and a fine working environment, without which this thesis work would not have been so exciting and stimulating.

I am indebted to Dr. C. Anandan, Surface Science Group., National Physical Laboratory for suggesting to me the a-Si:H growth experiments with modified pulsing scheme and also for the crucial discussions and other suggestions for this study. I greatly appreciate the pains taken by Dr. P.N. Dixit, Scientist, Thin Film Technology Group, NPL to impart to me various skills to handle PECVD silane discharges and other systems. I am also indebted to Dr. A. Basu, Dr. B.S. Verma, Dr. O.S. Panwar, Dr. M. Kar and Mr. Rajput for their support during the various stages of the experimental work.

A special word of thanks to Dr. Tanay Seth, Mr. S. Kumar, Mr. D. Sarangi and Mr. B.S. Satyanarayan for their constant technical help throughout my experimental work in the Thin Film Technology Group in NPL.

I am thankful to Mr. T.K. Bhattacharyya, Mr. T.K. Chakraborty, Mr. R.K. Sodhi, Mr. J. Chand and Mr. A. Singh for their technical help and co-operation.

I would like to acknowledge the contributions of Director, Nuclear Science Centre, New Delhi and his colleagues Mr. B.P. Ajithkumar and Mr. Venkatramanan for fabricating the CW/Pulsed 100 MHz generator according to the requirements of the present study, without which the success in conducting pulsed plasma studies would not have been achieved. Similarly I would like to thank Director, National Physical Laboratory for making available extensive R&D and other facilities at NPL.

I would like to thank Dr. K.L. Narashimhan, TIFR, Bombay and Dr. S.C. Agarwal, IIT, Kanpur for valuable discussions regarding Photothermal Deflection Spectroscopy.

I express my sincere thanks to Dr. B.K. Das, NPL and to Prof. L.K. Maheswari, BITS, Pilani for organising useful course-work during the first year of the thesis period.

BIRLA INSTITUTE OF TECHNOLOGY & SCIENCE
PILANI, RAJASTHAN

CERTIFICATE

This is to certify that the thesis entitled **Study of Hydrogenated Amorphous Silicon Films Grown By A Novel Pulsed Plasma Discharge** and submitted by Chandrachur Mukherjee ID No 92PZYF009 for award of Ph D Degree of the Institute, embodies original work done by him under my supervision.

Signature in full of the Supervisor ----------

Name in capital block letters ----------

Date: 14/1/03 Designation ----------

Synopsis

Amorphous silicon is no more a new electronic material; both it's material and application aspects have been explored extensively. It has been realised that the plasma processes involved in a-Si:H deposition are largely nonintuitive and, therefore, basic studies relating to the creation and maintenance of glow discharge plasma remain a relevant topic of continued intensive investigation. Again some technological goals yet to be achieved are i) increase of film deposition rate for low cost production, ii) attainment of improved surface homogeneity for the fabrication of large area devices and iii) improved material quality for still higher efficiency and stabler devices. For achieving the above goals basically two different approaches have been largely experimented. These are optimisation of i) external macroscopic parameters and ii) internal plasma microscopic parameters (electron density, electron decay time constant, electron temperature).

In the present study the second approach is further explored by utilising pulsed plasma discharge wherein internal plasma microscopic parameters are expected to attain higher values compared to conventional continuous wave (CW) discharges. Thus a-Si:H films (undoped) were deposited away from the so called standard deposition conditions. Films were deposited using a low frequency amplitude modulation of RF (13.56 MHz) and VHF (100 MHz) discharges in the same reactor. In recent years VHF (70 - 200 MHz) growth of this material has been performed by various groups internationally and this promises to be a rather easy way to enhance growth rates without any drastic change in the existing reactors. Pulsed plasma mode of discharge was adopted with the basic aim to attain high deposition rate with acceptable optoelectronic properties for different device applications. The other reason behind choosing pulsed discharge was to attain better thickness uniformity than obtainable by CW discharge and to avoid the deleterious effect of powder formation. However, the mode of pulsing that is used in the present study is novel in the sense that modulation depths were kept below 100% to avoid complete extinction of the plasma (otherwise films with poor interface properties are grown as observed by Hishikawa et al. in Sanyo, Japan).

Following is the chapter wise brief summary of the thesis.

In Chapter - I first a brief review of the journey of amorphous silicon research from 1969 onwards is presented. After that the structure of the amorphous material is discussed in detail

was developed at National Physical Laboratory, New Delhi, during the period of the present investigation. In addition to all these material characterisation techniques silane plasma is also characterised using optical emission spectroscopy. The procedure (time resolved optical emission spectroscopy) adopted for this spectroscopy is discussed in the last section of this chapter. This particular measurement has been found to be very much useful for correlating different observations.

Chapter - III contains results of the modified pulsed plasma discharge (**MPPD**) of 13.56 MHz excitation. First a general introduction of the pulsed plasma discharge technique is given. Then this chapter is divided in three sections 3A, 3B & 3C for the sake of proper presentation and comparison of the effect of different source gas combinations used. In section 3A undiluted MPPD grown film properties are included. In section 3B, H_2 diluted MPPD grown film properties are discussed. In the last section He and $He+H_2$ diluted MPPD grown film properties

are presented. In all these sections interpretation of the results obtained are given. Optical and electrical characterisations used are common for all the sections. Finally, under conclusion section, three subsections contain the important results and their interpretation as discussed under section 3A, 3B & 3C are presented.

In **Chapter - IV** modified pulsed plasma discharge of 100 MHz (VHF) excitation is discussed. In the introduction part of this chapter a detailed review of the VHF plasma decomposition work carried out so far by the various groups are presented. This is followed by the experimental details which includes detailed description of the VHF generator used for the present study. Different characterisation results are furnished thereafter for the VHF MPPD grown films. These results are presented in the same order as in the previous chapter. Finally discussions and conclusions of the results are given to highlight the novelty of the experiment conducted and implications of the results in the light of the advancement of a-Si:H technology.

Chapter - V gives a summary of the results of all the investigations carried out during the course of this work and indicates the scope of further research work that needs to be carried out to consolidate the gains of the present research effort documented in the thesis.

Contents

which includes role of hydrogen in a-Si:H. Defects in hydrogenated amorphous silicon is also discussed in detail. Under this heading different growth models are discussed. Standard deposition conditions are identified so that the deposition conditions used for the present study being called as 'away from the so called standard condition' is easily appreciated. Recently, dusty plasma has drawn wide attention and since pulsed plasma discharge impedes powder growth, therefore formation and suppression of powder is discussed in detail in the next section. Finally, a review of the plasma modelling, for both CW and pulsed plasma reactors, are presented because attainment of high rate and high thickness uniformity is contextual to the present investigation. A detailed reference list containing most of the important works done so far is also provided.

Chapter - II, named Experimental details - growth and characterisation, contains first a brief description of the different efforts / techniques to grow a-Si:H at high rate. Under this head different plasma excitation methods, dissociation and transport of the reactive species, dependence on excitation power, effect of buffer gas and effect of RF power modulation are discussed. This is followed by the description of the system used and the methodology employed for the deposition of a-Si:H films. After this different characterisation techniques used are described. These involve a brief theory of the particular technique used, the description of the system used and methodology employed for the measurement. Special emphasis is given for the defect density measurement using photothermal deflection spectroscopy because the setup used was developed at National Physical Laboratory, New Delhi, during the period of the present investigation. In addition to all these material characterisation techniques silane plasma is also characterised using optical emission spectroscopy. The procedure (time resolved optical emission spectroscopy) adopted for this spectroscopy is discussed in the last section of this chapter. This particular measurement has been found to be very much useful for correlating different observations.

Chapter - III contains results of the modified pulsed plasma discharge (**MPPD**) of 13.56 MHz excitation. First a general introduction of the pulsed plasma discharge technique is given. Then this chapter is divided in three sections 3A, 3B & 3C for the sake of proper presentation and comparison of the effect of different source gas combinations used. In section 3A undiluted MPPD grown film properties are included. In section 3B, H_2 diluted MPPD grown film properties are discussed. In the last section He and $He+H_2$ diluted MPPD grown film properties

are presented. In all these sections interpretation of the results obtained are given. Optical and electrical characterisations used are common for all the sections. Finally, under conclusion section, three subsections contain the important results and their interpretation as discussed under section 3A, 3B & 3C are presented.

In **Chapter - IV** modified pulsed plasma discharge of 100 MHz (VHF) excitation is discussed. In the introduction part of this chapter a detailed review of the VHF plasma decomposition work carried out so far by the various groups are presented. This is followed by the experimental details which includes detailed description of the VHF generator used for the present study. Different characterisation results are furnished thereafter for the VHF MPPD grown films. These results are presented in the same order as in the previous chapter. Finally discussions and conclusions of the results are given to highlight the novelty of the experiment conducted and implications of the results in the light of the advancement of a-Si:H technology.

Chapter - V gives a summary of the results of all the investigations carried out during the course of this work and indicates the scope of further research work that needs to be carried out to consolidate the gains of the present research effort documented in the thesis.

Contents

CHAPTER - I

Introduction

In this chapter a brief resume of the present understanding of the amorphous material in general, and hydrogenated amorphous silicon in particular is presented. First the material aspect of amorphous silicon is discussed. Under this, the role of hydrogen on disorder, mechanism of defect formation of a-Si:H and other material properties are described. Then the growth aspect of amorphous silicon is presented and various growth models are discussed. This is followed by a detailed description of the powder formation and inhibition processes which are of great relevance to the theme of the present investigation. Since the main emphasis here is the study of pulsed plasma deposition, therefore, relevant aspects of CW and pulsed plasma discharge are discussed in detail. The results obtained during the present investigation are analysed in the subsequent chapters in the light of the available information and in the frame work of various modeling studies of the plasma processes. These are compiled and presented here.

1.1 Introduction

The second most common element on earth: Silicon was identified by the Swede Jons Jacob Berzelius in the year 1823. In 1930 scientists decided that crystalline silicon is a metal and not an insulator. After 20 years of intensive research pure crystalline silicon was recognised as a semiconductor and the first transistor was developed in December 1947 at the Bell laboratories, New Jersy. Today crystalline silicon is the core material for all computers.

In Scotland in 1954 a group of scientists working on the production of high purity single crystal silicon, using thermal decomposition of silane by RF heating, noticed a deposit of non crystalline form of silicon on the unheated parts of the reaction vessel: hydrogenated amorphous silicon was discovered - as published by Chittik et al.[1] in 1969. The most crucial breakthrough for amorphous silicon was the substitutional introduction of impurities, as published in a famous paper by Spear and LeComber[2] in 1975. This discovery made possible

the fabrication of thin film transistors, solar cells and other devices with hydrogenated amorphous silicon. The main milestones in the history of amorphous silicon are also depicted in **Fig.1.1**.

Amorphous materials are those where the long range order in the atomic distribution is completely broken while the short range order is maintained, in the sense that the co-ordination number of the corresponding ordered crystal remains unchanged. However the bond lengths and angles in the amorphous system fluctuate[3]. As an amorphous material it has all the disorder due to variations in atomic arrangement. Zachariasen[4] has proposed the continuous random network model for covalently bonded amorphous solids. **Fig.1.2** is a three dimensional illustration of a-Si:H network.

The significant advantage of amorphous hydrogenated silicon in comparison to crystalline silicon is that it offers the important technical advantage of being deposited inexpensively and uniformly over a very large area. The technology which has received most attention is the photovoltaic solar cell. Large scale power production obviously depends on the ability to cover very large areas at low cost.

1.2 Various a-Si:H based devices

First solar cell on amorphous hydrogenated silicon was developed by Carlson and Wronski in RCA laboratories in 1976[5]. Subsequent research by RCA and many other groups increased the cell efficiency by roughly 1 percentage point each year to about 12 in 1989. In Japan, under the 'Sunshine Project' the conversion efficiency achieved was 13.2% for 1 cm^2, 12% for 100 cm^2 and 10.5% for 1200 cm^2 solar cells[6].

It was reported by Steabler and Wronski[7] in 1977 that this material exhibits a light-induced degradation effect. The instability of the conversion efficiency during light soaking has been suppressed largely by optimising the multijunction (Tandem) structure to achieve a stable 10% efficiency[8]. For 1 cm^2 solar cells, stabilised conversion efficiencies above 10% have been achieved[8]. The best solar cell reported to date is a triple junction solar cell having 14.6% initial efficiency and 13.0% stable efficiency made in United Solar Systems Corporation, USA[9]. For tandem submodules, a continuous light soaking at NREL, USA showed that the initial total area conversion efficiency of 10.2% decreased to 8.9% after 1000

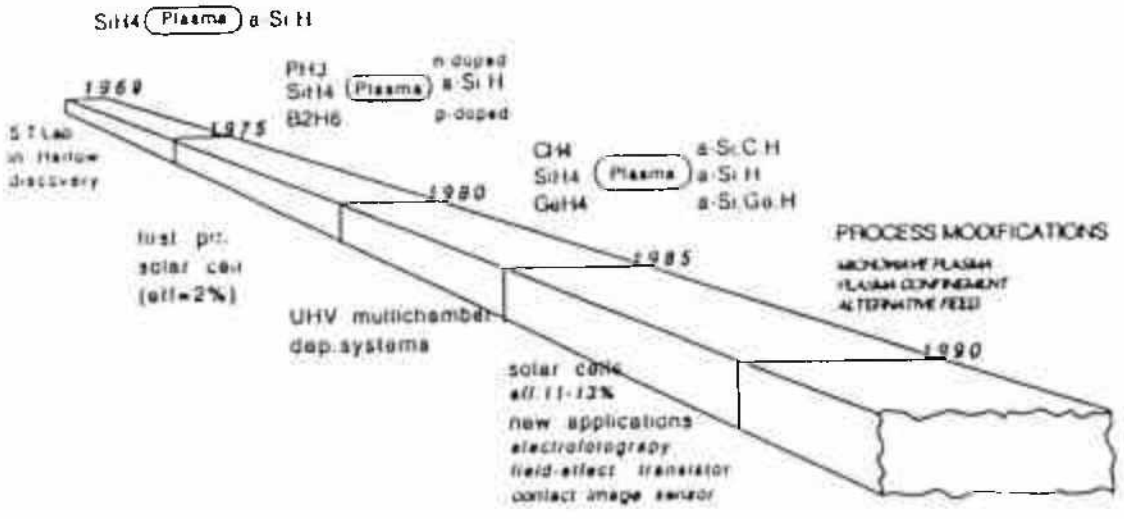

Fig. 1.1 History of Amorphous silicon: Process and Technology developments

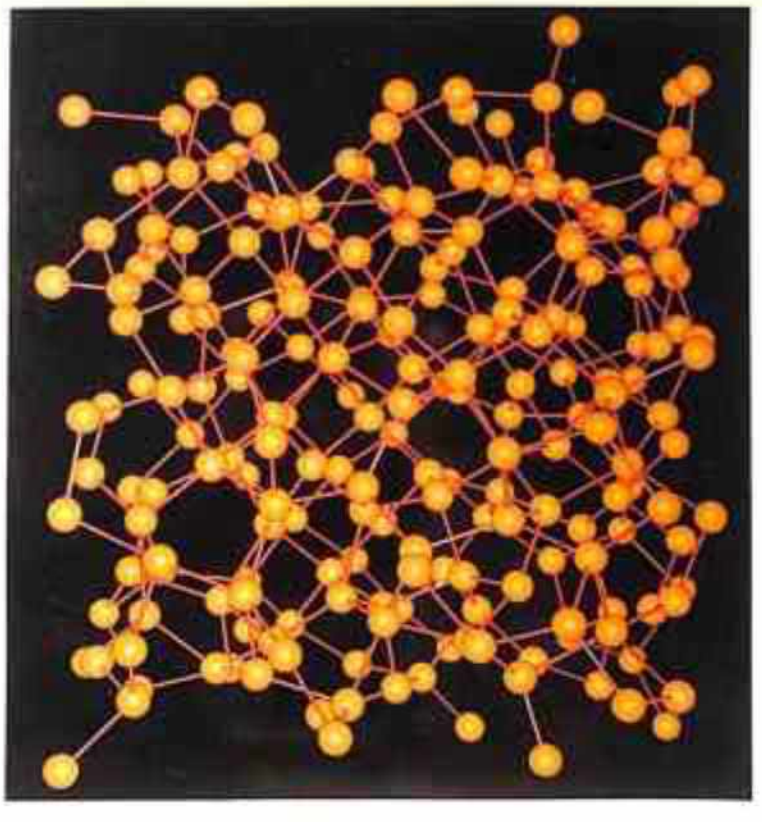

COMPUTER MODEL OF AMORPHOUS SILICON
(PHYSICS TODAY, July '88)

Fig. 1.2 Three dimensional computer modelled illustration of a-Si:H network.

hrs. light exposure, so that degradation was about 13% of the initial value[10]. One recent interesting recipe is from United Solar Corporation, USA, where Sugiyama et al.[11] have suggested total elimination of hydrogen from the gas mixture by deuterium, and achieved percentage degradation of solar cell efficiency around 10%. This certainly provides a new lease of life to amorphous silicon industry, but the cost of these specialised gases again blurs the future.

Today a-Si:H is being used as photoreceptors in copiers, utilising the ability to deposit the material over large areas. The most exciting and rapidly growing technological development is in the area of matrix addressed arrays. Mass production of liquid crystal displays driven by amorphous silicon transistors is particularly rapid now. The prospects for large area detector devices, including medical X-ray imaging, nuclear radiation detectors appear attractive.

The other issue in amorphous silicon technology that remains still unsolved is the low cost production of these devices; this requires achievement of high growth rate but certainly not at the cost of the quality of the material. In the year 1992 the cost status of solar cell was ≈ 1.5 $/Watt[12]. Although the shipment data for a-Si:H solar cell in 1996 is very much encouraging (≈25%) but still it is too costly compared to conventional power production technologies. Intensive research for the past 20 years has shown that, by and large, material quality and high deposition rate are mutually exclusive. Presently amorphous silicon technology demands a window with trade offs between these two parameters. This in a way is the aim of the present research effort.

1.3 Hydrogenated amorphous silicon - the material aspect

1.3.1 Electronic structure of amorphous materials

In the past there was considerable debate over whether the amorphous semiconductor had a band gap at all. Subsequent work explained that the band gap is equivalently described by the splitting of the bonding (or lone pair) and anti-bonding states of the covalent bond. The bands are most strongly influenced by the short range order, which is the same in amorphous and crystalline silicon, and the absence of periodicity is only a small perturbation.

Based on Anderson's theory[13], Mott[14] argued that the spatial fluctuations in the potential caused by configurational disorder in amorphous materials may lead to the formation of localized states, which do not occupy all the different energies in the band, but form a tail above and below the normal band. These states are called localized in the sense that an electron placed in a region will not diffuse, at zero temperature, to other regions with corresponding potential fluctuations. This is schematically shown in **Fig. 1.3(a).**

The model proposed by Cohen-Fritzshe-Ovshinksky[15] (CFO model of the band structure of the amorphous semiconductor) is shown in **Fig. 1.3(b).** At energies E_c and E_v a sharp transition between the localized and extended states is assumed to occur. These are known as mobility edges, since mobility changes by an order of magnitude from one region to another.

Another model suggested originally by Davis and Mott[16] and later improved by Mott[17] is illustrated in **Fig. 1.3(c)** and **1.3(d)** respectively. Due to the absence of Long Range Order (LRO) the electron states near the band edges, E_A and E_B are localized.

1.3.2 Role of Hydrogen in a-Si:H

Hydrogenated amorphous silicon typically contains 10 at% hydrogen and so may be properly considered as an alloy of silicon and hydrogen. Hydrogen is usually incorporated into the amorphous silicon during the growth process. Hydrogen in a-Si:H passivates dangling bond defects and also modifies the amorphous silicon network. Evaporated amorphous silicon (unhydrogenated) typically contains $\approx 10^{19}$ cm^{-3} dangling bond defects as determined by electron spin resonance measurements while in a-Si:H (produced by SiH_4 glow discharge) the density of dangling bonds is 10^{15}-$10^{16}cm^{-3}$ [18,19]. These dangling bonds occur as states in the mobility gap and are the dominant recombination centers for excess electron and holes. Their removal via hydrogen passivation thereby greatly increases the lifetime of photo excited charge carriers and allows efficient photoconductivity and photoluminesence to occur.

Photoemission studies have shown that H not only removes electronic states from the band gap but also from the top of the valence band as well[20]. Hence, the band gap is a function of the hydrogen concentration in the material and is larger than the band gapof crystalline silicon. Surprisingly it has been found that total number of H atoms in a-Si:H greatly exceeds the number one would require to passivate existing midgap defects[21]. However, it must be emphasised here the number of defects created in any metastable process

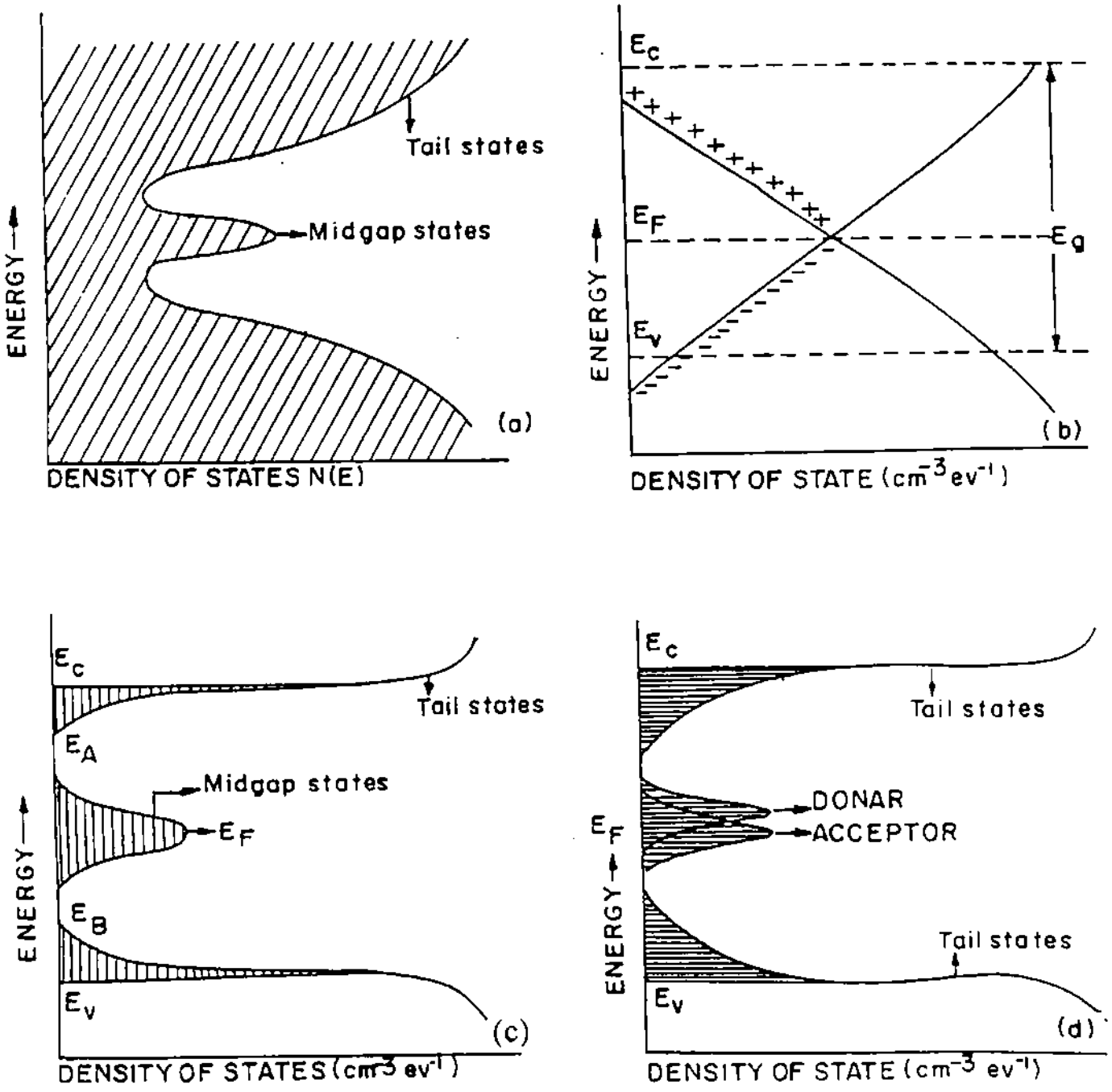

Fig. 1.3 Schematic diagrams of energy level versus density of states of a) Amorphous silicon, b) CFO model, c) Davis & Mott model and d) improved Davis & mott model.

in a-Si:H is typically a factor of 10^3 smaller than the number of H or silicon atoms present in the network.

Hydrogen has been shown to diffuse quite easily in a-Si:H at moderate temperature of 200°C. As H diffuses it breaks silicon-silicon weak bonds, leaving behind new dangling bonds, and it can passivate preexisting defects states. Thus the nature of H motion in a-Si:H results in atomic rearrangement of the amorphous silicon structure and can lead to either defect removal or creation, depending on the circumstance. It has been well established through the work of Jackson and Zhang[22] that H prefers to bond in separated pairs. A particular configuration of these pairs explain the metastability (S-W effect) in these materials rather well. Metastability typically involves less than 10^{19} cm^{-3} sites in a-Si:H.

1.3.3 Defects in hydrogenated amorphous silicon

The most important difference between a-Si and C-Si is the disorder induced localisation of electronic states near and in the otherwise forbidden band gapof the amorphous phase. In a silane discharge the surface mobility of silane fragments are low and the accumulation rate is high ($\approx$ 3 $A^{\circ}s^{-1}$), significant disorder is frozen into the resulting a-Si:H network structure. The incorporation of typically 10 at% H, in this process, relieves much of the accompanying strain, but the residual disorder gives rise to the localisation of electronic states both near the band edge and deep in the band gap. Tremendous progress in the understanding of defects in a-Si:H has been made in last few years in four important areas: i)the microscopic structure of defects, ii)the distribution of localised defect states, iii) theories of defect formation and iv) optimal growth for defect minimisation.

1.3.4 Microscopic structure of defects

The simplest picture, "strained" Si-Si bonds are the origin of localised band edge states and "broken" or "dangling" bonds are the origin of localised deep gap states. A dangling bond floating bond pair is shown in **Fig.1.4**. The main differences between dangling bond and floating bond defects are i) the electronic wave functions of the dangling bond is expected to be strongly localised, while the wavefunction of the floating bond should be strongly delocalised[23] and, ii) dangling bonds should be essentially immobile compared to the high mobility of floating bonds. This high mobility arises from the fact that floating bonds can be passed from one Si atom to another Si atom without the need for costly bond breaking. Thus

floating bonds should be able to self-annihilate, which should lead to significant defect annealing at elevated temperatures. Also high mobility of floating bonds has been proposed to drive H diffusion in a-Si:H via a simple "kick-out" mechanism which, if correct would require a defect diffusion coefficient significantly larger than that of H[24]. However, the experimental results show i) defects do not self annihilate at elevated temperatures, ii) upper limit for defect diffusion is 0.6 times the rate of H diffusion, iii)defects act as traps for H rather than enhancing H diffusion as the floating bond model would suggest, and iv) H is intimately involved in the defect formation process.

1.3.5 Distribution of localized states in a-Si:H

The sources of structural disorder that lead to localisation can be classified as follows: i) strained Si-Si bonds which give rise to band tail states, ii) impurity atoms such as phosphorus (P), which give rise to shallow doner states, and iii) dangling bonds which give rise to electronic states deep in the band gap. The distribution of these band gap states are shown schematically in **Fig.1.5**.

1.3.5.1 Optical and mobility band gaps in a-Si:H

Localized electronic states which lie in the gap, has led to two band gap definitions: the mobility gap and optical gap. Theoretically, the mobility gap separates extended and localized electronic states and, therefore, high mobility and low mobility charge carrier transport regions. The optical gap is the separation between supposedly parabolic band edges derived from the deconvolution of the optical absorption coefficient. The optical gap has little fundamental significance. The mobility gap, on the other hand, is fundamentally important, and it has only recently been reliably measured by internal photoemission measurements[25]. The measured value of mobility gap in a-Si:H is 1.89 ± 0.03 eV at 300 K where as optical gap (by Tauc's method) comes out to be 1.73 eV. **Fig. 1.5** depicts these concepts schematically.

1.3.5.2 Exponential valance and conduction-band tails

The origin of exponential absorption (Urbach) edges is generally attributed to the exponential tailing into the gap of the conduction and valance band densities of states, which result from a combination of thermal and structural disorder. The results of a sensitive electron

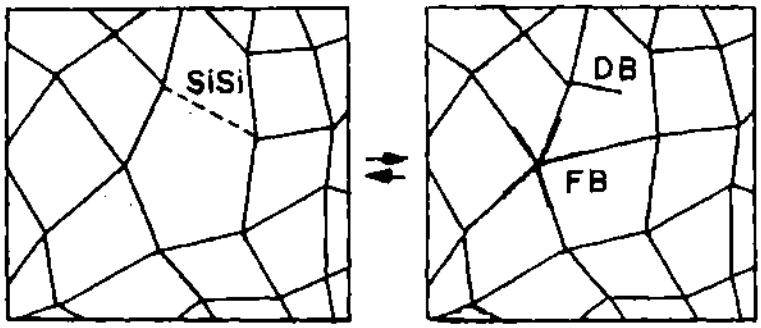

Fig. 1.4 Illustration of Frenkel defect formation of a dangling bond/floating bond pair in a-Si.

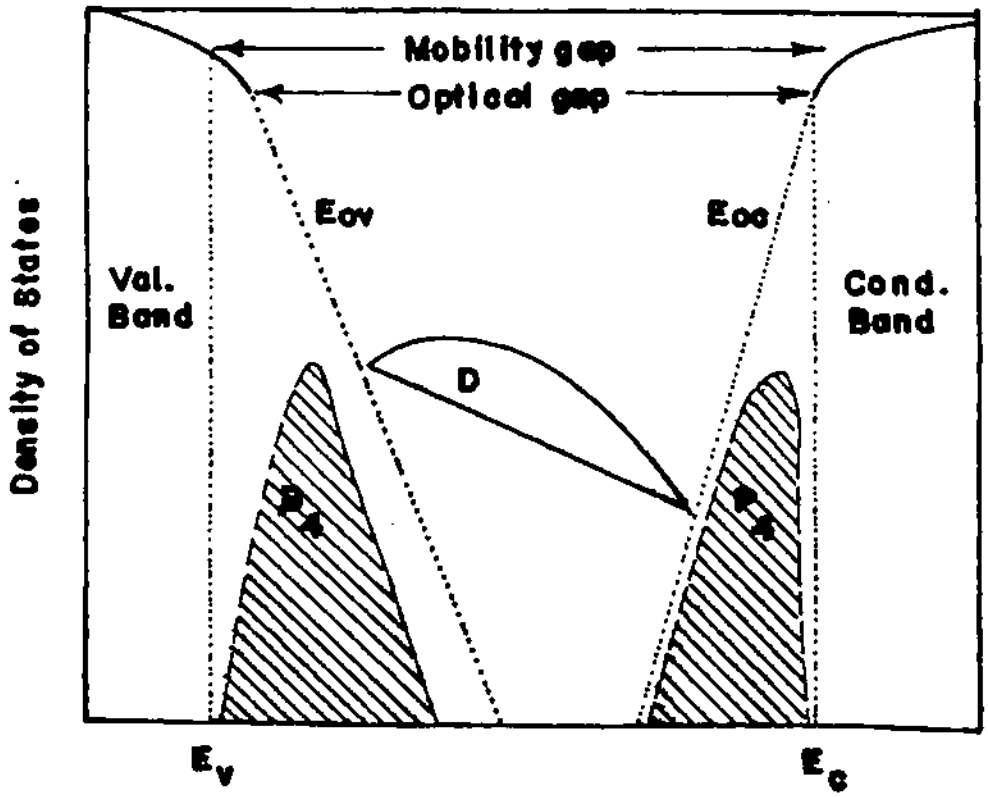

Fig. 1.5 Schematic distribution of localised electronic states in the bandgap of a-Si:H.

spectroscopy [26] show that these distributions are exponential over a wide dynamic range as expected.

The results show that the intrinsic valance band tail of a-Si:H is exactly exponential over atleast four orders of magnitude in the density of states with a logarithmic slope $E_{ov} \approx 45$ meV. Likewise, the conduction band tail is exactly exponential over three orders of magnitude with a characteristic slope $E_{oc} \approx 35$ meV. Again conduction band tail slope increases much more rapidly with temperature than that of the valance band tail i.e. conduction band tail is more susceptible to thermal disorder than structural disorder.

1.3.5.3 Distribution of localised defect states

One of the first and simplest model of the distribution of dangling bond (D) defect states in a-Si:H was the energy level ordering scheme for a single isolated defect with a positive correlation energy. Assume that a lone, singly occupied defect state has an energy E_D° in the a-Si:H gap. If the electron is removed by adding shallow acceptors, for instance, the resulting D^{+} (positively charged DB) state will appear at the same energy $E_D^{+} = E_D^{\circ}$. Adding a second electron to an isolated D° (neutral DB) state results in a defect state energy shift to $E_D^{-} = E_D^{\circ} + U$, as illustrated in **Fig.1.6**. U is the electron correlation energy , required to place a second electron on a singly occupied isolated defect level. This defect energy ordering scheme served as the basis for interpreting a number of transport, luminescence and other optical experiments for many years[27].

An alternative explanation proposes a pool of defect sites from which the system can choose to create or destroy defects in order to minimize the system free energy[28-31].

1.3.6 Theories of defect formation in a-Si:H

Unlike c-Si, the creation of extrinsic carriers in a-Si:H by doping is always accompanied by the formation of large concentrations of charged defects. Street in 1982 proposed the defect compensation model of doping, the first defect formation model[32]. It is based on the following chemical reaction for dopant, P (for example), incorporation into the growing a-Si:H film from the plasma,

$$P_{(gas)} \Rightarrow \alpha Si_3^{+} + P_4^{+} + (1-\alpha)\, e^{-} \qquad (1.1)$$

Where the subscripts denote coordination. Since a is measured to be about 0.9 [26], this simple reaction immediately accounts for the observed square root dependence of dopants or defects i.e.

$$[Si_3^-] \approx [P_4^+] \approx ([Si_3^-][P_4^+])^{1/2} \propto P_{gas}^{1/2} \quad (1.2)$$

However, both the active dopant[33] and deep defect[34] concentrations in a-Si:H were found to depend reversibly on the sample temperature after deposition, a characteristic signature of solid-state chemical equilibrium processes. Furthermore, it has been shown that a chemical equilibrium model can accurately describe the incorporation of charge defects and active dopants during a-Si:H growth, even though the host a-Si network is far from equilibrium[35].

1.3.6.1 Solid-state chemical equilibria

The equilibrium concentrations of species that participate in solid-state chemical reactions depend on temperature α. If the temperature is varied more rapidly than the system can respond, non-equilibrium concentrations can be frozen-in and the time dependence of their equilibrium is characteristic of the kinetics of the reaction. The corresponding chemical reactions for active dopants and deep defects in a-Si:H can be approximately described for n-type (say, P-doped) a-Si:H as follows:

$$P_4 + e^- \Rightarrow P_3 \quad (1.3)$$

$$Si_4 + e^- \Rightarrow Si_3^- \quad (1.4)$$

The reactions are independent but are linked by their dependence on electron concentration.

1.3.6.2 Hydrogen glass model

Hydrogen diffuses readily in a-Si:H at 200°C the temperature above which the reactions (1.3 & 1.4) are always in equilibrium. Hydrogen motion provides the flexibility to rearrange the bonding structure, which cannot be accomplished by Si motion alone at these low temperatures. Hydrogen forms a mobile sub-lattice coexisting within the rigid a-Si host network. The mobility of hydrogen at 200°C allows the sub-lattice to rearrange itself to attain a minimum free energy configuration within the constraints of the rigid a-Si network. There the hydrogen diffusion constant in a-Si:H is found to be dispersive i.e. time dependent[36]. As

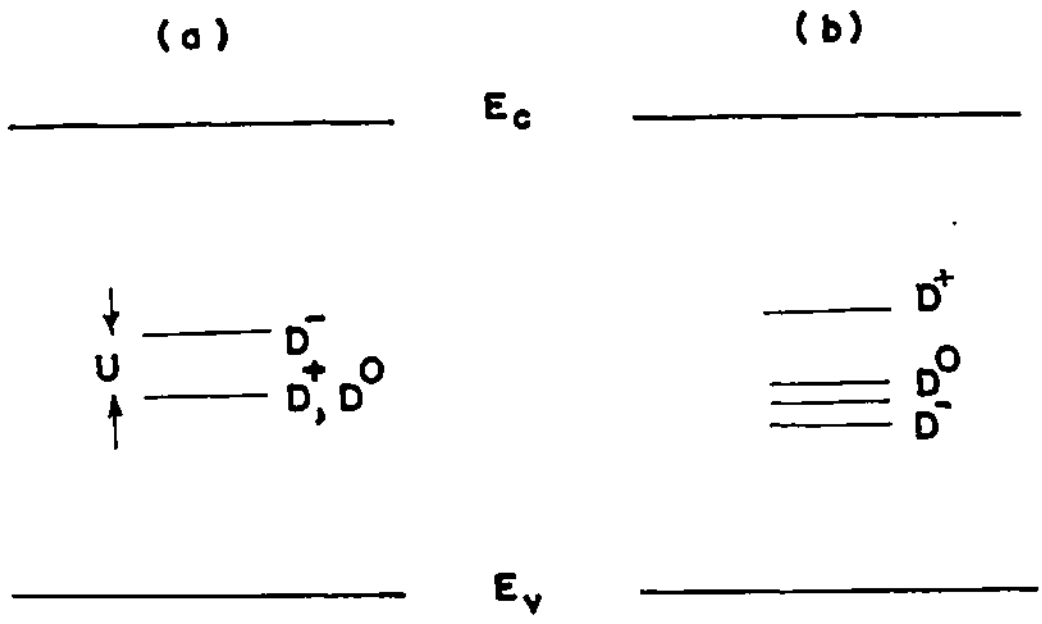

Fig. 1.6 Defect level ordering a) for single, isolated defect and b) measured by a variety of methods in a-Si:H.

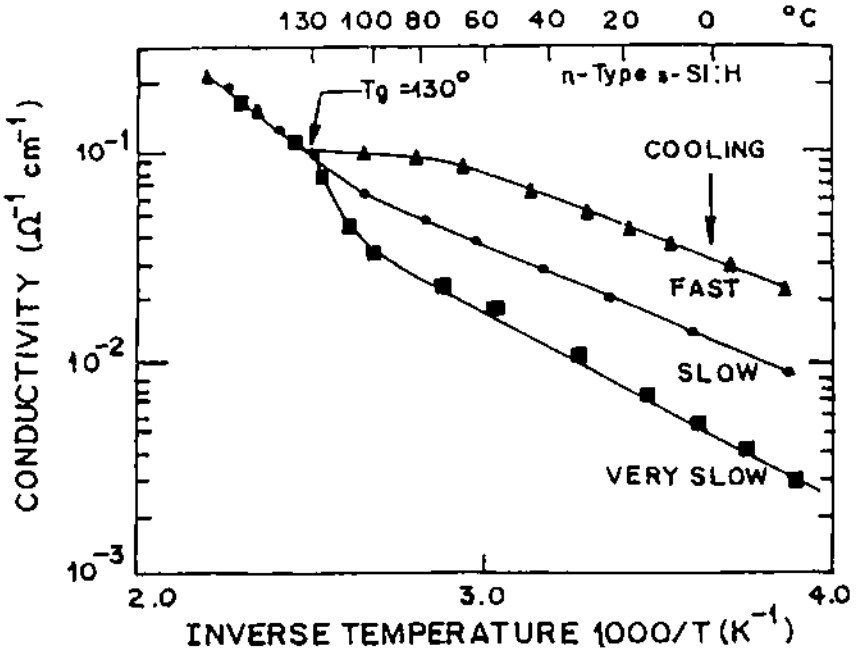

Fig. 1.7 Temperature dependence of DC conductivity of a slightly n-type amorphous silicon film after annealing at 200°C, Below T_g = 130°C ("glass transition temperature") the energy-activation curve depends upon the cooling rate.

the temperature is lowered, the diffusion rate decreases until it becomes so low that the hydrogen becomes nearly frozen into a non-equilibrium configuration. The temperature at which this occurs is called the hydrogen glass transition temperature since the behavior of hydrogen sub-lattice has all the attributes of a glass[37]. The rearrangements of the hydrogen sub-lattice can affect the concentration and distribution of defects in a-Si:H.

The above phenomena is best illustrated on **Fig. 1.7**, showing a set of activation energy curves (log σ Vs 1/T) for a typical sample of slightly phosphorous-doped amorphous silicon. Above a certain temperature T_E, Equilibrium temperature, a well defined activation energy can be estimated from these curves. Below this temperature a discontinuity can be observed, in the σ (1/T) curve depending upon the cooling rate, with an activation energy varying with cooling rate.

This is the famous HYDROGEN GLASS MODEL as proposed by Street and his coworkers[33] and is very appealing and explains many of the physical properties of hydrogenated amorphous silicon. In particular, combined with the defect-compensation model of doping[32], it provides an accurate phenomenological description of the transport properties of the material. It also provides an interesting tool for the explanation of the Staebler-Wronski effect[7]. In the framework of hydrogen glass model an intense light irradiation can displace some elements of the hydrogen glass, creating new defects which can be annealed by heating above the glass fusion temperature T_E[38].

1.3.6.3 Hydrogen mediated weak bond/dangling bond conversion

Neutral defect formation in undoped a-Si:H can be described by a reaction

$$SiH + SiSi = D^{\circ} + SiHSi \qquad (1.5)$$

where SiH are hydrogen atoms bonded to Si, whose motion enables the equilibration. SiSi are weak Si-Si bonds that give rise to the exponential valance band tail and SiHSi are H trapped at a SiSi weak bond site as illustrated in **Fig.1.8**. In fact several such reactions are possible and the temperature dependence of the defect concentration at equilibrium will strongly depend on the details of the reaction[39]. More importantly, because of the disordered nature of a-Si:H , there is an exponential distribution of enthalpies $2\Delta E$ required to form a D°-SiHSi pair; $\Delta E = E_D^{\circ} - E$ is the energy separating the initial valance band tail (SiSi) state at E and the final defect state at E_D°.

1.4 Device quality a-Si:H material properties

Some of the present state-of-the-art parameters obtained for undoped a-Si:H[40] are summarised below Standard deposition conditions (discussed in detail in section 1.5.2) are generally employed to produce these "device" quality optoelectronic properties of a-Si:H. Dark conductivity $\approx 10^{-10}\ \Omega^{-1}cm^{-1}$

Activation energy	$\approx$ 0.8 - 0.9 eV	
Optical band gap	$\approx$ 1.7 - 1.8 eV	
Hydrogen content	$\approx$ 10 at%	
Valance band tail slope	$\approx$ 40 meV	
Conduction band tail slope	$\approx$ 25 meV	
Defect density at the minimum	$> 10^{15} - 10^{17}\ eV^{-1}cm^{-3}$	
Extended state mobility		
	electrons	$> 10\ cm^2V^{-1}s^{-1}$
	holes	$\approx 1\ cm^2V^{-1}s^{-1}$
Drift mobility		
	electrons	$\approx 10\ cm^2V^{-1}s^{-1}$
	holes	$\approx 10^{-2}\ cm^2V^{-1}s^{-1}$

1.5 Hydrogenated amorphous silicon the growth aspect

Hydrogenated amorphous silicon is a broad class of materials produced by variety of plasma assisted processing technique like plasma CVD (DC, RF, Microwave, ECR, Remote, Homo-CVD), sputtering (RF / DC with or without magnetron) in which presence of hydrogen is crucial in determining its optoelectronic properties.

1.5.1 A description of the basic growth process

Molecules of the source gases for example, silane, gain energy through inelastic collisions with high energy electrons and are excited to their dissociative states. This may lead to spontaneous decomposition into neutral atoms and radicals (primary radical generation process). The collisions of the energetic electrons with the gas molecules cause many

processes in addition to the ionization. Gas molecules may be excited into a higher electronic state, from which recombination to the ground state results in the emission of photons and is the origin of the plasma glow, although many of the transitions are in the UV region of the spectrum. The gas molecules are also excited into higher vibrational or rotational states. The average electron energy is given by $eE\lambda_e$, where E is the electric field and λ_e is the mean free path of the electrons for collisions with molecules. At high gas pressure which results in a small λ_e, therefore requires a high field to cause ionization. On the other hand, a low pressure reduces the number of collisions which occur before the electron reaches the electrode, and a high field is again needed to increase the ionization rate and sustain the plasma. In the secondary reaction process neutral atoms and radicals produced by the generation process collide and react mostly with SiH_4 parent molecules. Neutral atoms and radicals migrate to the substrate surface by diffusion and condense to form a-Si:H (surface reaction process). Although a small amount of ionic species (10^9 - 10^{10} cm^{-3}) and emissive species (10^5 - 10^6 cm^{-3}) exist in the steady state plasma, their contribution to the deposition of a-Si:H is marginal/negligible.

Some possible dissociation, excitation and ionisation reactions are given below[41]:

Dissociation reactions:

$$e^- + SiH_4 \Rightarrow SiH_2 + H_2 + e^- \quad (\Delta H = 2.2\ eV) \qquad (1.6)$$
$$\Rightarrow SiH_3 + H + e^- \quad (\Delta H = 4.0\ eV)$$
$$\Rightarrow Si + 2H_2 + e^- \quad (\Delta H = 4.2\ eV)$$
$$\Rightarrow SiH + H_2 + H + e^- \quad (\Delta H = 5.7\ eV)$$
$$e^- + H_2 \Rightarrow 2H + e^- \quad (\Delta H = 4.5\ eV) \qquad (1.7)$$

Excitation reactions:

$$e^- + SiH_4 \Rightarrow Si^* + 2H_2 + e^- \quad (\Delta H = 9.5\ eV) \qquad (1.8)$$
$$\Rightarrow SiH^* + H_2 + H + e^- \quad (\Delta H = 8.9\ eV)$$
$$\Rightarrow H^* + SiH_3 + e^-$$
$$e^- + H_2 \Rightarrow H^* + H + e^- \qquad (1.9)$$

Ionisation reactions:

$$e^- + SiH_4 \Rightarrow SiH_2^+ + H_2 + 2e^- \quad (\Delta H = 11.9\ eV) \qquad (1.10)$$
$$\Rightarrow SiH_3^+ + H + 2e^- \quad (\Delta H = 12.3\ eV)$$
$$\Rightarrow Si^+ + 2H_2 + 2e^- \quad (\Delta H = 13.5\ eV)$$

$$\Rightarrow SiH^{\cdot} + H_2 + H + 2e^{\cdot} \ (\Delta H = 15.3 \text{ eV})$$

There are many other possible reactions involving increasingly higher energies. In the absence of radical radical reactions in the gas phase , as is appropriate for low power regime primary production of higher silanes can occur either by gas phase insertion of SiH_2 into silane

$$SiH_2 + SiH_4 \Rightarrow Si_2H_6 \text{ and} \quad (1.11)$$

$$SiH_2 + SiH_4 \Rightarrow H_3SiSiH + H_2 \quad (1.12)$$

followed by $H_3SiSiH + SiH_4 \Rightarrow Si_3H_8$ (1.13)

or surface recombination of physisorbed SiH_3 and Si_2H_5 radicals,

$$(SiH_3)_s + (SiH_3)_s \Rightarrow Si_2H_6 \quad (1.14)$$

$$(SiH_3)_s + (Si_2H_5)_s \Rightarrow Si_3H_8 \quad (1.15)$$

It has also been found that secondary reactions greatly modify the mix of radicals within the plasma.

Dissociations in inert gas diluted SiH_4 discharge differ significantly from undiluted silane discharge. As He/SiH_4 ratio increases a major fraction of the silane dissociation is by $He^{\cdot}$ and He^{*} (metastable) collisions rather than electron collisions. The principal effect of $He^{\cdot}$ and He^{*} reactions with silane will be to increase the silane dissociation into ions versus neutrals.

Fig. 1.9 shows a typical RF plasma set up for producing these films, together with different steps which lead to a-Si:H film formation on a heated substrate.

Real time spectroscopic ellipsometry studies during growth of a-Si:H has revealed that basically there are three different types of nucleation processes in a-Si:H growth. The most simplest is homogeneous growth with a constant refractive index. In the hemispherical nucleation model, a hexagonal network of spherical nuclei of a-Si:H is created. The radius of an isolated nucleus increases continuously until the different hemispheres come into contact. This results in a density deficient layer of growing thickness. The other model is named as coalescence model, which basically leads to a columnar microstructure in the film[42].

1.5.2 Standard deposition conditions:

Conscious efforts over the past two decades resulted into identification of a parameter space (as given below) which yields device quality a-Si:H films (in a typical research reactor), known as standard condition of growth of a-Si:H (CVD growth regime).

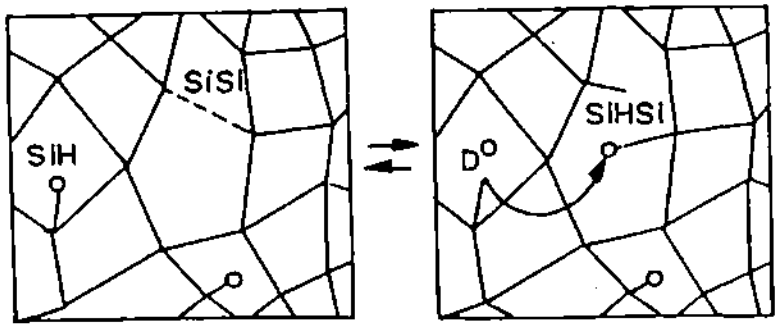

Fig. 1.8 Illustration of Frenkel defect formation in a-Si:H according to reaction 1.5.

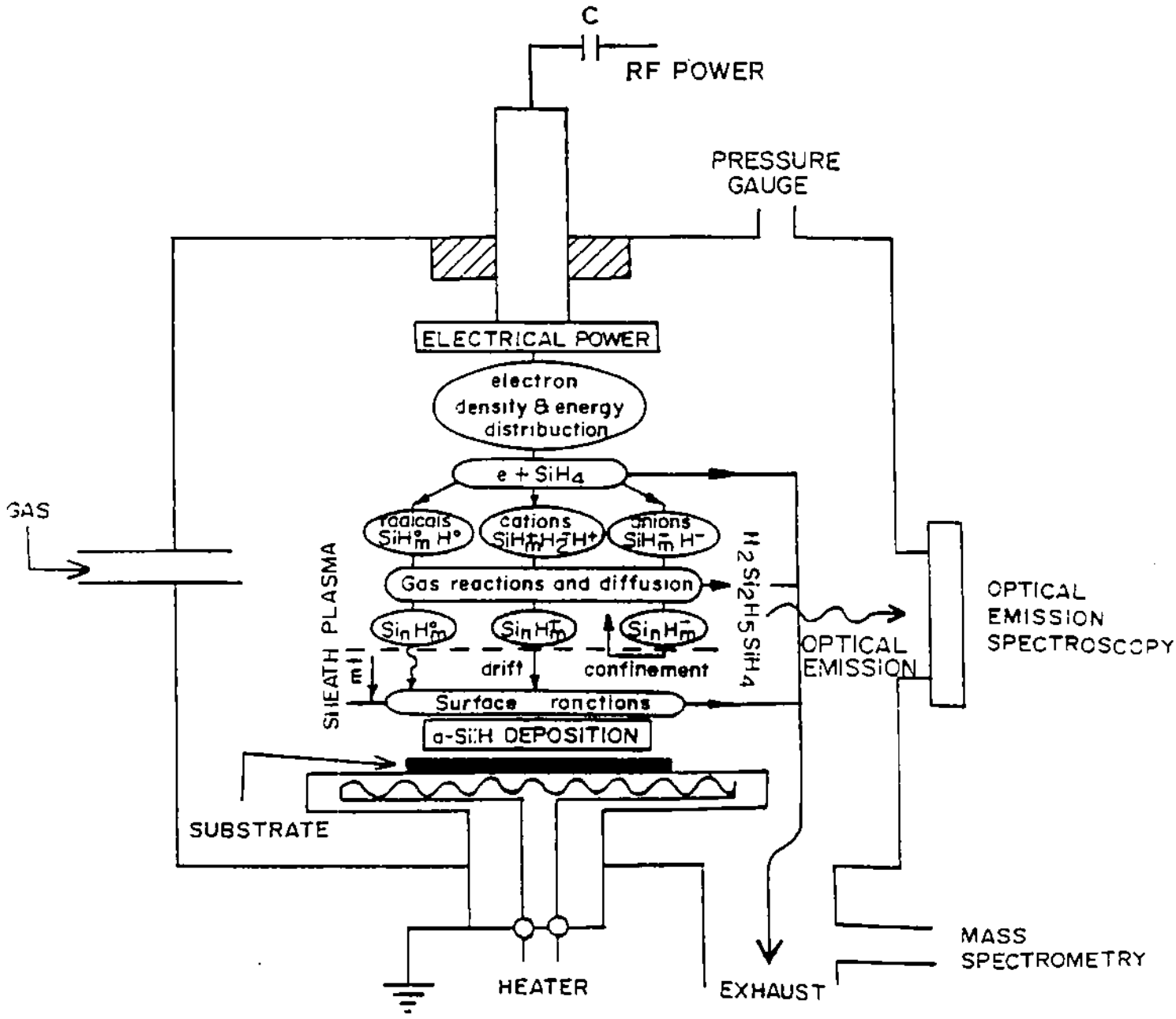

Fig. 1.9 Synopsis of a-Si:H deposition mechanisms from SiH_4 glow discharge.

Deposition Temperature	≈ 250°C
R.F. Power	< 25 mW cm^{-2}, CW
Gas flow rate	> 40 sccm (100% SiH_4)
Pressure	≈ 200 - 600 mTorr

Deposition parameters away from the above standard conditions for CVD growth leads ultimately to PVD type growth. A PVD process is limited by the flux of the reactants arriving on the growth surface[43]. Under this condition occurrence of various secondary plasma reaction is very common which may finally lead to powder formation (discussed in detail in section 1.5.4).

Further, those radicals with a high reaction rate have a low concentration and a short diffusion length and are less likely to reach the growing surface. The least reactive species is SiH_3, which does not react with SiH_4. Thus the silane plasma contains a combination of long-lived primary radicals, and the secondary products of the more reactive gas species.

The growth of a-Si:H film involves two further processes beyond the primary excitation of ions and radicals, and their secondary reactions. First is the adsorption of the molecular fragments onto the growing surface. There is still considerable doubt about exactly which species cause deposition[44], but the common view is that under low power deposition with undiluted silane, it is SiH_3. The second process is the release of atoms or molecules from the surface. The resulting a-Si:H material has a hydrogen content of about 10 at%, but the radicals arriving at the surface bring far more hydrogen with them. Clearly hydrogen must be released from the surface during growth.

Fig. 1.10 illustrates some of the processes which may occur at the growing surface on an a-Si:H film[45]. A surface which is completely terminated by Si-H bonds will not take up SiH_3 radicals.

1.5.3 Optimal growth of a-Si:H for defect minimisation

Optimal growth of a-Si:H refers to the conditions of deposition (mainly determined by growth rate (r_d) and substrate temperature (T_s) that result in films with the lowest defect concentrations. For example, a-Si:H grown at very high temperature becomes hydrogen deficient and, therefore, highly defective while low-substrate temperature growth also results in a-Si:H films with high defect densities and broad valance-band tails, post-deposition annealing at the

growth temperature can reduce the defect concentration by an order of magnitude and the slope of the valance-band tail by a factor of two.

There exists three types of growth models depending on the thickness of the layer which in principle determines the film defect density. Going from the free a-Si:H surface down to the bulk, these models are as follows:

1.5.3.1 Surface limited optimal growth model

Matsuda and Tanaka[46] consider that the a-Si:H defect density is controlled by surface diffusion kinetics of SiH_3 precursors during a-Si:H growth. According to their model, optimal growth occurs when the diffusion length of the precursors on the a-Si:H growing surface is long enough to allow these precursors to find energetically favorable sites for their incorporation. Low substrate temperature kinetically limit SiH_3 surface reactions that would ordinarily remove surface defects.

Recently Ganguly and Matsuda[47] have further refined this model where they postulated that the dangling bond (DB) density in the bulk of PECVD a-Si:H films are determined by the Steady-state DB density on the surface during growth. This is schematically shown in **Fig. 1.11**.

At optimum temperature, the diffusion coefficient determined diffusion length (l),

$$l = [2D_s\tau_s]^{1/2} \qquad (1.16)$$

where τ_s is the staying time of the precursor on the surface and is sufficient to locate optimum growth sites. As the temperature is lowered, the movement of the precursors becomes sluggish i.e. surface diffusion coefficient, D_s decreases. Therefore, l decreases and poor quality material is formed. Above optimum growth temperature, the surface hydrogen begins to disrobe, thus creating surface DB's which reduces τ_s and, hence l.

1.5.3.2 Growth-zone equilibrium model

Winer's model[48] is based on thermodynamics of three chemical reactions which account for silicon incorporation , defect formation and strain reduction respectively.

Si incorporation: Si incorporation during growth may be described stoichiometrically by the following reactions[49].

$$SiH_3(g) + Si_3Si\text{–}(s) \Rightarrow Si_3Si\text{-}SiH(s) + H_2(g) \qquad (1.17)$$

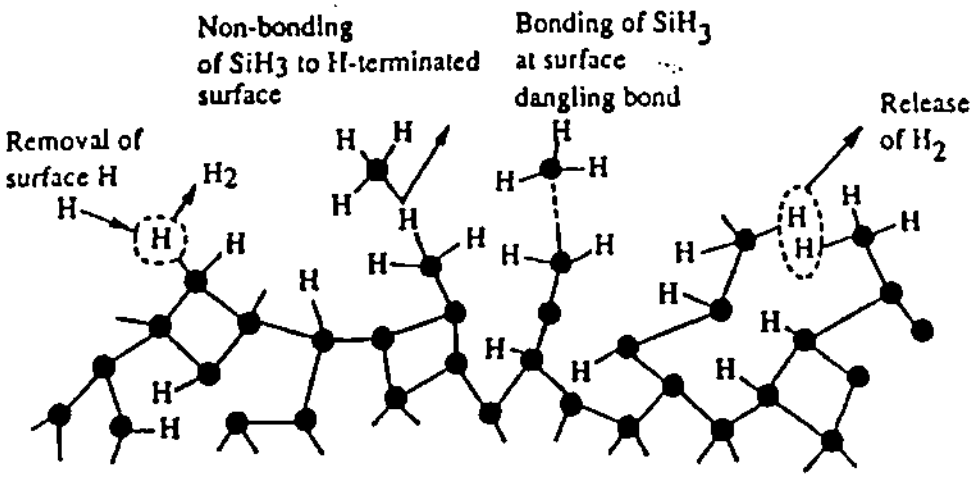

Fig. 1.10 Illustrates some of the processes which may occur at the growing surface on an a-Si:H film.

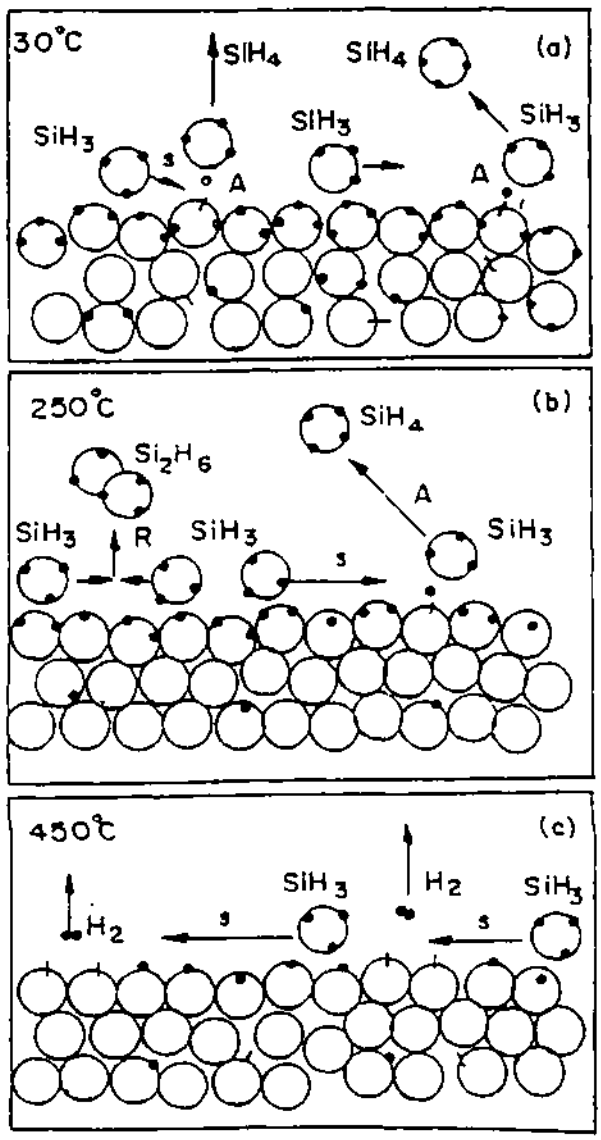

Fig 1.11 Schematic representation of the growth surface region of a-Si:H at a) room temperature, b) 250°C and c) 450°C. A, S & R stand for abstraction, sticking and recombination reaction respectively.

Where Si_3Si–(s) is a surface dangling bond (D^o), (g) and (s) refer to gas - and solid - phase species. This reaction proceeds at a rate proportional to the plasma power P.

Neutral defect formation: Defect formation occurs via

$$SiH + SiSi \Leftrightarrow D^o + SiHSi \qquad (1.18)$$

Both the forward and reverse rates depend on the rate of dispersive hydrogen diffusion.

Strain reduction: Reduction of valance band tail slope is associated with strain reduction. This can be accomplished by the following reaction[41].

$$SiHSi + SiSi_{weaker} \Leftrightarrow SiSi_{stronger} + SiHSi \qquad (1.19)$$

which is exothermic in the forward direction. The forward reaction proceeds until the valence-band tail is sufficiently narrowed to reach equilibrium if there is sufficient time to do so near the surface during growth. Below the surface, bulk constraints increase the kinetic barriers of the reaction. The equilibration rate depends on the rate of H diffusion and, therefore, on T_s.

In order for optimal growth to occur, the average rate of H diffusion μ_H in the time interval dt should be roughly equal to the growth rate R,

$$\mu_H = (4D_H/\delta t)^{1/2} \approx R \approx 4D_H/L \qquad (1.20)$$

where D_H is the H diffusion constant in a-Si:H[50] and L equivalent $R\delta t$, such that the time available for equilibration in the less constrained near-surface layer of thickness L decreases as R increases. Agreement with the experimental data is obtained with L = 1 A°, which suggests a surface-limited equilibrium growth process. Of course, Eqn. 1.20 is approximate, and does not take into account the dispersive nature of H diffusion. For typical deposition parameters μ_H and R equals at $\approx 250^oC$.

1.5.3.3 Hydrogen chemical potential model

Street[50] has proposed a growth model of amorphous hydrogenated materials based on the hydrogen chemical potential (μ_H). This model assumes the following.

(1)During deposition from hydrogen-containing gases the bonding structure of the film is in large part controlled by the effective hydrogen chemical potential (μ_H) in the plasma. Hydrogen influences the structure through its reaction with weak and broken silicon bonds.

(2) At sufficiently high growth temperature, μ_H in the plasma and the film tend to equalize because of the rapid interchange of hydrogen across the growth surface. The

structure then approaches an equilibrium distribution of Si-Si and Si-H bonds, limited by the network (topological constraints) and is indicated by the valence-band tail slope which is not less than $E_o \approx 40$-50 meV.

(3) At low growth temperature there is a kinetic constraint to the structural equilibration because insufficient hydrogen motion does not allow the network to rearrange between alternative configurations. Material grown in the kinetically limited regime has a higher disorder manifested by a broader distribution of weak bonds.

The hypothesis of this model is that the hydrogen reactions beneath the surface of the film change the structure from that which is created by the attachment of radicals at the surface of a structure which approaches a constrained equilibrium. This model explains hydrogen mediated defect minimisation in terms of energy distribution of hydrogen density of states (HDOS) as illustrated in **Fig.1.12**.

Hydrogen resides in the occupied states below μ_H, which in a-Si:H, are the Si-H bonds. The band of unoccupied states above includes the distribution of weak Si-Si bonds into which hydrogen can insert with low energy, and stronger Si-Si bonds at high energy. E_M, is the hydrogen migration energy and corresponds to the average energy at which hydrogen can diffuse freely.

The equilibration of the bonding structure induces a minimum in the hydrogen density of states at μ_H, because this configuration corresponds to the minimum defect density[50]. This interaction between μ_H and the HDOS allows hydrogen to influence the distribution of weak Si-Si bonds and the density of dangling bonds. When the growth temperature is high enough to allow the hydrogen chemical potentials in the gas and within the near surface growth region of the a-Si:H film to become equal, the structural order and, therefore, the defect concentration in the resulting a-Si:H film is determined by the H concentration in the gas. μ_H can be increased by H_2 dilution to such a point that there is no amorphous structure available with such a small amount of disorder; this makes the transition to μc-Si.

The model predicts the conditions for optimum growth of a-Si:H as follows. The surface layer formed by attaching highly hydrogenated gas radicals (e.g. SiH_3) has a high hydrogen concentration and is assumed to be highly disordered[50]. The final film structure is determined in the subsurface region though the motion and elimination of the excess hydrogen, and the reduction in structural disorder. In order to obtain the optimum growth

structure, it is assumed that a large fraction of the bonded hydrogen must redistribute within the time τ_s in which the subsurface reactions establish the final film structure. The rate limiting step in this process is attributed to the excitation of hydrogen to the mobile state at E_M, which occurs with rate $\omega_o \exp [-(E_M-E)/kT]$, where E is the hydrogen energy. A redistribution energy E_R is therefore defined by equating the inverse of the excitation rate of the time τ_s, giving

$$E_M - E_R = kT \ln(\omega_o \backslash \tau_s) \qquad (1.21)$$

where E_M is the hydrogen migration energy (see Fig. 1.10) and $\omega_s = 10^{13}$ sec^{-1}. E_R is indicated in (**Fig. 1.10**) and separates those hydrogen atoms of higher energy which can move in time τ_s, but it is expected to be usually of the order 10 sec, this being the typical time to grow a few atomic layers of the film.

1.5.3.4 Bulk equilibrium model

To explain the thickness dependence of the sub gap optical absorption, Hata et al.[51,52] have developed a model based on the annealing, during growth, of the growth induced surface defects. From this point of view the equilibrium may develop across the whole thickness of the film, which explains both the temperature and the thickness (deposition rate) dependence of the a-Si:H defect density.

1.5.3.5 Chemisorption based deposition model

Bruno et al.[42] have reported a chemisorption based deposition mechanism able to describe the surface growth from the kinetic point of view, i.e. to define the relationship between deposition rate and species concentration. Basically this relationship follows from the analysis of a chemical model whose concise scheme is as follows:

$$SiX_4(gas) \Rightarrow^{K} \Rightarrow SiX_2(ads) \Rightarrow SiX_2(gas)$$

$$K \Downarrow H$$

$$-SiX(FB\text{-}Si) \Rightarrow a\text{-}Si\text{-}film.$$

The most important features of this model are

1) The dissociative chemisorption of silicon volatile compounds (SiX_4) giving active species (SiX_2) adsorbed at the growing surface.

2) The surface reaction of H atoms to give free-bond silicon species (FB-Si) that are reactive intermediates for the silicon-to-silicon bond formation on the surface.

1.5.4 Powder formation

Recently dusty plasma has drawn wide attention and has been studied in detail. In the following formation, growth of powders and its effect on the a-Si:H film properties are discussed in certain detail. It is felt that the information presented here will make comprehension of what is being said subsequently in chapter-III & IV much easier.

Particulate contamination presents a major problem by limiting manufacturing productivity and device reliability[53]. The maximum achievable deposition rate for device quality intrinsic a-Si:H is limited by plasma polymerisation which results in poorer electronic quality[54] and rough films[55]. The density of particles occluded in the film has been found to rise with the increasing deposition rate, no matter how this increase is obtained. Neutral radicals are the likely candidates for particle precursors and their propagation is supposed to be by insertion of lower silane radicals into higher saturated molecules[56,57]. Plasma polymerisation is expected to be more rapid for ions. Experiments show that activation energy barrier prevent the formation of high mass positive ions. The fact that negative ions are retained in the plasma by the sheath potentials has led several authors to suggest that plasma polymerisation might proceed via negative ion pathways[58,59]. Negative ions upto mass 500 amu have been detected in RF SiH_4 plasma[60].

The formation of powder was observed the same day as the first silane plasma deposition[61]. It is very often suspected to be a source for particulate contamination. The initial observation of Spears[62] is that particulates are confined in the sheath edge. Normally particulates would be negatively charged as any object at floating potential immersed in the plasma. The charge is expected to be of the order of 1000 electron charge for a 0.2 mm spherical particulates. Particulates should be confined in the plasma potential well and be evenly distributed inside the uniform zone of the plasma.

According to Schmitt[63]

- a particulate is negatively charged,
- it attracts positive ions, increases recombination rate,
- it deflects by coulomb force slow electrons,

- it increases plasma resistivity,
- it preferentially collects fast electrons,
- it cools down the fast electron tail

L. Boufendi et al.[64] have proposed a three step process for powder formation and its growth. (i) rapid formation of crystalline clusters (2 μm) with concentrations upto 10^{10} cm^{-3}, ii) formation of aggregates of diameter upto 50 nm, by coagulation (during coagulation particle concentration decreases dramatically) and (iii) growth of particles with a constant concentration by surface deposition of SiH_x radicals.

Again Perrin et al.[65] have proposed a five successive step scenario for particle formation in SiH_4 discharges.

i) during the 1st step (t_o) the fast electron population is quickly established (≈ 10msec) and does not evolve as revealed by constancy of SiH^* emission.

ii) during the 2nd step (t_1) from a fraction of a second[66] to several minutes[67] the discharge remains in the α regime and no particles are yet detected by most sensitive techniques. In this stage Si-cluster growth proceeds.

iii) in this critical step (t_2) (few seconds) drastic α to γ transition occurs accompanied by the onset of monodispered particles whose density drop by two orders of magnitude and their radius increases by aggregation of primary clusters (2 - 5 nm)[77]. Plasma becomes more resistive.

iv) In this long step (t_3) the discharge power dissipation is dominated by attachment to particles of mean radius 40 nm[68]. Particle aggregation stops and growth slowly continues by condensation of radicals.

v) in the last step, for mean particle radius 100 nm the increasing charge on particles makes the plasma unstable which leads to a partial expulsion of particles. Then new generations of particles take place with dispersed particle sizes.

In high power high pressure silane plasmas, where particles form in a fraction of a second[69], a rapid neutral pathway via SiH_2 insertion into higher silanes have been proposed[69,70]. If neutral clusters reach critical size[71] and become large enough to be negatively charged by the RF plasma, there is no need to invoke a slower, parallel anionic pathway[72] (this is schematically shown in the **Fig.1.13**). Once a critical particle density and

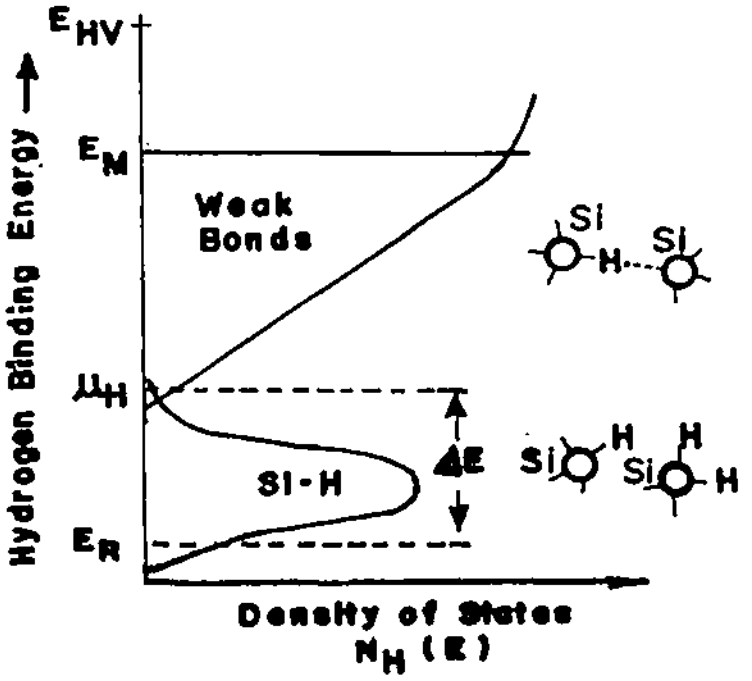

Fig. 1.12 Illustration of hydrogen density of states for a-Si:H, showing the Si-H bonds and the energy of H in the distribution of Si-Si bonds. E_{HV} is the energy of hydrogen in vacuum.

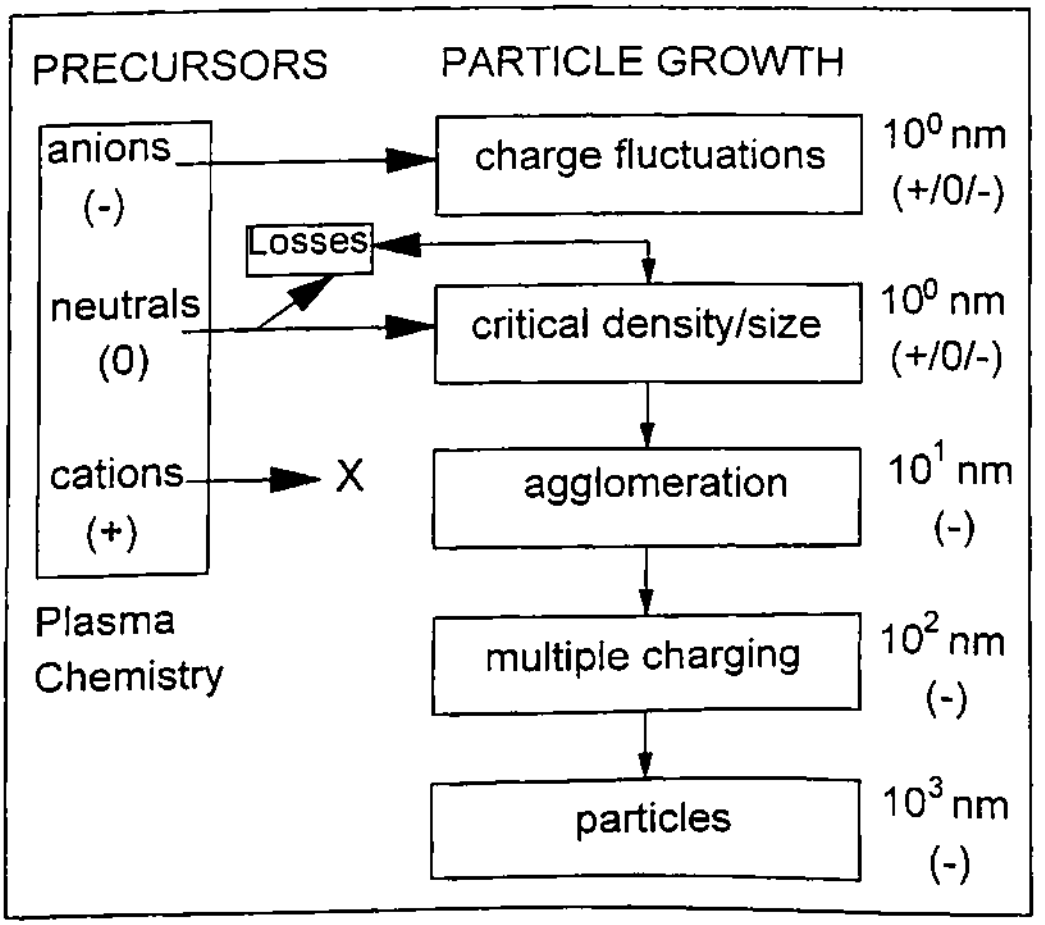

Fig. 1.13 Relationship between different precursors origins in a tentative scheme for a particle growth in silane plasma. The time interval for each step, which can range from subseconds to minutes, depends sensitively on plasma parameters.

size is reached, agglomeration and growth would continue independently of the precursor stage.

According to Howling et al.[73] the initial phase of powder formation produces macromolecules or clusters which although invisibly small, introduce electron coulomb scattering, attachment and recombination centers[74] and alter EEDF[75]. These molecular scale reactions modify the plasma impedance and RF power matching conditions. A change in reflected power is, thus, a precursor to visible particle formation, and this information can be fruitfully utilised because even 20A° particles could be deleterious to the electronic properties of a growing layer[76]. The reflected power could be incorporated into a feedback loop to keep the input power below the threshold for particle production.

1.5.5 Powder inhibition

It is difficult to find a completely powder free deposition plasma. It has been found in a plasma powder (heated) experiment that for a given flow above a given box temperature, the appearance time for powder goes to infinity, i.e. plasma becomes dust free. It was speculated that the important influence of the ambient temperature may be related to the thermally activated electron detachment from negative ions. The powder formation threshold is increased when the velocity of the carrier gas is increased. The drag force on the particulate pushes the powder out of the trapping potential well. The larger the flow the most likely is the powder to be driven away and carried out by the gas flow towards the pump as revealed by careful analysis of powder patterns left on the walls of all sorts of reactor geometry. This implies that, at least when plasma disruptions are avoided, there is no reason for powder to contaminate the film. Therefore, a gradual decrease of RF power along with an increase of gas flow should avoid powder from landing up on the substrate. The most important way of controlling powder is to use the concept of Intermittent plasma as introduced by Watanabe et al.[77]. The explanation is based on the assumption of powder to be negatively charged ions. During plasma interruption the charged species recombine. Neutral diffusion takes place. Light negative ions become light neutral which can diffuse rather fast. When dust is present it is so heavy that it requires a longer time to disappear. It disappears not by diffusion but rather by sweeping by the gas flow.

Intermittent plasma may avoid the build up of large size powder but, in contrast to the continuous plasma, it allows the powder seed to reach the wall, hence it may affect the film

quality. It has been found that surface roughness varies drastically. For smaller modulation frequency the powder size is too large for it to reach the surface. At higher frequency, the surface recovers the smoothness of the DC experiment. This implies that for modulation frequency of the order of 2-5 KHz the negatively charged powder seed has not enough time to reach a significant size and when it diffuses to the surface in the remaining time it is small enough to get incorporated into the film without perturbing the film structure.

The bulk material is also modified by intermittence. The loosely bound hydrogen as revealed by exodiffusion study, increases when powder makes a contribution to the growth.

A structural change is observed by low angle scattering and by the slope of the Urbach optical absorption tail. The continuous trend for material compactness improvement in high modulation frequency range (0.4 to 5 KHz) can be explained by the change in the size of the powder seed reaching the surface but it can also be attributed to the change of the plasma equilibrium itself due to the absence of big negative clusters. It has been found that these clusters can affect the plasma equilibrium. Therefore, they may indirectly affect the film growth by, for example, decrease of soft ion bombardment or shift of the radical source location from the sheath edges to the center.

Watanabe et al.[78] have found, for low (20%) duty cycle (D) the scattered laser light (LLS) intensity was too low to be observed. Decrease in D makes the high intensity region shift away from the RF electrode and brings about a significant decrease in particulate amount. Therefore RF power modulation is really effective in decreasing not only the amount of particulates throughout the discharge space but also their size. From the balance between the electrostatic and ion drag forces it appears, particulates of smaller size should reside far away from the RF electrode.

Mechanism of negative ion extraction:

In power modulated plasmas, provided that the modulation depth is atleast 90% [79], the sheaths collapse sufficiently for negative ions to escape if the after glow period is long enough. When the electrode voltage is applied at the beginning of each cycle, energetic electrons (at least 8 eV) are created which dissociate SiH_4 and give rise to sharp SiH* emission peaks in less than few msec. Equilibrium between the power source and the various plasma species is established on a slower time scale of around few tens of msec. When RF power is removed the most energetic electrons rapidly leave the plasma and the SiH* emission completely disappears in few msec. Thereafter positive ions and electrons undergo ambipolar

diffusion to the electrode surfaces and positive ion flux falls. After a delay of about 100 msec. from the end of the power period the negative ion flux appears abruptly and gradually decays until the next power period starts when the flux is cut off by sheath formation. When the electron density decays during the afterglow, the negative ion density eventually becomes large compared to the electron density. The plasma potential then no longer needs to be positive to retain electrons since the mobilities of the remaining positive and negative ions are comparable and the sheath field collapses[80]. Because of the mass dependent delay times and decay time constants, the loss rates and hence negative ion densities depend on the modulation frequency in different ways according to their mass.

The sheath electric field above 15 kHz modulation frequency does not have time to reverse and so the negative ions remain trapped in the plasma volume and continue to accumulate during successive plasma cycles and polymerise indefinitely leading to powder particles as observed[81].

Formation of polysilicon hydride anions:

Experimental results suggest that a polymerisation pathway proceeds via negative ion clustering. The negative ions are not simply by- products formed by electron attachment to a neutral species pathway. High mass negative ions are not formed by attachment to heavy neutrals because i) no neutrals with masses as high as negative ions are detected in the mass spectra. ii) negative ions and neutrals have very different abundance ratios which can not be reasonably explained by assuming attachment probabilities which are orders of magnitude larger for higher masses and iii) no attachment peak exists in the time resolved measurements for negative ions heavier than trisilicon hydride anions

One possible polymerisation pathway which propagates via negative ions is by silane addition[82].

Alternately negative ions can lose their excess energy by a stabilisation collision with a 3rd body which must occur within its auto detachment lifetime if the parent ion is to survive.

Autodetachment: $(SinH_x^-)^* \Rightarrow Si_nH_x + e^-$ (1.22)

Ion-Ion recombination is the second possible pathway for polymerisation. Ion-molecule and ion-ion reactions both eventually lead to stable, higher mass negative ions.

Dependence on modulation frequency for powder formation in modulated plasmas would be as follows:

At modulation frequency << 1kHz : Large clusters or even particles form within a single plasma period and some may become too large to be ejected in the subsequent off period; these particles would then continue to grow during successive cycles and eventually become visible[59].

At modulation frequencies < 1kHz : Clusters do not grow too large in one plasma cycle to be ejected in the off period and the plasma appears powder free[69].

At modulation frequency ≈ 1kHz : Plasma period is too short for polymerisation to propagate and powder production is suppressed[69,77]. The best quality film is obtained at this modulation frequency.

At modulation frequency > 1kHz : Negative ions are trapped by the sheath potential which do not have time to reverse and polymerisation continues in successive modulation cycles, ultimately forming particles in the plasma. These particles acquire a multiple electronic charge in the plasma and therefore remain trapped.

Measurement of negative ions and powder in silane plasmas as a function of power modulation frequency, partial depth modulation and after glow duration reveals the following:

i) particles formation is strongly reduced by square wave power modulation at kHz frequencies[81]. Previous work[81] demonstrated that powder does form when the anions do not have time to be evacuated in the after glow (modulation frequency > 3 kHz). Suppression of polymerised anions near 1 kHz modulation frequency is due to too short plasma period for anions to reach high masses before the reservoir of low mass anions is evacuated in each subsequent after glow period[67].

ii) with ON/OFF power modulation (100% modulation depth) at 1 kHz no powder is formed. If the RF voltage during the afterglow is then increased so that the sheath no longer fully collapses (≈ 85% modulation depth), the anion flux abruptly disappears and powder eventually forms. Neutrals are not affected by the sheaths and the flux of polysilicon neutrals undergoes no significant variation during a modulation cycle. Therefore any neutral polymerisation pathway to particle formation that may exist would not be affected by kHz power modulation[83].

1.5.6 Plasma Modelling

Mathematical models, in concert with experimental measurements, can assist in rational design of plasma deposition and etching reactors. One can distinguish two levels of complexity in the plasma deposition process. First, the concentration and energy distribution of electrons, ions and radicals in the plasma must be determined as a function of reactor operating conditions. Second, the relation between the flux (and energy distribution) of particles bombarding the substrate and the resulting film deposition rate and uniformity, as well as film structure and properties must be established. The earlier proposed models concerned with reactor operation consider the transport and reaction of the precursor gas in the plasma.

Pulsed plasma operation is relatively new approach to PECVD which has been implemented by plasma deposition equipment manufacturers, presumably to improve the film uniformity in channel reactors. Recently pulsed plasma discharge has been used to obtain superior properties of a-Si:H films and suppression of powder formation were obtained by low frequency modulation of SiH_4/He plasma[77]. In the following a simplified mathematical model of pulsed plasma CVD process is discussed[44].

The average deposition rate and uniformity are defined as

$$r_{av} = Da_n \int C_i(F)dF \qquad (1.23)$$

where $F = x/L$ is a dimensionless parameter, x is axial coordinate, L chamber dimension, $C_i(F)$ concentration distribution of radicals.

Uniformity index is defined as

$$UI = [C_{i,max} - C_{i,min}]/2C_{i,av} \qquad (1.24)$$

This is a measure of the deposit thickness uniformity. The lower the value of UI the better the uniformity.

An important parameter Da_n, Damkohler No. for deposition

$$Da_n = [(s/v)_n K_n L^2]/D_i \qquad (1.25)$$

D_i diffusivity of species, (s/v) surface to volume ratio, K_n rate constant of an heterogeneous reaction of the main radical containing deposition species.

Pictel number, P_e is a measure of convection as compared to axial diffusion

$$P_{ei} = uL/D_i \qquad (1.26)$$

u is the average fluid velocity.

Another important parameter is Da_p, Damkohler No. for radical generation

$$Da_p = K_p n_e L^2 / D_1 \qquad (1.27)$$

K_p rate constant for gas phase reaction, n_e electron density.

1.5.6.1 Plasma modeling for CW reactor

For a given pictel number (P_e), the precursor gas concentration decreases monotonically along the reactor due to electron impact dissociation in the plasma. For $P_e < 10$ there is complete conversion of precursor gas. For very high P_e gas residence times become very short and the chance of dissociation diminishes. In such case, most of the gas passes through the reactor unconverted. For $P_e > 1$, a maximum appears in the radical concentration profile. As P_e increases the position of maximum shifts away from the reactor entrance and it depends on the balance between rate of radical production and its consumption.

In a simulation study, for $Da_n = 40$ and $Da_p > 5$, UI was found to decrease sharply with P_e, attained a minimum for $P_e \approx 10$ and then increased monotonically with further increase in P_e. Under these conditions, the uniformity index for CW reactor was 0.707.

1.5.6.2 Plasma modeling for pulsed plasma reactor

For a conventional pulsed plasma discharge the deposition rate increases during the plasma on fraction of the cycle, and decreases during the plasma off fraction. The decay time is determined by various radical loss mechanisms such as convective flow and deposition. Deposition continues well after the plasma extinction, provided off period is not much longer than the radical lifetime. Compared to CW operation, pulsed plasma operation has the effect of decreasing the reaction rate near the reactor inlet, and increasing the rate near the exit. The result is a smoother reaction rate distribution and improved uniformity. For a given duty cycle, the reaction rate attains limiting values for very low and very high values of the pulse period. For very low pulse period species concentration cannot follow rapidly changing applied waveform. For very large pulse periods, the system reaches the corresponding CW state. Similarly an UI identical to CW reactor is attained at high pulse period regardless of the duty cycle. Whereas, for low pulse periods, uniformity is improved by pulsing the plasma and gradually improves with lower and lower duty cycle as shown in **Fig. 1.14**. In some pulsed plasma reactors the precursor gas depletion is minimised by allowing the reactor to "refill"

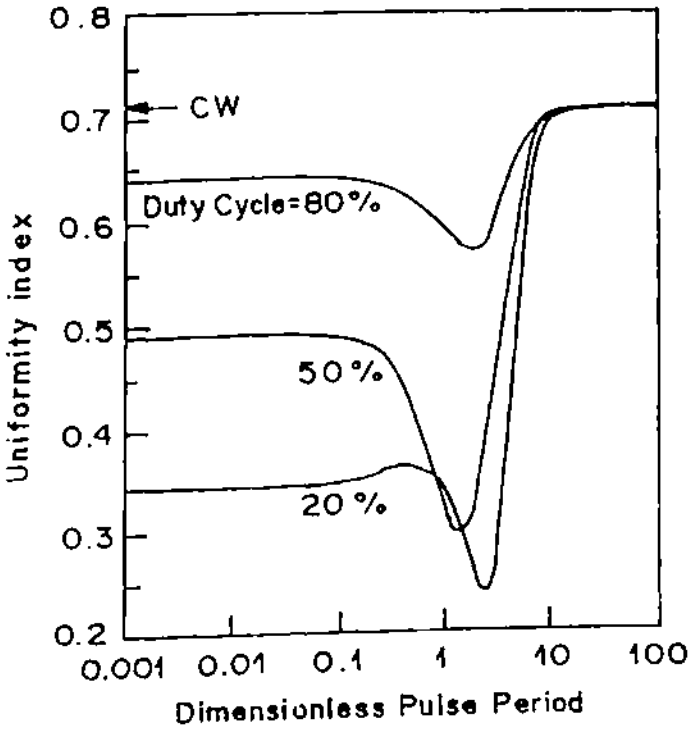

Fig. 1.14 Uniformity index in a pulsed plasma reactor without recycle as a function of pulse period with the duty cycle as a parameter. $P_e = 10$, $Da_p = 100$ and $Da_n = 40$.

with fresh gas during the plasma off fraction of the cycle. This results in smoother deposition rate profiles and in general improved uniformity.

For a given pulse period the average deposition rate decreases with decreasing duty cycle Hence, by controlling the duty cycle, better uniformity may be obtained at the expense of throughput. By selecting appropriate values of pulse period and duty cycle uniformity may be substantially improved without significant loss of the deposition rate. Park et al. [84] further suggested that under conditions of low depletion of precursor gas and/or low reactivity of the radicals, recycle of the exhaust can result in improvements in both deposition rate and uniformity.

1.6 Definition of the problem

In the proceeding review an attempt has been made to bring to focus how by maintaining the so called 'standard' deposition conditions one can deposit a-Si:H films capable of exhibiting "device" quality. However, further technological innovation in the area requires that a-Si:H films be grown away from the standard conditions and yet presently obtainable opto-electronic qualities of the material are not compromised. The technical goals to be achieved can be stated as follows:

1. Achieving high growth rate without sacrificing excellent set of optoelectronic properties of a-Si:H films.
2. Achieving tailorable band gap of basic a-Si:H material without drastically altering its optoelectronic properties i.e. without alloying. This is particularly attractive for a tandem solar cell structure for replacing the alloy materials.
3. Achieving good optoelectronic properties on temperature sensitive substrates.

However, research conducted during the last several years indicate that it may well be possible to realise one or more of these desirable technological requirements. Specifically, a body of experimental evidences is slowly building up by which one can explain the dependence of optoelectronic properties of a-Si:H as a process out of equilibrium in which plasma plays an important role. Further, some recent experimental studies[85] indicate that in order to produce low defect density a-Si:H, increase in the deposition rate must be accompanied by an increase of the substrate temperature (through thermal enhancement of precursor diffusion length). It

also appears that the subtilities of the plasma processes are the limiting step in the production of low defect density films.

In view of what has been said it becomes imperative to optimise, at great length, a particular PECVD process and look for a window where one could possibly observe one or more of above stated desirable properties, away from standard conditions of growth.

Thus, in carefully trying to optimise a-Si:H deposition processes, away from standard conditions, one is not only trying to test the limits of applicability of the existing models but also creating a body of experimental data based on which these models can, perhaps, be further refined or some new models proposed.

The aim of the present investigations, therefore, is precisely to generate these new evidences by careful experimentation of a-Si:H growth, away from so called standard conditions. Specifically the following two PECVD processes are considered.

(1) Modified pulsed plasma CVD at RF (13.56 MHz).

(2) Modified pulsed plasma CVD at VHF (100 MHz)

Each of these have some distinct advantages and limitations. But when one combines VHF processing in a pulsed plasma mode many interesting results are expected. One expects not only to exceed presently achievable growth rate (VHF advantage), but also the limitations of VHF i.e. finite wavelength effect leading to nonuniformity of deposition can possibly be overcome by pulsing the source.

1.7 References

1. R.C. Chittick, J.H. Alexander and H.F. Sterling, *J. Electrochem. Soc.* **116**, 77 (1969).
2. W.E.Spear and P.G. LeComber, *Solid State Comun.* **17**,1193 (1975).
3. F. Yonezawa and T. Ninomiya, *Topological Disorder in condensed Matter* Proc. 5th Taniguchi Int. Symp. Japan (1982) p-2.
4. W.H. Zachariasen, *J. Am. Chem. Soc* **54**, 3841 (1932).
5. D.E.Carlson and C.R.Wronski, *Appl. Phys. Lett.* **28**, 671 (1976).
6. Y. Ichikawa, S. Fujikake, T. Takayama, S. Saito, HY. Ota, T. Oshida, T. ihara and H. Sakai, Proc., *23rd IEEE Photovoltaic Specialists Conf.*, Louisvillo (1993).
7. D.E.Stabler and C.R.Wronski, *Appl. Phys. Lett.* **31**, 292 (1997).
8. E. Maruyama, K. Sayama, A. Terakawa, K. Nonomiya, H. taraui. S. Tsuda, S. Nakano and Y. Kuwano, Proc., *23rd IEEE Photovoltaic Specialists Conf.*, Louisvillo (1993).
9. J. Yang, A. Banerjee and S. Guha, *Appl. Phys. Lett.* **70**, 2975 (1997).
10. Y. Ichikawa, T. Ihara, S. Saito, H. Ohta, S. Fujikawe and H. Sakai, Proc. *11th EC PVSEC*, Montreux, Switzerland, p-203 (1992).
12. H. Sakai, *Solar Energy Materials & Solar Cells* **34**, 9 (1994).
11. S. Sugiyama, J. Yang and S. Guha, *Appl. Phys. Lett.* **70**, 378 (1997).
13. P.W. Anderson, *Phys. Rev.* **109**, 1492 (1958).
14. N.F. Mott, *Phil. Mag.* **22**, 7 (1970).
15. M.H. Cohen, H. Fritzsche and S.R. Ovshinsky, *Phys. Rev. Lett.* **22**, 1065 (1969).
16. E.A. Davis and N.F. Mott, *Phil. Mag.* **22**, 903 (1970).
17. N.F. Mott, *Phil. Mag.* **42**, 911 (1971).
18. T.D. Moustakas and W. Paul, *Phys. Rev. B* **15**, 1564 (1977).
19. M.H. Brodsky and R.S. Title, *Phys. Rev. Lett.* **23**, 581 (1969).
20. B.Von. Roedern, L. Ley and M. Cardona, *Phys. Rev. Lett.* **39**, 1576 (1977).
21. M. Vanecek, A.H. Mahan, B.P. Nelson and R.S. Crandall, in Proc. *11th Ec PVSEC*, 1992.
22. W.B. Jacson and S.B. Zhang, in *Transport, Correlation and Structural Defects*, ed. H. Fritzsche (World Sientific, Singapore, 1990), p.63.
23. P.A. Ledders and A.E. Carlsson, *Phys. Rev. B* **39**, 1134 (1989).
24. S. Pantclides, *Phys. Reb. Lett.* **58**, 1344 (1987).
25. C.R. Wronski, S. Lee, M. Hick and S. Kumar, *Phy. Rev. Lett.* **26**, 1541 (1989).
26. K. Winer, I. Hirabayashi and L. Ley, *Phys. Rev. B* **38**, 7860 (1988).

27. R.A. Street, D.K. Beigelsen and R.L. Weisfield, *Phys. Rev. B* **30**, 5861 (1984).

28. Y. Bar-Yam , D. Adler and J.D. Joannopoulos, *Phys. Rev. Lett.* **57**, 467 (1986).

29. K. Winer and L. Ley, *Advances in Disordered Semiconductors: Amorphous Silicon and Related Materials*, Vol. 1, ed. H. Fritzsche, World Scientific Singapore (1988), p-365.

30. Z.E. Smith and S. Wagner, *Advances in Disordered Semiconductors: Amorphous Silicon and Related Materials*, Vol. 1, ed. H. Fritzsche, World Scientific Singapore (1988), p.409.

31. L. Ley and K. Winer, *Proc. 19th Int. Conf. Phys. semiconductors*, Warsaw, PIOP Warsaw (1989), p.1609.

32. R.A. Street, *Phys. Rev. Lett.* **49**, 1187 (1982).

33. R.A. Street, J. Kakalios and T.M. Hayes, *Phys. Rev. B* **34**, 3030 (1986).

34. Z.E. Smith, S. Aljishi, D. Slobodin, V. Chu, S. Wagner, P.M. Lenahan, R.R. Arya and M.S. Bennett, *Phys. Rev. Lett.* **57**, 2450 (1986).

35. K. Winer and R.A. Street, *Phys. Rev. Lett.* **63**, 880 (1989).

36. R.A. Street, C.C. Tsai, J. Kakalios and W.B. Jackson, *Phil. Mag. B* **56**, 305 (1987).

37. J. Kakalios and W.B. Jackson, in *Advances in Disordered Semiconductors: Amorphous silicon and related materials*, Vol - 1, (World Scientific, Singapore, 1988), p.207.

38. R.A. Street, J. Kakalios, C.C. Tsai and T.M. Hayes, *Phys. Rev. B* **35**, 1316 (1987).

39. R.A. Street and K. Winer, *Phys. Rev. B* **40**, 6236 (1989).

40. A. Madan and M.P. Shaw in *The physics and applications of Amorphous Semiconductors* (Academic Press Inc., 1988).

41. Hydrogenated Amorphous Silicon , ed. by J.I. Pankova, Vol. 21A in *Semiconductors and Semimetals* (Academic Press, New York, 1984).

42. G. Bruno in *Plasma Deposition of a-Si:H Based Materials* (Academic Press Inc., 1995) p.115.

43. R.A. Street, *Hydrogenated Amorphous Silicon* (Cambridge Univ. Press, 1991).

44. S. Veprek, *J. Appl. Phys.* (1989).

45. A. Gallagher, *Mat. Res. Soc. Symp.* Proc. **70**, 3 (1986).

46. A. Matsuda and K. Tanaka, *J. Non-Cryst. Solids* **97&98**, 1367 (1987).

48. K. Winer, *Phys. Rev. B* **41**, 12150 (1990).

47. G. Ganguli and A. Matsuda, *Phys. Rev. B* **47**, 3661 (1993).

49. A. Gallagher, *J. Appl. Phys.* **63**, 2406 (1988).

50. R.A. Street, *Phys. Rev. B* **43**, 2454 (1991).

51. N. Hata, S. Wagner, P. Roca i Cabarrocas and M. Favre, *Appl. Phys. Lett.* **56**, 2448 (1990).

52 N. Hata, E. Larson, J.Z. Liu, Y. Okada, H.R. Park and S. Wagner, *Proc. of the Materials Research Society Spring Meeting*, 1990 (Pittsburg, Pennsylvania).

53. G.S. Selwyn, J. Singh and R.S. Bennett, *J. Vac. Sci. & Tech.* A7, 2758 (1989).

54. R.C. Ross and J. Jaklik, jr., *J. Appl. Phys.* **55**, 3785 (1984).

55. N. Morosoff, in *Plasma deposition, treatment and etching of polymers*, ed. R. d'Agostion (Academic Press, New york, 1990).

56. M.J. Kushner, *J. Appl. Phys.* **63**, 2532 (1988).

57. S. Veprek, K. Schopper, O. Ambacher, W. Reirer and M.G.J. Veprek-Heijman, *J. Electrochem. Soc.* **140**, 1935 (1988).

58. J.T. Verdeyen, J. Beberman and L. Overzet, *J. Vac. Sci. & Tech.* **A8**, 1851 (1990).

59. A. Lloret, E. Bertran, J.L. Andujar, A. Canilles and J.L. Morenza, *J. Appl. Phys.* **69**, 632 (1991).

60. A.A. Howling, L. Sansonnens, J.-L. Dorier and Ch. Hollenstein, *J. Phys. D: Appl. Phys.* **26**, 1003 (1993).

61. J. Ogier, *Bl.Soc. Chem.* **8**, 116 (1879).

62. K.G. Spears, R.P. Kampf, T.J. Robinson, *J. Chem. Phys.* **92**, 5297 (1988).

63. J.P.M. Schmitt, *Mat. Res. Soc. Symp. Proc.* Vol. 219, 631 (1991).

64. L. Boufendi and A. Bouchoule, *Plasma Sources Sci. & Tech.* **3**, 262 (1994).

65. J. Perin, C. Bohm, R. Etmadi and A. Lloret, *Plasma Sources Sci. & Tech.* **3**, 252 (1994).

66. A. Bouchoule, A. Plain, L. Blondeau, J.Ph. Boludeau and C. Laure, *J. Appl. Phys.* **69**, 1991 (1991).

67. Ch. Hollenstein, J.L. Dorier, J. Dutta, L. Sansonnens and A.A. Howling, *Plasma Sources Sci. & Tech.* **3**, 278 (1994).

68. J.P. Boeuf, *Phy. Rev. A* **46**, 7910 (1992).

69 Y. Watanabe, M. Shiratani & H. Makino, *Appl. Phys. Lett.* **57**, 1616 (1990).

70. S. Veprek, K. Schopper, O. Ambacher, W. Rieger & M.G.J. Veprek-Heijman, *J. Electrochem. Soc.* **140**, 1935 (1993).

71. S.J. Choi and M.J. Kushner, *J. Appl. Phys.* **74**, 853 (1993).

72. Ch. Hollenstein, W. Schwarzenbach, A.A. Howling, C. Courteille, J. -L. Dorier and L. Sansonnens, *J. Vac. Sci & Tech.* **A14**, 535 (1996).

73. A.A. Howling, Ch. Hollenstein and P. -J. Paris, *Appl. Phys. Lett.* **50**, 1409 (1991).

74. A. Garscadden, In *Non eqilibrium processes in partially ionised gases*, ed. M.Capitelli and J.N. Bradsley (Pelnum, NewYork, 1990) p.541.

75. M.J. McCaughey and M.J. Kushner, *Appl. Phys. Lett.* **55**, 951 (1989).

76. K.G. Spears and T.J. Robinson, *J. Phys. Chem.* **92**, 5302 (1988).

77. Y. Watanabe, M. Shiratani, Y. Kubo, I. Ogawa and S. Ogi, *Appl. Phys. Lett.* **53**, 1263 (1988).

78. Y. Watanabe and M. Shiratani, *Plasma Sources Sci. & Tech.* **3**, 286 (1994).

79. L.J. Overzet, J.H. Beberman and J.T. Verdeyen, *J. Appl. Phys.* **66**, 1622 (1989).

80. R.A. Gollscho and C.E. Gasbe, *IEEE Trans. Plasma Sci.* **Ps-14**, 92 (1986).

81. A.A. Howling, P. -J. Paris and Ch. Hollenstein, *Appl. Phys. Lett.* **62**, 1341 (1993).

82. J. Perrin, A. Lioret, G. de. Rosny and J.P.M. Schmitt, *Int. J. Mass Spectrom. Ion Processes*, **57**, 249 (1984).

83. Y. Watanabe, M. Shiratani and M. Makino, *Appl. Phys. Lett.* **57**, 1616 (1990).

84. S.K. Park and D.J. Economou, *J. Electrochem. Soc.* **137**, 2103 (1990).

85. P. Roca i Cabarrocas, *Proc. of ICAS* 15, 1993 (Cambridge, UK).

CHAPTER-2

Growth and Characterisation of a-Si:H Films

In this chapter first a brief review of different innovations that have been made to enhance growth rates of a-Si:H is presented. Details of the plasma reactors used for the present investigations are subsequently given. This is followed by brief descriptions of different characterisation techniques used during the present investigation. Silane glow discharge is also studied by optical emission spectroscopy. A brief description of this technique has been presented.

2.1 Different techniques to grow a-Si:H films at high deposition rate

There are many ways to prepare a-Si:H films. The most widely used method is the glow discharge decomposition of silane, wherein an electric field is used to produce a plasma containing ions and other reactive species which condense on a heated substrate (200 to 400°C typically) to form an amorphous solid.

There are many variants of the basic glow discharge method. In RF discharge, power is coupled either inductively or capacitively. Additional DC electric field can be used to stabilise the discharge or DC magnetic field to confine the plasma. Basically RF power controls the rate of dissociation of gas and, therefore, the film growth rate. The gas pressure determines the mean free path of the gas molecules and dictates whether the reactions will take place on the growing surface of the film or in the bulk of the plasma. The gas flow rate and the pumping speed determine the residence time of the gas species in the reactor. Temperature of the substrate controls the chemical reactions and the surface mobility of the species on the growing surface.

A complete understanding of the silane plasma chemistry has not yet been reached and in the absence of a quantitative model, optimisation of the deposition parameters requires a

lengthy and tedious "exploration of the space of preparation"[1]. Some of the parameters, in an approximate order of importance are:

- deposition temperature;
- geometrical dimension of the chamber and the electrodes;
- RF power and electrical bias of the substrate;
- gas parameters: total and partial pressures, flow rates, pumping speed, etc.

If one assumes a modest number of five parameters and five measurements of each parameter, the 'exploration of the space of preparation' require the deposition of $5^5 = 3125$ samples. This kind of tedious work is a lengthy exercise. This kind of exercise has already been done by different groups and have revealed the following set of parameters, better known as 'standard condition of growth of a-Si:H':

- deposition temperature around 200 to 250°C
- inter-electrode distance of few centimeters (2 - 4 cm)
- RF power density of around 0.1 Wcm^{-2}

High deposition rates are expected to be achieved from the following three different approaches[2].

(1) Increasing the generation rate of radicals in the plasma.

(2) Shortening the transport path from the plasma to the growing surface.

(3) Increasing the sticking coefficient of the radicals reaching the growing surface.

Different efforts based on the above guiding principles are briefly discussed below.

2.1.1 Plasma excitation methods

DC, RF and Microwave plasma excitation are commonly used for the deposition of amorphous silicon. The first two types of plasma excitations have mostly been employed by workers in this field and also these two are the only methods adopted so far by the industry. The substrates are generally placed on a grounded electrode (anode) in the case of RF discharge, largely to avoid ion bombardment resulting in the deterioration of the film properties[3], and at the same time ground electrode is usually kept at the top to avoid large size powder incorporation.

Ross et al.[4] have examined the deposition rate on the anode, using both RF and DC discharges in the same reactor, and explained why the deposition rate under RF glow discharge is higher than that for the DC glow discharge.

By using electron-cyclotron resonance plasma, Kato et al.[5] achieved high deposition rates, r_d upto 250 A^0s^{-1} from decomposition of SiH_4+H_2 mixture, without much deterioration of the optoelectronic properties of the films so produced.

Conde et al.[6] have demonstrated that in their Concentric Electrode-PECVD technique high band gapa-Si:H films could be grown at low substrate temperature at considerably high rates by varying silane flow rates over wide limits.

Hamasaki et al.[7] proposed a novel design by incorporating a grounded mesh surrounding the electrodes and a high deposition rate of more than 50 $A°s^{-1}$ was achieved in this case without much deterioration of the film quality. Hamasaki et al.[8] further proposed another new technique for the modification of the potential profile in a capacitively coupled reactor, by employing a tuning network connected to the substrate electrode. In this case, the potential drop in the sheath near the substrate electrode could be increased under the resonance conditions and it was found that the glowing region spreads toward the substrate. A high deposition rate, exceeding 40 $A°s^{-1}$ could be obtained with no appreciable degradation in structural and electronic properties of the films so produced.

Sanyo group[9] prepared high quality a-Si:H films with a photosensitivity, σ_{ph}/σ_d of $7x10^5$ at a high deposition rate of 10 $A°s^{-1}$ with the use of magnetic fields (Controlled Plasma Magnetron, CPM technique); a-Si:H solar cells, with the i-layer deposited at high deposition rate by CPM technique, were found to have a higher open circuit voltage and a higher conversion efficiency than those grown without the use of magnetic fields. They confirmed with the help of optical emission studies that a high electron density plasma could be produced under a magnetic field, at low RF power, which in turn decreased the ionic bombardment on the substrate.

Curtins et al.[10] reported a strong dependence of the deposition rate on the excitation frequency in the range of 25-150 MHz. The deposition rate was found to be maximum at about 70 MHz. The a-Si:H films prepared at rates exceeding 20 $A°s^{-1}$, at a frequency of 70 MHz, were found to show properties comparable to films prepared at 13.56 MHz at a typical rate of 3 $A°s^{-1}$.

Chatham et al.[11] also used very high frequency discharges (10-110 MHz) to deposit high quality amorphous silicon at high deposition rates using disilane. They also incorporated intrinsic layers deposited at rates upto 20 $A^{\circ}s^{-1}$ in p-i-n devices by using 110 MHz discharge and achieved solar cell efficiencies greater than 9.5% over 1 cm^2.

Scarsbrook et al.[12] have discussed the limitation of continuous plasma processes like incomplete gas dissociation or proper gas utilisation , gas depletion , powder formation and requirement of substrate heating. They proposed a novel pulsed plasma discharge, wherein very high power is applied for a short duration (typically few hundred sec) and discharge remained off for the rest of the period. They even pulsed the gas flow in phase with the RF power pulsing. The dramatic consequences of the above procedure are i) many fold increase in the deposition rate, ii) enhanced thickness uniformity and iii) substantial decrease in powder formation. They achieved deposition rate of 50 $A^{\circ}s^{-1}$ for the growth of a-Si:N:H using 50 KW power having a pulse width of 250 msec. Interestingly, their film properties were comparable to those of the films grown by using more conventional techniques with deposition rates a few $A^{\circ}s^{-1}$.

Scott et al.[13] used higher silanes to increase the deposition rate of amorphous silicon and a rate as high as 65 $A^{\circ}s^{-1}$ was obtained. Thus, the rates obtainable using disilane are many times higher than what could be obtained using monosilane. However, Kuboi et al.[14] reported that this tendency becomes less pronounced with increasing excitation power. Ross et al.[4] further reported that the deposition rate, in the case of an RF glow discharge method, at 0.50 Torr and 10 sccm flow rate, increased upto 11 $A^{\circ}s^{-1}$, with increasing Si_2H_6 fraction in SiH_4 + Si_2H_6 mixture.

2.1.2 Dissociation and transport of the active species to the substrate

The discharge deposition chemistry is initiated by electron impact dissociation of SiH_4, and under normal conditions more than 95% of the resulting deposition is by reactive neutral species (radicals) and only a small contribution comes from ionised species[15]. Discharge deposition of a-Si:H is normally done at power/flow ratios that decompose 10 to 50% of the silane gas, as well as most of the higher silane produced in the discharge. Gallagher et al.[16] proposed that radicals with an odd number of H atoms (H, SiH & SiH_3) ultimately lead to formation of a-Si:H film, whereas radicals with even number of H atoms (Si & SiH_2) react

with SiH_4 before reaching the surface producing higher silanes. Different dissociation pathways with their corresponding enthalpies are listed in section 1.5.1.

Ischihara et al.[17] deposited a-Si:H films by RF glow discharge by changing anode-cathode spacing (d) and chamber pressure (p) simultaneously. They found that the deposition rate was dependent not only on p but also on d. They further found that for deposition rate, in the p-d space, there were two distinct boundaries. One was pd = constant; other followed a relation pd^2 = constant. The RF plasma could be stably sustained between the two boundaries.

A variety of species exist in the excited silane plasma and they are transported onto the substrate for the deposition of a-Si:H film. However, on way to the substrate, they undergo collisions and the flux of the active species decreases. The deposition rate is, therefore, dependent on the distance between the center of the plasma glow and the substrate. Matsuda et al.[18] used a triode type reactor in which a discharge is maintained between the powered electrode and a grounded mesh electrode. It was argued that log (r_d) would be proportional to p^2L^2, where p is the pressure, for a specified precursor and L is the distance between substrate and mesh. The above relation is valid under the condition that deposition is determined by the survival of the active species.

Das et al.[19] have studied the effects of interelectrode spacing on the properties of a-Si:H. They found that in high RF power regime r_d increases with an increase in interelectrode spacing in a capacitively coupled PECVD system having arrangement for cathode heating and this is in contrast to the opposite trend in r_d at low RF power densities.

2.1.3 Dependence on the excitation power

An increase of the deposition rate with the excitation power is expected in the conventional RF glow discharge system[20]; RF planar magnetron system[21], capacitively coupled RF system with a ground mesh[6], and microwave systems[22] also generally follow this pattern. Tsai et al.[23] reported that the deposition rate of a-Si:H, on either electrodes of a PECVD system, increases linearly with RF power in a capacitively coupled RF (13.56 MHz) plasma system.

Nishikawa et al.[24] reported the possibility of depositing device grade a-Si:H films grown at higher power levels with appreciably high deposition rates. They obtained a deposition rate upto $70A°s^{-1}$ with $\sigma_{ph} = 1.2x10^{-5}\ \Omega^{-1}cm^{-1}$ by increasing the silane flow rate and the power. At RF powers lower than a threshold value, the concentration of SiH_2 bonds and

$(SiH_2)_n$ groups were found to increase with increasing RF power. However, at RF powers higher than the threshold value the concentration of SiH_2 bonds and $(SiH_2)_n$ groups decreased with increasing power.

2.1.4 Gas dilution effects, dual use of a buffer gas

Deposition of a-Si:H is not very sensitive to a moderate dilution of silane in a buffer gas, e.g. molecular hydrogen. The operational definition of a buffer gas is schematically shown in **Fig. 2.1**; it is a gas having very high threshold energy E_2 of decomposition by the electrons of the plasma, so that the collisions with the molecules of the buffer gas are mostly elastic. This is the case for gases like H_2, N_2 or He which are chemically very stable and have very high ionisation energy. It is to be noted that the heavy rare gases (Ar, Kr, Xe) have relatively low ionisation energy and, in that sense, are not good buffer gases and, indeed, have a negative influence on the quality of the deposited material[25]. It is to be marked that in the case of production of very high energy electrons (very high power plasma), collisions with the buffer gas become inelastic and thus is not a "buffer" gas anymore and the glow discharge process is deeply affected: this is the case for a large dilution in hydrogen and application of high power levels where microcrystalline rather than amorphous material is obtained[26]. On the other hand, at very low plasma power, a gas like CH_4, which is chemically stable and has a threshold of decomposition higher than that of silane can be considered as a buffer gas so far as plasma chemistry is concerned.

Knight et al.[25] have reported that (using SiH_4) increasing the RF power density to a high value leads to rapid gas phase reactions resulting in the formation of powder and deterioration of the film properties. To avoid this powder formation they diluted the silane with an inert gas (He or Ne) and obtained $r_d > 10$ A°s^{-1}.

Kampas et al.[27] studied Ar dilution of SiH_4 and found that maximum deposition rate occurred for a silane fraction of around 2%, with a total pressure of 0.1 Torr.

Vanier et al.[28] investigated hydrogen dilution of SiH_4 and reported a maximum r_d of 3.5 A°s^{-1} for a silane fraction of 25%. The decrease in the deposition rate for the silane fractions larger than 25% was attributed to a decrease in the concentration of energetic electrons in the discharge.

Messen et al.[29] investigated H_2 and D_2 dilution of silane to clarify the origin of hydrogen in the films and observed that r_d for samples grown with D_2 was consistently 25%

higher than that grown with H_2, using capacitively coupled RF discharge system (at 5 - 30W, 10 sccm SiH_4, 30 Pa, and 250°C). They suggested a contribution of the larger D_2 emission to the dissociation of silane (photo CVD) as a possible explanation.

Device quality a-Si:H films have been deposited at high growth rate using variety of diluent gases. Often the use of noble gas mixture lead to columnar growth [30] whereas high hydrogen dilution leads to the creation of a microcrystalline phase[31]. Vanier et al.[28] have reported that dilution of SiH_4 with H_2 resulted in an increase of r_d by as much as one order of magnitude over the rate obtained by pure SiH_4.

Hamasaki et al.[32] used pulsed RF discharges for 11% SiH_4 (H_2) and showed that r_d is nearly constant for each repetition frequency (at 67 sccm flow and pressure 0.18 Torr) when the total period was kept constant.

Kato et al.[33] experimented with H_2 dilution in an ECR plasma and found that r_d increases with the silane fraction upto 50% and saturates there after.

Bruno et al.[34] investigated the effect of Ar dilution in $SiCl_4$ + H_2 and found r_d to increase with Ar addition and attains a maximum at 27% Ar.

Nakayama et al.[35] investigated H_2 dilution of Si_2H_6 and reported the deposition rate obtained to be proportional to the square root of the Si_2H_6 fraction x, for $x < 30\%$ and it was found to be proportional to (3/2) for $x > 30\%$. The maximum r_d obtained was about 30 μm/hour (≈ 83 $A^{\circ}s^{-1}$).

2.1.5 Effect of RF power modulation

Generally silane plasma is operated in a continuous wave (CW) mode, but very recently a novel approach to the PECVD technique has been proposed, which consists in producing the plasma under modulated wave (MW) condition. With respect to CW plasma operation some substantial improvements in the deposition process[36,37,38], the uniformity in both thickness and composition[39] and the suppression of powder in the plasma phase[36,40,41] have been reported to occur in modulated plasmas. This has been ascribed to the fact that the typical time constant, about 1 min for particle formation, is much larger than the normally used pulse period. Hence the modulation prevents the growth in size of particles, and thereby reducing the negative effects of their formation.

2.2 System description and methodology employed for the deposition

The plasma glow discharge deposition system used for growing films on the grounded electrode is a Multizone PECVD system (Glasstech Solar INC., USA). It consists of a central load lock chamber and three deposition chambers. Each chamber is a four way stainless steel cross (Φ = 150mm). In the cross two parallel electrodes have been installed and the insulated one (bottom electrode) is connected to CW/pulsed, RF/VHF power supplies. The other electrode (12 mm away) is grounded and heated externally to reach a temperature anywhere from room temperature to a high temperature ($\approx$ 400°C). The substrates were placed on the earthed electrode. In view of Hamasaki et al.'s[7] work, a stainless steel grounded shield, surrounding the two parallel electrodes was used for confining the plasma and also for suppressing the diffusion of reactive species towards the chamber wall. Some holes were made on the region of the grounded shield which was just behind the viewing window. Reacting gases were allowed to enter the chamber through a flange placed 180° opposite to the viewing window. The deposition systems used in this study is shown in **Plate no. 2.1** and also schematically in **Fig. 2.2**. This multizone reactor is a versatile system with ultra-high vacuum compatibility and is adapted to a wide range of applications including p-i-n solar cells, thin film transistor, very thick intrinsic layer for X-ray and nuclear detectors, plasma etching and so on. Substrates with dimensions of 100mm x 100mm area are easily handled and upward deposition is utilised to minimise particulate incorporation in films. As mentioned earlier there are three deposition chambers and one loadlock chamber which is common to all the deposition chambers. For the present study all the films were deposited in the intrinsic chamber. To avoid any possibility of cross contamination between the doping and intrinsic chamber, the later one is provided with a separate set of pumps. All pumping lines are finally connected to a scrubber in which residual gases are neutralised by reacting with KOH solution.

According to Hamasaki et al.[7] plasma potential, V_p in a PECVD reactor is related to the area ratio A1/A2 of the powered and ground electrodes and to the developed selfbias V_s, by the following equation;

$$V_p[1-(A1/A2)^n] \approx (A1/A2)^n V_s \qquad (2.1)$$

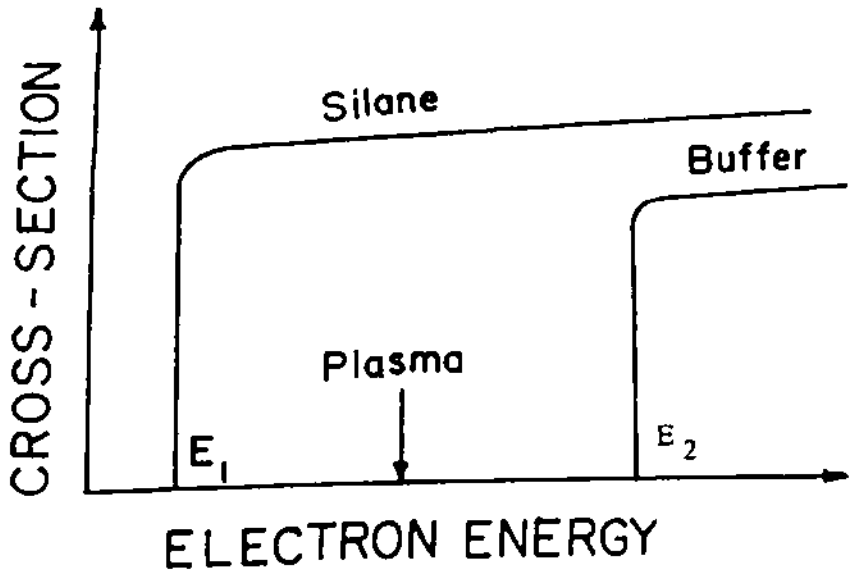

Fig. 2.1 Cross-section of decomposition of the gases in the plasma. For silane gas, all the electrons having an energy higher than the threshold E_1 participate to the deposition of a-Si:H. For other gases (H_2 or He) if almost all electrons have an energy smaller than the threshold E_2, then collision of the gas are elastic: It is a buffer gas with little effect on the deposition.

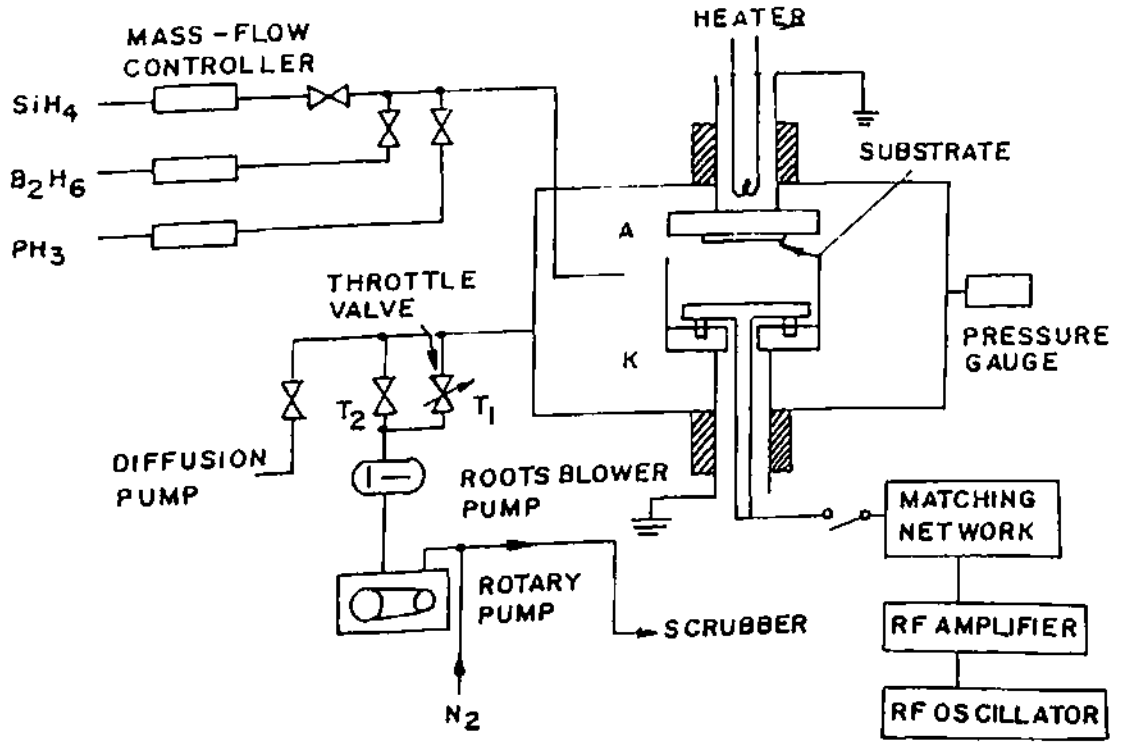

Fig. 2.2 Schematic diagram of the diode type plasma reactor used for deposition of a-Si:H.

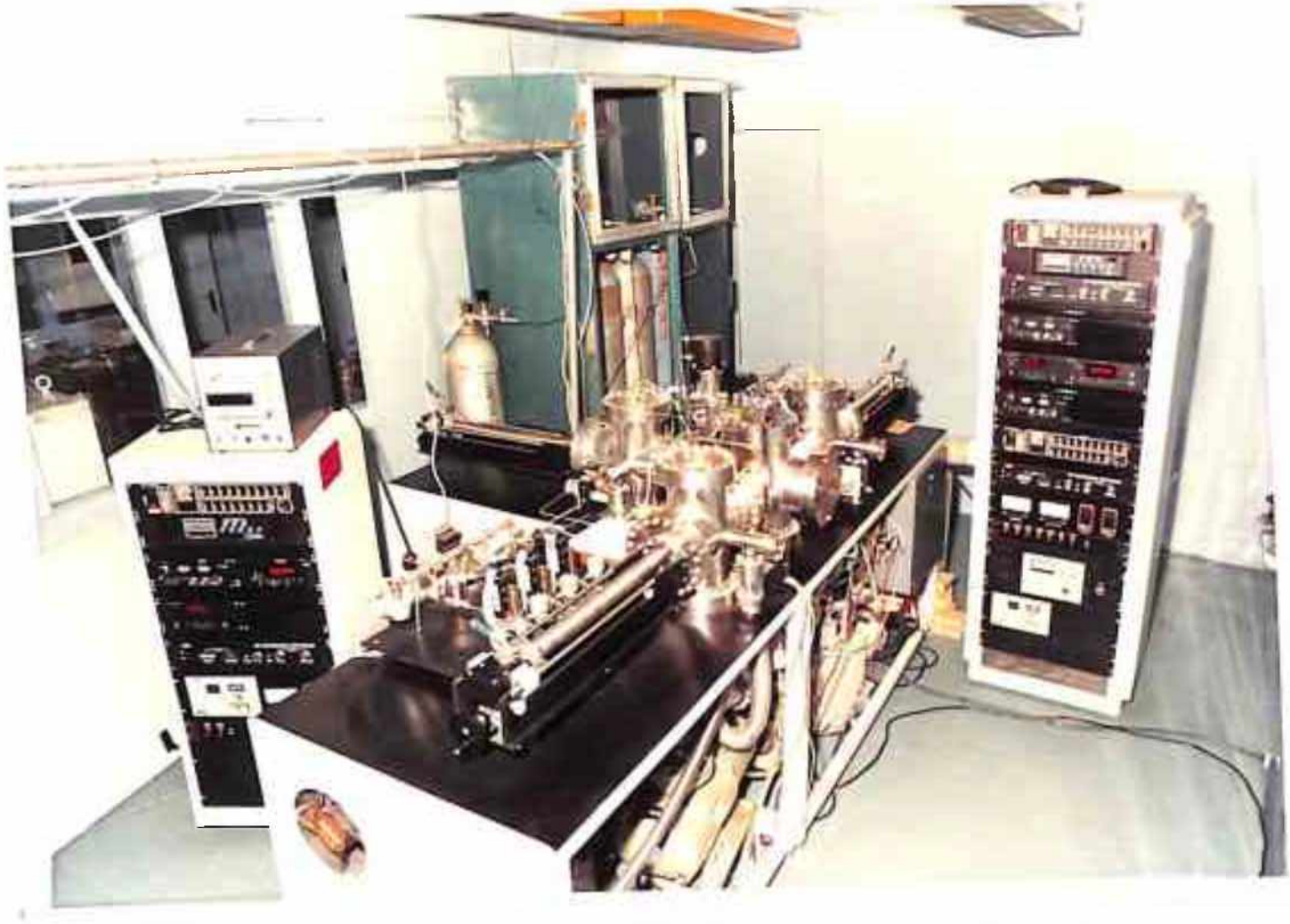

Plate 2.1 Photograph of multizone PECVD system used for the deposition of a-Si:H

Here, $n \approx 1$ is empirically satisfied[42,43]. Since the value of A1/A2 is significantly increased to near unity by the presence of the shield, an appreciable increase of V_p together with a decrease of V_s should occur in the shield system. Consequently, the potential drop on the grounded electrode becomes close to that on the powered electrode. This change in potential distribution results in spreading of the positive column towards the grounded electrode, which is otherwise localized near the powered electrode. This in turn, implies that the substrates placed on the grounded electrode suffer significant ion bombardment by the presence of mesh as in the case of films grown on the powered electrode although the energy of impinging ions in the mesh system is small compared to that obtained in a conventional system. As reported by Cabarrocas et al.[44], finite ion bombardment of growing a-Si:H films does, indeed, help in obtaining a compact film. Subtle changes in optoelectronic properties due to this ion bombardment effect are also expected.

2.3 Experimental procedure

The substrates used for deposition of a-Si:H films were Corning 7059 glass and single crystalline silicon wafers (5-10 Ωcm, optically polished, p-type). The procedure adopted for cleaning the glass substrates comprises of an initial wash with soap solution (Extran-01) and then rinsing in deionised water (5 MΩ) followed by hot air dry. After this ultrasonic cleaning for 5 minutes is done in deionised water. Finally, substrates are exposed to hot Iso-Propyle alcohol vapor and then dried in dry nitrogen. The c-Si wafers were however given an HF etch to remove the native oxide layer and then an ultrasonic cleaning in distilled water was carried out. The above cleaning methods were found to provide good adhesion of the films with the substrates.

The substrates cleaned in the above mentioned way, were fixed in the slots of the upper electrode. The chamber as well as the gas lines were evacuated to a vacuum of 10^{-7} Torr by using a turbo molecular - rotary pump stack and the substrates were heated to the desired temperature by suitably setting the temperature controller. The process gas (Semiconductor grade, Matheson Gas Products, USA) was introduced into the chamber and the flow rate and pressure were adjusted using the mass flow controller (Sierra Instruments Inc. USA), baratron (MKS) and throttle valve controller (MKS Type 252 C). The process gas

was pumped out by roots - rotary combination. The excitation sources used were RF5S (RF Plasma Products Inc. USA) for RF discharge and a locally made (Nuclear Science Centre, New Delhi) VHF source (details in section 4.2) for obtaining VHF discharge. For pulsed discharges RF/VHF power was amplitude modulated using low frequency modulation (2 - 10 Hz). In the modulation scheme employed in this study, RF/VHF power was never allowed to go to zero, in fact power was switched between a low and high power level. For the present study low power level was maintained at 10W. Details of pulse parameters used are given in chapter-III (**Table 3A.1**). Plasma was struck after the pressure and flow of the gas were stabilized. The matching network was tuned to have minimum reflected power. The deposition was carried out for the required amount of time to yield the desired film thickness. The films were taken out from the chamber after allowing it to cool for sufficient time and the thickness was measured by the Talystep (a stylus type apparatus manufactured by Rank, Taylor and Hobson, U.K.). For this, part of the film was required to be removed by pulling with an adhesive tape.

2.4 Optical gap of a-Si:H

The optical band gap of amorphous semiconductors can be found from the dependence of the absorption coefficient α on the photon energy $h\nu$. The forms of α as a function of $h\nu$ are determined by the energy dependence of the density of state, N(E) for the bands containing the initial and final states. For simple parabolic bands [$N(E) \propto E^{1/2}$] and for direct transitions (as becomes allowed in case of a-Si:H) the absorption coefficient data of amorphous semiconductors follow the relationship[45];

$$\alpha(h\nu)h\nu = B(h\nu - E_g)^{nc + nv + 1} \qquad (2.2)$$

provided matrix elements are independent of energy. E_g is optical band gapenergy defined by the separation of the two extrapolated band edges. For parabolic band edges $n_c = n_v = 1/2$. Thus Eq. (2.2) becomes,

$$\alpha h\nu = B(h\nu - E_g)^2 \qquad (2.3)$$

where B is a constant containing the average matrix element. Thus, a plot of $(\alpha h\nu)^{1/2}$ vs $h\nu$ shows a linear variation, which gives the value of E_g by extrapolation to zero. The square of the slope of this linear variation gives the value of B.

The optical measurements were carried out, both in transmission and reflection mode, on a Shimadzu 3101PC spectrophotometer in the wavelength range 500 to 800 nm.

α at all the different wavelengths are calculated from the relation,

$$\alpha = [1/t\{\ln(1 - R)\}]/T \qquad (2.4)$$

where R is reflectance, T is transmittance and t is thickness and then $(\alpha h\nu)^{1/2}$ is plotted against energy ($E = h\nu$). A straight line is fitted and extrapolated to intercept the E axis which gives the value of E_g. This is known as Tauc's plot. **Fig.2.3** shows the Tauc's plot for the estimation of optical band gap of a-Si:H films grown.

2.5 Electrical properties

According to the Davis-Mott[46,47] model the band structure of amorphous semiconductors consists of a narrow tails of localized states at the extremities of the valence and conduction bands and a band of localized levels near the middle of the gap. This leads to basically three different mechanisms for conduction.

2.5.1 Conduction in extended state

In the non-degenerate case and under the assumption of a constant density of states and constant mobility, the conductivity due to electrons excited beyond the mobility edge into the extended states is given by,

$$\sigma = \sigma_o \exp[-(E_C - E_F)/kT] \qquad (2.5)$$

where prefactor, σ_o is found to be between $10\text{-}10^3\ \Omega^{-1}cm^{-1}$ and k is the Boltzmann constant. This is an activated process whose activation energy $\Delta E_D = (E_C - E_F)$ gives the location of the Fermi level in the mobility gap.

2.5.2 Conduction in band tails

If the wave functions are localized, so that $\sigma_{(E)} = 0$, conduction can only occur by thermally activated hopping. Every time an electron moves from one localized state to another, it will exchange energy with a phonon. The conductivity will depend on the energy distribution of the density of localized states. Hopping conduction in the band tail is given by

$$\sigma_{tail} = \sigma_{ot} \exp[-(E_{CT} - E_F)/KT] \qquad (2.6)$$

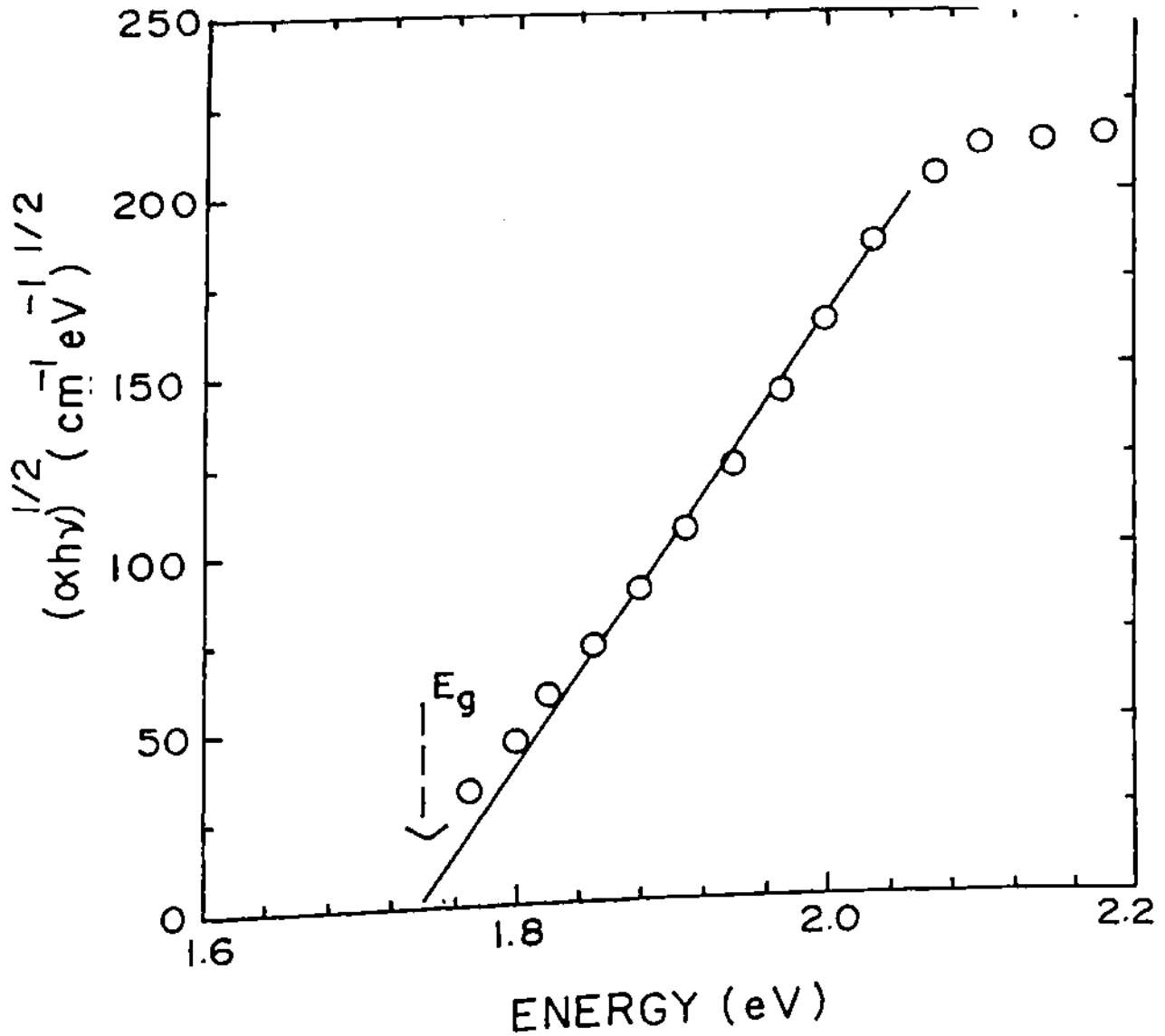

Fig. 2.3 Typical Tauc's plot for a-Si:H film. E_g indicates the optical bandgap.

where E_{CT} is the average energy of the band tail conduction path. The prefactor σ_{ot} depends on the overlap of the wavefunctions and is smaller than σ_o. On the other hand, E_{CT} is closer to E_F than is E_C, so that the exponential term offsets the smaller prefactor, particularly at low temperature.

2.5.3 Hopping conduction at the Fermi energy

Conduction at the Fermi energy occurs when the density of states is large enough for significant tunneling of electrons. The conductivity is small but weakly temperature dependent and consequently this mechanism tends to dominate at low temperatures. Mott's treatment of variable range hopping leads to a temperature dependence for the conductivity of the form

$$\sigma = \sigma_o(T) \exp[-(T_o/T)^{(1/4)}] \qquad (2.7)$$

where T_o is a temperature independent constant.

2.5.4 Measurement procedure

Conductivity measurements were carried out on samples deposited on 7059 corning glass substrates having aluminum contacts above the a-Si:H film in a coplanar configuration with a gap spacing of 0.08 cm. Annealing at 180°C for an hour at $1x10^{-4}$ Torr was done before undertaking conductivity measurements. A highly regulated (± 5 mV) DC voltage of 20 volts was applied to the electrodes and the current passing through the film was measured by an electrometer (Keithley, Model 610 C or 617).

After the measurement of dark current in different temperatures, the sample is allowed to cool down to room temperature at a slow rate and then the specimen was illuminated by a tungsten halogen lamp through a set of filters (Oriel corp., USA) to produce AM1.5 spectrum with an intensity of ≈ 100 $mWcm^{-2}$. Intensity was calibrated using a standard silicon photodiode (S-2281, Hamamatsu, Japan). The value of dark conductivity (σ_D) and photoconductivity (σ_{ph}) was calculated from the relation,

$$\sigma = \{I_{D/ph} \times l\}\{V \times t \times w\}\ \Omega^{-1}cm^{-1} \qquad (2.8)$$

where V is applied voltage in volts, $I_{D/ph}$ is measured current in amperes, t is thickness in cms., w is width in cms. and l is the distance between the electrodes in cms. A typical graph of σ_d vs 1000/T of some undoped a-Si:H films are shown in **Fig. 2.4**.

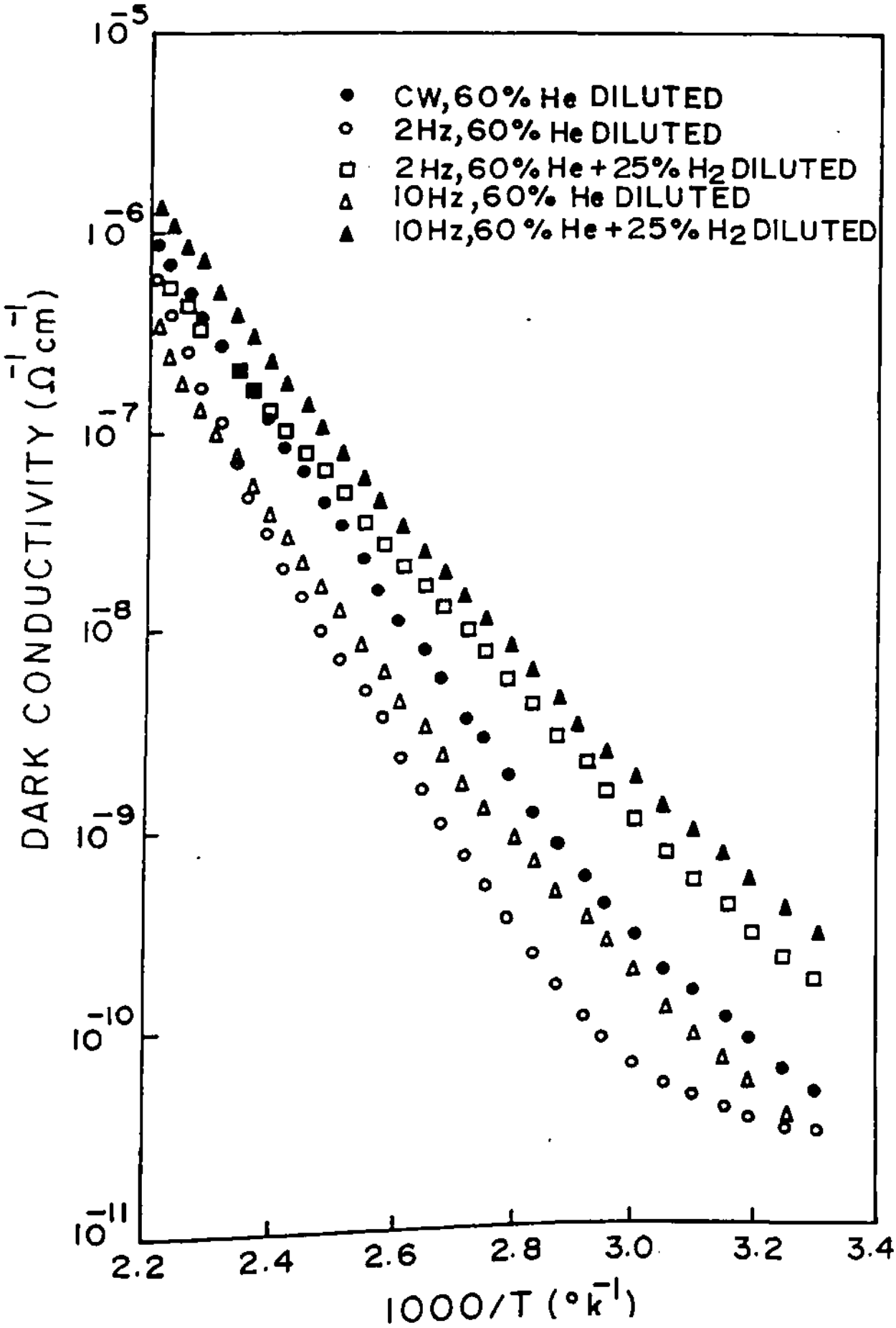

Fig. 2.4 Temperature dependence of DC conductivity of few a-Si:H films grown for the present study.

2.6 IR studies

IR spectroscopy technique has been used in the present investigation to determine the hydrogen content and the microstructure factor (to be defined in the following). The presence of hydrogen was first detected in a-Si:H, produced by the GD process using both hydrogen evolution[48] and IR absorption[49]. The atomic arrangements of bonded H-atoms in a-Si:H were first identified through the pioneering IR measurements of Broadsky et al.[50], and then given additional clarification through the experiments and modeling of Lucovsky and Co-workers[51-55]. Hydrogen is a light atom, so the vibration is almost entirely confined to the hydrogen atom and the analysis of the modes are relatively simple. A single hydrogen atom bonded as Si-H has three degrees of freedom. The first stretching mode has a frequency near 2000 cm^{-1} and the degenerate bending modes has a frequency at 630 cm^{-1}. The difference is because the bond stretching force is stronger than bond bending force. The modes originating from $=Si=H_2$ or $-Si\equiv H_3$ bonding configurations lie in the range 800 - 900 cm^{-1}. The extra degrees of freedom introduced by the additional hydrogen allow many more vibrational modes of both the bond stretching and bending types. **Fig. 2.5** gives the calculated frequencies of all the modes of the various Si-H configurations[54].

During present investigations, a-Si:H films were grown on optically polished c-Si wafers. IR spectra were recorded on a Nicolet 510P FTIR spectrophotometer, in the transmission mode. After subtraction of the reference spectra, the integrated intensity under the stretching mode[53] in the range 1900 - 2200 cm^{-1} was used for the estimation of the bonded hydrogen content. For this estimation, the method given by Freeman and Paul[56] has been followed.

$$C_H = n_H \int [\alpha(\omega)/\omega]d\omega \qquad (2.9)$$

n_H is a constant multiplied by square of local field factor ($n_H = Af^2$). The microstructure parameter (R) of the films was also determined from the ratio of the integrated band intensity of the IR mode centered at 2080 cm^{-1} to the sum of the integrated band intensities of modes centered at 2080 cm^{-1} and 2000 cm^{-1} [57-58]. Thus microstructure fraction R, ($0 < R < 1$) is expressed as,

$$R = [2080]/\{[2000] + [2080]\} \qquad (2.10)$$

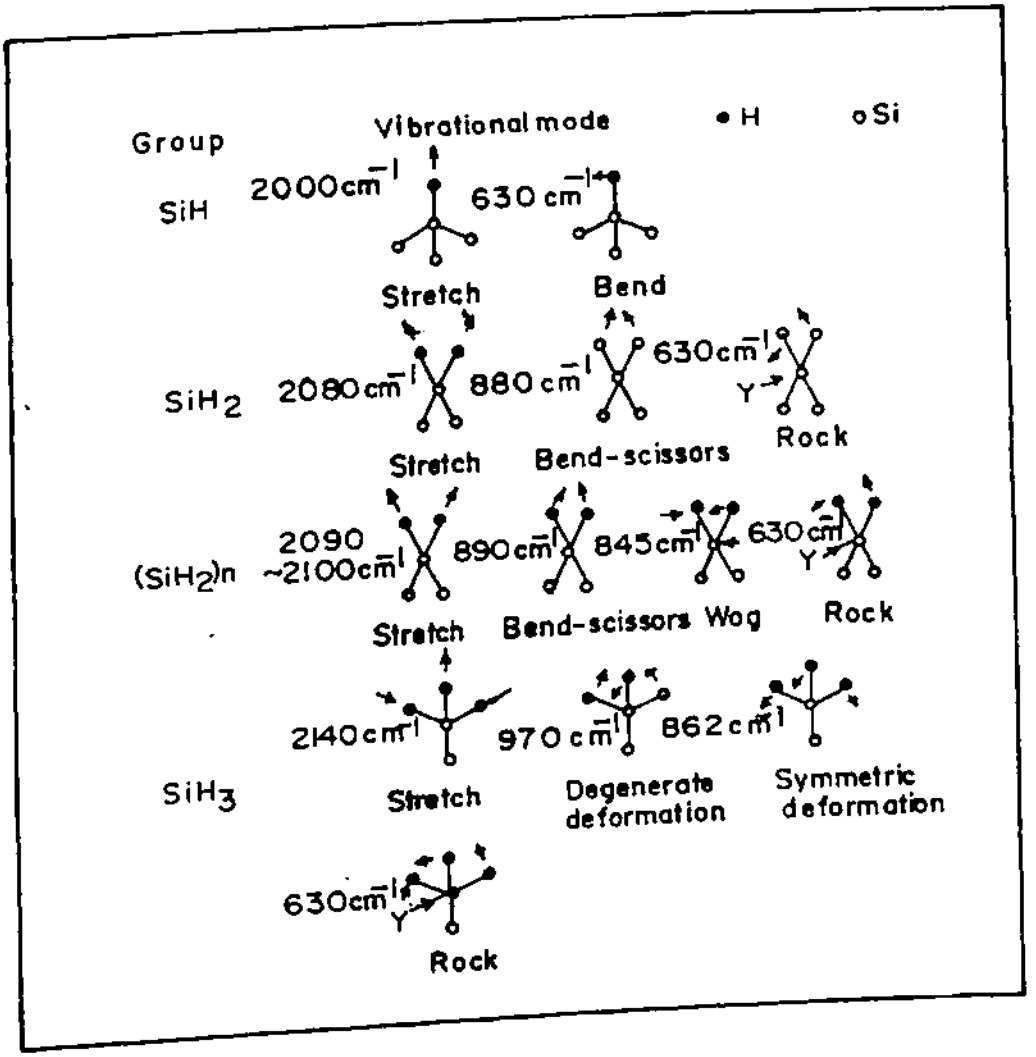

Fig. 2.5 The set of Si-H vibrational modes for SiH, SiH_2, $(SiH_2)_n$ and SiH_3 groups with calculated frequencies as indicated.

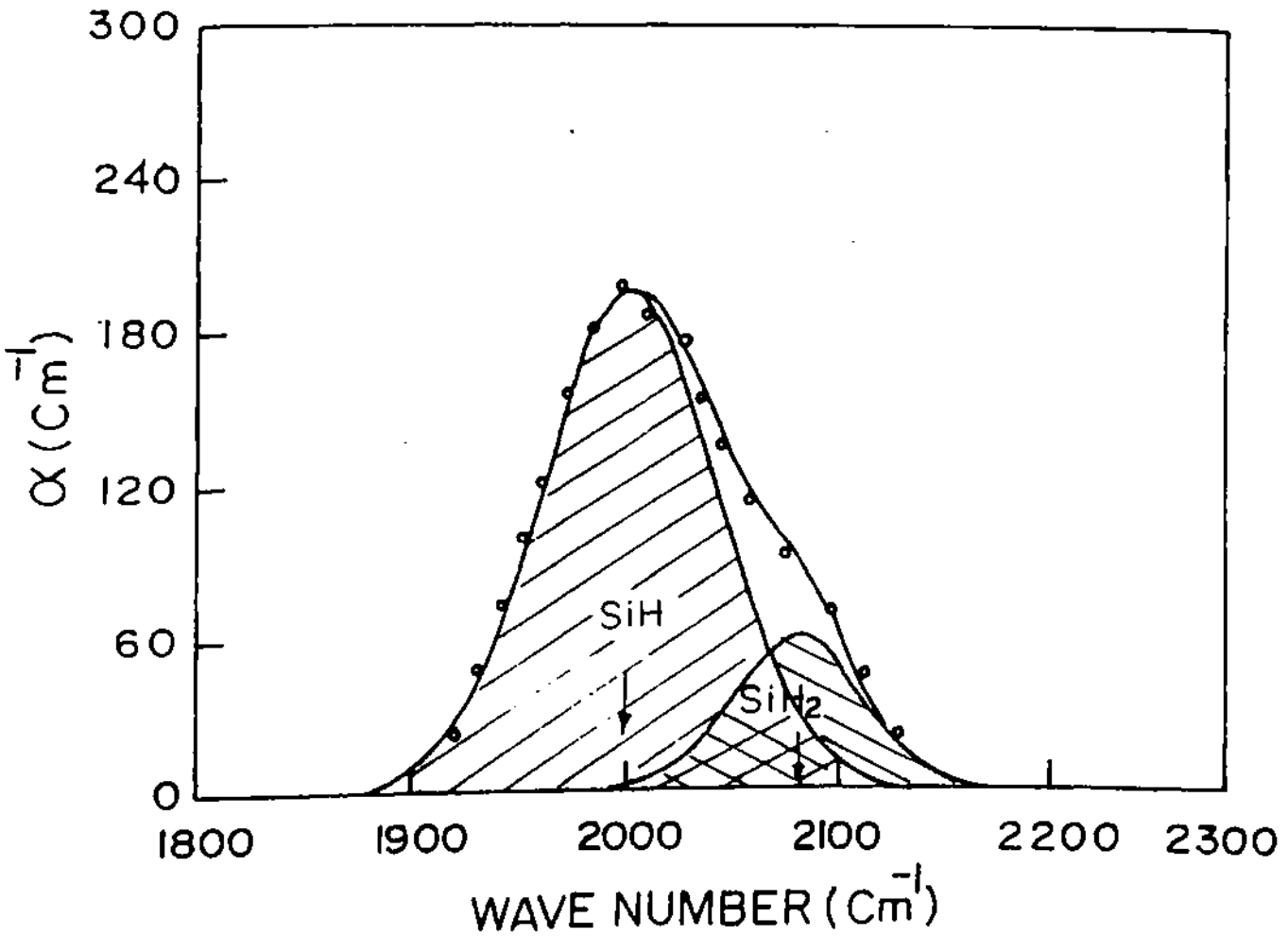

Fig. 2.6 Deconvolution of a typical IR absorption peak around 2000 cm^{-1} into SiH stretching (2000 cm^{-1}) and SiH_2 symmetric stretching (2080 cm^{-1}) modes.

where the square brackets denote the integrated band intensities of the respective modes.

Determination of R requires the deconvolution of the IR spectra in the 1900-2200 cm^{-1} region using Gaussian line shapes fitted to the absorption peaks at 2000 cm^{-1} and 2080 cm^{-1}. A typical deconvolution of the IR spectra is shown in **Fig.2.6**.

2.7 Subgap absorption in a-Si:H

A technique, using which one can measure low absorption can be used as a technique to characterise impurities, defects, etc. For example, in hydrogenated amorphous silicon (a-Si:H) the band edges are not as sharp as in crystalline silicon and there are electronic states distributed continuously within this gap (mobility gap) (**Fig.2.7**) as a result of the lack of long range order in the material. For photon energies less than the band gapof silicon, as shown in **Fig.2.8**, the absorption due to these states is orders of magnitude lower. The distribution of states within this gap is believed to be exponential and is characterised by a slope E_o, an important parameter in deciding the quality of the material. The parameter E_o determines the broadness of the states distribution; higher the value of E_o, more will be the disorder in the amorphous network. The defect states N_D, near the middle of the gap, due to dangling bonds etc. is another important quantity that determines the electronic (device) grade of the material. Higher the density of these states, higher will be the recombination loss.

As shown in **Fig.2.8**, the absorption edge spectrum of a typical amorphous semiconductor can be roughly divided into three regions:

- high absorption region A ($\alpha > 10^3$ cm^{-1}),
- exponential edge B ($10^1 < \alpha < 10^3$ cm^{-1}) and
- weak absorption tail C ($\alpha < 10^1 cm^{-1}$).

The optical transitions responsible for each region are shown in the simplified gapstate profile of **Fig.2.7**.

The optical transition of region A is usually described by the Tauc's expression (Eqn. 2.3). In region B (10^1 $cm^{-1} < \alpha < 10^3$ cm^{-1}), variation of α with hv follows the following eqn.,

$$\alpha = \alpha_o \exp(-h\nu/E_o) \qquad (2.11)$$

where α_o is a constant and E_o the characteristics energy representing the slope of the exponential tail state distribution and reflects the randomness of an amorphous network. The

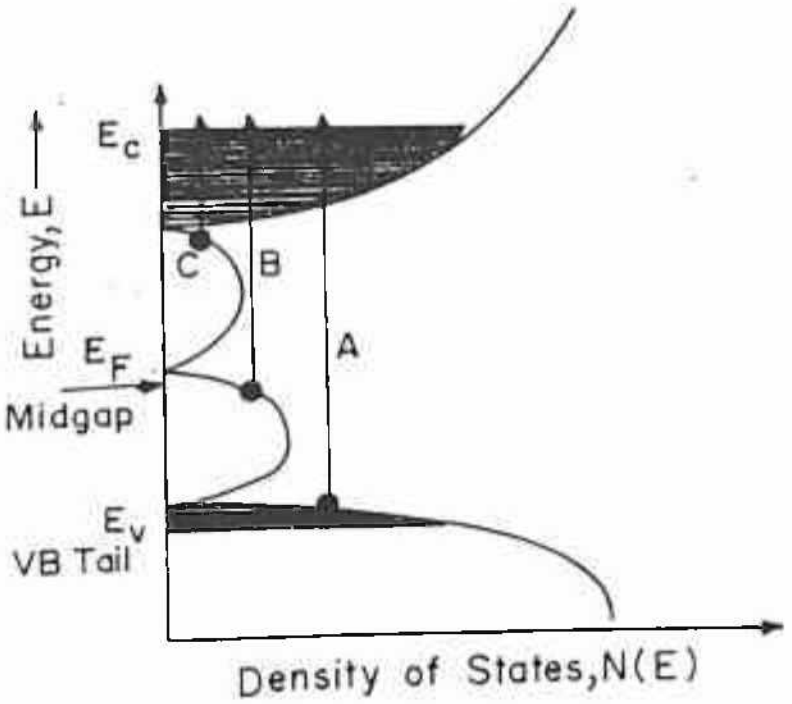

Fig. 2.7 Density of states distribution in a-Si:H.

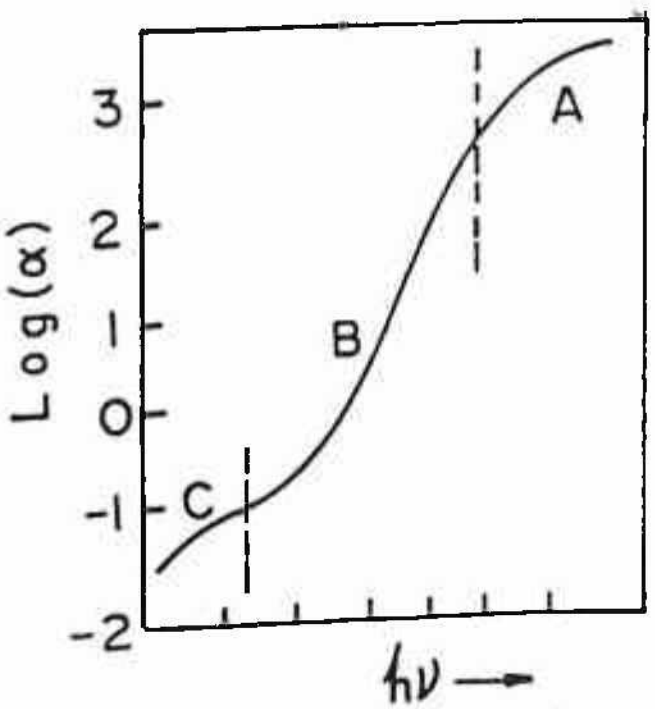

Fig. 2.8 Typical absorption spectrum of a-Si:H film.

weak absorption tail of region C is attributed to the deep defect states in the midgap, mostly originating from dangling bonds and impurities. Therefore, measurement of α in the appropriate wavelength regions provides useful information about the electronic states within the band gapof the material.

Optical absorption spectra of a-Si:H have been obtained by a variety of techniques, such as the spectrophotometer based transmission method, constant photocurrent method[59], photothermal deflection spectroscopy[60] and photoacoustic spectroscopy[61]. Photothermal deflection spectroscopy (PDS) is one of the most sensitive methods in this respect. In the present investigation we have adopted the transverse PDS[64] technique.

2.7.1 Transverse photothermal deflection spectroscopy

Transverse photothermal spectroscopy is based on the commonly observed "mirage" effect during a hot day. The mirage effect takes place due to the refraction / deviation of the light beam when it travels through a medium (air) in which a gradient of refractive index exists in a perpendicular direction. The gradient is the result of heat dissipation by the hot surface (earth) in contact with the medium. This heat is produced by the absorption of the sun's radiation by the surface. This principle is used in PDS to measure the absorption coefficient of various materials as a function of wavelength. The magnitude of refraction/deviation φ of a beam of light, such as a laser beam, propagating close to the sample surface which is absorbing the incident monochromatic light flux (pump beam) under investigation is related to the optical absorption coefficient of the material in the following manner:

$$\varphi = K(1-\exp(-\alpha t)) \qquad (2.12)$$

where t is the film thickness. The proportionality constant K depends on various system parameters such as the diameter of the probe beam in relation to the pump beam and its closeness to the sample surface, the thermophysical properties of the fluid medium in contact with the sample, the modulation frequency of the pump beam etc. In order to increase the sensitivity of the technique it is advantageous to have a medium with higher temperature coefficient of refractive index in contact with the sample. Carbon tetra chloride (CCl_4) for which $dn/dT=5\times10^{-4}$ $^{\circ}K^{-1}$ (for air $dn/dT=5\times10^{-6}$ $^{\circ}K^{-1}$) has been found to possess such a property. The deflection is measured using a position sensitive detector.

It is emphasised here that PDS technique is contactless and requires no special device structure. Second, it is all-seeing, in the sense that any level that can have an electron lifted into or out of it, whether it is at the surface or in the bulk, should be observable. Third, unlike electron spin resonance (ESR), it does not require the state to be paramagnetic to be observable. Unfortunately these same properties can be disadvantageous as well. Studies of PDS spectra versus film thickness[62,63] indicate a density of defects at or near the surface (exposed surface or film/substrate interface) of $N_{ss} \approx 10^{12}$ cm^{-2}. Recently, Frye et al.[64] published their data showing N_{ss} to depend critically on the post deposition procedures. For the commonly encountered film thicknesses ($\approx$ 1 μm), $N_{ss} \approx 10^{12}$ cm^{-2} means that in high quality films (with bulk deep defect density $N_{def} < 10^{16}$ cm^{-3}), there is more optical absorption due to the surface states than due to the bulk.

2.7.1.1 Experimental set up

The schematic diagram of the PDS set up developed for the present investigations is shown in **Fig.2.9**. The whole arrangement was made on a vibration damping optical table (M/s Holooptics Ltd., New Delhi). The table consists of aluminium honeycomb structure in between thick stainless steel plates and is supported on three air filled cylinders to damp out low frequency vibrations.

The broad band light source used in our experiment is an air cooled 350 watt tungsten-halogen lamp. The beam is focused on the entrance slit of a 0.25 metre monochromator (Thermo Jarrell Ash Corporation, model 82-410). The monochromatic beam coming out of the exit slit of the monochromator is chopped at a low frequency typically 12 Hz by a mechanical chopper (Stanford Research Systems model 540) and is focussed on the sample surface by means of a combination of lenses. The a-Si:H sample is immersed in doubly distilled CCl_4 in a cuvette of 10x10x70 mm size. The top of the cuvette is tightly closed to prevent the escape of CCl_4 vapor into the atmosphere. The cuvette is mounted on a tilting stage attached to a manipulator capable of three axes i.e X, Y & Z translation. The sample's position was manipulated so that the 5 mW He-Ne laser probe beam travels close and parallel to the surface of the sample. The position of the quadrant detector mounted on an X, Y & Z translation stage was adjusted so that the laser beam falls perpendicularly on the active area of the quadrant position detector (Silicon Detector Corporation Ltd. USA).

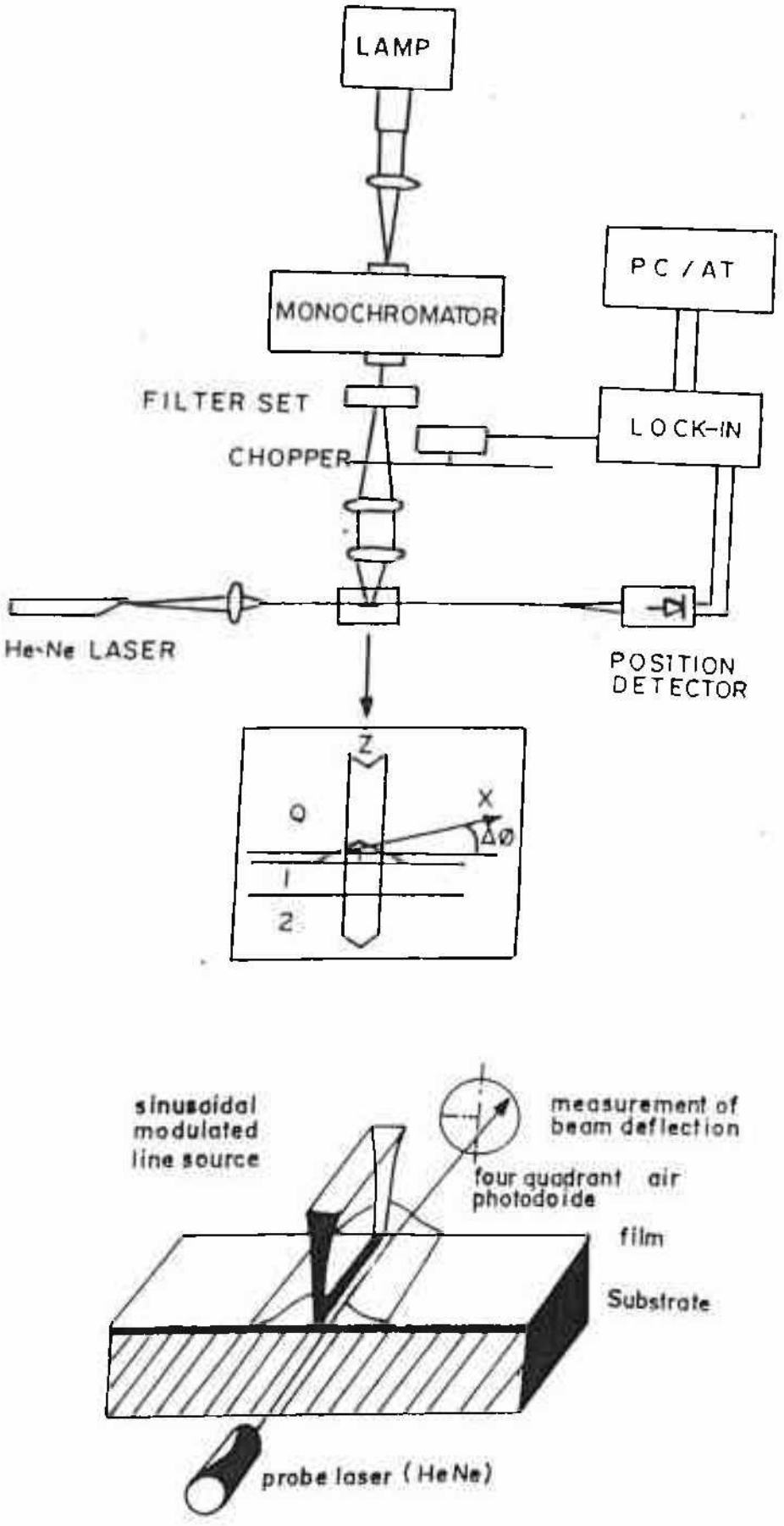

Fig. 2.9 Schematic diagram of the transverse photothermal deflection spectroscopy (PDS) setup.

2.7.1.2 Signal detection

The position sensitive detector employed here is basically a photodiode whose output depends on the position of the light spot on the surface of the photodiode for a given intensity of the light beam. The sum of output currents from the two top electrodes (say A & B) is proportional to the intensity of the incident beam whereas the position dependence of the signal is given by the difference in the two output currents. The output currents of the detector is converted into a voltage output by the current to voltage convertors and then fed to the inputs of the sum and difference amplifiers. After computing (A-B) and (A+B) electronically, the two values are fed to the inputs of the analog divider. The output of the divider gives the relative change of the position of the light spot on the position sensor. The relative position of the light beam on the photodiode is given by computing (A-B)/(A+B) in one direction.

According to the manufacturers specification this detector is linear if (A-B)/(A+B) is in the range -1.0 to +1.0 . In our experiment (A-B)/(A+B) never exceeds 0.5. The intensity of the probe beam was adjusted in order to keep (A+B) $\approx$ 10V, as required by the electronics.

The analog signal (A-B)/(A+B) is fed to a lock-in-amplifier (Stanford Research Systems, SR-530) after computing it electronically. The reference signal to the lock-in amplifier is provided by the mechanical chopper driver. By varying the wavelength of the incident (pump beam) radiation, the PDS signal and its phase with respect to the probe beam were recorded using the lock-in-amplifier at various wavelengths. The absolute absorption spectrum can be obtained by comparing the results in the high absorption region with that obtained by conventional spectrophotometric method and calculating a for the remaining part of the spectra.

The dominant factor that determines the precision in the measurement of E_0 in our system is the bandwidth of the monochromator. In order to get adequate signal strength especially in the longer wavelength region the band width has been kept at 25nm. In order to ascertain the repeatability of the measurement system, the same sample was studied a number of times. It was found that the measured values are scattered with a standard deviation of 1.4 meV.

2.7.1.3 Noise

The ultimate sensitivity of any method depends on the total noise level in the experimental set up. There are three sources of noise in the present PDS set up: (l) noise due to the mechanical stability of the overall system, (2) noise in the signal detection/processing electronic system and (3) noise due to the instability of the probe beam.

The pump beam is modulated at low frequencies, typically at 12Hz. Therefore, the low frequency vibrations of the entire system consisting of the probe beam, sample holder and detector has to be shielded against the low frequency mechanical interferences. This is achieved in the present system by mounting them on a vibration damping optical table supported by three air filled cylinders.

The electrical noise originates from the detector, signal conditioning circuits and the lock-in amplifier. By shielding the detector in a metal box and preventing stray light falling on the detector by means of a narrow band filter at 632 nm (laser wavelength) the detector noise is reduced. Further noise reduction is achieved by using coaxial cables for connecting the detector to the electronic systems and high tolerance resistors and low noise operational amplifiers. Operational amplifier AD549 has been chosen for the current to voltage converter stage due to its very low noise characteristics and OP07 for the sum and difference amplifiers. The feed back resistors are of 1% tolerance. The divider used is AD742 and does not contribute significantly to the noise.

In order to minimise the effects of background illumination the pump beam was modulated using a mechanical chopper and the signal detected using the lock-in technique.

The whole experimental set up mounted on the optical table is kept in a darkened enclosure to prevent probe beam deflection due to convective air currents and also stray light absorption by the sample and the detector.

Absorption spectra of few a-Si:H films as obtained by the present PDS set up is shown in **Fig. 2.10.**

2.8 Optical Emission Spectroscopy

At present, the intricacies of the plasma chemistry that lead to the growth of a-Si:H film is still not fully understood because of the great complexity of the chemical processes that proceed in

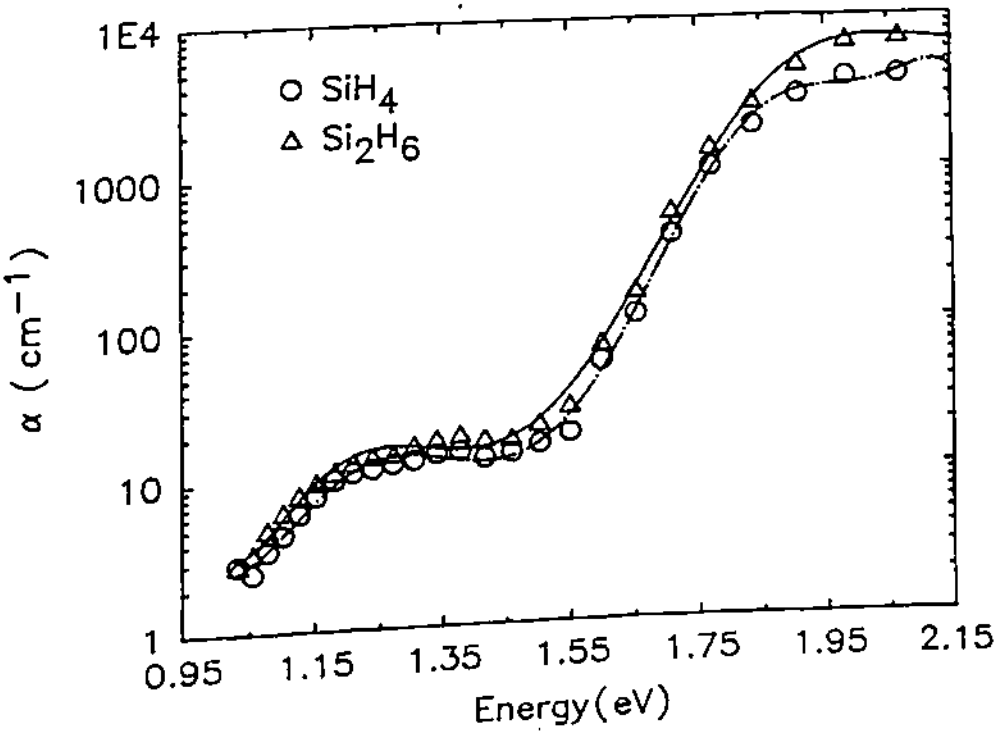

Fig.2.10 Absorption spectra of few a-Si:H films determined by PDS setup.

the silane plasma and hence the material properties are empirically controlled by finding a good combination of the deposition parameters. In situ observation of some of the reactive species created in the glow discharge is necessary for obtaining satisfactory reproducibility of the film properties and for more general understanding of the plasma chemistry. Details of the emission species studied in the present investigation is listed in **Table 2.1.** The reactive species identified by the emission spectrum is rather limited and there is no emission from SiH_2 and SiH_3, which are generally regarded as the potentially important species in a-Si:H deposition. However it is worthwhile to note that the number of SiH bonds incorporated in the a-Si:H matrix and the deposition rate are proportional to the optical emission intensity of SiH[65]. The advantage of optical monitoring is that the silane plasma is not perturbed.

Table 2.1 Optical emission details of the species studied

Species	Emission wavelength	Transition	Energy of emitting state above ground
H	656.28 nm	$H_\alpha 4d^2D - 2p^2P^o$	12.09 eV
SiH	414.23 nm	$A^2\Delta - X^2\Pi$	3.02 eV
Si	288.16 nm	$3p^{21}D - 4s^1P^o$	5.08 eV

The diagnostics of the modulated plasma requires the utilisation of a time resolved techniques. Among these, time resolved optical emission spectroscopy (TROES) is particularly suitable. This way some additional information becomes available on the formation and decay of active species, and a better understanding of the various plasma processes involved is expected[66,67,68]. The Optical emission spectroscopy set up used for this study is shown schematically in **Fig. 2.11**. One 1/8m monochromator (Oriel Corp., USA) was directly coupled to the viewing flange of the deposition chamber. Plasma emission was allowed to fall on the monochromator entrance slit through a quartz window. The entrance and exit slit width were kept same (2 mm) and slit height used was 12 mm. The grating used was blazed at 500 nm having 1200 lines/mm. At the output slit of the monochromator a photodiode (S-2281, Hamamatsu, Japan) was placed. It is a large diameter (Φ = 11 mm) C-Si detector having a UV enhanced spectral range (190 to 1100 nm). The detector photocurrent was converted to a voltage signal by using a photosensor amplifier having ultra low noise

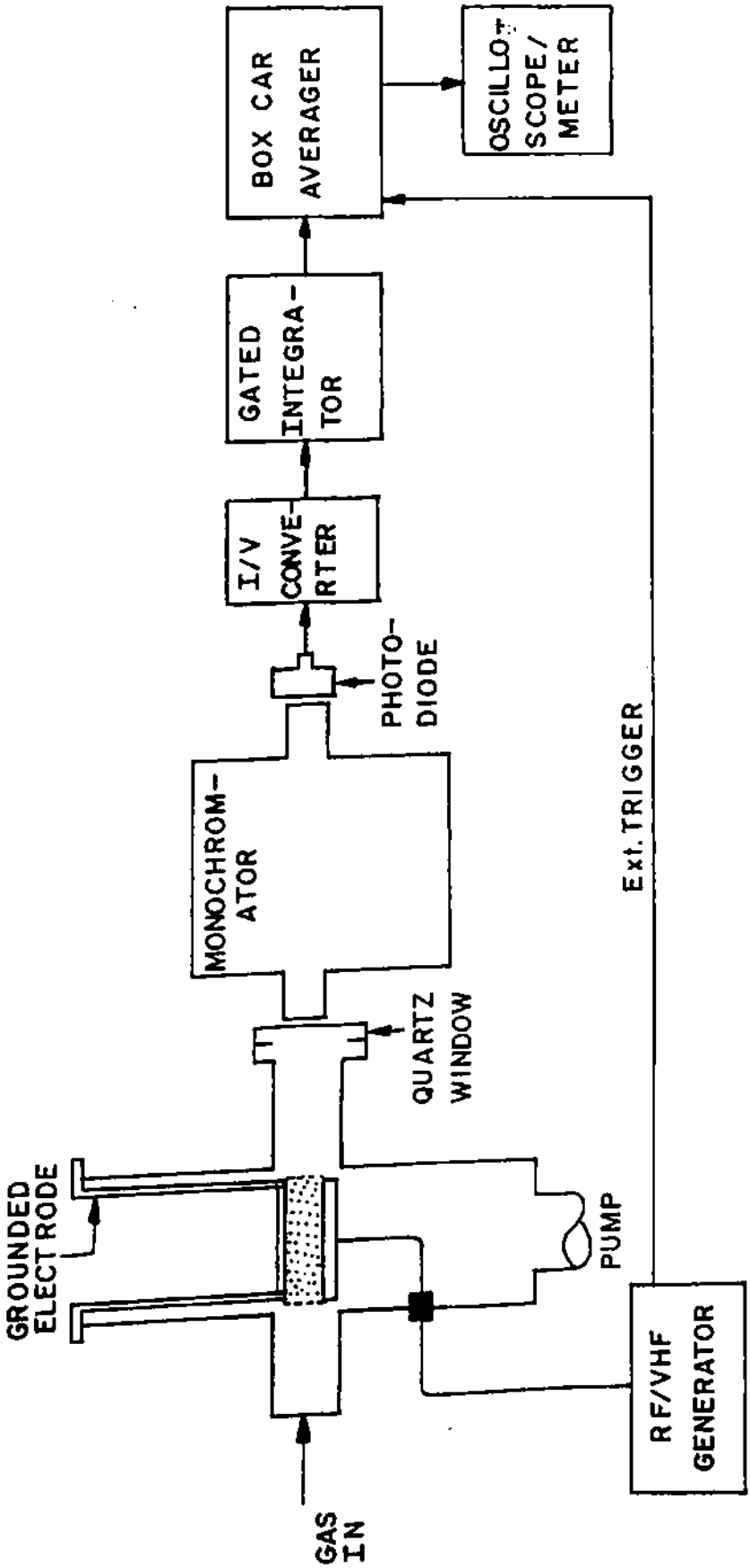

Fig. 2.11 Schematic diagram of the optical emission spectroscopy (OES) setup.

characteristics (C-2719, Hamamatsu). This amplifier has transimpedances varying from 10^9 to 10^5 Ω. This output is fed to the input of the gated integrator (EG & G Model 164) of a boxcar averager. The time constant used for the gated integrator was 10 msec. Exponential averaging is used in the gated integrator. The external triggering pulse for the boxcar (EG & G Model 162) was made available from the RF/VHF generator. Aperture duration and aperture delay range settings in the averager were kept at 50 nsec and 50 msec respectively. The signal to noise improvement ratio achieved with the current settings is given by SNIR = $(2TC/AD)^{1/2} = 20$, where TC is the time constant used in the gated integrator and AD is the aperture duration in the averager. Single point analysis mode was used to study the pulsed emission intensities.

2.9 References

1. I. Solomon, *Appl. Solar Energy* **28**, 1 (1992).
2. A Matsuda and N. Hata, in *Glow-Discharge Hydrogenated Amorphous Silicon*, ed. K.Tanaka (KTK Scientific Publishers, Tokyo, 1989), p. 28.
3. M. Hirose, *in Semiconductor and Semimetals* 21 A, ed. J.I. Pankove (Academic Press, New York, 1984), p. 9.
4. R.C. Ross and J. Jaklik Jr., *J. Appl. Phys.* **55**, 3785 (1984).
5. S. Kato and T. Aoki, *J. Non-Cryst. Solids* **77 & 78**, 813 (1985).
6. J.P. Conde, K.K. Chan, J.M. Blum, M. Arienzo and J.J. Cuomo, *J. Appl. Phys.* **71**, 3981 (1992).
7. T. Hamasaki, M. Ueda, A. Chayahara, M. Hirose and Y. Osaka, *Appl. Phys. Lett.* **44**, 600 (1984).
8. T. Hamasaki, M. Ueda, A. Chayahara, M. Hirose and Y. Osaka, *Appl. Phys. Lett.* **44**, 1049 (1984).
9. M. Nishikuni, K. Ninomiya, M. Tanaka, T. Matsuoka, S. Nakano, Okuda, H. Shibuya, M. Ohnishi, Y. Kishi, Y. Kuwano and S. Ohara in *Proc. of 4th PVSEC*, Sydney, Australia (1989) p.14.
10. H. Curtins, N. Wyrsch and A.V. Shah, *Electron. Lett.* **23**, 228 (1987).
11. H. Chatham, P.Bhat, A. Benson and C. Matovich, *J. Non-Cryst. Solids* **115**, 201 (1989).
12. G. Scarsbrook, I.P. Liewellyn, S.M. Ojha and R.A. Heinecke, *Vacuum* **38**, 627 (1988).
13. B.A. Scott, M. Brodsky, D.C. Green, P.B. Kirgy, R.M. Phecenik and E.E. Simonyi, *Appl. Phys. Lett.* **37**, 725 (1980).
14. O. Kuboi, M. Hastimoto and Y. Yatsurugi, *Appl. Phys. Lett.* **45**, 543 (1984).
15. J. Perrin, P. Roca i Cabarrocas, B. Allain and J. Freidt, *Jpn. J. Appl. Phys.* **27**, 2041 (1988).
16. A. Gallagher, *J. Appl. Phys.* **63**, 2406 (1988).
17. S. Ischihara, M. Kitagawa, T. Hirao, K. Wasa, T. Arita and K. Mori, *J. Appl. Phys.* **62**, 485 (1987).
18. A.Matsuda, T. Kaga, T. Tanaka and K. Tanaka, *J. Non-Cryst. Solids* **59 & 60**, 687 (1983).
19. D. Das, S. Chattopadhyay, A.K. Barua and R. Banerjee, *J. Appl. Phys.* **78**, 3193 (1995).

20 J Kanne, M. Knagai, K. Takahashi, *Appl. Phys. Lett.* **44**, 695 (1984).

21 H Watanabe, H. Warashino and T. Nagashima, *Thin Solid Films* **129**, L 65 (1985).

22. R. Manory, E. Grossman, R. Avni and A. Grill, *Thin Solid Films* **121**, 135 (1984).

23 C C. Tsai and H. Fritzsche, *Sol. Energy Mater.* **1**, 29 (1979).

24 S Nishikawa, H. Kakinuma, T. Watanabe and K. Nihei, Jpn. *J. Appl. Phys.* **24**-1, 639 (1985).

25 J.C. Knight, R.A. Lujan, M.P. Rosenbulm, R.A. Street and D.K. Biegelsen, *Appl. Phys. Lett.* **38**, 331 (1981).

26 S Usui and M. Kikuchi, *J. Non-cryst. Solids* **36**, 1 (1979).

27 F.J. Kampas, *J. Appl. Phys.* **54**, 2276 (1983).

28 P E. Vanier, F.J Kampas, R.R. Corderman and G. Rajeswaran, *J. Appl. Phys.* **56**, 1812 (1984).

29 K M H. Maessen, M.J.M. Pruppers, F.H.P.M. Habraken, J. Bezeme r and W.F. van der Weg, *J. Non-Cryst. Solids* 77**& 78** , 785 (1985).

30. J C. Knights and R.A. Lujan, *Appl. Phys. Lett.* **35**, 244 (1979).

31 W E. Spear and P G. LeComber in *The Physics of Hydrogenated Amorphous Silicon* - I, ed J.D Joannopoulos and G. Lucovsky (Springer Verlag, Berlin, 1984), p. 63.

32. T Hamasaki, M. Ueda, M. Hirose and Y. Osaka, *Proc. Int. Ion Energy Congress,* Keyoto, Japan Vol-3, P.1403 (1983).

33 S Kato and T. Aoki, *J. Non-Cryst. Solids* **77&78**, 813 (1985)

34 G. Bruno, P Capezzuto and F. Cramarossa, *Thin Solid Films* **129**, 217 (1985).

35 Y. Nakayama, Y. Takuma, K. Akiyama, T. Otsuchi, T. Kawamura, *Jpn. J. Appl. Phys.* **23**, L 470 (1984).

36. L.J. Overzet and J.T. Verdeyen, *Appl. Phys. Lett.* 48, 695 (1986).

37. Y. Watanabe, M. Shiratani, Y. Kubo, I. Ogawa and S. Ogi, *Appl. Phys. Lett.* **53**, 1263 (1988).

38. T. Yoshida, Y. Ichikawa and H. Sakai *Proc 9th ECPVSEC* (freiburg) ed. W. Pabs et al. p. 1006 (1989).

39. G. Bruno, P. Capezzuto, G. Cicala and P. Manodoro *Mat. Res. Symp. Proc.* on Chemical Perspectives of Microelectronic Materials II, ed. H. Bubois et al. p. 289, (1991).

40 A.A. Howling, Ch. Hollenstein, J-L. Dorier, P. Paris and M. Fabre *Proc 10th EC-PVSEC* (lisbon) ed. A. Lugue et al. p. 169 (1991).

41 A. Bouchoule, A. Plain, L. Boufendi, PH.J. Bloudean and C. Laure, *J. Appl. Phys.* **70**, 1991 (1991).

42. C. M. Horwitz, *J. Vac. Sci. Technol.* **A1**, 60 (1983).

43. J.W. Coburn and E. Kay, *J. Appl. Phy.* **43**, 4965 (1972).

44 P. Roca i Cabarrocas, P. Morin, V. Chu, J.P. Conde, J.Z. Liu, H.R. Park and S. Wagner, *J. Appl. Phys.* **69**, 2942 (1991).

45 R.A. Street in *Hydrogenated Amorphous Silicon* (Cambridge Univ. Press, 1991), p. 87.

46. P. Nages, in *Amorphous Semiconductors*, ed. M.H. Brod sky (Springer, New York, 1979), p. 116.

47. E. A. Davis and N.F. Mott, *Phil. Mag.* **22**, 903 (1970).

48. A. Triska, D. Dennison and H. Fritzsche, *Bull. Am. Phys. Soc.* 20, 392 (1975).

49. J.C. Knights, in *AIP Conf. Proc.* **31**, 296 (1976).

50. M.H. Brodsky, M. Cardona and J. Cuomo, *Phys. Rev. B* **16**, 3556 (1977).

51. G. Lucovsky and W.B. Pollard, in *The Physics of Hydrogenated Amorphous Silicon* - II 56, eds. J.D. Jannopoulos and G. Lucovsky (Springer, Berlin, 1984), p. 301.

52. G. Lucovsky, *J. Non-Cryst. Solids* **141**, 241 (1992).

53. G.N. Parsons, D.V. Tsu and G. Lucovsky, *J. Vac. Sci. Technol.* **A6**, 1912 (1988).

54. J.C. Knight, G. Lucovsky and R.J. Nemanich, *Phil. Mag. B* **37**, 467 (1978).

55. G. Lucovsky, R.J. Nemanich and J.C. Knight, *Phys. Rev. B* **19**, 2064 (1979).

56. E.C. Freeman and W. Paul, *Phys. Rev. B* **18**, 4288 (1978).

57. A.H. Mahan, P. Raboisson, D.L. Williamson and R. Tsu, *Solar Cells* **21**, 117(1987).

58. A.H. Mahan, P. Raboisson, and R. Tsu, *Appl. Phys. Lett.* **50**, 335(1987).

59. J. Kocka, M. Vanecek and A. Triska, in *Advances in Disordered semiconductors*, Vol. 1, Amorphous Silicon and related materials, ed. H. Fritzsche (World Scientific, Singapore, 1989), p. 297.

60. H. Cartins and M. Favre, in *Advances in Disordered semiconductors*, Vol. 1, Amorphous Silicon and related materials, ed. H. Fritzsche (World Scientific, Singapore, 1989), p. 329.

61. G. Amato, G. Benedetto, L. Boarino, M. Maringelli and R. Spagnolo, *IEE Proc.* A **139**, 181 (1992).

62. W.B. Jackson, D.K. Biegelsen, R.J. Nemanich and J.C. Knights, *Appl. Phys. Lett.* **42**, 105 (1983).

63. F. Boulitrop, N. Proust, J. Magarino, E. Criton, J.F. Peray and M. Dupre, *J. Appl. Phys.* **58**, 3949 (1985).

64. R.C. Frye, J.J. Kumler and C.C. Wong, *Appl. Phys. Lett.* **50**, 101 (1987).

65. M. Hirose, *Jpn. J. Appl. Phys.* Suppl. **21-1**, 275 (1982).

66. A. Bouchoule and P.Ranson, *J. Vac. Sci. Tech.* **A9**, 317 (1991).

67. J.P. Booth and N. Sadeghi, *J. Appl. Phys.* **70**, 661 (1991).

68. G.H. Hansen, G. Luckman and S.D. Colson, *Appl. Phys. Lett.* **53**, 1588 (1988).

CHAPTER -III

Modified Pulsed Plasma Discharge at 13.56 MHz

3.1 Introduction

From the scientific point of view, even though the plasma enhanced chemical vapour deposition (PECVD) process for the deposition of device quality hydrogenated amorphous silicon films has been extensively investigated, many issues still remain to be resolved satisfactorily, for instance

i) the identity of growth precursors,

ii) the plasma-surface interactions, and

iii) the microscopic parameters affecting the film quality, are not very well understood.

From the technological point of view, the PECVD technique, although already widely practised in the industry for the preparation of a-Si:H and some other related materials, has not reached its complete development since some important goals remain to be realised. These are,

i) the increase of deposition rate, r_d from it's present value of 1 - 2 $A^{\circ}s^{-1}$ to more than 10 $A^{\circ}s^{-1}$ for low cost production of a-Si:H based devices,

ii) the obtainable material quality at high growth rates for their utilisation in the high efficiency devices, and

iii) the improvement of surface homogeneity for large area devices.

To give answers to the open questions and to achieve the stated technological goals, two different approaches have been adopted. First, the optimisation of the growth process and the material so produced have been carried out by acting on the external macroscopic plasma parameters. Second, investigations relating to the role played by the internal plasma microscopic parameters on the deposition process and the material quality have also been simultaneously carried out.

Hydrogenated amorphous silicon (a-Si:H) can be deposited by a variety of techniques; for the device quality material, however, it is the RF plasma enhanced CVD at 13.56 MHz

using silane that is widely used. Even this technique is at a disadvantage when high power densities are employed in an attempt to achieve higher growth rates, since such high power densities are found to lead to powder formation in the discharge which deteriorate the film properties[1]. The various ways powder formation sets in a plasma discharge and its deleterious effects have already been documented in Chapter-I and therefore these issues will not be mentioned again.

The deposition rate and the optoelectronic properties of a-Si:H deposited by PECVD at 13.56 MHz have been found to depend critically on the deposition conditions such as substrate temperature (T_s), flow rate of gases, gas composition, pressure and applied power for a given reactor geometry. The Sanyo group[2] has experimented with a large number of such PECVD reactors and has identified a parameter space for the deposition of a-Si:H material over which one is expected to get reasonably good quality films. These efforts have shown that for a set of given deposition conditions (using 100% silane), increasing RF power to enhance deposition rate, r_d leads to gas phase reactions (secondary plasma reactions[3] of the type $SiH_x + SiH_4 \rightarrow$ a-Si:H with Si_nH_m + powder), which do not contribute to the film growth and instead enhance powder formation in the reaction zone, thus, limiting the achievable deposition rates[1]. Further, films grown under these conditions are found to possess inferior optoelectronic properties[1]. Therefore, it became necessary to explore other techniques to overcome this handicap. Efforts involving use of very high frequency (VHF) power sources etc. have been tried with reasonable success[4].

Recently much interest has been devoted to the study of the effect of 'new' and 'unusual parameters', such as frequency of the RF field, plasma confinement and plasma modulation. Among these, insufficient information is presently available on the plasma modulation. An attempt has been made during the present investigation to identify its role on the deposition process and on the material properties.

A modulated plasma is characterised by a periodical switching of the plasma between a high and low power levels and so causes completely different conditions in comparison to the continuous wave (CW) discharges. In fact, Yoshida et al.[5] have reported that in the deposition of a-Si:H under pulsed discharge condition a strong variation of hydrogen content as well as of microstructure factor is observed; obviously, all the properties correlated are effected. Also, it has been observed, a reduction of the nucleation process which results in solid particulates in the plasma phase, that leads to an improvement of the material quality.

As compared to CW discharges, particular improvements in the deposition process[6-8], improvements in thickness and compositional uniformity[9] and the suppression of powder in the plasma phase[6,10,11] have been reported to occur in modulated plasmas. These have been ascribed to the fact that the typical time constant, about 1 min, for particle formation, is much longer than the normally used pulse periods. Hence the modulation prevents the growth in size of particles, so reducing the negative effects of their formation.

It may be noted other approaches which depend on CW discharges, even though circumvent this problem of high r_d vis-a-vis quality of material at hand, do not provide any additional process parameter which can be manipulated for further advantage. In contrast to CW discharges, pulsed plasma discharges offer some additional process parameters which can be used to tailor the material properties. In this method, for instance, the RF power can be either square wave modulated (SQWM) with variable dwell time (τ) and duty cycle or applied as bursts of high power periodically. Other attractive features of this technique that have been cited are

i) basic equipment and system configuration remains the same as conventional RF PECVD,

ii) lends itself to a variety of manipulations (digital processing for instance) and

iii) uniformity of deposition is generally improved in this technique.

To overcome the limitations of the continuous plasma processing like incomplete gas dissociation, gas depletion, powder formation and the requirement of substrate heating, Scarsbrook et al.[12] have proposed a novel pulsed plasma discharge wherein very high power is applied for a short duration (typically few hundred msec) and discharge remains off for the rest of the period. They even pulsed the gas flow in phase with the RF power pulsing. The dramatic consequences are many fold increase in the deposition rate, better thickness uniformity and substantial decrease in powder formation. They achieved deposition rate of $\approx$ 50 $A^{\circ}s^{-1}$ for the growth of a-Si:N:H using 50 KW power having pulse width of 250 msec. Interestingly their film properties were comparable to the films grown at few $A^{\circ}s^{-1}$ by the so called standard technique of growth. These initial results appear to be very encouraging though the equipment complexity increases many folds. This technique will not be discussed any further in the present thesis.

In the more common pulsed plasma growth experiments RF generators of moderate power are amplitude modulated by a square wave[13-15]. Previous reports on the square wave

modulation (SQWM)[12-14] technique employing 100% modulation of 6.0 - 13.56 MHz RF sources have shown r_d to depend on dwell time, τ, of the high power cycle. In these investigations, apart from using highly diluted silane (5% silane in He or H_2) the applied power was kept high for less than a few msec and for the remaining part of the pulse, plasma was completely extinguished. Since in such cases growth is periodically perturbed, the growth surface is also disturbed periodically. Watanabe et al.[14] attributed the higher growth rate, in such discharges, to the higher life time of SiH_3 film forming precursors which succeed in forming optimal network even after the applied RF pulse has decayed. Hamasaki et al.[15] used the pulsed discharge technique to study the growth kinetics of a-Si:H and did not find any perceptible gas phase nucleation in the discharge. It may be noted, in the above experiments source gases were heavily diluted (H_2 or He).

When a mixture of gases is used as feed stock in a PECVD reactor, the plasma parameters are governed by the gas component for which the ionisation rate is larger. Thus, it is very difficult to decompose a gas component having a high threshold energy for dissociation. Moreover, the potential difference between the plasma and the substrate, which accelerates ions and leads to the bombardment of the substrate, is not controllable. One can overcome the above difficulties by using pulsed plasma discharge. The main features of this technique are the following:

i) In the period the pulse voltage is applied one can transiently obtain a higher electron energy than the stationary discharge. This results in an advantage when a mixture of gases having different ionisation energies are used as feed gas.

ii) The electron temperature, T_e in the afterglow plasma decays rapidly. Thus the collision energy of ions on the substrate surface is reduced significantly since the acceleration voltage across the space charge region between the plasma and the substrate is of the same order as the electron temperature.

A more recent study from Simens group[16] shows that even for continuous RF discharges, at 13.56 MHz, the deleterious effect of powder formation becomes perceptible only during the time steady state plasma is disturbed and more importantly during p/i interface formation of a p-i-n solar cell.

Recently use of hydrogenated amorphous silicon, alloyed with other tetrahedral elements (C, Ge and Sn) has resulted in an increase of the solar cell efficiencies with the added advantage of the extension of the spectral sensitivity range offered by the tandem type solar

cells. One such candidate is a-Si:Ge:H. The use of fluorinated source gas (SiF_4, GeF_4) results in better quality a-Si:Ge:H,F material compared to that grown by SiH_4 and GeH_4 mixture. A recurrent problem in these fluorinated material is the presence of high inhomogeneity in thickness and composition. According to Bruno et al.[17] this is due to the large difference in reactivity of SiF_4 with respect to GeF_4 and GeH_4. Now the credit for the growth of a-Si:Ge:H,F with better homogeneity goes to plasma modulation as suggested by Yoshida et al.[5] and subsequently demonstrated by Bruno et al.[17].

Kawasaki et al.[18] have deposited amorphous superlattice structure consisting of a-Si:H well layer and a-Si:C:H barrier layer by utilising pulsed plasma discharge from a mixture of disilane and carbon tetra fluoride. They found pulsed plasma discharge as an alternative to the inefficient physically controlled method of making superlattices wherein mechanical alteration of source gases and evacuation of system for each layer deposition are required.

Park et al.[19] have proposed a mathematical model to calculate the deposition rate and surface uniformity in a pulsed plasma reactor (already discussed in Chapter-I). They show how a good selection of gas flow (residence time) and the modulation parameters (period and duty cycle) can maximise the film uniformity without sacrificing the deposition rate. The beneficial effects of modulation are observed when the pulse period is shorter than the species residence time in the reactor, in contrast, for pulse periods larger than the residence time, the system reaches a state similar to the CW conditions and the modulation becomes ineffective.

A detailed study by Overzet et al.[20] suggests that during the high power part of the pulse a large number of negative ions are formed. Some of these negatively charged ions may grow in size under suitable conditions and may reach the cathode sheath as negatively charged particles. These negatively charged particles land on the substrate due to fast decaying sheath electric field in the afterglow during the period when RF power vanishes (if not fully driven away by gas flow etc.). In view of this, MPPD can be thought of as a discharge where sheath electric field never vanishes, rather switches between a very high to a low value almost in a similar fashion as that of the power variation. In such environments negative ions and/or particles are rather forced to stay outside the growth zone i.e. in the vicinity of the substrate.

In the present study a novel pulsed plasma growth process is proposed, where deviating from earlier such experiments, a non zero low power condition is maintained instead of 100% modulation and henceforth this process is called "Modified Pulsed Plasma Discharge" (MPPD). By creating a large number of reactive species during the

high power condition and by sustaining the glow discharge by using a low power for the remaining part of the cycle it was anticipated that higher deposition rates for a-Si:H will be achieved.

Another reason for keeping a non zero low power condition is that it is widely known that extinguishing the plasma completely during the film growth is not conducive to the growth of good quality film. In fact it is an accepted practice to initiate the plasma before the substrates are introduced into the growth zone, and also initiating the growth using a low power plasma and then switching to high power growth to obtain better quality interfaces.

In the present experiments, the low power level is chosen as the one which was found to produce good quality films in a CW discharge, at a reasonable rate in the present deposition system. The different high power levels chosen are those that result in powder formation in a normal discharge. By varying the duration of the high power level it was expected to achieve higher growth rates without compromising the optoelectronic properties of the films so grown. However, as will be shown later, the results are surprising. Additional advantage of this technique is, apart from the various pulse parameters such as High power level (HPL), τ, duty cycle, one can use the low power level (LPL) as an additional variable in order to arrive at the desired results.

3A Undiluted MPPD

3A.1 Experimental Details

The a-Si:H films were deposited in a capacitively coupled RF glow discharge system (Multizone PECVD system, GSI. INC), (described in chapter-II), using a 13.56 MHz generator and 100% silane and disilane were used as feed gases The films were deposited at 0 5 Torr. In the case of deposition involving silane, the substrate temperature was 275°C and the flow rate was 40 sccm. For disilane discharges, a higher substrate temperature of 300°C and a lower flow rate of 3.5 sccm was used. The pulse parameters namely the pulse high power level and its dwell time were systematically varied while keeping the pulse low power level constant. Here, the duty cycle in percentage is defined by the following equation:

Duty cycle in percentage = [(pulse high power duration)/(Total pulse period)] x100.

The pulse low power in the case of silane discharge is 10W and for disilane discharge it is 15W. The following table gives the range of pulse parameters used in the present study.

Table-3.1 Range of pulse parameters used for the present study

Gas used	Low Power	High Power	Dwell Time (msec)	Duty Cycle
SiH_4	10W	50W	50ms	10%
			25 ms	5%
SiH_4	10W	75W	50ms	10%
			25ms	5%
			10ms	2%
SiH_4	10W	100W	50ms	10%
			25ms	5%
			10ms	2%
Si_2H_6	15W	75W	50ms	10%
			25ms	5%
			10ms	2%

For the dark conductivity (σ_D), the photoconductivity (σ_{ph}) and the optical band gap(E_g) measurements, samples were deposited on 7059 corning glass substrates. A coplanar geometry was used for σ_D and σ_{ph} measurements. σ_{ph} was evaluated using a light source giving 100 $mWcm^{-2}$ intensity and having AM 1.5 spectrum. Reflection and transmission measurements were carried out for E_g determination. Films deposited on polished c-Si wafers were used for FTIR measurement. Film thicknesses were determined by a step height measurement equipment (Talestep, Rank, Tailor & Hobson). Average thickness values were used for plotting the data points. Time resolved optical emission spectroscopy (TROES) studies were carried out using the set up discussed in section 2.8.

3A.2 Results

3A.2.1 Deposition rate

The dependence of the deposition rate (r_d) on the dwell time (τ) is shown in **Fig. 3A.1** for different high power conditions for silane and disilane discharges. The figure also displays the deposition rate for the CW discharge with the power applied equal to the low power level of the pulsed discharge. **Fig. 3A.2** shows the dependence of r_d on the high power level for a given dwell time.

It is evident from **Fig. 3A.1** that r_d depends on τ; in fact it seems to have a nearly linear relationship with τ for all the high power levels used here for both silane as well as disilane discharges. Similar dependence of r_d has been reported by Hamasaki et al.[15] for silane discharges. Another important observation, not to be missed from a study of **Fig. 3A.1**, is the lower r_d in the case of the pulsed discharges upto a certain τ as compared to CW discharges at the corresponding low power levels, despite the fact that for a part of the pulse period the applied power is substantially higher. This is observed for all the high power levels experimented. After a certain τ, which seems to depend on the HPL, the r_d under MPPD is found to be higher than the that the r_d obtained under CW discharge. As the cross over point is approached, that is, when r_d increases above the normal value, powder begins to appear along the periphery of the powered electrode. Watanabe et al.[13] have also observed limited powder formation in their pulsed discharge experiments.

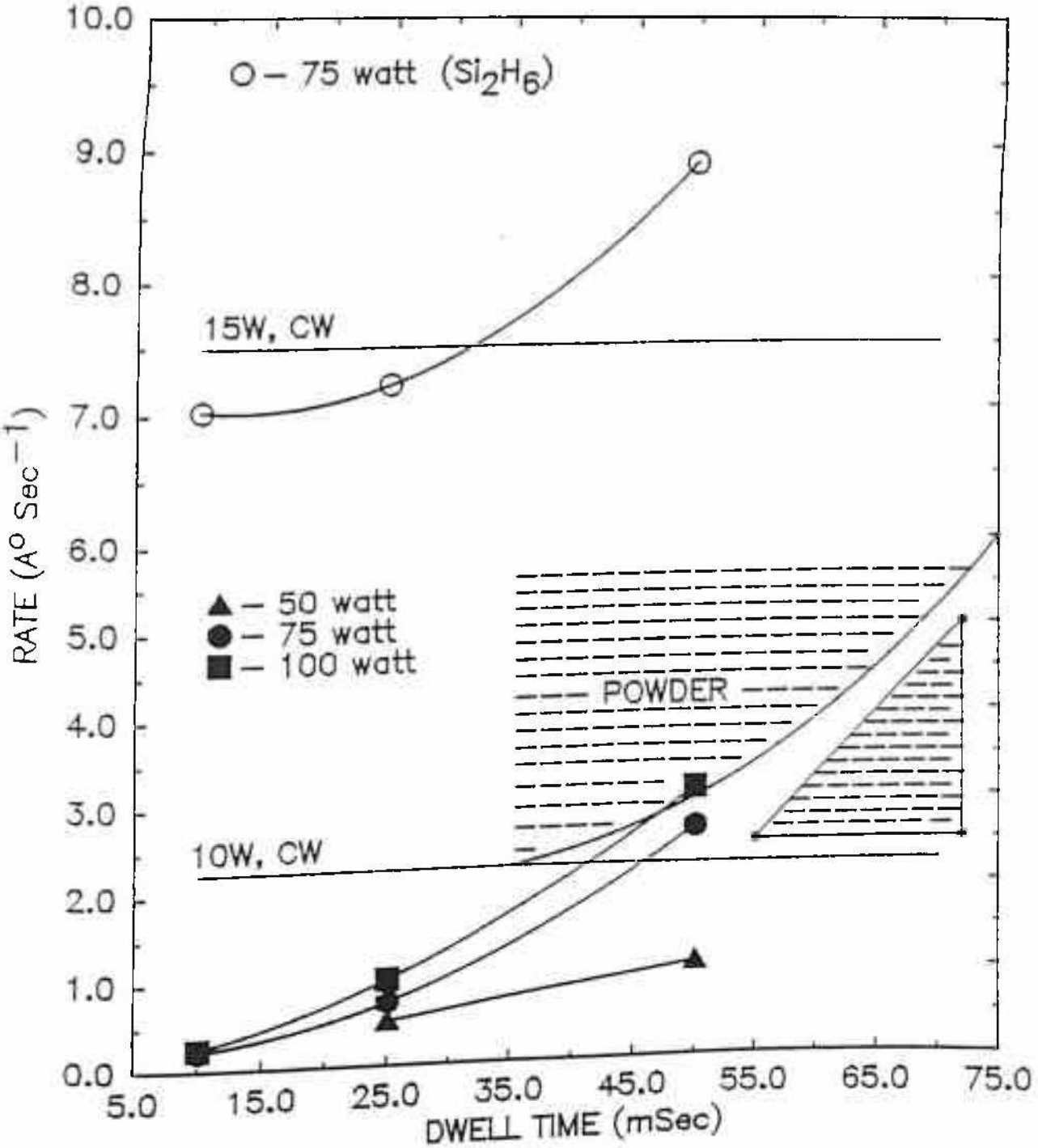

Fig.3A.1 Dependence of the deposition rate on the dwell time of the high power level. The rate for CW discharge is shown by horizontal lines.

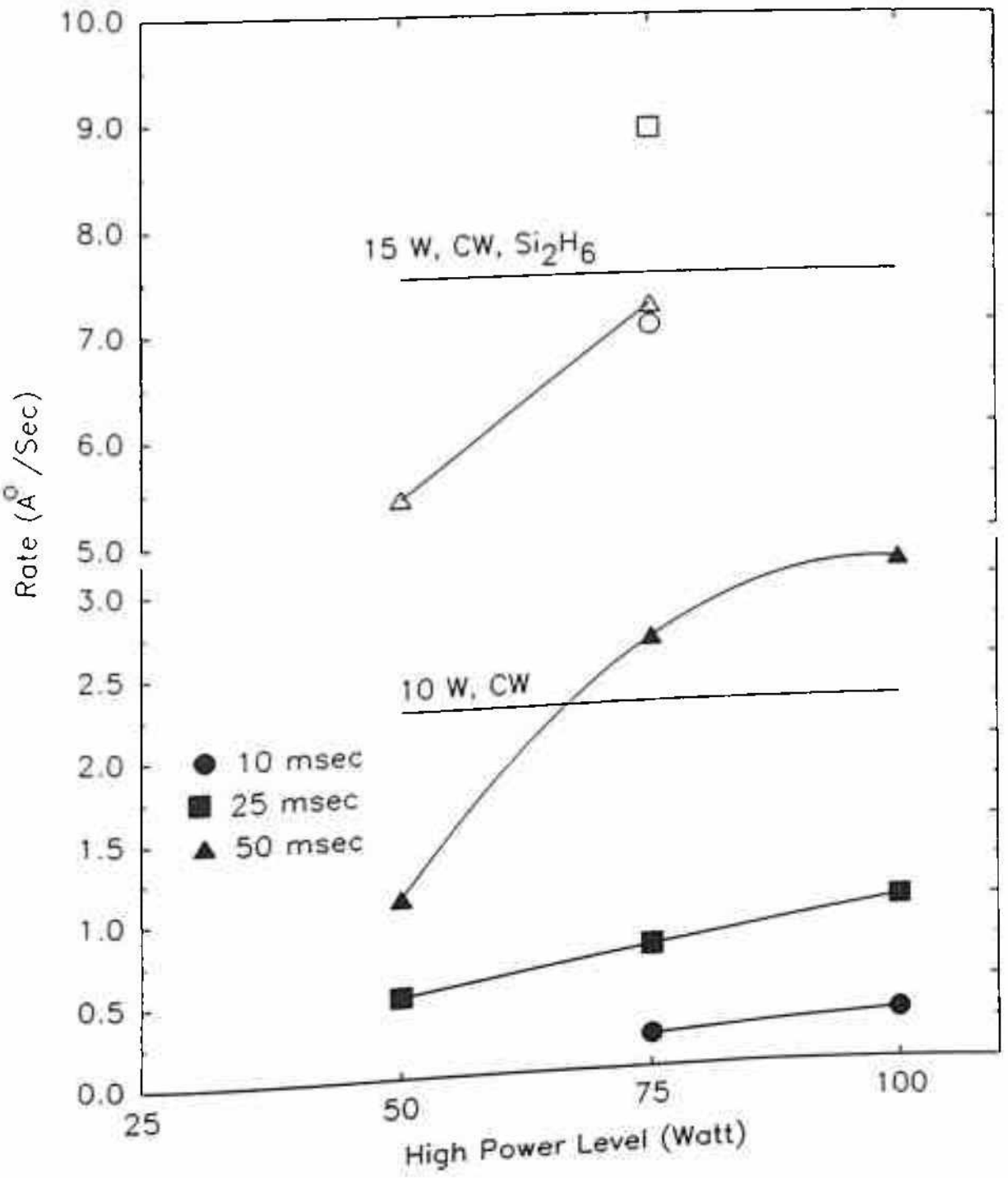

Fig.3A.2 Dependence of deposition rate on the applied high power level for a given dwell time. Open symbols are for disilane discharge.

It is clear that r_d increases monotonically with t for a particular HPL. As the HPL increases the slope of the above dependence increases. Similar dependence holds true for the Si_2H_6 discharges as well. For a given τ, it is observed that as HPL is increased, r_d is limited by powder formation[15] as happens in the case of CW discharges as well. It was observed that as r_d (MPPD) exceeds that of CW discharge r_d values, onset of powder formation takes place only around the periphery of the powered electrode. To illustrate this point in **Fig. 3A.1** the expected powder formation zone is shown as a shaded area.

Another significant observation that needs to be stressed is the uniformity of film thicknesses It was found that in all the cases (different HPL and τ) film uniformity was never less than that is obtainable for CW discharges. Uniformity was checked by measuring film thicknesses at various places of a 10 cm x 10 cm a-Si:H coated substrate. Regarding thickness uniformity it may be said that the switching of the discharge between LPL and HPL hardly disturbs the process that determine the growth of the film.

The other two inferences that can be drawn from a close study of **Fig. 3A.2**, are i) the deposition rate increases with HPL for a given τ and ii) as in the case of CW discharges, application of higher HPL results in powder formation for a given τ. This value of τ, however, depends on the HPL; higher the power level, shorter will be the τ at which powder formation sets in.

3A.2.2 Optical band gap

Fig. 3A.3(a) & (b) depict the variation of E_g with HPL and with τ, respectively. Study of **Fig. 3A.3(a)** indicates that for a given τ, E_g increases in all cases with the increase of HPL. It is interesting to see that E_g can be tailored over a fairly wide window of 0.35 eV, i.e. from 1.75 eV to 2.1 eV by just varying τ. On a closer look of **Fig. 3A.3(a)** one finds that the rate of increase of E_g with HPL varies inversely with τ. From Fig. 2(b), it seems that E_g vs τ has a maximum around τ = 25 msec and E_g drops on the either side of this τ value.

3A.3.3 Conductivity measurements

Fig. 3A.4(a) & (b) show respectively the variation of σ_D, σ_{ph} and σ_{ph}/σ_D with τ for various HPLs experimented upon. It is seen that σ_D increases with τ and at high τ value (50 msec), for all the three HPL values experimented, it attains a value close to $10^{-11}\Omega^{-1}cm^{-1}$. For HPL

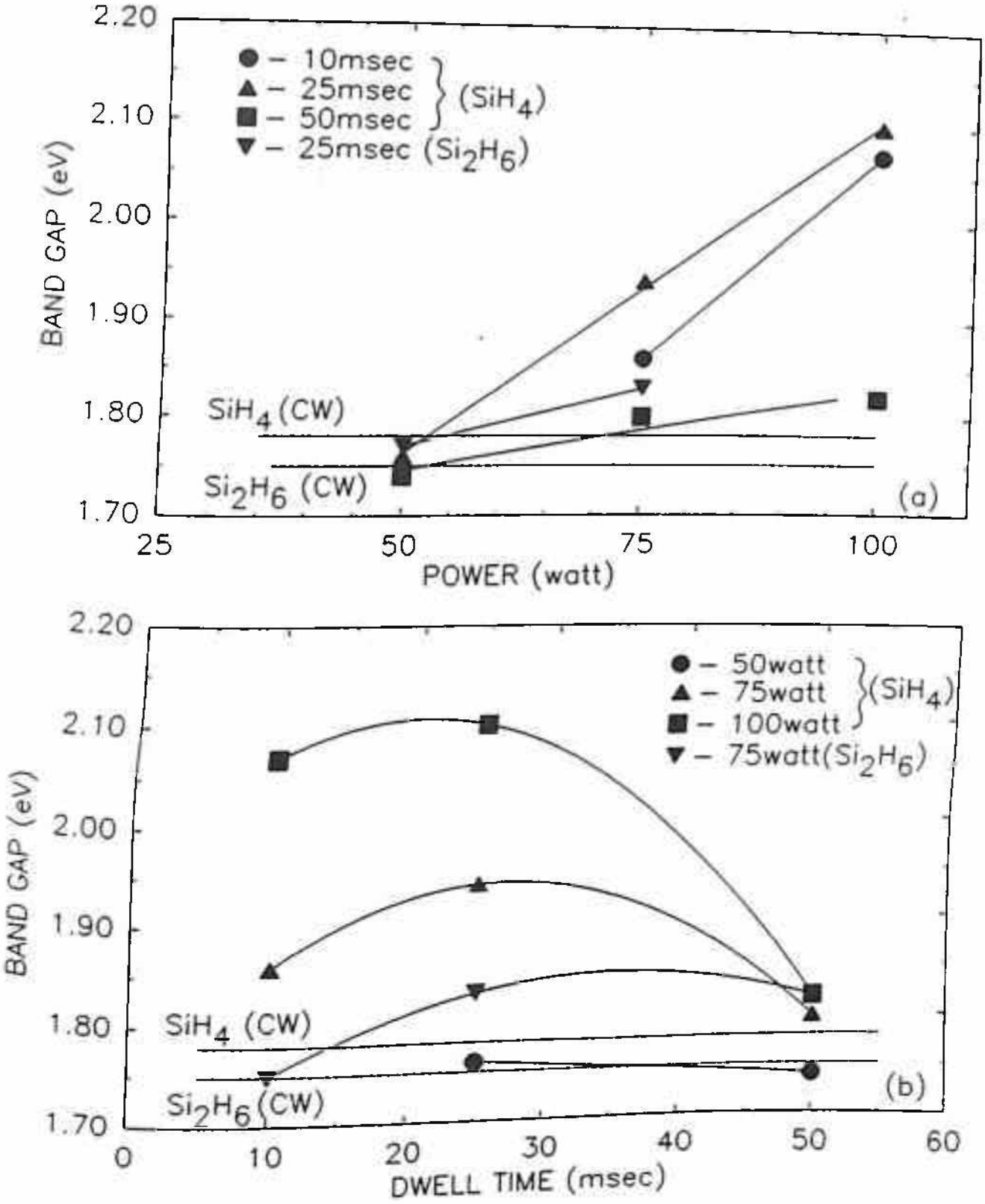

Fig.3A.3 Variation of E_g on (a) HPL and on (b) dwell time. Horizental lines show the E_g values for CW discharges.

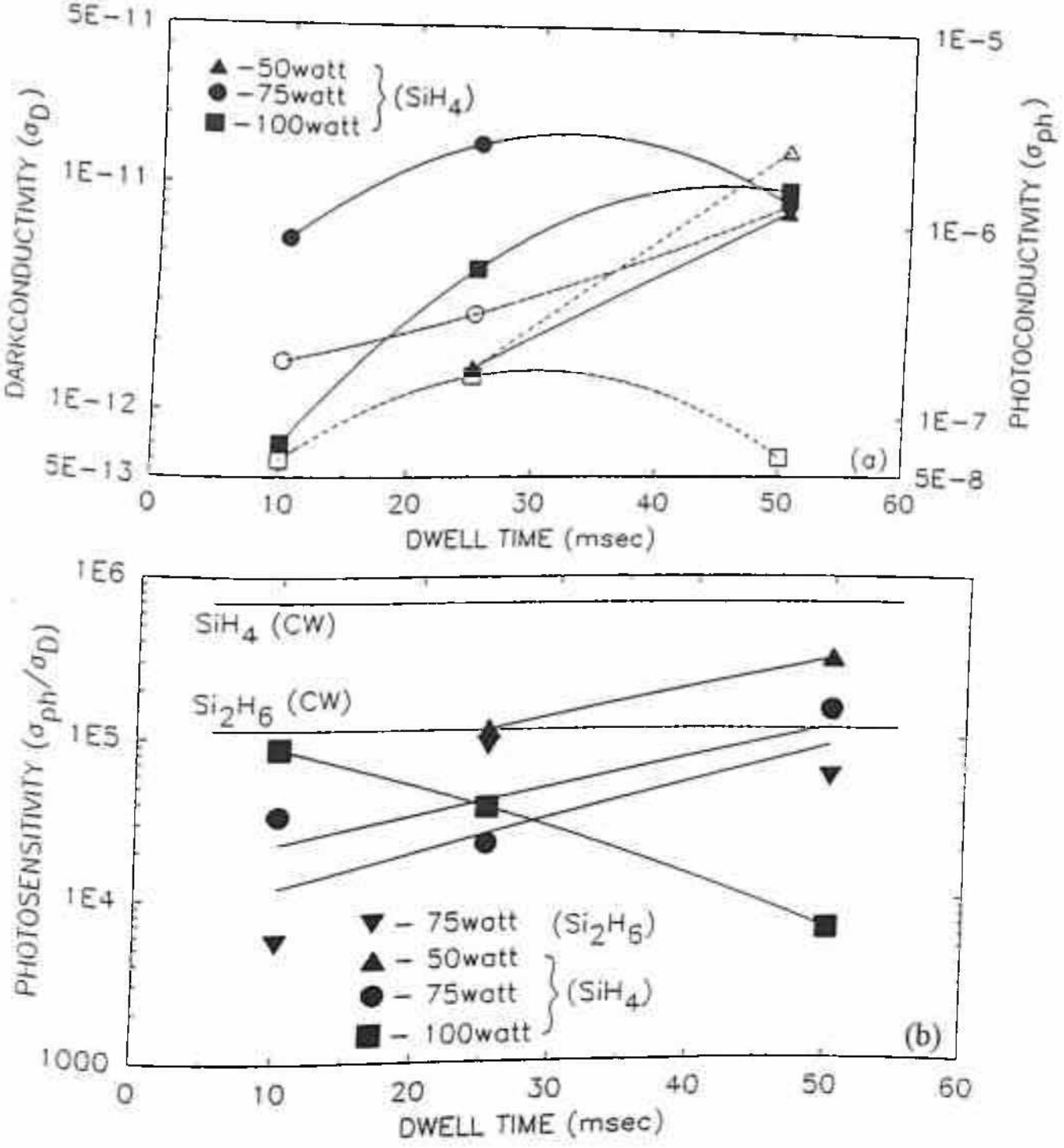

Fig.3A.4 Dwell time dependence of (a) σd and σph and (b) for various HPL used. Open symbols correspond to σ_{ph}.

values of 50 and 75 Watt an increasing trend in σ_{ph} and σ_{ph}/σ_D with τ is observed for both silane and disilane discharges. However, at 100W HPL a reverse trend is noticed.

3A.3.4 IR Studies

FTIR traces in the 2000 cm^{-1} range of some selected samples are shown in **Fig. 3A.5**. Pulse parameters used and hydrogen contents of these films are also mentioned in the figure itself. The possibility of polyhydride formation is supported by the FTIR traces obtained (PD2, PD3, PD4) as shown in **Fig.3A.5**. Again, hydrogen content, C_H calculation (indicated in **Fig. 3A.5**) reveals no one-to-one correspondence of C_H with E_g.

3A.3 interpretation of the results

The results obtained relating to MPPD growth of a-Si:H during the present investigation will now be discussed.

The following explanation based on experimental results reported in the literature appears plausible in the present case as well. Fleddermann et al.[21] have shown that in a pulsed SiH_4/He discharge, addition of SiH_4 drastically reduces electron density (n_e) and electron decay time constant (τ_e). This is thought to be due to the electron attachment to the silane dissociation products. As the pulse width increases obviously, n_e also increases and electron attachment process appears to saturate. This view is further supported by Overzet et al.'s[6] electron density measurements. Therefore, it may be that the higher concentration of dissociation products in undiluted silane and disilane, generated during the initial part of the high power pulse, strongly influences n_e even in the remaining part of the pulse. At lower τ values the overall effect is a restricted growth rate. This negative influence decreases with the increase of dwell time and beyond a critical value of τ (dependent on HPL) r_d exceeds the value obtained for CW discharges.

In the literature conflicting reports are mentioned. While Overzet et al.[6] reported enhancement of the deposition rate with increasing duty cycle in a pulsed discharge, Watanabe et al.[14] observed a decrease in r_d in SiH_4/H_2 discharge with respect to duty cycle. In the above studies a zero low power condition was maintained while in the present study non zero low power conditions were maintained. One wishes to emphasise here that the

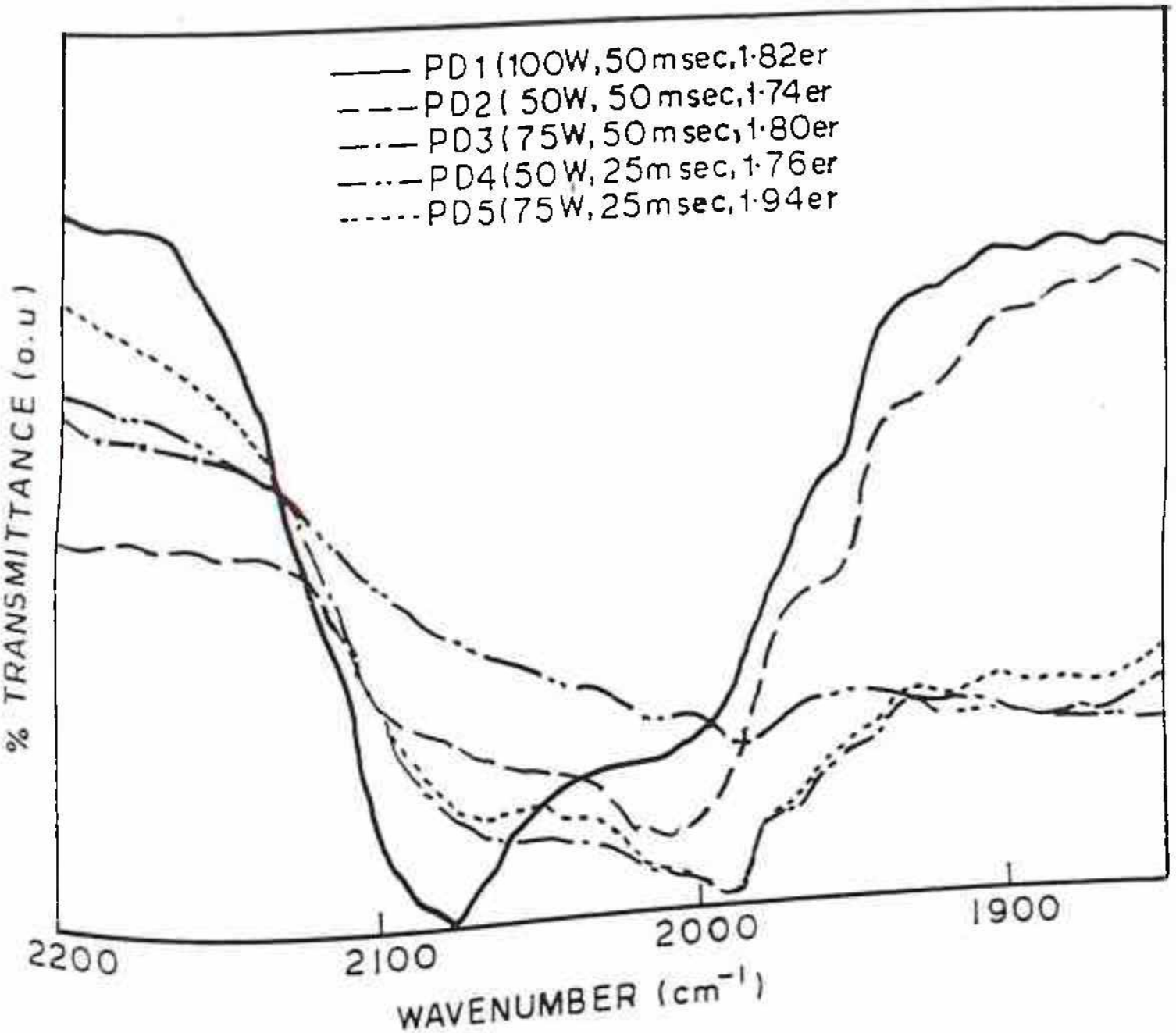

Fig.3A.5 FTIR transmission spectra for some undiluted silane MPPD grown films.

deposition conditions are not yet fully optimised and source gases in the present case have not been diluted. It may be noted that in a highly diluted feed stock the plasma chemistry is entirely different (even for normal RF discharges). This has been discussed in general under section 2.1.4.

From **Fig. 3A.1** it is not clear whether there is an inherent limitation in pushing the r_d values much beyond what are obtainable under CW discharge conditions. However, a better understanding of plasma chemistry and interplay of process parameters in pulsed discharges may allow one to identify a process parameter space (shaded triangle in **Fig.3A.1**) where growth rate is higher than that obtainable for CW discharges without, of course, any powder formation.

The 1st observation from **Fig.3A.2** i.e. increase of r_d with increasing HPL is expected since increasing the RF power density is known to enhance r_d. However, in the present case these values are below those one would expect for these power levels. This is partly due to the fact that these power levels are maintained only for a short duration. Even then one would intuitively expect an arithmetic sum of the individual deposition rates for the high power and low power levels; but surprisingly this is not the case.

Regarding the 2nd observation from **Fig. 3A.2** relating to the saturation of r_d at higher HPL, it can be said that powder formation is, perhaps, the only explanation behind the flattening of the curves in **Fig. 3A.2** at higher power levels since these powder forming [illegible] growth.

[illegible] are fairly common. Earlier workers[23] have demonstrated that the [illegible] films accompanied by high hydrogen content (C_H in at%) and higher E_g in a CW discharge. Conde et al.[24] have also shown E_g tailoring by utilising the residence time of the precursors although a different reactor geometry (CE-PECVD) was used for such experiment. Thus, initially it was thought that high E_g values in these films could be due to more polyhydride incorporation in the films. However, at higher τ, E_g values were found to approach the CW value irrespective of HPL used. This is suggestive of a counter process operative under such circumstances which may, perhaps, be inhibiting the polyhydride forming reactions, presumably at work at higher τ regime.

A higher band gapis the expected result for higher HPLs with larger τ values since under these conditions it is possible for the reactions that lead to polymerisation to take place. This is because normally at this power level in a CW discharge polymerisation reactions are fairly common. However, this seems not to be the case here, since the band gap, after the initial increase seems to approach the CW value for higher τ irrespective of the HPL used. *This result, coupled with the higher σ_{ph} (section 3A.3.3) for the films, with the exception of that grown at 100W, indicates that a counter process that may inhibit the polymer forming* reactions may be at work at higher τ.

It would thus be interesting to perform some plasma diagnostic experiments and to confirm whether there exists two different processes at work in the low and high τ regimes. In fact an exhaustive study by the Sanyo group[2] (E_g = 1.73 eV & C_H = 25 at%) and the results obtained in the present study (E_g = 1.89 eV & C_H = 5 at %) have failed to confirm such a correlation, earlier believed to have existed (i.e. high C_H and high E_g).

The IR results (stretching mode of vibration), shown in Fig. 3A.5. supports this view (no one to one correspondence of E_g with C_H) since there is no substantial increase in the absorption due to polyhydrides which fall around 2100 cm^{-1}. As far as the lower τ regime (<10 msec) is concerned, it appears more exhaustive investigations are needed to confirm whether these high powered shorter duration (<10 msec) pulses act as disturbances in a CW plasma and influence significantly the film properties.

The observed decrease in σ_{ph}/σ_D and σ_{ph} at 100W HPL with increasing τ may, perhaps, be due to the onset of gas phase polymerisation (secondary plasma reactions) in the plasma as evidenced by the powder formation around the powered electrode. The IR absorption spectra of these films, specifically that of PD1 as shopwn in **Fig. 3A.5** also support the above contention. The best σ_{ph} and σ_{ph}/σ_D values for silane discharges are 2.5 x 10^{-6} $\Omega^{-1}cm^{-1}$ and 3 x 10^5 respectively and, the films grown by Si_2H_6 discharge seems to have slightly better σ_{ph} (4.4 x 10^{-6} $\Omega^{-1}cm^{-1}$). A density of states measurement by PDS gives a typical value of 1.2 x 10^{16} cm^{-3} for these films having a band gap of 1.83 eV. This is comparable with the values reported for a-Si:C:H of similar E_g[25].

3B H_2 diluted MPPD

3B.1 Introduction

In the previous experiments (discussed in section 3A) it was found that at very low modulation frequency (2 Hz), for RF 13.56 MHz excitation deposition rates were less than those obtained by CW discharges. It was thought to be due to higher electron attachment to silane [illegible] al [21] These authors concluded from their [illegible] to hydrogen may not be a significant process and perhaps H_2 addition increase electron decay time constant (τ_e). Therefore, anticipating a longer τ_e and higher n_e in SiH_4/H_2 discharges compared to undiluted silane discharge, modified pulsed plasma discharge of SiH_4/H_2 mixture was carried out systematically with an aim of achieving higher growth rate. It was also found that optoelectronic properties of undiluted MPPD grown films were inferior to CW discharge grown films. In fact, consequences of plasma polymerisation were also reflected in the properties of undiluted MPPD films. Therefore, it should be interesting to investigate H_2 dilution of the feed stock for obtaining better quality films grown at high rates, presumably by suppressing plasma polymerisation and by increasing n_e and τ_e.

In this context it should be mentioned that Capitelli et al.[26] have predicted an increase of average electron energy with H_2 addition to silane plasma through their theoretical calculations. They have concluded that in 100% SiH_4 plasma the vibrational impact is 100 times more efficient than the electronic one, whereas in SiH_4-H_2 diluted plasmas the electronic excitation frequency becomes comparable to that of vibrational excitation. Thus in pure silane "soft" plasmas the vibrational excitation is the most probable dissociation channel, whereas in "hard" 3% SiH_4 in H_2 plasma the electronic excitation could be predominant.

In the present study while attempting some plausible explanations for different observations, variation of the above mentioned plasma parameters (n_e and τ_e) are utilised and referred at many places. In fact, in the present study OES has been extensively utilised for probing the growth process. It is to be noted, that above plasma parameters are indirectly related to OES intensities and such correlations are very well documented in the existing

literature. Therefore no additional attempt has been made to estimate these parameters through separate measurements.

3B.2 Experimental Details

The deposition system used was the same Multizone unit, discussed in section 2.2. Two different schemes of H_2 dilution were experimented to understand the basic kinetics involved in the deposition process. In one scheme the total flow of the mixture was maintained constant (40 sccm) while changing the flow of the diluting gases. In the other scheme silane flow was maintained constant (20 sccm) and different amount of dilutions were used while keeping other parameters unchanged. Time resolved optical emission spectroscopy (TROES, see section 2.8) studies were carried out to see whether excited species can give some insight into the reaction kinetics involved.

Dark conductivity (σ_D), photoconductivity (σ_{ph}), Photothermal deflection spectroscopy (PDS) and FTIR measurements were carried out on these H_2 diluted samples also.

3B.3 Results

3B.3.1 Deposition rate

Fig. 3B.1 shows the variation of deposition rate (r_d, $A^o s^{-1}$) with dwell time (τ msec). For this study the pulse power levels used were 75 W high power level (HPL) and 10 W low power level (LPL). These parameters were chosen because this combination, at τ= 25 msec and 5% duty cycle, yielded the best quality film ($\sigma_{ph} \approx 10^{-5}$ $\Omega^{-1}cm^{-1}$). As expected, r_d increased after hydrogen dilution of the feed gas and τ dependence of r_d could be pushed up by diluting silane.

It also appears from **Fig. 3B.1** that as τ increases the difference between the r_d values for undiluted and 25% H_2 diluted silane decreases and, at τ = 50 msec, this difference becomes almost zero.

Fig. 3B.2 shows the variation of r_d with dilution for the two different flow rate schemes experimented. Different H_2 dilution [$H_2/(SiH_4+H_2)$] experiments were carried out at constant HPL, LPL, τ and duty cycle. In both cases it was found that r_d increases with the

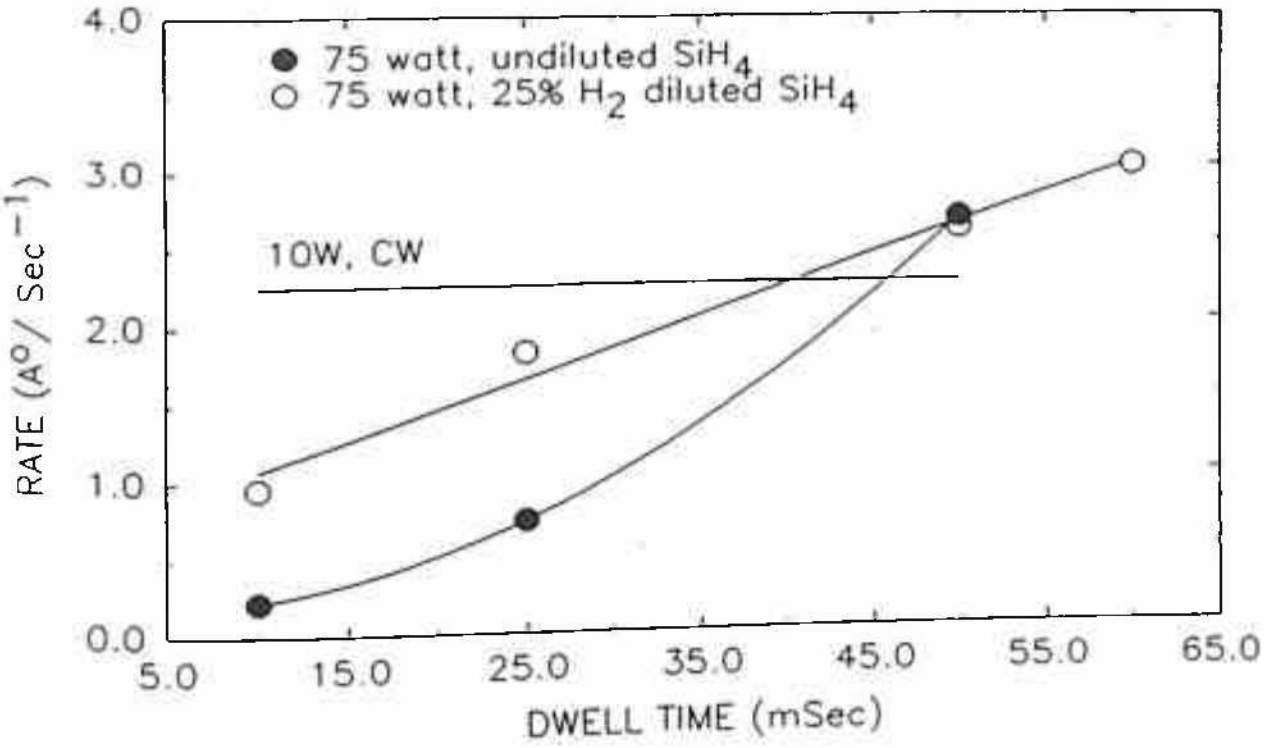

Fig.3B.1 Deposition rate as a function of dwell time for undiluted and H_2 diluted silane discharges.

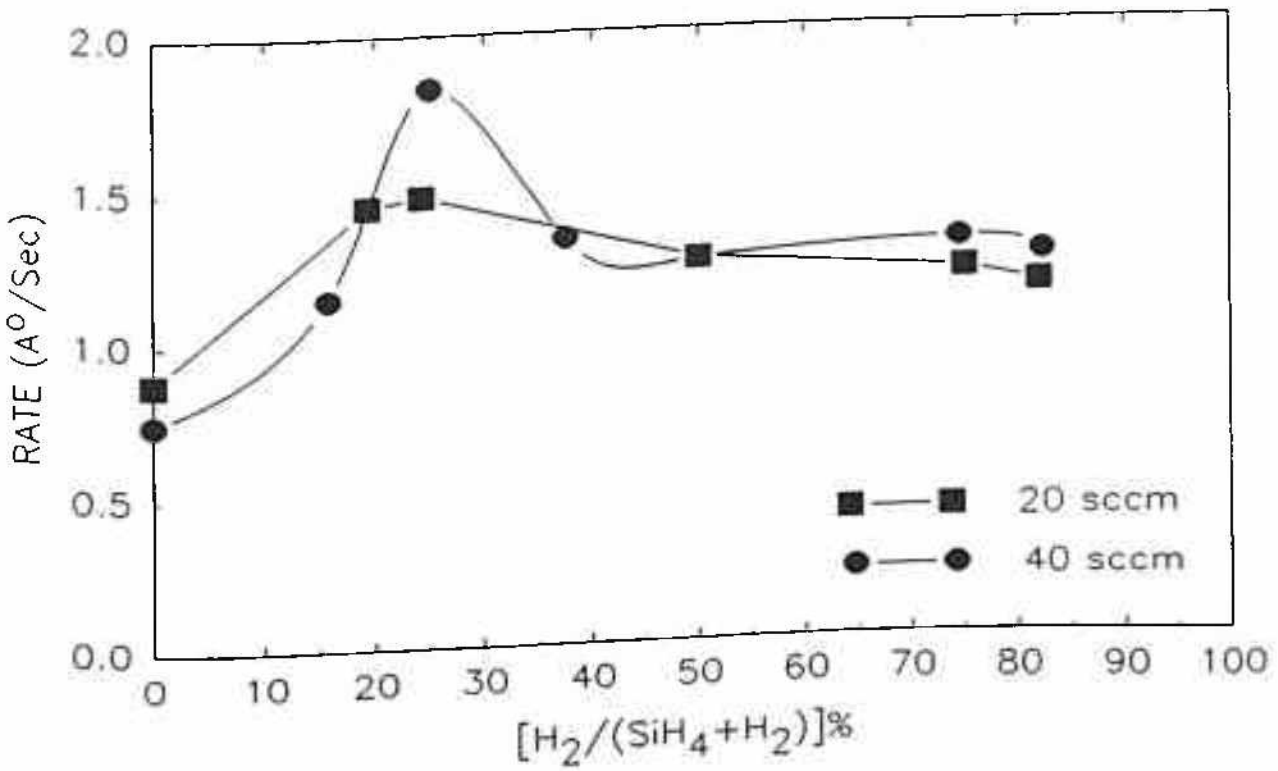

Fig.3B.2 Deposition rate as a function of percentage H_2 dilution for two different flow rate schemes used.

dilution upto approximately 25% H_2 dilution. Further increase of hydrogen dilution leads to a slow decrease of r_d with dilution and finally r_d seems to attain a steady value around 80% dilution. It is also seen that the initial rate of increase of r_d with dilution is higher than the subsequent rate of decrease of r_d.

3B.3.2 Optical Emission Spectroscopy

Emission spectra were recorded for some selected species only like SiH^*, H^* and Si^*. Spectra were recorded for both the dilution schemes studied. **Fig. 3B.3(a), (b) & (c)** show the variations of emission intensities with H_2 dilution for the above mentioned species, respectively.

Emission from SiH^* at 414 nm was found to increase with dilution upto 70% H_2 and to drop thereafter in case of 40 sccm total flow rate. In the case of 20 sccm fixed silane flow, the peak around 70% H_2 dilution in SiH^* emission intensity was missing and instead it increased steadily in the whole dilution range studied.

In case of Si^* emission intensity (288 nm), almost similar trend as that of SiH^* emission was found.

Emissions from H^* were measured at two wavelengths, 656 nm (H_α, 12.09 eV) and 486 nm (H_β, 12.7 eV) for both the dilution schemes experimented. Emission intensity in all these cases were found to increase steadily with H_2 dilution. Beyond 50% H_2 dilution H^* emission intensities were found to increase much rapidly deviating from it's linear increase below 50% H_2 dilution.

3B.3.3 Optical band gap

Fig. 3B.4 gives the variation of E_g vs dwell time (τ) for 25% H_2 dilution and 40 sccm (10 H_2, 30 SiH_4) total flow case. It is seen that band gapincreases linearly with τ i.e. from 1.77 eV to 1.88 eV. It is to be noted that without dilution the tailorability in band gapwas more and E_g vs τ showed a maxima at around 25 msec.

Variation of E_g with H_2 dilution for both the dilution schemes are presented in **Fig. 3B.5**. In both the cases a drastic drop in E_g value occur after 25% H_2 dilution. At higher dilutions E_g remains within a limit 1.77 to 1.82 eV. In case of 20 sccm constant SiH_4 flow E_g

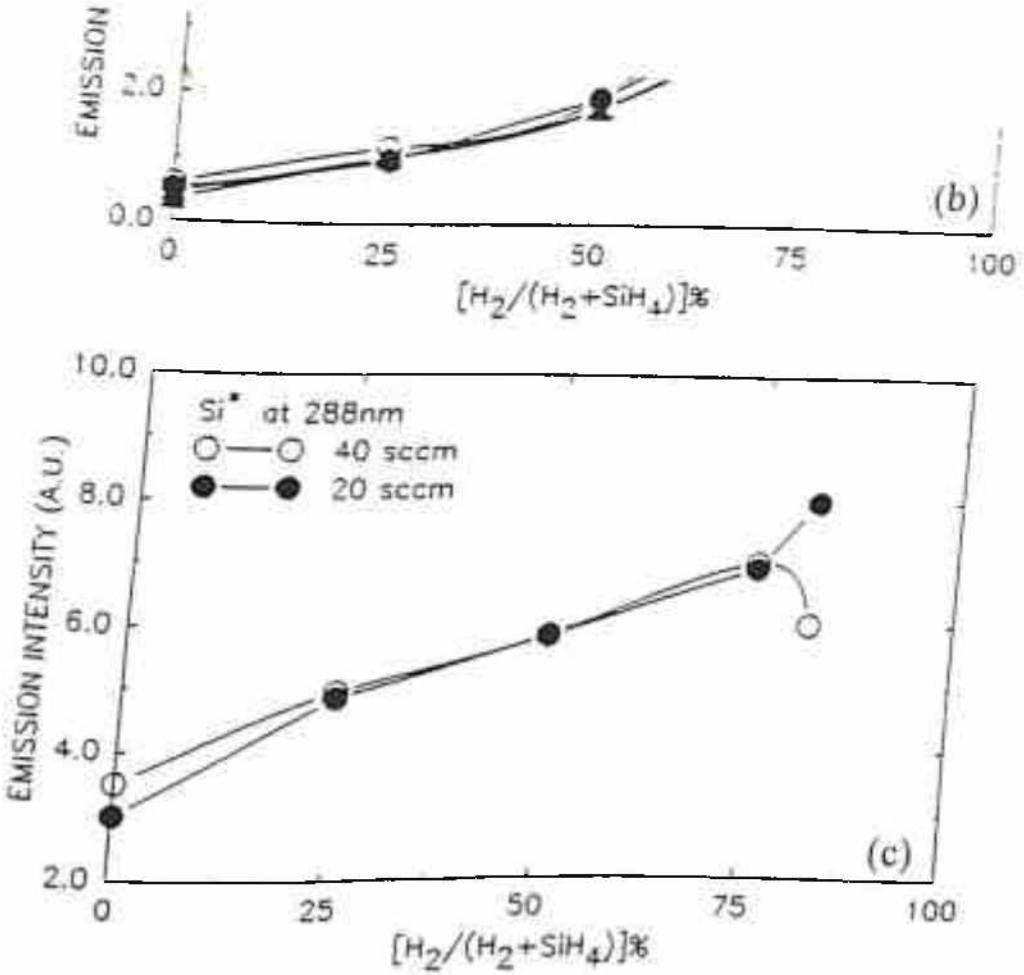

Fig.3B.3 *Emission intensities of excited a) SiH^*, b) H^* and c) Si^* species as a function of H_2 dilution.*

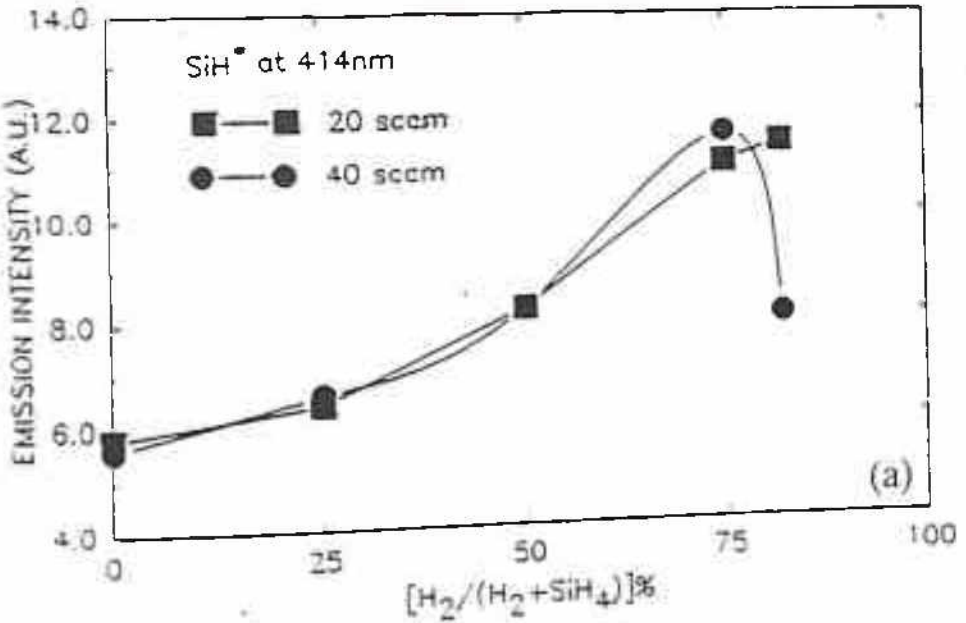
14.0
12.0
10.0
8.0
6.0
4.0
EMISSION INTENSITY (A.U.)
SiH* at 414nm
20 sccm
40 sccm
(a)
0
25
50
75
100
[H2/(H2+SiH4)]%

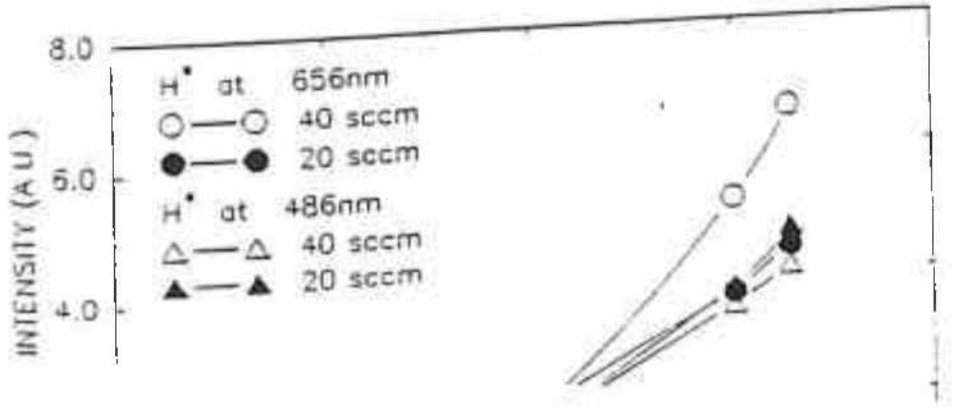
8.0
6.0
4.0
INTENSITY (A.U.)
H* at 656nm
40 sccm
20 sccm
H* at 486nm
40 sccm
20 sccm

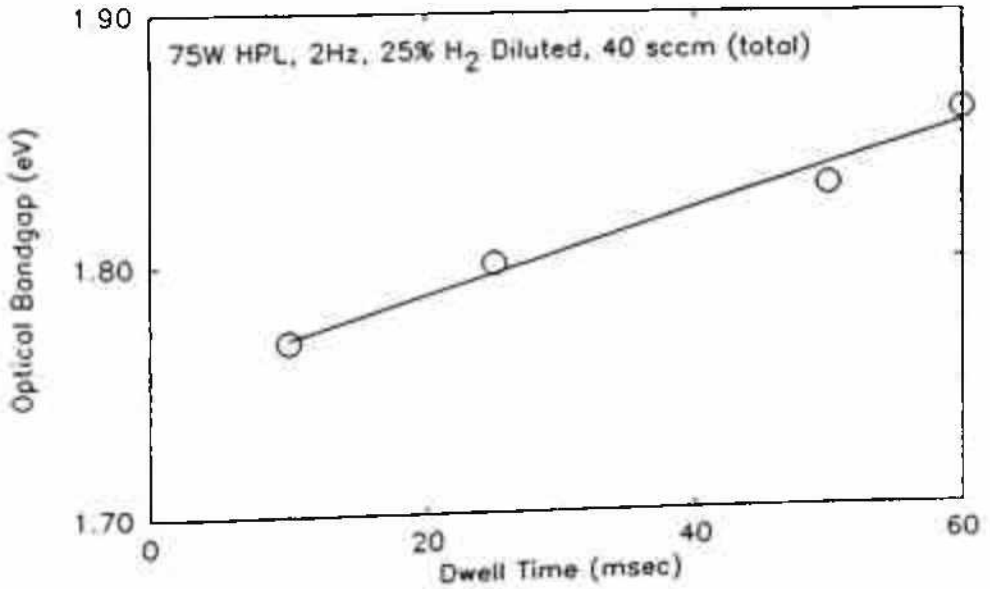

Fig.3B.4 Variation of E_g with dwell time for 25% H_2 dilution.

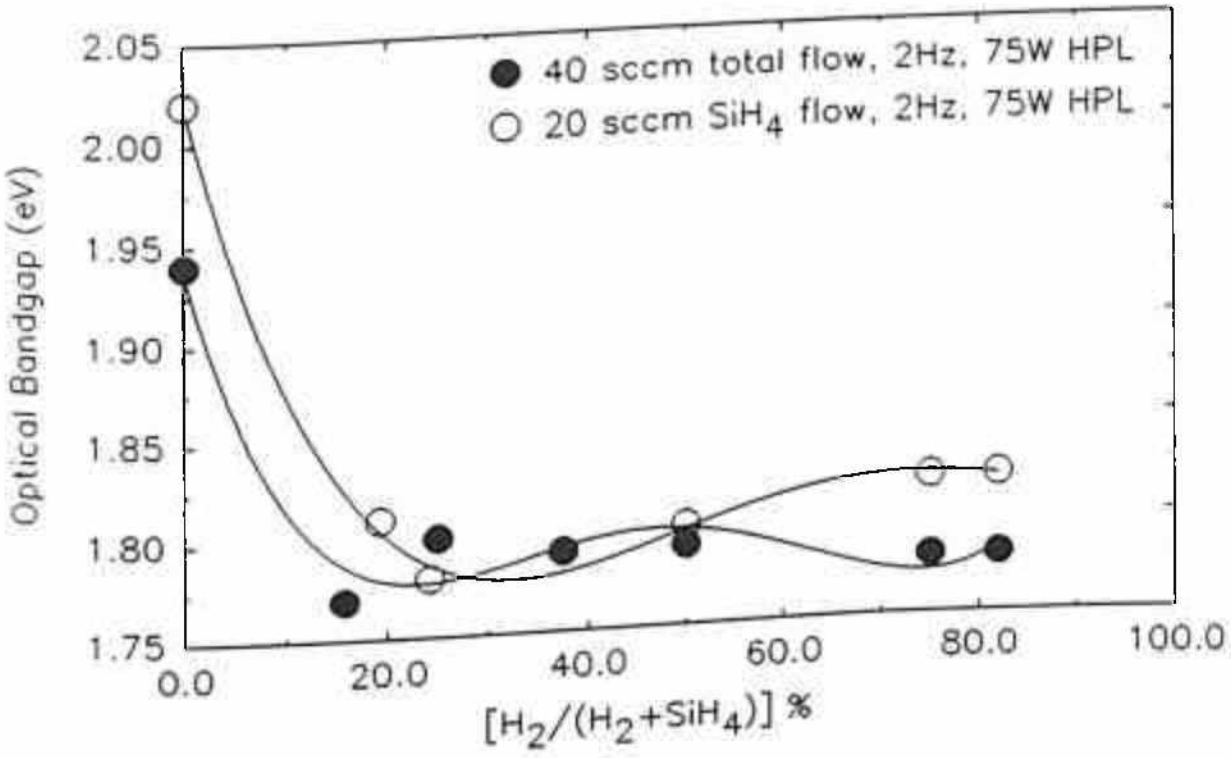

Fig.3B.5 Variation of E_g with % H_2 dilution for two different flow rate schemes used.

increases slowly with H_2 dilution beyond 25% dilution, whereas for 40 sccm total flow case it decreases slowly.

3B.3.4 Dark and Photoconductivity

Fig. 3B.6 shows variations of σ_d and σ_{ph} versus τ. Results for both undiluted and 25% H_2 dilution grown films are provided for comparison. Horizontal lines show the conductivity values for CW discharge produced films. For 25% H_2 diluted discharge produced films σ_{ph} decreases steadily with increasing τ while σ_d increases marginally upto τ = 50 msec and increases sharply thereafter. It is quiet clear that modulated discharge produced films always show less σ_{ph} than the CW discharge produced films as also higher σ_d than CW discharge produced films. The increase in σ_{ph} with τ for undiluted silane discharge has already been discussed in earlier section (3A.2.3). Increasing τ from 10 msec to 60 msec reduces σ_{ph} by almost an order of magnitude.

Fig. 3B.7 shows the variation of σ_{ph} with H_2 dilution for both the dilutions schemes experimented. Initially there is a steep rise in σ_{ph} (around two orders of magnitude) with dilution and beyond 25% H_2 dilution the dependence of σ_{ph} with H_2 dilution becomes less pronounced. Finally σ_{ph} decreases with H_2 dilution beyond 75% H_2 dilution for 40 sccm total flow case and beyond 50% H_2 dilution for 20 sccm constant silane flow case.

3B.3.5 Hydrogen content and microstructure factor

Fig. 3B.8 shows the FTIR traces in the range 2300 to 500 cm^{-1} for samples grown with different H_2 dilutions as mentioned in the figure itself. The common feature is that all these films show predominant SiH bonding. **Fig. 3B.9(a)** shows the variation of hydrogen content, C_H with τ for films grown at 25% H_2 dilution. Initially C_H increases very fast with τ i.e. from 10 to 25 msec and after that rate of increase of C_H with τ becomes less and less. For 75W HPL and τ = 60 msec C_H attains a value as high as 16 at%. It may be mentioned at this point that band gapfor this particular film is 1.85 eV. **Fig. 3B.9(b)** depicts the dependence of microstructure factor, R with τ for those films which are shown in **Fig. 3B.9(a)**. It is clear from the **Fig.3B.9(b)** that R increases linearly with τ and becomes as high as 0.75 for the film grown at τ = 60 msec. For the films grown at 10 msec E_g, C_H and R factor all are comparatively lower and comparable to the values expected for the device quality material.

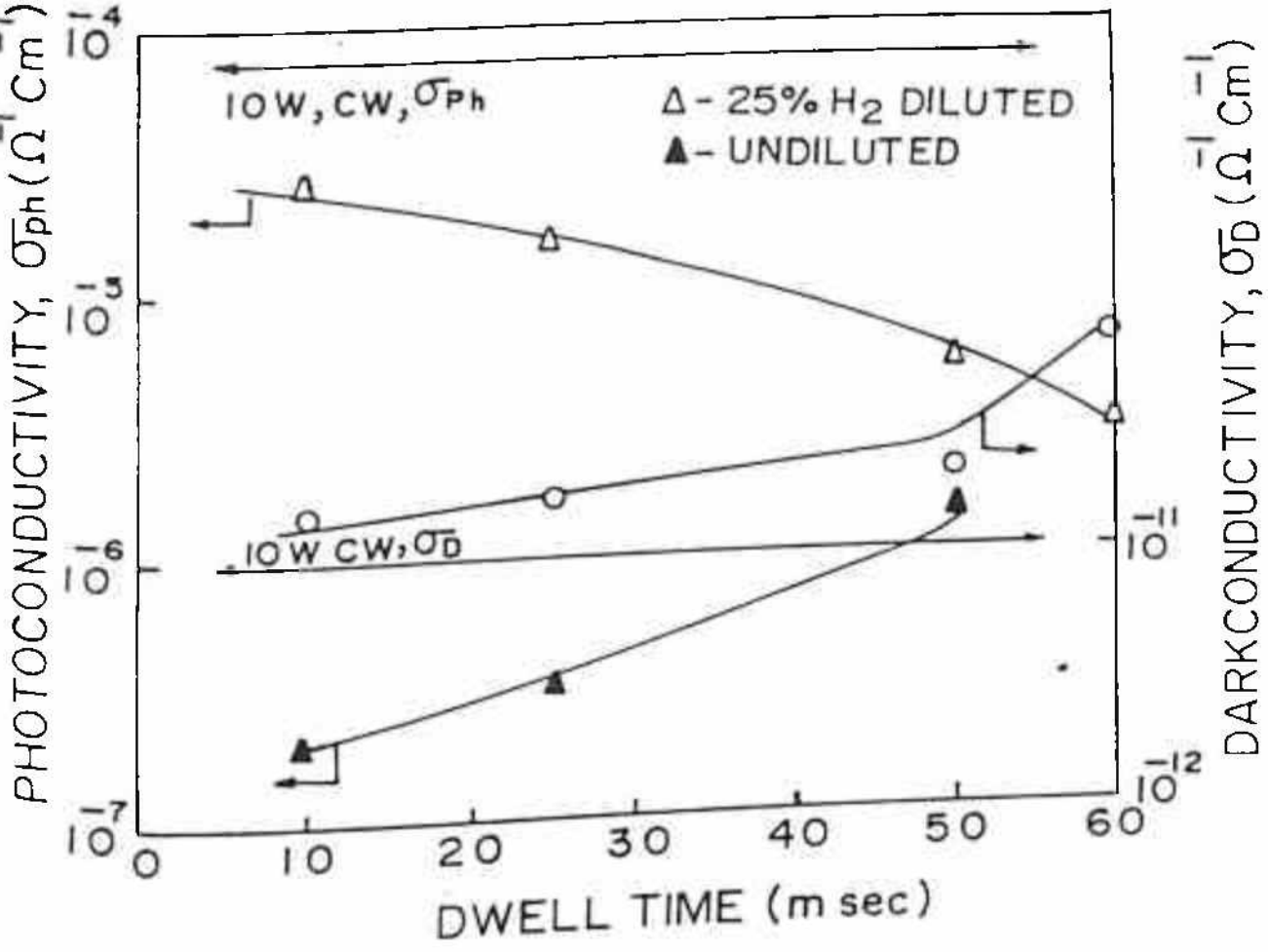

Fig.3B.6 Variation of σ_d and σ_{ph} with dwell time

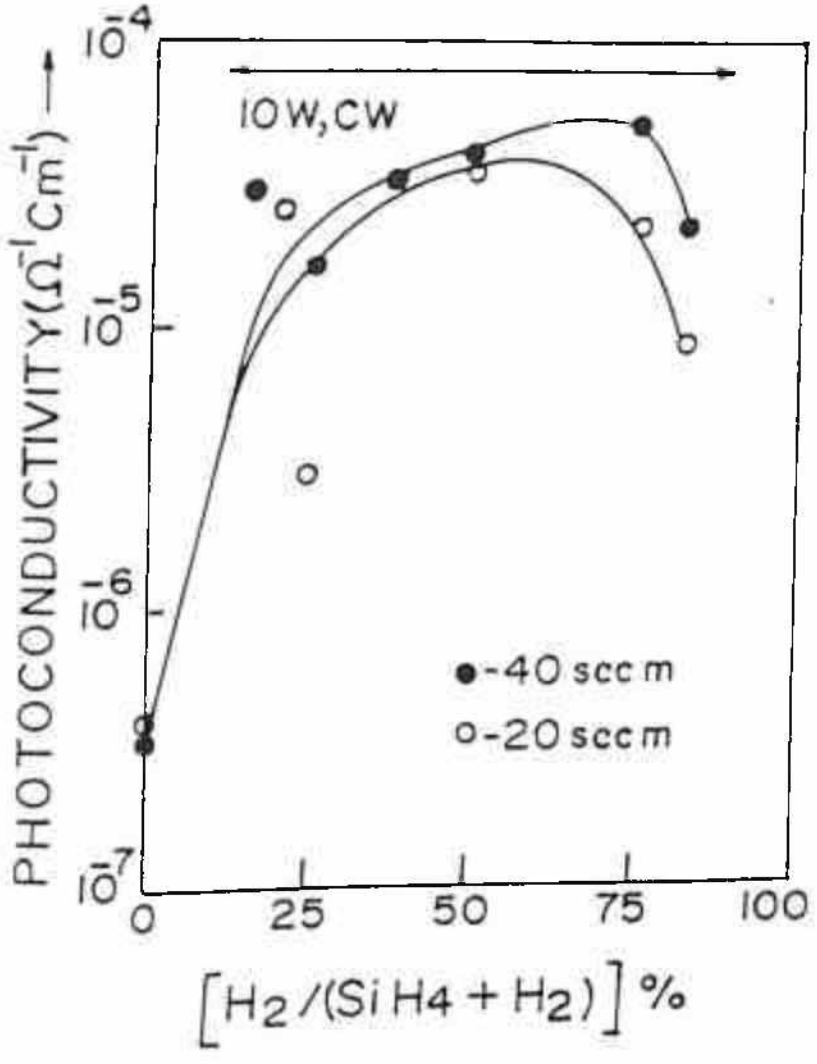

Fig.3B.7 Variation of σ_{ph} with $\%H_2$ dilution for both the dilution schemes used.

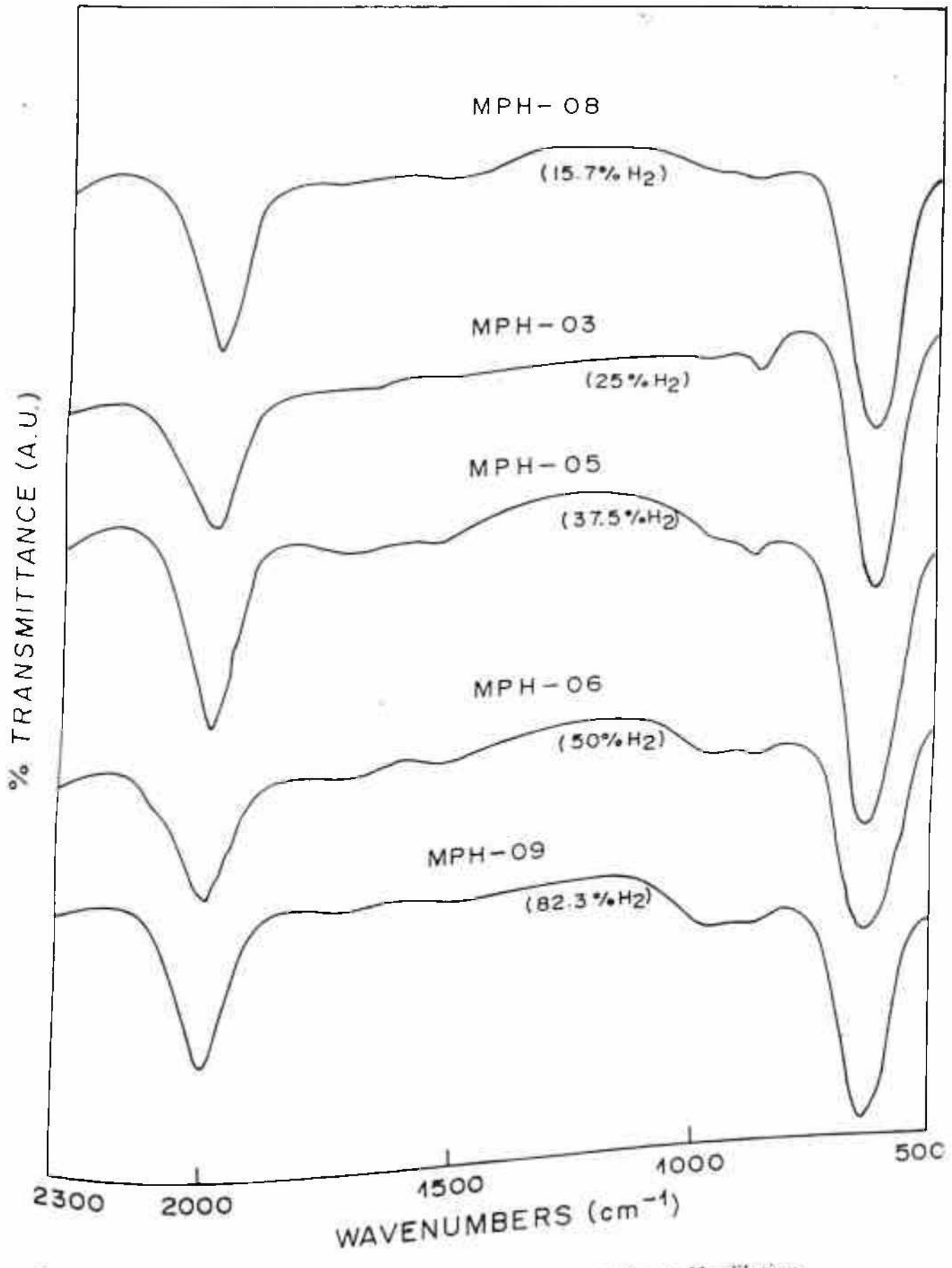

Fig.3B.8 FTIR traces of a-Si:H films grown at different H_2 dilution.

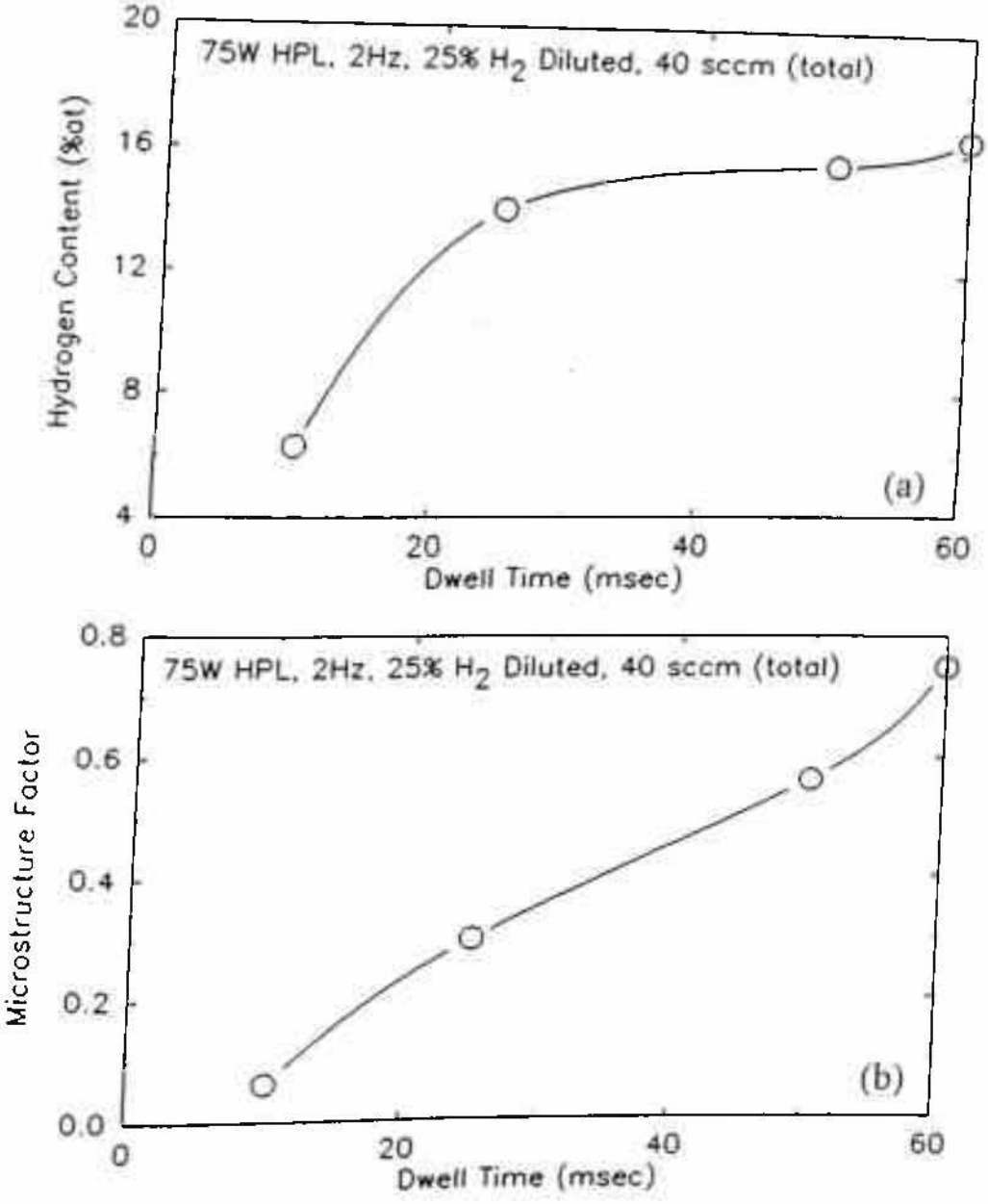

Fig.3B.9 Variation of a) hydrogen content and b) microstructure factor with dwell time for 25% H_2 dilution.

Fig. 3B.10 shows variation of C_H (at%) with H_2 dilution. For the films grown at 40 sccm total flow, C_H is found to be higher than those grown at constant silane flow and decreases sharply with the increasing dilution upto 50% H_2 and, thereafter, it remains almost constant (≈ 6 at%). In case of 20 sccm fixed silane flow the films show lower C_H values (<10 at%) and again there is a decreasing trend upto 25% H_2 dilution but thereafter value of C_H remains between 5 to 6 at% only. One interesting point that emerged from these studies is that from 50% H_2 dilution onwards whatever be the SiH_4 or H_2 flow rates, C_H in the films so deposited remains almost constant and lies between 5 to 6 at% and R factor between 0.06 to 0.07.

3B.3.6 Defect density studies

Fig. 3B.11 shows PDS spectra in the range 0.9 to 2.2 eV for samples grown at different H_2 dilution as mentioned in the figure. For CW discharge grown films (r_d = 2.25 A°s^{-1}) average values of defect parameters are E_o = 47 meV and N_D = 4.6 x 10^{16} cm^{-3}. It is to be noted that σ_{ph} for this film is quiet high, σ_{ph} = 7.5 x 10^{-5} $\Omega^{-1}cm^{-1}$. For undiluted MPPD (2Hz) grown film this value was, σ_{ph} = 3.4 x 10^{-7} $\Omega^{-1}cm^{-1}$. H_2 dilution, thus, improves significantly optoelectronic behaviours of a-Si:H films over that could be obtained by MPPD in undiluted silane discharge (σ_{ph} increases by orders of magnitude). The best set of properties were obtained under MPPD at 75% H_2 dilution, with N_D = 9.5 x 10^{16} cm^{-3}, E_o = 48.6 meV, σ_{ph} = 5 x 10^{-5} $\Omega^{-1}cm^{-1}$, C_H = 5.7 at% grown at r_d = 1.35 A°s^{-1}.

3B.3.7 Effect of modulation frequency

Effect of modulation frequency was studied only for undiluted discharge grown films. Modulation frequency was simply varied by changing the duty cycle of the pulse while maintaining τ constant. Exactly linear increase in r_d was observed in the frequency range studied. At 10 Hz modulation frequency r_d was found twice that of CW deposition rate. The variation of r_d due to change of modulation frequency is as shown in **Fig. 3B.12**.

For the films grown at different duty cycles only σ_{ph} and σ_{ph}/σ_d were measured. Their variations with modulation frequency is shown in **Fig.3B.13**.

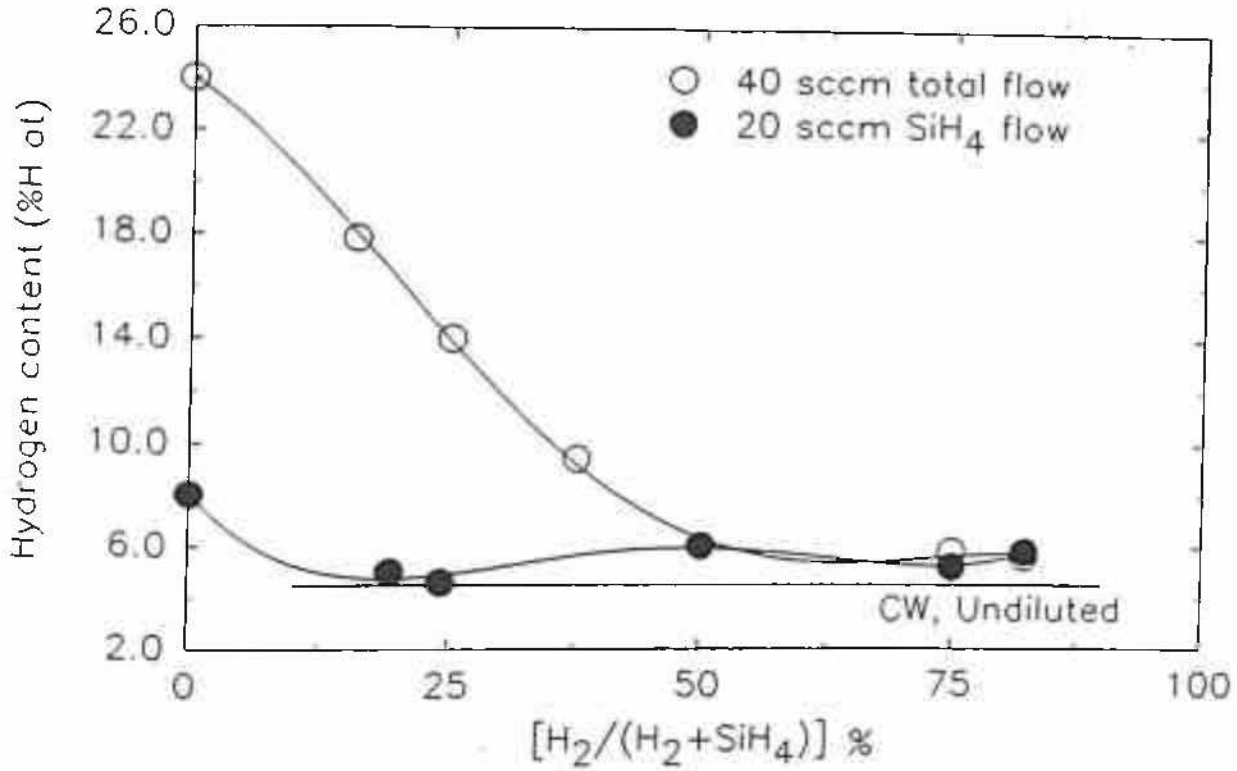

Fig.3B.10 Variation of C_H with % H_2 dilution for two different dilution schemes.

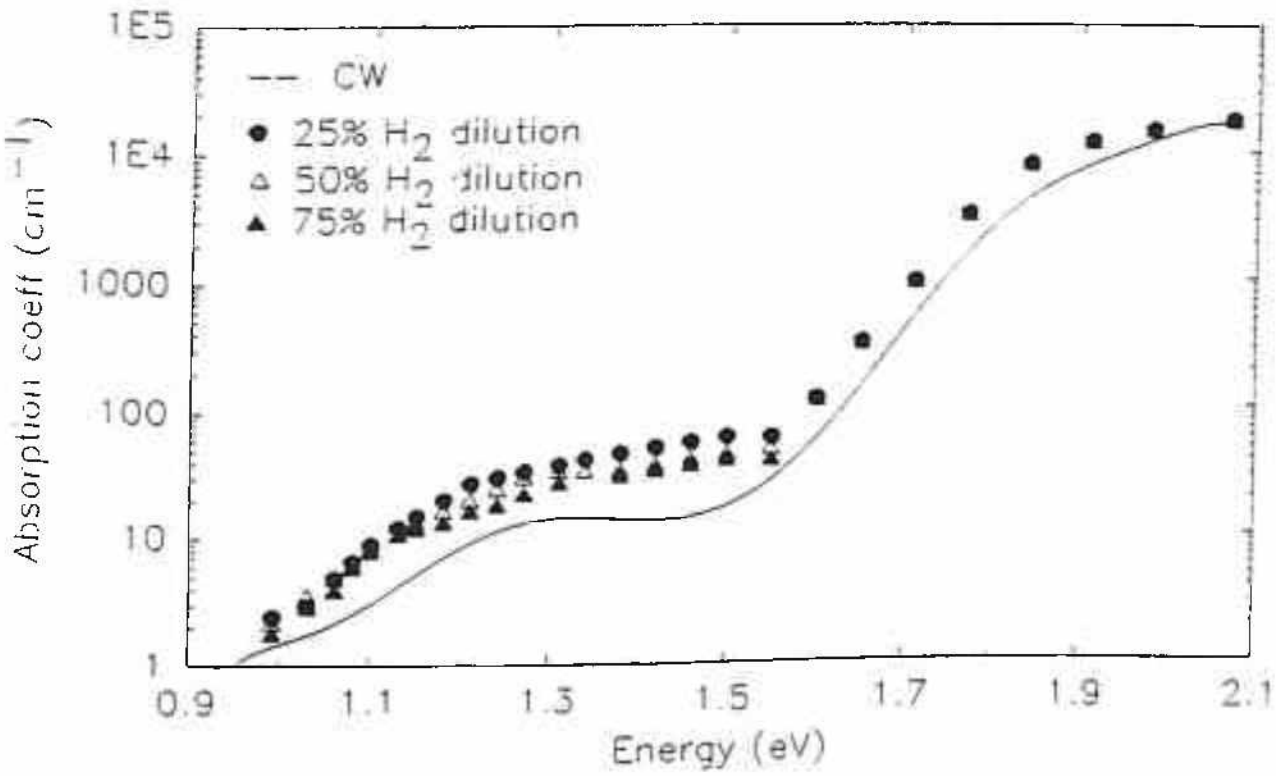

Fig.3B.11 PDS spectra of a-Si:H films grown at different H_2 dilutions.

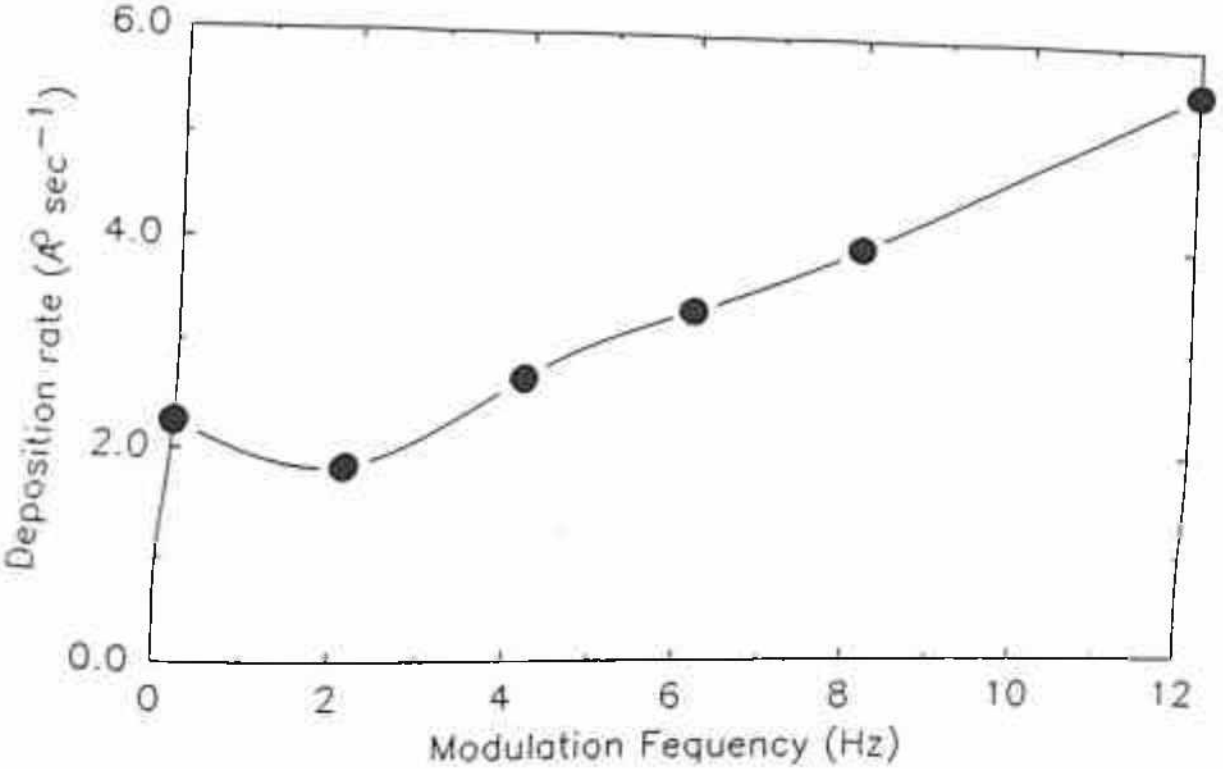

Fig.3B.12 Variation of r_d with modulation frequency for undiluted discharge grown films.

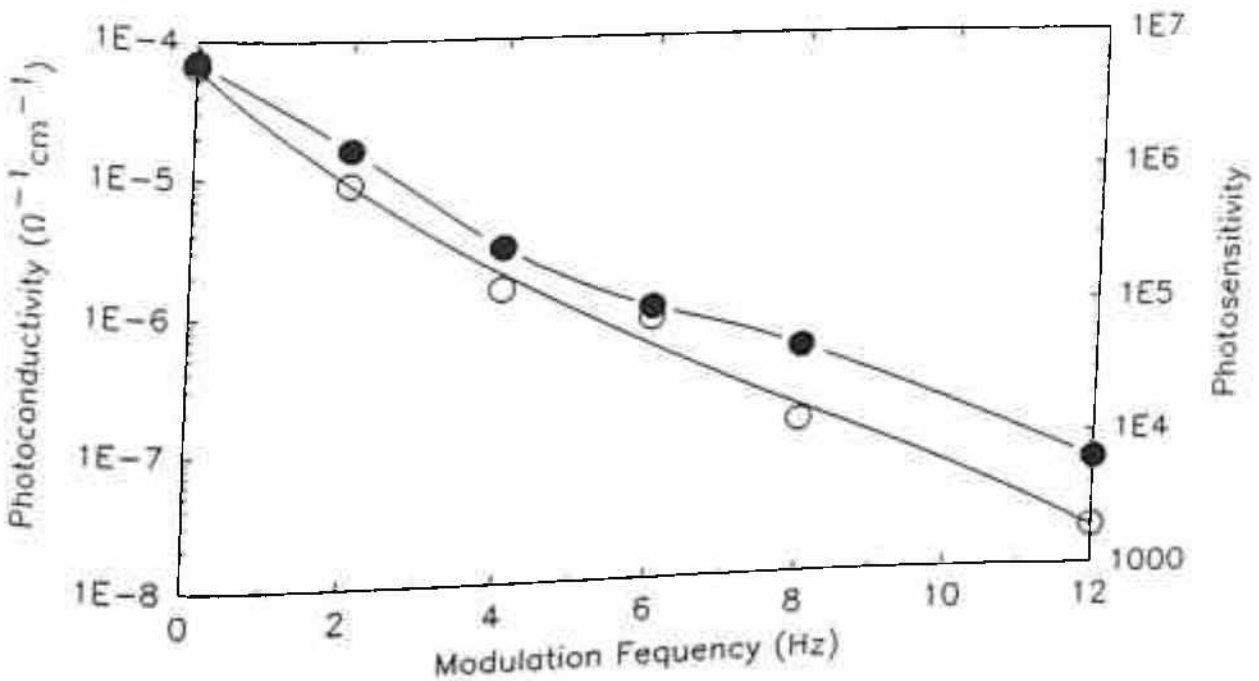

Fig.3B.13 Variation of σ_{ph} and σ_{ph}/σ_d with modulation frequency for undiluted discharge grown films.

3B.4 Interpretation of results

The observed increase in r_d after H_2 dilution would have been possible because of the following reasons:

i) higher dissociation of silane due to enhancement of n_e and τ_e compared to undiluted silane discharges, during both HPL & LPL[21].

ii) the suppression of gas phase secondary plasma reactions[3] due to hydrogen dilution, mainly during HPL, may have lead to enhancement of the arrival rate of a-Si:H film forming precursors to the substrate and thereby contributing to useful film growth.

It would be interesting to explore whether the observation of significant enhancement of σ_{ph} values (nearly two orders of magnitude) over the undiluted silane grown films appears related to the containment of the said secondary plasma reaction. Taking clues from Overzet et al's.[6] and Fleddermann et al.'s[21] work it appears that τ also has some influence on n_e and τ_e which, in turn, determine the change in r_d after dilution. The above linearly increasing trend in r_d continues for $\tau > 50$ msec, then although the enhancement of r_d on dilution is ultimately lost, the basic advantage of H_2 dilution still remains i.e. higher r_d than CW discharge conditions without any perceptible powder formation. On the other hand in undiluted silane discharges r_d enters the powder formation regime under these deposition conditions.

This dependence of r_d on dilution as observed in **Fig. 3B.2** was as expected from the results of CW discharge experiments with silane diluted with H_2 and inert gases. But the difference lies in the degree of dilution at which this maximum has occurred. Earlier Vanier et al.[27] have found that r_d increases with hydrogen fraction upto 75%, the increase being as much as an order of magnitude, and then r_d was found to decreases. They correlated this with the distribution of electron energy. Hamasaki et al.[28] used pulsed RF discharges for 11% $SiH_4(H_2)$ and found r_d to be nearly constant for every repetition frequency experimented (at 67 sccm flow and 0.18 Torr pressure, when the total ON period was kept constant). In another study[29], using 50% $SiH_4(H_2)$, saturation at a lower power than in pure silane was observed. Kato et al.[30] investigated H_2 dilution effects in an ECR plasma and found r_d to increase with the silane fraction upto 50% and then a saturation was noticed. Bruno et al.[31] have also investigated the effects of Ar dilution in $SiCl_4$+H_2 and found an increase in r_d with Ar addition with a maximum at 27% of Ar.

To verify whether the decrease in r_d beyond 25% H_2 dilution was due to lower and lower silane fraction under these flow conditions or due to other reasons, another scheme of gas mixture flow (constant 20 sccm silane flow with varying H_2) was experimented. Again, as can be seen in **Fig.3B.2** r_d was found to follow the previous r_d dependence (total gas flow = 40 sccm) i e r_d peaked around 25% dilution.

The intensity of SiH^* emission line, generally regarded as an indicator of film growth rate, was found to increase upto 75% dilution as shown in **Fig.3B.3(a)**. It leads one to believe that there must be some other process at work which inhibits r_d from further increase as dilution increases beyond 25%. In order to get a better picture, TROES was carried out for H^* at 656 nm. Interestingly it was found that H^* emission intensity increased substantially after 25% H_2 dilution, whereas, its increase was gradual below 25% (**Fig.3B.3(c)**). Therefore, it is plausible to invoke the concept of an etching mechanism, presumably by hydrogen atoms, to explain the decrease in r_d beyond 25% dilution. The following reaction may be involved (Reference No. 41, Chapter-I).

$$e^- + SiH_4 \Rightarrow SiH^* + H_2 + H + e^- \quad (\Delta H = 8.9\ eV) \qquad (3B.1)$$

This reaction takes care of SiH^* emission intensity increase with dilution because, as dilution increases n_e and τ_e increase. In fact this view is also supported by Hamasaki et al.'s[15] observation, although the increase in SiH^* emission intensity is rather slow in their case. The above reaction suggests that as dilution increases generation of H_2 molecule also increases. At the same time feed gas dilution also increases the H_2 partial pressure by many folds. However, as mentioned earlier according to Fledderman et al.[21] electron attachment to H_2 molecule may not be a significant process. Therefore, in the present case (high dilution, high power, high n_e) the reaction cross sections of the following reactions may increase many folds. Additionally these reactions require lower energy electrons compared to the requirements of reaction (3B.1).

$$e^- + H_2 \Rightarrow 2H + e^- \quad (\Delta H = 4.5\ eV) \qquad (3B.2)$$

or it can proceed as

$$e^- + H_2 \Rightarrow H + H^* + e^- \qquad (3B.3)$$

This view is strongly supported by the observed H^* emission intensity at 656 nm. Thus, availability of high concentration of H atoms determines the film growth under high dilution conditions.

It is noted that the decrease in r_d, in the present case beyond 25% dilution, is not so dramatic as observed by previous workers[27] for CW discharges. Perhaps, it may be due to the fact that τ values, for which high powers were applied, were shorter as compared to the CW discharge in SiH_4/H_2 plasma. It may be that etching is predominant in the high power part of the pulse because electrons having energy $\approx$ 10 eV will be available in abundance during HPL. That the etching reactions predominantly taking place under higher dilution conditions, are indeed relevant is further supported by the gradual improvement in σ_{ph} values between 25% and 75% dilution range. The nearly identical values of r_d in both the flow rate conditions implies that, in highly diluted feed stock, r_d seems to attain a steady state value, determined by competing etching and deposition reactions and further increase in the silane concentration seems to have only marginal effect.

In the context of atomic hydrogen assisted etching Veprek[32] has found that H atoms act as etchant species and, during deposition, a reversible chemical equilibrium ($SiH_x \Leftrightarrow Si + xH$) is established. Again Blayo et al.[33] have demonstrated, by in-situ phase modulated ellipsometry, the role of etching by H atoms while treating as deposited a-Si:H films in pure H_2 discharges. They found that H atoms preferentially etch the SiH_2 groups.

It is very clear from FTIR studies that as the duration of high power period increases beyond τ = 20 msec the proportion of hydrogen in polyhydrides increases rapidly even though C_H shows an increase of $\approx$ 4 at% only. This is also reflected in E_g and C_H values which increase steadily with τ.

The kind of variation that is observed in **Fig. 3B.12** is quiet expected because the amount of power delivered during a certain interval of time to the plasma certainly increases linearly with the duty cycle.

Again as expected, both σ_{ph} and σ_{ph}/σ_d were found to degrade by several orders of magnitude as a result of an increase in the modulation frequency, merely 5 - 6 times.

3C He and He+H_2 diluted MPPD

3C.1 Introduction

As discussed under section 3A.2.1 - the deposition rate in MPPD as compared to other pulsed plasma discharges are found to be lower and even lower than that is obtained in CW discharge, operated at the low power level (LPL) of MPPD (**Table 3.1**). Also the optoelectronic properties of these films are found to be generally not as good as that of CW discharge grown films. In earlier sections (section 3A.3 & 3B.4) the above observations have been analysed. In section 3B. effect of H_2 dilution on growth of a-Si:H films in MPPD has been discussed. The main idea behind diluting SiH_4 by H_2 was to obtain higher r_d through achieving higher electron density (n_e) and also higher electron decay time constant (τ_e).

In search for producing device quality films, a-Si:H films have been deposited using diluent gases other than H_2, for example noble gases[34,35]. Proper choice of the diluent gases and their concentrations in a particular mixture determines whether material will be of device quality or not. It has been found that noble gas dilution of SiH_4 leads generally to a columnar growth,[36] whereas a high hydrogen dilution leads to onset of microcrystalline phase[37] in the material. Through these experiments it has been found that high quality material can be grown only at low growth rates. Helium dilution however produces some very interesting results. For instance i) Knights et al.[34] have found He dilution to be useful to increase the deposition rate(>10 $A^{\circ}s^{-1}$) of a-Si:H films while maintaining a low defect density in the material, ii) Cabarrocas et al.[35] have found lower equilibrium temperature suggesting thereby higher stability of a-Si:H films produced through He diluted silane discharge and iii) Hollenstein et al.[38] have found that with increasing rare gas dilution the contribution of hydrogen deficient ions becomes comparable to SiH_3^+, which is predominant in 100% SiH_4 discharge. The other motivation behind the use of He dilution was to utilise higher n_e and τ_e that are observed in pulsed plasma discharge of noble gases. Fledderman et al.[21] have reported that addition of even 1% of SiH_4 in pure He discharge reduces n_e by almost an order of magnitude and similar is the case for τ_e. However, when H_2 is added in SiH_4+He mixture, τ_e increases. They have also found that n_e increases in a discharge of molecular hydrogen and He mixture, which is in marked contrast to SiH_4+He discharge. Another study by Vignole et al.[39] on the kinetics of

defect creation by pulsed laser illumination in a-Si:H films deposited from SiH_4 + He mixture has revealed several interesting features specially a better stability of hydrogen in He diluted films suggesting an improved stability against light soaking. Exodiffusion spectra indicate that hydrogen is more strongly bonded in He diluted films[40] and the less mobile hydrogen in a-Si:H network leads to lower Stabler-Wronski type light induced degradation. At the same time light induced annealing via hydrogen diffusion must be reduced too.

Therefore, low to moderate He dilution of SiH_4 was studied in a MPPD environment during the present investigation. Very high dilutions $\approx$ 90% and above were not tried because they result in very low growth rates and onset of microcrystalline phase.

First in He diluted SiH_4 case, total gas flow in discharge chamber was maintained constant at 40 sccm. Therefore, with increasing He flow SiH_4-He ratio decreases sharply. Now in each He diluted condition an additional amount of H_2 was added keeping the other individual flow rates constant. This was tried with the hope of separating out the kinetics involved with the above two diluents to an extent.

3C.2 Experimental details

The a-Si:H films were deposited at 0.5 Torr in the same Multizone PECVD system (section 2.2). Similar to previous MPPD work (section 3A & 3B) a non zero low power level was maintained. Two different He dilutions were tried, i.e. 25% and 60%, while keeping the total gas flow constant at 40 sccm. For He + H_2 dilution studies, H_2 was added to the He diluted SiH_4 while keeping the SiH_4 and He flows unaltered so that 25% of the total flow is H_2 i.e. $H_2/(H_2+He+SiH_4)$ = 25%. In all these cases substrate temperatures were kept at 275°C, same as that used in undiluted (section 3A) and H_2 diluted (section 3B) discharges. Films were deposited for three different RF Power conditions

(i) CW discharge at the low power level of MPPD

(ii) 2Hz MPPD (dwell time τ = 25 msec, duty cycle = 5%) and

(iii) 10 Hz MPPD (τ = 25 msec, duty cycle =25%).

TROES studies were carried out using the set up described in section 2.8.

Dark conductivity(σ_D), photoconductivity (σ_{ph}), Photothermal deflection spectroscopy (PDS) and FTIR measurements were carried out on these samples.

3C.3 Results

3C.3.1 Deposition Rate

Fig. 3C.1 gives a comparative picture of growth rates (r_d) that are obtained at various dilution conditions in terms of a bar graph. For each dilution condition r_d values obtained at CW, 2 HZ and 10 Hz modulation conditions are shown. Undiluted, H_2 diluted, He diluted and H_2 + He diluted cases are shown in **Fig. 3C.1**. As discussed in section 3B, it was found that r_d increases with H_2 dilution upto 25% of H_2 and then decreases slowly and finally attains a steady value at around 80% H_2 dilution. In case of He dilution, a different picture emerges from **Fig. 3C.1.** Although effect of He dilution was not studied in as much detail as H_2 dilution still a comparative study of the two different dilutions provide the following picture.

i) deposition rates are higher in the He diluted plasmas than in H_2 diluted plasmas and these are higher than the r_d values obtained from 100% SiH_4 at 2 Hz MPPD.

ii) at 2 Hz modulation r_d increases in the manner - 0% He → 25% He → 60% He dilution. From 0% He dilution to 25% He dilution, the increase in r_d is 250% whereas the increase in r_d is comparatively very small when He dilution increases from 25% to 60%. Since in all these cases total gas flow was kept constant, therefore, r_d values normalised with respect to SiH_4 flow increases steadily with the increasing He dilution. Thus it appears, so far as SiH_4 utilisation is concerned, He dilution in MPPD environment is an advantage. The other encouraging picture is the improvement in photosensitivity (σ_{ph}/σ_D), (as discussed in section 3C.3.4) with increasing He dilution.

iii) r_d at 2Hz modulation seems to saturate with increasing He dilution whereas, at 10 Hz modulation r_d decreases as dilution increases from 25% He to 60% He.

iv) addition of H_2 to He diluted SiH_4 at 2 Hz does not show any perceptible drop in r_d, whereas at 10 Hz modulation r_d drops substantially for both the 25% and 60% He diluted conditions. These drops in r_d are also accompanied by a significant improvement in σ_{ph} and in σ_{ph}/σ_D values as discussed later (section 3C.3.4).

v) It is also observed that at a particular dilution obtained by using a single diluent, r_d values are much different from that obtained at the same total dilution obtained by mixing two different diluents. For example at 50% H_2 dilution r_d is 1.2 $A^{\circ}s^{-1}$, whereas for 25% H_2 + 25%

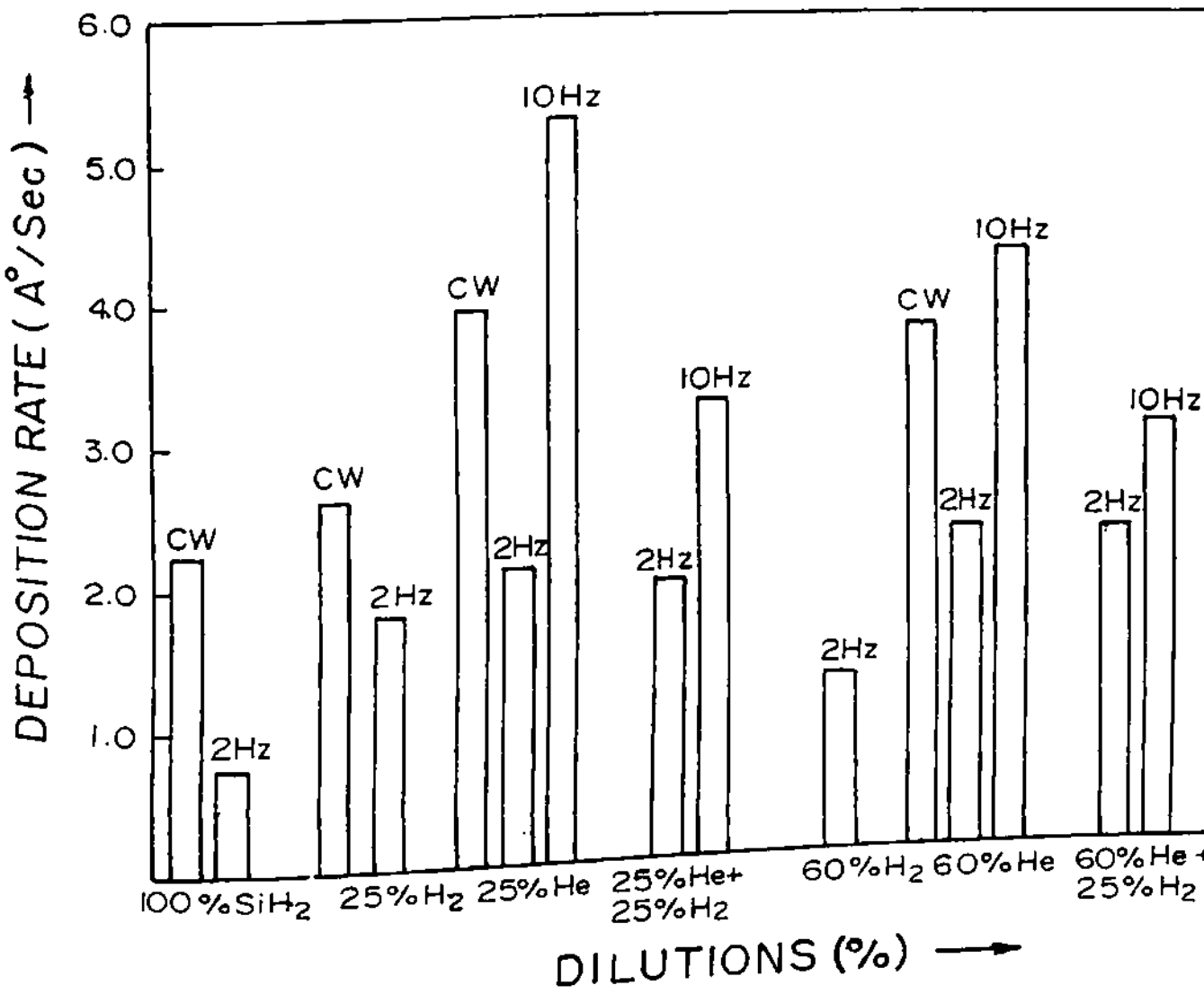

Fig.3C.1 Bar graph representation of growth rates at various dilution and modulation conditions.

He dilution r_d is 2.0 $A^{\circ}s^{-1}$. Similarly at 82% H_2 dilution r_d is 1.3 $A^{\circ}s^{-1}$ whereas for 60% He + 25% H_2 dilution r_d is 2.3 $A^{\circ}s^{-1}$.

3C.3.2 Optical emission spectroscopy

Time resolved OES (TROES) signals corresponding to emission from different excited species at different dilution conditions are plotted in **Fig. 3C.2**. Emission intensities only at 2 Hz modulation was studied. The horizontal axis of **Fig.3C.2** is the same as that of **Fig.3C.1** with the only difference that the different dilution conditions are denoted by 1,2,3 etc. The main observations are the following:

(i) With increasing He dilution (0% to 25% to 60%) SiH^* and Si^* intensities hardly change but the addition of H_2 in the above conditions always cause an increase in the intensity of the above two species.

(ii) Below 60% total dilution H^* intensities at both 656 nm and 486 nm increase with the increasing total dilution. Above 60% dilution it becomes independent of diluent gases. At 60% He dilution it is found that H^* intensities, at both the above wavelengths, are even lower than that at 25% He dilution. On the contrary addition of H_2 in 60% He diluted SiH_4 raises the OES signal upto the 60% H_2 diluted case.

3C.3.3 Optical Band gap

Fig. 3C.3 represents the variation of optical band gap(E_g) in terms of a bar graph for various dilution conditions studied. The most common feature is that for CW discharges E_g values are always less than the E_g values for MPPD. Again E_g values for the films grown under MPPD remain within the range 1.75 ± 0.05 eV except for undiluted SiH_4 films. In undiluted SiH_4 MPPD grown films high E_g (1.94 eV) is rather due to more polyhydride incorporation in the film[3] as evidenced by a very high microstructure factor (0.6). In 25% He diluted SiH_4 MPPD grown films, as modulation frequency is increased E_g also increases. Similar trend with frequency is observed when H_2 is added to SiH_4 + He mixture with their individual magnitudes having increased. On the other hand in 60% He diluted SiH_4 MPPD grown films this frequency dependence of E_g is just opposite i.e. E_g decreases with the increase of modulation frequency as can be seen in **Fig.3C.3**.

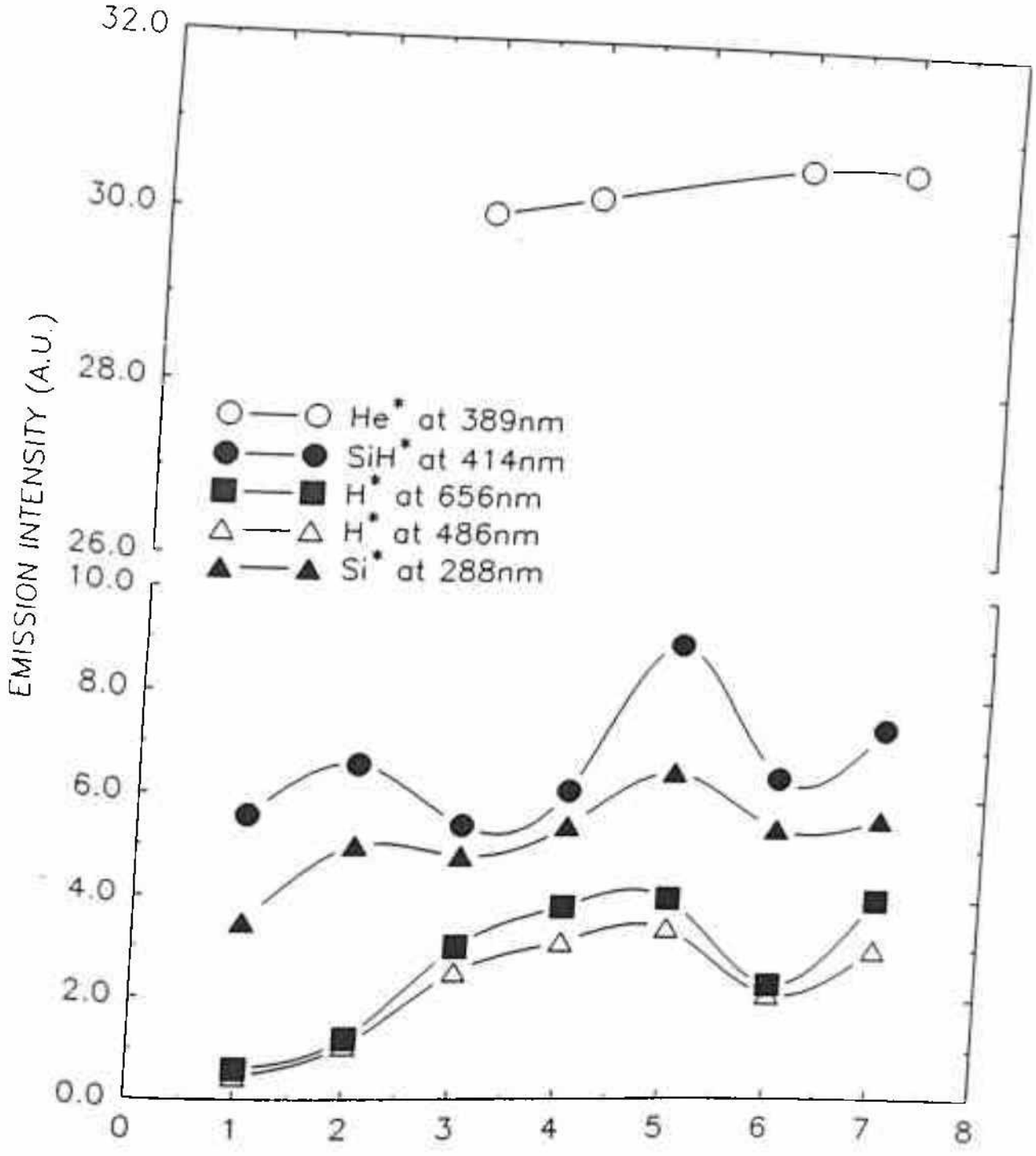

Fig.3C.2 Emission intensities of different excited species at different dilution. 1, 2, 3 ... in the X-axis chronologically corresponds to the dilution conditions as mentioned in Fig.3C.1.

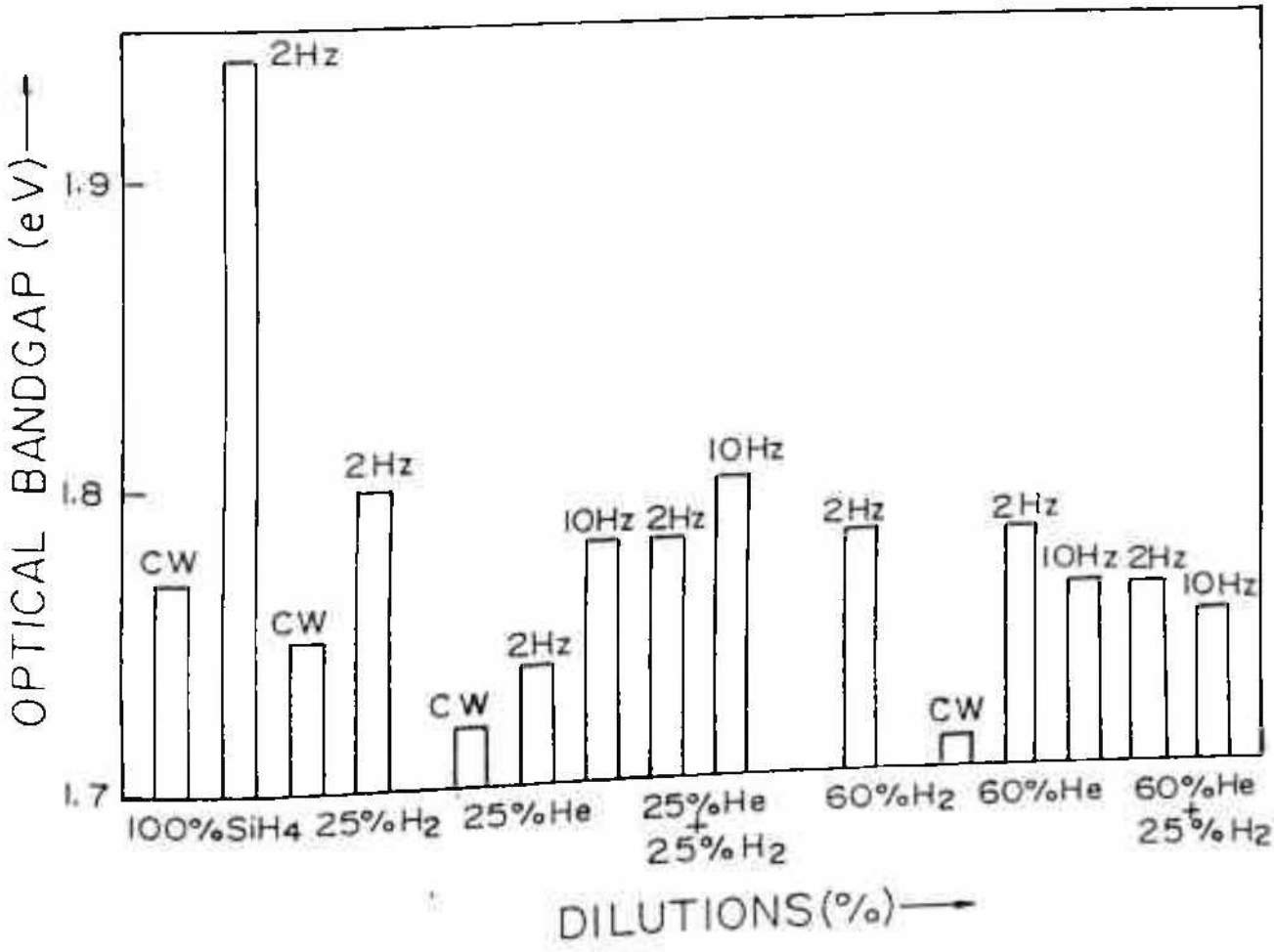

Fig.3C.3 Bar graph representation of E_g at different dilution and modulation conditions

3C.3.4 Photoconductivity and Photosensitivity Measurements

Fig. 3C.4 and **Fig. 3C.5** depict the variations of σ_{ph} and σ_{ph}/σ_D values obtained at different dilutions and modulation conditions in terms of bar graphs. For CW discharges σ_{ph} and σ_{ph}/σ_D values are high. Generally σ_{ph} and σ_{ph}/σ_D values are found to decrease in the sequence, CW to 2 Hz to 10 Hz. At 2 Hz modulation a dramatic improvement in both the parameters are observed only when SiH_4 is diluted either by H_2 or He. The most encouraging picture is that when H_2 is added either in 25% or 60% He diluted SiH_4, σ_{ph} values improve significantly and even become higher than σ_{ph} (CW) values. Another point that should not be missed in **Fig.3C.4** is that improvement in σ_{ph} values after dilution for the films grown at 10 Hz are quiet substantial. Although both σ_{ph} and σ_{ph}/σ_D are $5 \times 10^{-5}\ \Omega^{-1}cm^{-1}$ and 2×10^6 , respectively, for 60% H_2 diluted SiH_4 at 2 Hz MPPD, the growth rate was low $\approx 1.2\ A^o s^{-1}$. In comparison to this at 10 Hz MPPD and 60% He + 25% H_2 diluted SiH_4 discharge grown film σ_{ph} and σ_{ph}/σ_D values are $2 \times 10^{-5}\ \Omega^{-1}cm^{-1}$ and 10^5 respectively and the corresponding growth rate is $\sim 3\ A^o s^{-1}$.

3C.3.5 Hydrogen content (C_H) and Microstructure factor (R)

FTIR traces of He diluted films are shown in **Fig.3C.6(a) & (b)**. The first figure is for set of films with 25% He dilution and the second one is for 60% He dilution. FTIR traces of CW discharge grown films are also shown in the figures (MPHE-03 & MPHE-06).

Fig. 3C.7(a) show hydrogen content, C_H different dilution and modulation conditions in terms of a bar graph. C_H is determined from the IR absorption band around 2000 cm^{-1} similarly, **Fig.3C.7(b)** represents microstructure factor, R of the a-Si:H films grown at different dilution conditions. The important observations are the following:

(i) with increasing total dilution either by He or by H_2, C_H shows a decreasing trend whereas, R factor for films grown at 2 Hz and 10 Hz decreases initially at a faster rate and then only slowly at higher dilutions. Interestingly, it is found that for 60% He dilution R factors are lower than even CW values.

(ii) C_H and R factor both increase sharply when films are grown by modulating the plasma and these values also increases with the increase of modulation frequency.

(iii) It is also observed that as 25% H_2 is added in 60% He diluted SiH_4, C_H values increase for both 2 Hz and 10 Hz modulation by marginal amount ($\approx$ 1 at %). However when 25% H_2 is added in 25% He diluted SiH_4 then for films so grown C_H value for 2 Hz

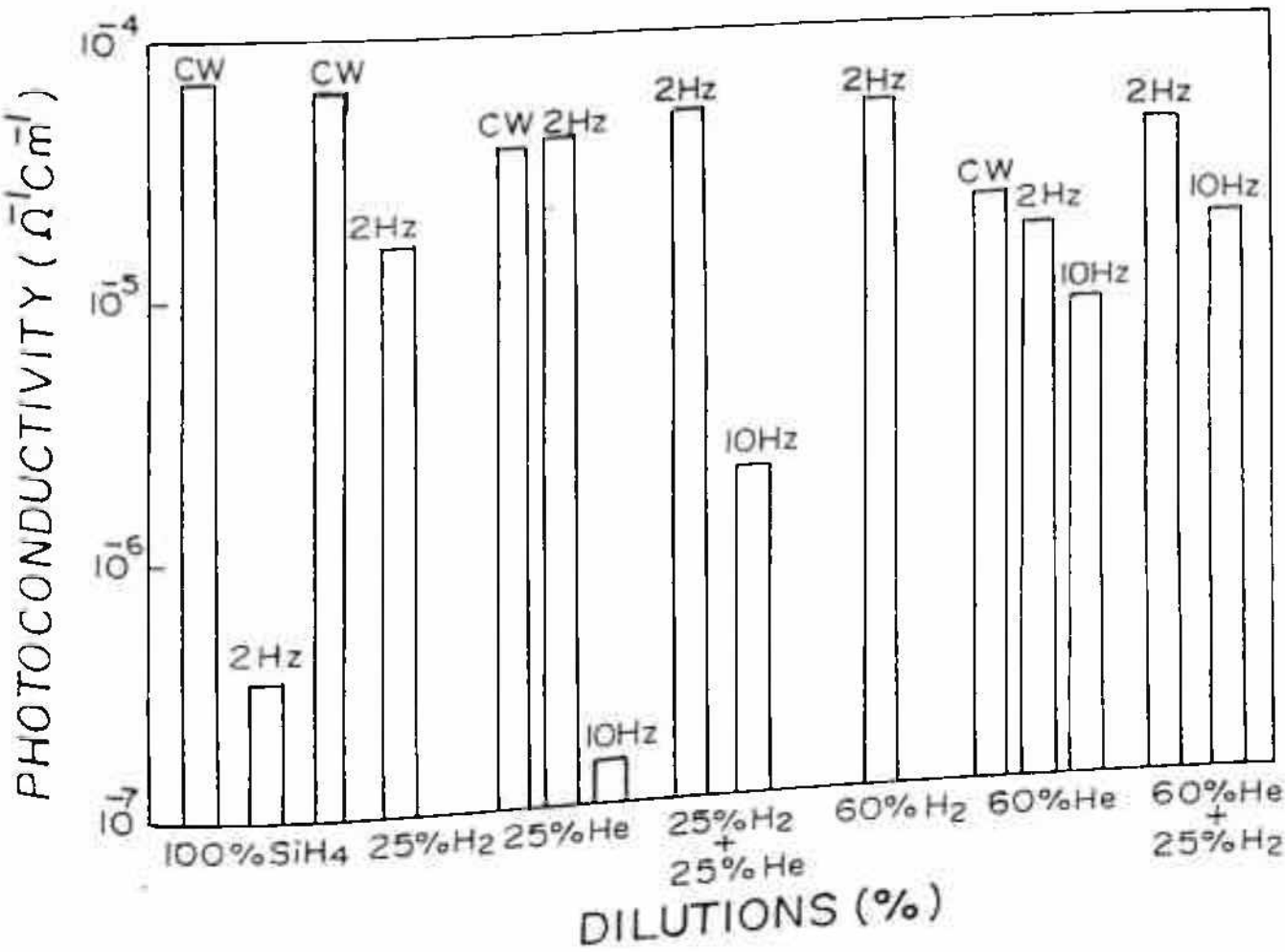

Fig.3C.4 Bar graph representation of σ_{ph} at different dilution and modulation conditions.

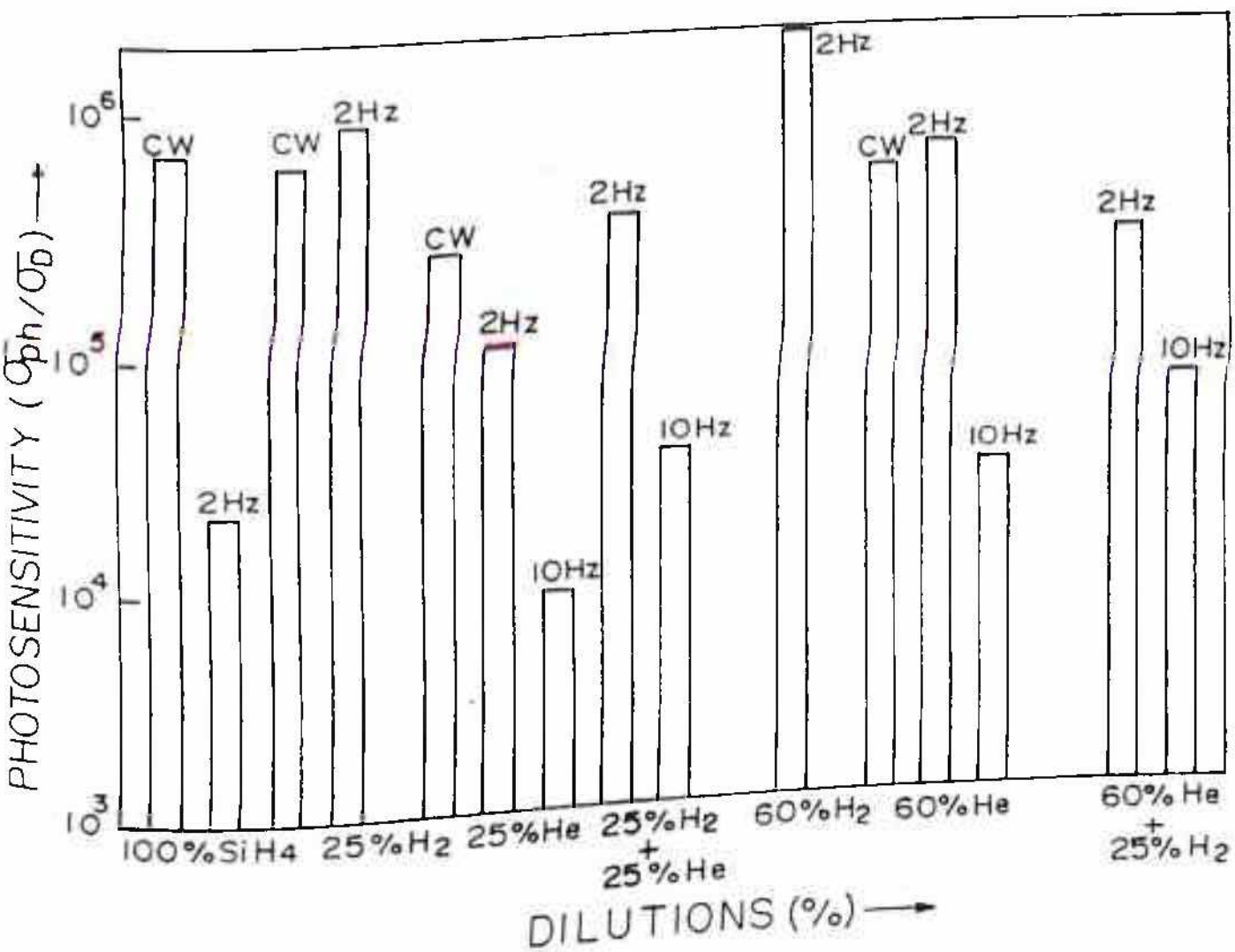

Fig.3C.5 Bar graph representation of σ_{ph}/σ_d at different dilution and modulation conditions.

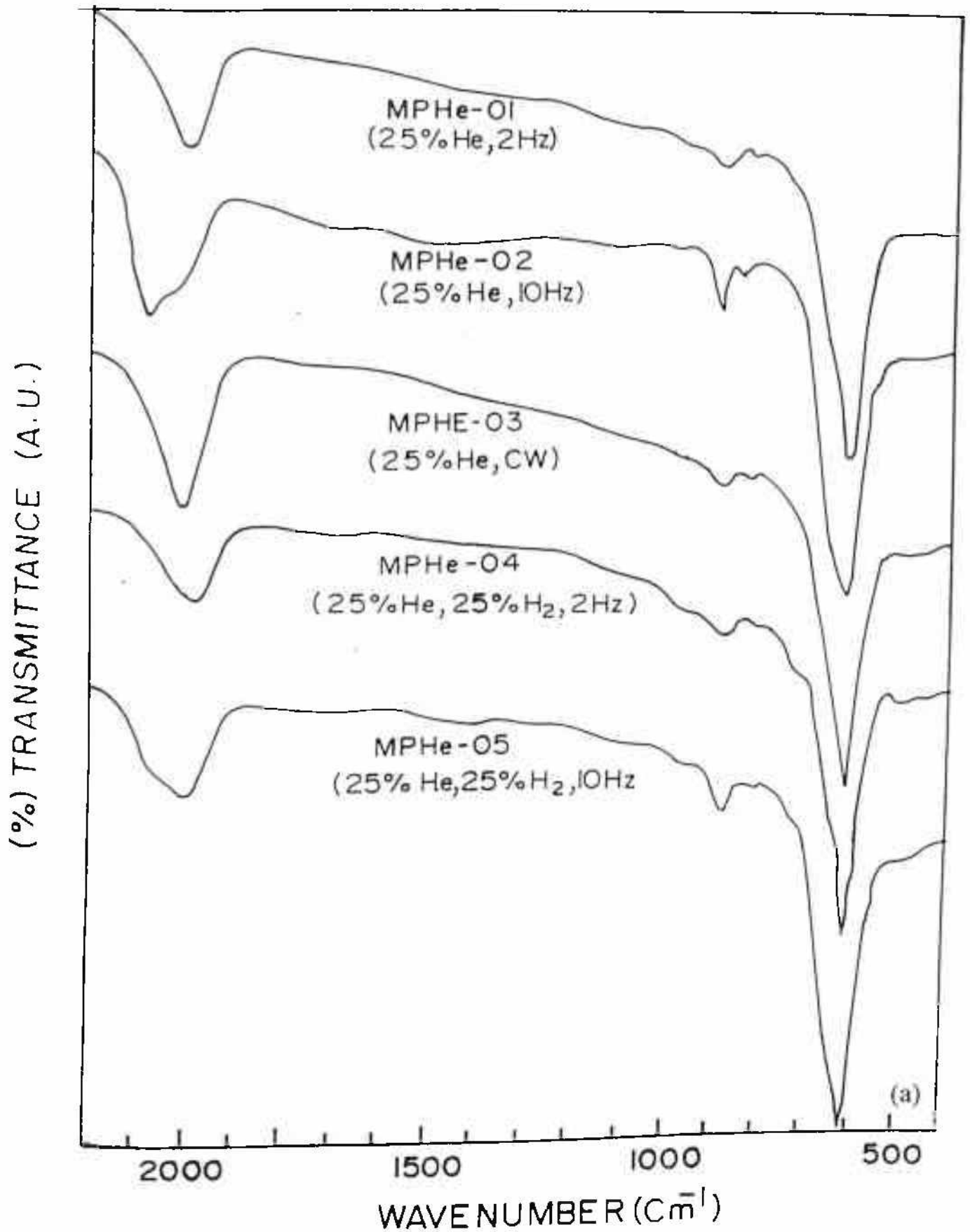

Fig.3C.6 FTIR traces of (a) 25% and (b) 60% He diluted a-Si:H films.

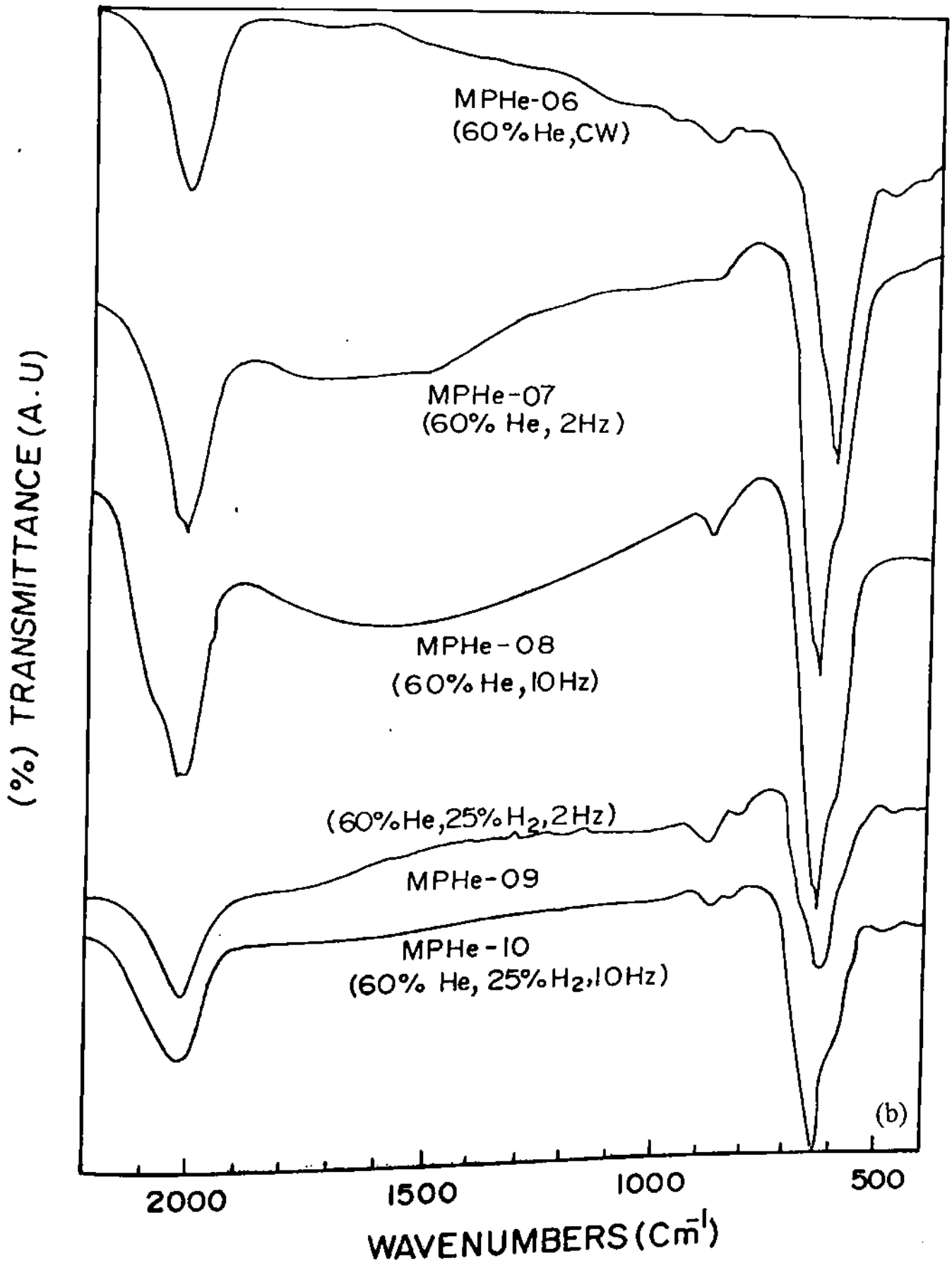
MPHe-06
(60% He,CW)
MPHe-07
(60% He, 2Hz)
MPHe-08
(60% He, 10Hz)
(60%He,25%H2,2Hz)
MPHe-09
MPHe-10
(60% He, 25%H2,10Hz)
(b)
(%) TRANSMITTANCE (A.U)
2000
1500
1000
500
WAVENUMBERS (Cm-1)

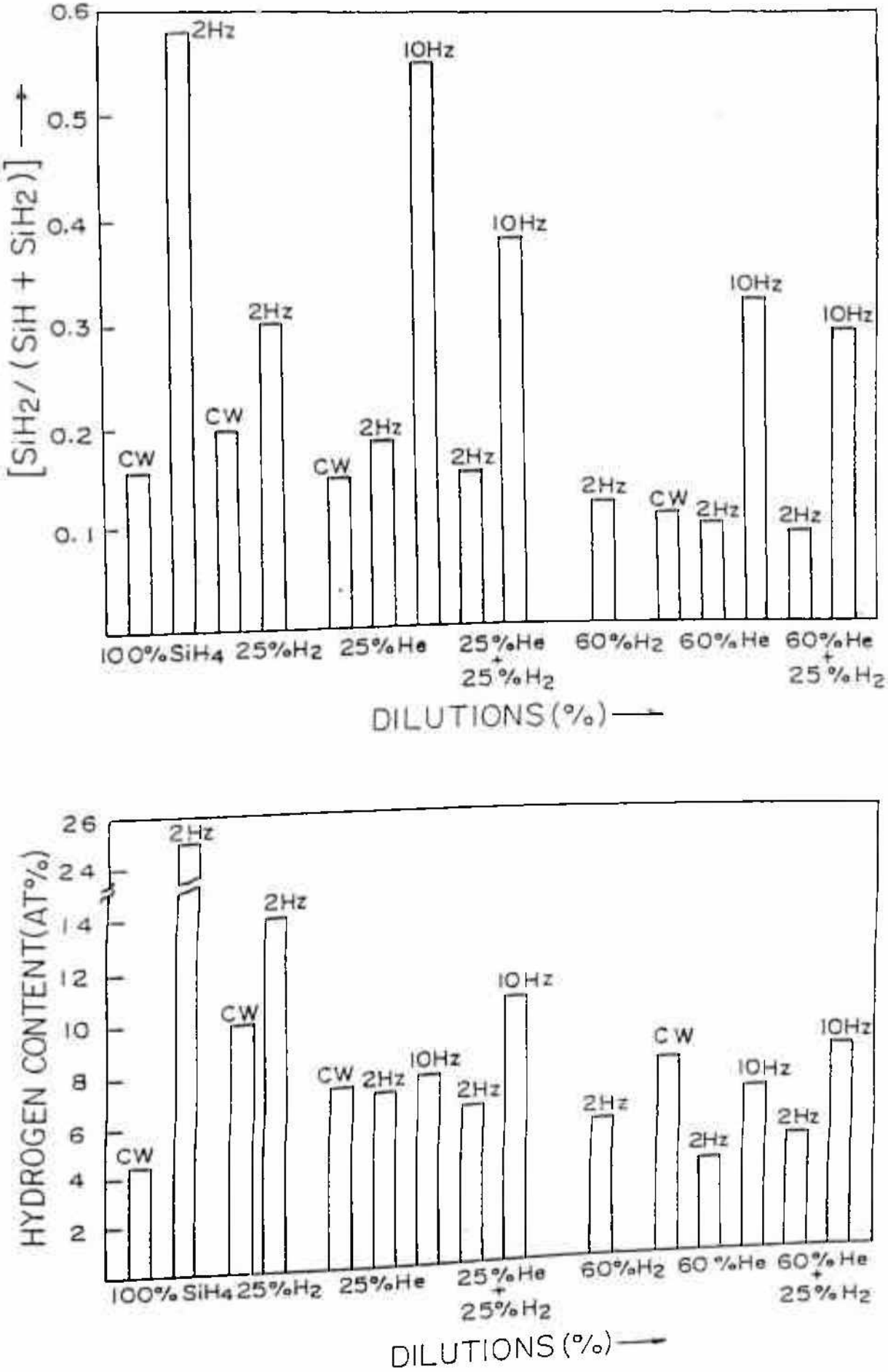

Fig. 3C.7 Bar graph representation of (a) hydrogen content and (b) microstructure factor at different dilution and modulation conditions

modulation changes marginally but for 10 Hz it increases substantially by ≈ 3 at %. In the case of R factor as H_2 is added in He diluted SiH_4, for both the modulation frequencies it is found to decrease and the lowest value obtained is 0.09 at 60% He + 25% H_2 dilution at 2 Hz. At this dilution both σ_{ph} and $\sigma_{ph}\sigma_D$ **(Fig.3C.4 & 3C.5)** values are comparable to the device quality material.

(iv) The difference between the C_H values for films grown at 10 Hz and 2 Hz also increases with increasing He dilution.

3C.3.6 Defect density studies

The PDS spectra from 2.1 eV to 0.9 eV for some of the He diluted films grown at different MPPD environments are shown in **Fig. 3C.8**. It was found that N_D and E_o values are almost similar for 25% He diluted films grown by CW and 2 Hz MPPD. N_D increases by a factor of 2 for 10 Hz grown film but hardly there is any effect of modulation frequency on E_o. As H_2 is added in SiH_4+He mixture N_D and E_o decrease but by small amounts. N_D and E_o values are almost similar for 25% and 60% He diluted films, and also changes in a similar fashion with H_2 addition. Recently Cabarrocas et al. [41] have reported that in highly He diluted SiH_4 (98% He) modulation frequency (f) does not have any effect on N_D. Whereas, for moderate He diluted SiH_4 (40% He) N_D values increase with f and show maxima at 10 Hz. In the present investigation MPPD grown films it is found that N_D increases with f under both 25% and 60% He dilution conditions.

3C.3.7 Dark conductivity Measurement

Temperature dependence of dark conductivity (σ_D) for 25% and 60% He diluted cases are shown in **Fig. 3C.9(a)** and **(b)** respectively. Activation energy values (ΔE_D) for 60% He + 25% H_2 diluted SiH_4 case is lowest compared to all other films. ΔE_D values are nearly equal for all the cases of 25% He dilution grown films, but their σ_D values at room temperature differ by an order of magnitude from 2 Hz and 10 Hz modulation. Whereas in 60% He diluted cases σ_D values at room temperature are almost similar their ΔE_D values are quiet different as shown in the table below:

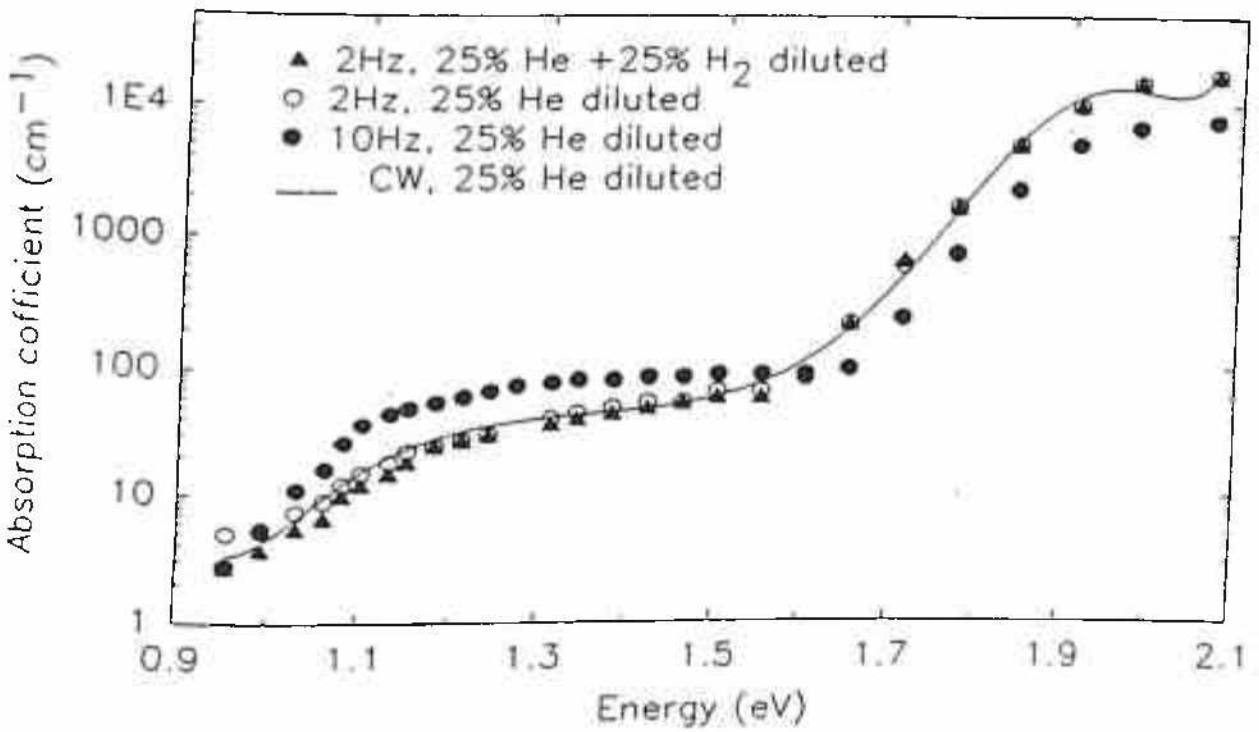

Fig.3C.8 PDS spectra of He diluted a-Si:H films grown at different MPPD environments.

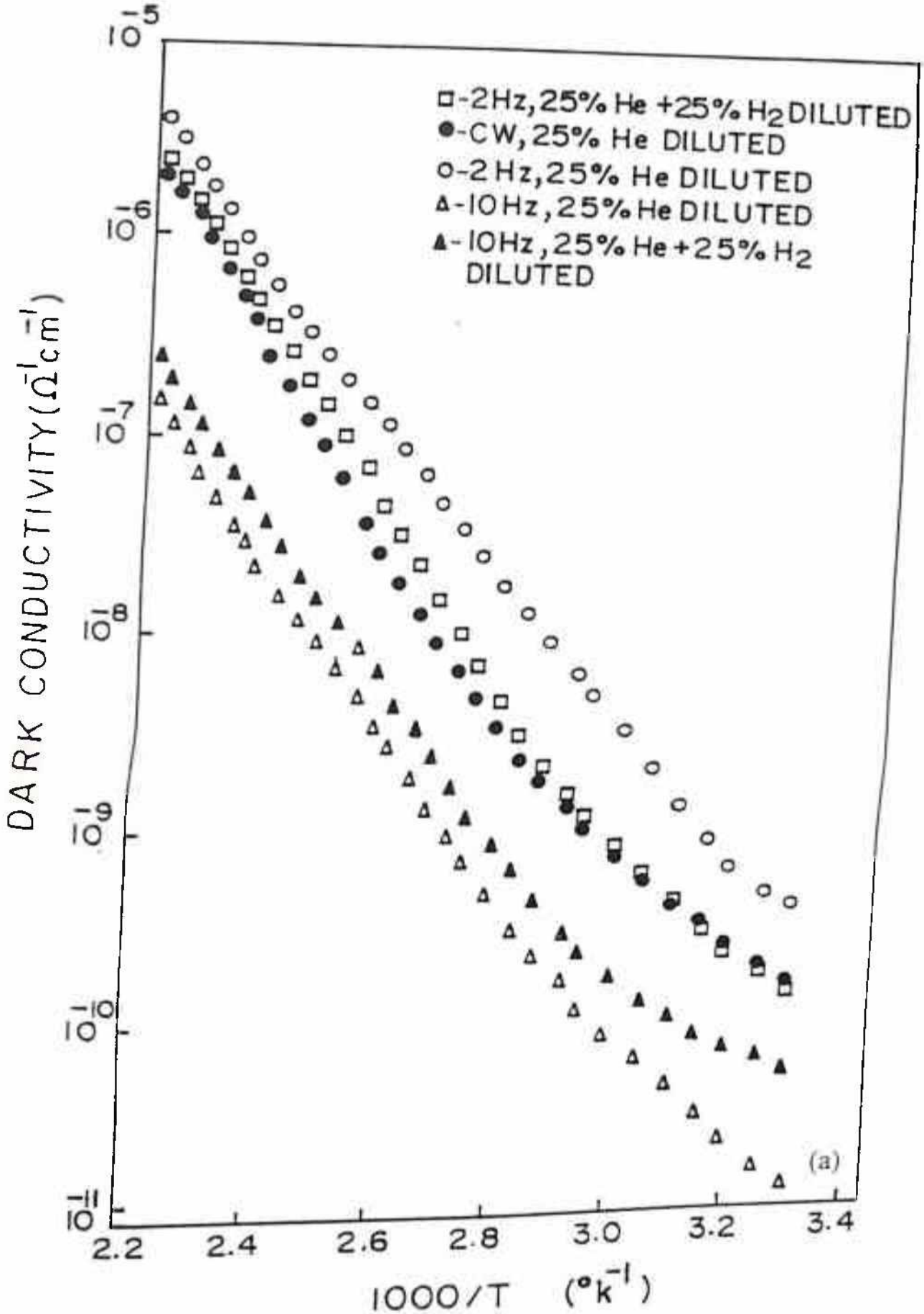

Fig. 3C.9 Temperature dependence of dark conductivity for (a) 25% and (b) 60% He diluted RF MPPD grown a-Si:H films

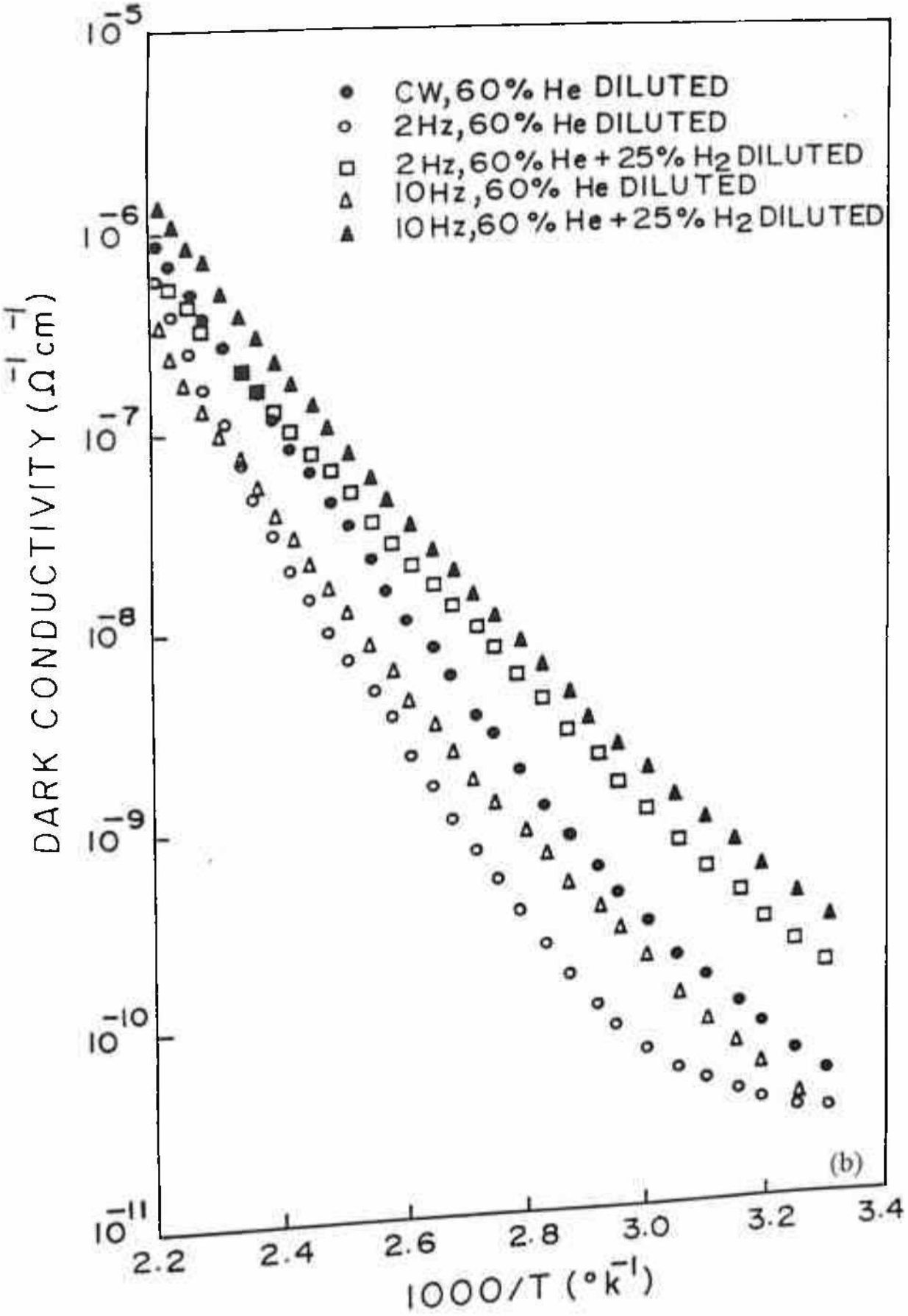
CW, 60% He DILUTED
2Hz, 60% He DILUTED
2Hz, 60% He + 25% H2 DILUTED
10Hz, 60% He DILUTED
10Hz, 60% He + 25% H2 DILUTED
DARK CONDUCTIVITY (Ω cm)⁻¹
10⁻⁵
10⁻⁶
10⁻⁷
10⁻⁸
10⁻⁹
10⁻¹⁰
10⁻¹¹
2.2
2.4
2.6
2.8
3.0
3.2
3.4
1000/T (°k⁻¹)
(b)

Table 3.2 Activation energy and dark conductivity values at different He dilution and modulation conditions.

	25% He dilution		60% He dilution	
	ΔE_D (eV)	σ_D ($\Omega^{-1}cm^{-1}$)	ΔE_D (eV)	σ_D ($\Omega^{-1}cm^{-1}$)
CW	0.97	$1.7x10^{-10}$	0.92	$4.2x10^{-11}$
2 Hz	0.83	$4.0x10^{-10}$	0.94	$2.7x10^{-11}$
10 Hz	0.81	$1.2x10^{-11}$	0.86	$2.6x10^{-11}$

For CW discharges grown films both ΔE_D and σ_D values are higher for 25% He dilution case as compared to 60% He dilution films. It is to be noted here that C_H is less in 25% He dilution grown films as compared to 60% He dilution films, but R factor is less in 60% He diluted MPPD. E_g values are almost similar in both these types of He diluted films.

3C.4 Interpretation of results

At 2Hz modulation, the higher r_d values obtained by discharge in 25% He diluted silane as compared to discharge in 25% H_2 diluted silane shows that the dissociation is higher in He diluted plasma as evidenced from the higher emission intensities of H^*. This is expected from the higher electron density reported in such noble gas plasmas[21]. For still higher He dilution r_d tends to saturate. It is to be noted that at 2 Hz modulation r_d increases slightly at increasing He dilution. Whereas, at higher modulation frequency (10 Hz) i.e. more frequent occurrence of HPL, and with increasing He dilution, increasing ratio of power/SiH_4 flow appears to be the main cause behind the drop in r_d. At 2Hz modulation, drop in r_d is observable only for higher H_2 dilution or when H_2 is added to SiH_4-He mixture.

TROES results do indicate that as H_2 is added to SiH_4+He mixture, H^* and SiH^* intensities both increase. Therefore, indirectly it can be said that addition of H_2 in SiH_4+He mixture increases n_e and τ_e. Fledderman et al.[21] have also observed similar behaviour, although they used different dilutions and measured n_e and τ_e directly. H^* intensities are hardly different in (25% He + 25% H_2) and (60% He + 25% H_2) and at these dilution conditions r_d values are comparable. This appears valid for both the modulation frequencies experimented.

The decrease in r_d and improvement in the optoelectronic properties appears correlated with the increase in H^* intensity with increasing H_2 dilution.

The decrease in r_d as observed at 10 Hz modulation on adding H_2 in SiH_4-He mixture can be explained by invoking the concept of etching mostly by atomic hydrogen, as discussed in section 3B.4. In such discharge conditions substantial improvement in σ_{ph} (as shown in **Fig. 3C.4**) and σ_{ph}/σ_D (as shown in **Fig. 3C.5**) are also observed. Similarly at 2 Hz modulation although no appreciable decrease in r_d is noticed after H_2 addition but increase in σ_{ph}/σ_D is noticeable in ***Fig. 3C.4 & Fig. 3C.5***. At 10 Hz modulation the frequent occurrence of the HPL results in higher density of higher energy electrons as compared to that at 2 Hz modulation. Therefore, amount of atomic hydrogen generated by higher energy electrons will naturally be higher at 10 Hz modulation. Similarly, that such a mechanism is operating not only at 10 Hz but also at 2 Hz modulation can be inferred from the increase in σ_{ph} and σ_{ph}/σ_D values; of course the magnitude of change is low at 2 Hz compared to 10 Hz. At 2 Hz modulation the so called etching effect appears only marginally effective. Another important point is that in the presence of He, preferential etching rate by atomic hydrogen appears to be different from He absent environments. As 25% H_2 is added in 60% He diluted SiH_4, a drop in r_d is noticed but this drop is less compared to the decrease in r_d when same amount of H_2 is added in 25% H_2 diluted SiH_4. Thus, in He rich environment etching by atomic hydrogen appears to be less inspite of the fact that H^* intensities (**Fig.3C.2**) are comparable in both cases. Intuitively it appears that some sort of a surface coverage or shading on the freshly grown top surface by He atoms may be the cause of lower etching rate in He rich environment. However, the differences in atomic sizes of H and He being not very much different (as compared to Ar and Xe) and absence of columnar growth in most of PECVD a-Si:H films studied preclude this possibility. It may be that He dilution provides a different mix of SiH_x[38] ions and radicals other than SiH_3 and this change in environment may explain this lower etching rate. At this point it may be mentioned that microstructure factor (as discussed in **Fig.3C.7(b)**) decreases in both cases i.e. on increasing He dilution or by adding H_2 to the SiH_4+He mixture.

As can be seen from **Fig. 3C.7(a)** films grown in He diluted MPPD environment have lower C_H values (7 at% for 25% He and 4 at% for 60% He dilution) as compared to those reported by other workers for films grown in similar conditions; also these values are found to

be lower than CW values. Kleider et al.[42] have demonstrated that hydrogen related structures of the He diluted a-Si:H films are very different from standard condition grown films (100% SiH_4, low RF power & low pressure etc.). They have found higher C_H & R values in He diluted films are comparable to standard films. In another detailed study on the discharge of SiH_4+He mixture, Mashima et al.[43] have suggested that the deexcitation cross section of long lived He^* (2^3S), where energy (19.81 eV) is much higher than ionisation potential of SiH_4 (12.36 eV). Penning ionisation is a major deexcitation process and excited He atoms (He^*) release energy to the film growth surface and/or subsurface which can help the relaxation of a-Si:H network structure during deposition so as to decrease C_H. In the present study for a fixed RF power as He flow rate increases, number density of He^* increases (evidenced by the TROES signal, **Fig.3C.2**) which in turn causes a further decrease in C_H. At this point it is worthwhile to mention that Cabarrocas et al. [41] have found in their SQWM discharge of 98% He diluted SiH_4 that C_H = 9.5 at% for CW and 15.5 at% at 10 Hz modulation and likewise for 40% He dilution their C_H values are 24.9 and 22.7 at % respectively. These values are quiet high compared to C_H values obtained in the present investigation. They have attributed this high C_H to the accumulation of H_2 in artificially generated interfaces in SQWM. On the contrary the films grown in MPPD environment at low (25%) and moderate (60%) He dilutions show quiet a low C_H values as compared to their films, like 7 at% at low dilution and 4 at% at moderate dilution. However, the said mechamism[41] may explain the increase in C_H when H_2 is added in SiH_4+He mixture at 10 Hz MPPD, but the changes in other parameters like R factor (**Fig. 3C.7(b)**) and optical band gap(**Fig. 3C.3**) rather obscures the picture. Again the same idea cannot explain the fact that C_H changes very little at 10 Hz while increasing He dilution from 25 to 60%. The most probable explanation for C_H increasing with modulation frequency, may perhaps be the following. According to Perrin et al.[44] the transition from α to γ regime is due to a better coupling of the RF power to the plasma. As modulation frequency increases the transition of the discharge from α to γ regime becomes more prominent accompanied by the appearance and subsequent growth of the particle sizes that are found close to the sheath boundaries. This is again supported by the fact that both R factor (**Fig.3C.7(b)**) and defect density, N_D (**Fig.3C.8**) increase. The general consensus regarding the particle formation and dynamics in plasma discharge is that they are negatively charged and are confined by the sheath electric field near the cathode. These particles

continue to grow in size unless they are driven away by gas flow, ion wind and so on. In MPPD environment particles are electrostatically confined for longer periods compared to the conventional pulsed plasma discharge. If such particles reach the growth surface through some suitable channel (Time during which sheath potential changes from very high to a low value) polymer rich defective layers are formed. It is more likely that by some means e.g. gas flow drag, ion wind during the transition of electric field they can reach the growth surface and severely damage the film surface causing an increase in C_H and N_D values. It is also to be noted that σ_{ph} and σ_{ph}/σ_D values decrease.

The enhanced optical absorption as seen by PDS measurement, at higher modulation frequency (10 Hz), may be due to the incorporation of particles in the films as discussed in the previous section. If reasonable powder growth rate is considered to be 500 $A^{\circ}s^{-1}$ [41] then during a period of 25 msec HPL a powder can grow upto 12.5 A°. But in MPPD environment these powders (supposed to be negatively charged) encounter number of HPL periods before they are driven out from the discharge zone and so can grow to a bigger size. Now if these powders get incorporated into the film they may increase excess absorption in the film.

3.2 Conclusions

Undiluted MPPD

In the present study a novel pulsed plasma growth of a-Si:H in which RF power is switched between a high power and a non-zero low power limits has been carried out. First both SiH_4 and Si_2H_6 without any dilution have been used as feed gases. It has been found that undiluted Si_2H_6 formed films grown at rates upto 9 $A^{\circ}s^{-1}$ to be of sufficiently good quality and perhaps can be further improved after optimisation of the process. From these results it appears that for such type of pulsed plasma growth, use of disilane has a distinct advantage. Highest σ_{ph} and E_g values obtained are 4.4×10^{-6} $\Omega^{-1}cm^{-1}$ and 2.07 eV respectively. The above values appear to be comparable to device quality a-Si:C:H. Further detailed optimisation of the process parameters may prove this pulsed plasma discharge suitable for fabricating Tandem Solar Cells and even multilayers by tailoring the band gap of the a-Si:H material as found possible in the present study.

It is found that dwell time can be used as an additional process parameter to tailor the material properties

It is also found that in all cases film uniformity is comparable to that of CW deposited films, implying that fast switching of plasma between LPL and HPL hardly has any effect on the uniformity of the plasma over a fairly large deposition area (100 cm^2).

It is also seen that higher τ is required for lower HPL and vice versa to cross the CW deposition rate. The lack of proper plasma diagnostics does not allow a proper picture regarding the mechanism for this lower growth rate to emerge. However, the electron density (n_e) and electron decay time constant (τ_e) measurement of Overzet et al.[6] and study of helium dilution in silane in a pulsed discharge by, Fleddermann et al.[21] suggest that electron attachment could be the reason behind the lower r_d in MPPD as well.

H_2 diluted MPPD

As in the case of CW discharges, for a given set of pulse parameters, r_d attains a maximum value at a particular H_2 dilution. This dilution value is significantly different from those reported by other workers. Thereafter, r_d slowly decreases to reach seemingly a steady state value at higher dilutions, controlled by an etching process, irrespective of the number of silane molecules present in the discharge. Again the etching reactions predominantly taking place under high hydrogen dilution conditions are further accompanied by a gradual improvement in σ_{ph} values between 25% and 75% dilution range. TROES results supports this view.

Further, it is shown that r_d can be increased by hydrogen dilution beyond CW value by varying τ and HPL without onset of powder formation and thereby improve the optoelectronic properties of the films.

In undiluted MPPD, as growth rate exceeds the CW value onset of powder formation occurs and the apparent advantage of achieving higher growth rate in MPPD does not remain. However, in the case of H_2 diluted MPPD it appears from the present investigations that CW growth rate can be exceeded appreciably without any visible powder formation.

He, He+H_2 diluted MPPD

Based on the observation made on He+H_2 dilution studies, it can be concluded that rate of deposition in an MPPD environment depends both on the partial pressures of the constituent gases and on the parameters of the modulating pulse.

In MPPD higher r_d is observed under He dilution as compared to H_2 dilution. This could be due to occurrence of higher n_e in He diluted discharges as suggested by Fleddermann[21].

H_2 seems to play a dual role since its addition increases n_e even in He diluted plasma as

The results of the investigations that have been presented in this chapter clearly reveal that it has been possible in only small measure to improve this situation. Firstly, unlike Cabarrocas et al.[35] a-Si:H films when produced by MPPD do not deteriorate in quality. In fact they could be grown to least upto 3 $A^{\circ}s^{-1}$ with as good a quality as is expected under the standard condition of growth. What however needs to be emphasised is that depth of modulation in the present case was always below 100%. In fact the conventional pulsed plasma technique (SQWM) specifically require that during certain part of excitation the plasma need necessarily be extinguished. It is during this time the dust particles at the sheath edge are driven out of the reactor. In the present experiment the silane plasma was never extinguished but only switched between a low and a high power level. The fact that neither σ_{ph} nor PDS signals showed deterioration raises doubt about the validity of the accepted mechanism of SQWM. However the results obtained are not very gratifying and the search should continue. In fact by setting a VHF plasma in the same reactor and pulsing the same in the said modified way marked improvement has been noticed in the film quality and this is being reported in the following chapter.

He, He+H_2 diluted MPPD

Based on the observation made on He+H_2 dilution studies, it can be concluded that rate of deposition in an MPPD environment depends both on the partial pressures of the constituent gases and on the parameters of the modulating pulse.

In MPPD higher r_d is observed under He dilution as compared to H_2 dilution. This could be due to occurrence of higher n_e in He diluted discharges as suggested by Fleddermann[42]

H_2 seems to play a dual role since its addition increases n_e even in He diluted plasma as also is found to improve optoelectronic properties of the material so grown presumably by suitably removing the weaker bonds.

Intuitively it appears that some sort of a surface coverage or shading on the freshly grown top surface by He atoms may be the cause of lower etching rate in He rich environment. However, the differences in atomic sizes of H_2 and He being not very much different (as compared to Ar and Xe) and absence of columnar growth in most of PECVD a-Si:H films studied precludes this possibility. It may be that He dilution provides a different mix of SiH_x ions and radicals other than SiH_3 and this change in environment may explain this lower etching rate.

The model proposed by Mashima et al.[43] that excited He atoms release energy to the film growth surface and/or subsurface which can help the relaxation of a-Si:H network so as to decrease C_H seems to be valid in these He diluted films as well. The idea of hydrogen accumulation in artificially generated interfaces as proposed by Cabarrocas et al.[41] does not appear to be valid in these He diluted films grown for the present study.

Therefore, it appears from these investigations that in order to optimise both r_d and the quality of a-Si:H films using MPPD one has to judiciously choose a mixture of diluents rather than a single diluent.

At this point it will be very instructive to compare the results that have been presently obtained with what Cabarrocas et al.[35] have obtained after a very careful study of square wave modulated RF discharge of SiH_4 + He mixture. Their main conclusion was "At both high and low deposition rates the modulation of RF discharge results in a negligible effect or deterioration of film properties, particularly in the σ_{ph} which we have found to be the most sensitive parameter".

The results of the investigations that have been presented in this chapter clearly reveal that it has been possible in only small measure to improve this situation. Firstly, unlike Cabarrocas et al [35] a-Si:H films when produced by MPPD do not deteriorate in quality. In fact they could be grown to least upto 3 $A^{o}s^{-1}$ with as good a quality as is expected under the standard condition of growth. What however needs to be emphasised is that depth of modulation in the present case was always below 100%. In fact the conventional pulsed plasma technique (SQWM) specifically require that during certain part of excitation the plasma need necessarily be extinguished. It is during this time the dust particles at the sheath edge are *driven out of the reactor*. In the present experiment the silane plasma was never extinguished but only switched between a low and a high power level. The fact that neither σ_{ph} nor *PDS* signals showed deterioration raises doubt about the validity of the accepted mechanism of SQWM. However the results obtained are not very gratifying and the search should continue. In fact by setting a VHF plasma in the same reactor and pulsing the same in the said modified way marked improvement has been noticed in the film quality and this is being reported in the following chapter.

3.3 References

1. J P M. Schmitt, *Mat. Res. Soc. Symp. Proc.* **219**, 631 (1991).

2. Y. Hishikawa, S. Tsuda, K. Wakisaka and Y. Kuwano, *J. Appl. Phys.* **73**, 4227 (1993).

3. P. Roca i Cabarrocas, *J. Non-Cryst. Solids* **162-164**, 37 (1993).

5. T. Yoshida, Y. Ichikawa and H. Sakai, Proc. of 9th EC PVSEC, Freiburg 1989, p.1006.

4. A. Shah, J. Dutta, N. Wyrsch, K. Prasad, H. Curtins, F. Finger, A. Howling and Ch. Hollenstein, *Mat. Res. Soc. Symp. Proc.* **258**, 15 (1992).

6. L.J. Overzet and J.T. Verdeyen, *Appl. Phys. Lett.* **48**, 695 (1986).

7. Y. Watanabe, M. Shiratani, Y. Kubo, I. Ogawa and S. Ogi, *Appl. Phys. Lett.* **53**, 1263 (1988).

8. T. Yoshida et al., Extended abstract of the 36th spring meeting (The Japan Society of Applied Physics) No. 1, p. 40, 390 (1989).

9. G. Bruno, P. Capezzuto, G. Cicala and P. Manodoro, *Mat. Res. Symp. Proc.* on Chemical Perspectives of Microelectronic Materials II ed. H. Bubois et al. p.289, (1991).

10. A.A. Howling, Ch. Hollenstein, J-L. Dorier, P. Paris and M. Fabre, *Proc 10th EC-PVSEC* (Lisbon) ed. A. Lugue et al. p-169 (1991).

11. A. Bouchoule, A. Plain, L. Boufendi, PH.J. Bloudean and C. Laure, *J. Appl. Phys.* **70**, 1991(1991).

12. G. Scarsbrook, I.P. Liewellyn, S.M. Ojha and R.A. Heinecke, *Vacuum* **38**, 627 (1988).

13. Y. Watanabe, M. Shiratani and H. Makino, *Appl. Phys. Lett.* **57**, 1616 (1990).

14. Y. Watanabe, M. Shiratani, Y. Kubo, I. Ogawa and S. Ogi, *Appl. Phys. Lett.* **53**, 1263 (1988).

15. T. Hamasaki, M. Ueda, M. Hirose and Y. Osaka, *J. of Non-Cryst. Solids* **59 & 60**, 679 (1983).

16. H. Kausch and R.D. Plattner, *Proc. 11TH E.C. Photovoltaic Solar Energy Conference*, edited by W. Palz (Montreux, Swizerland 12-16 Oct 1992), p. 195.

17. G. Bruno, P. Capezzuto, M. Losurdo, P. Manodoro and G. Cicala, *J. of Non-Cryst. Solids*, **137&138**, 753 (1991).

18. M. Kawasaki, Y. Matsuzaki, K. Fueki, K. Nakajima, Y. Yoshida and H. Koinuma, *Nature* **331**, 153 (1988).

19. S.K. Park and D.J. Economou, *J. Elec. Chem. Soc.* **137**, 2103 (1990).

20. L.J. Overzet, J.H. Beberman and J.T. Verdeyen, *J. Appl. Phys.* **66** 1622 (1989).

21. C.B. Fleddermann, J.H. Beberman and J.T. Verdeyen, *J. Appl. Phys.* **58**, 1344 (1985).

22. R.C. Ross and J. Jaklik, Jr., *J. Appl. Phys.* **55**, 3785 (1984).

23. S. Furukawa and N. Matsumoto, *Phy. Rev. B* **31**, 2114 (1985).

24. J.P. Conde, K.K. Chan, J.M. Blum, M. Arienzo and J.J. Cuomo, *J. Appl. Phys.* **71**, 3990 (1992).

25. F. Alvarez, M. Sebastini, F. Pozzilli, P. Fiorini and F. Evangelisti, *J. Appl. Phys.* **71**, 267 (1992)

26. M. Capitelli, C. Gorse, R. Winkler and J. Wilhelm, *Plasma Chem. Plasma Sources* **8**, 399 (1988).

27. P.E. Vanier, F.J. Kampas, R.R. Corderman & R. Rajeswaran, *J. Appl. Phys.* **56** 1812 (1984).

28. T. Hamasaki, M. Ueda, M. Hirose, Y. Osaka, Proc. *Int. Ion Engg. Cong.* Kyoto, Japan Vol. 3, p-1403 (1983).

29. T. Hamasaki, M. Ueda, A. Chayahara, M. Hirose & Y. Osaka, *Appl. Phys. Lett.* **44**, 600 (1984).

30. S. Kato & T. Aoki, *J. Non-Cryst. Solids* **77 & 78**, 813 (1985).

31. G. Bruno, P. Capezzuto & F. Cramarossa, *Thin Solid Films* **129**, 217 (1985).

32. S. Verrek, *Chimia*, **34**, 489 (1981).

33. N. Blayo and B. Drevillon, *J. Non-cryst Solids* **137&138**, 775 (1991).

34. J.C. Knights, R.A. Lujian, M.P. Rosenblum, R.A. Street, D.K. Beigleson and R.A. Reimer, *Appl. Phys. Lett.* **38**, 331 (1981).

35. P. Roca i Cabarrocas, Y. Bouizem and M.L. Theye, *Phil. Mag. B* **65**, 1025 (1992).

36. J.C. Knights and R.A. Lujian, *Appl. Phys. Lett.* **35**, 244 (1979).

37. W.E. Spear and P.G. LeComber in *'The Physics of Amorphous Silicon - I'* ed. J.J. Joannopoulos and G. Lucovsky (Springer Verlag, Berlin, 1984).

38. C. Hollenstein, U. Kroll, A.A. Howling, J. Dutta, J.-L. Dorier, J. Meier, R. Tschrner and A. Shah, *Proc., 11th E.C.PVSEC*, p-76 (Harwood Academic Publ., 1992).

39. S. Vognoli, R. Meaudre, M. Meaudre, L. Chanel and P. Roca i Cabarrocas, *15th ICAS, Cambridge/ J. Non. Cryst. Solid.*

40. R. Meaudre, M. Meaudre, S. Vignoli, P. Roca i Cabarrocas M. L. Theye, *Phil. Mag. B* **67**, 497 (1993).

41. P. Roca i Cabarrocas & A. Lloret, *Appl. Phys. A* **58**, 365 (1994).

42. J.P. Kleider, C. Longe and P. Roca i Cabarrocas, *15th ICAS, Cambridge/ J. Non. Cryst. Solid.*

43. S. Mashima, G. Ganguli and A. Matsuda, *Plasma Sources Sci. & Tech.* **2** 23 (1993).

44 J. Perrin, Ch. Bohm, R. Etemadi and A. Lloret, *Plasma Sources Sci. & Tech.* **3**, 252 (1994).

CHAPTER-IV

Modified Pulsed Plasma Discharge at 100 MHz

4.1 Introduction

Presently 13.56 MHz is the most commonly used frequency for low pressure plasma processing. This choice is dictated by convention and consequent availability of RF technology suited to this industrial frequency rather than by the optimisation of the physical processes in the discharge. Sustained efforts have been made, during the last decade in achieving high quality intrinsic a-Si:H films at high deposition rates essentially to enhance the production capacity of a-Si:H based devices (e.g. continuous production line of a-Si:H solar modules). The progress in terms of industrial developments is still limited by serious gaps in the understanding the process and control of material properties. In this context technological goals to be reached are the following:

i) increase of film deposition rate, for low cost production,

ii) improvement of surface homogeneity, for the scaling up process to large area devices and

iii) achievement of very high quality material (a-Si:H) for attaining higher efficiency and more stable devices.

To achieve the above goals two different approaches are possible. First, optimisation of the process and material so produced by acting on the external macroscopic parameters (power, substrate temperature, pressure, flow, reactor geometry etc.). Second, the role played by internal microscopic plasma parameters (electron density, electron temperature, neutral and ion density etc.) on the deposition process and material quality. However, the attainment of high deposition rates (r_d) requires a high radical generation rate and at the same time maximum utilisation of the precursors produced by plasma decomposition. To enhance radical generation the partial pressure of source gas needs to be increased as also the processes

leading to the ionisation processes to be highly efficient. However, high pressure discharges are known to lead to gas phase nucleation and polymerisation. On the other hand higher electron density, obtained by coupling higher RF power to the discharge may concurrently lead to significant ion bombardment on the growth surface and can indeed, damage the growth surface unless it is optimised for right energy and flux.

An elegant way of achieving higher electron density is by increasing the plasma excitation frequency. It has been found that a change of excitation frequency (ω) also modifies electron energy distribution function (EEDF) of the plasma; higher the excitation frequency higher will be the number of electrons at high energy end of the EEDF. Ferreira and Loureiro[1], Wertheimer and Moisan[2] demonstrated that the shape of EEDF in Ar plasma depends on the parameter ω/ν, where ν is the electron - neutral collision frequency for momentum transfer and ω is the angular frequency of the applied electromagnetic field. Various effects of ω/ν on the EEDF are listed in the following.

i) EEDF tends towards a maxwellian distribution with increasing ω/ν

ii) a relatively large population of electrons gets into the high energy tail of the EEDF (**Fig.4.1**)

iii) average electron energy decreases with increasing ω

iv) total electron density increases with ω at constant plasma power

ω/ν value approaches zero for DC plasma, ∞ for microwave plasma and it always remains less than unity for RF plasmas. For VHF plasmas ω/ν could be significantly higher than that at RF frequencies, depending upon operating pressure.

A comparison of the theoretical analysis of the frequency effects on the discharge characteristics with the results of Ar discharge and hydrocarbon polymer deposition[3] shows:

i) electron density increases significantly with frequency only above 200 MHz

and

ii) electron-electron interaction can not be neglected in low frequency plasmas and as a result, enhancement of high energy electrons with increasing frequency will not be as pronounced as predicted earlier.

Glow discharge deposition of a-Si:H at frequencies in the VHF range (30 to 300 MHz) has attracted considerable interest since the work of Curtins et al.[4]. It has been shown by them that high quality material can be prepared at deposition rates upto 20 $A^{\circ}s^{-1}$ as compared to 2 -

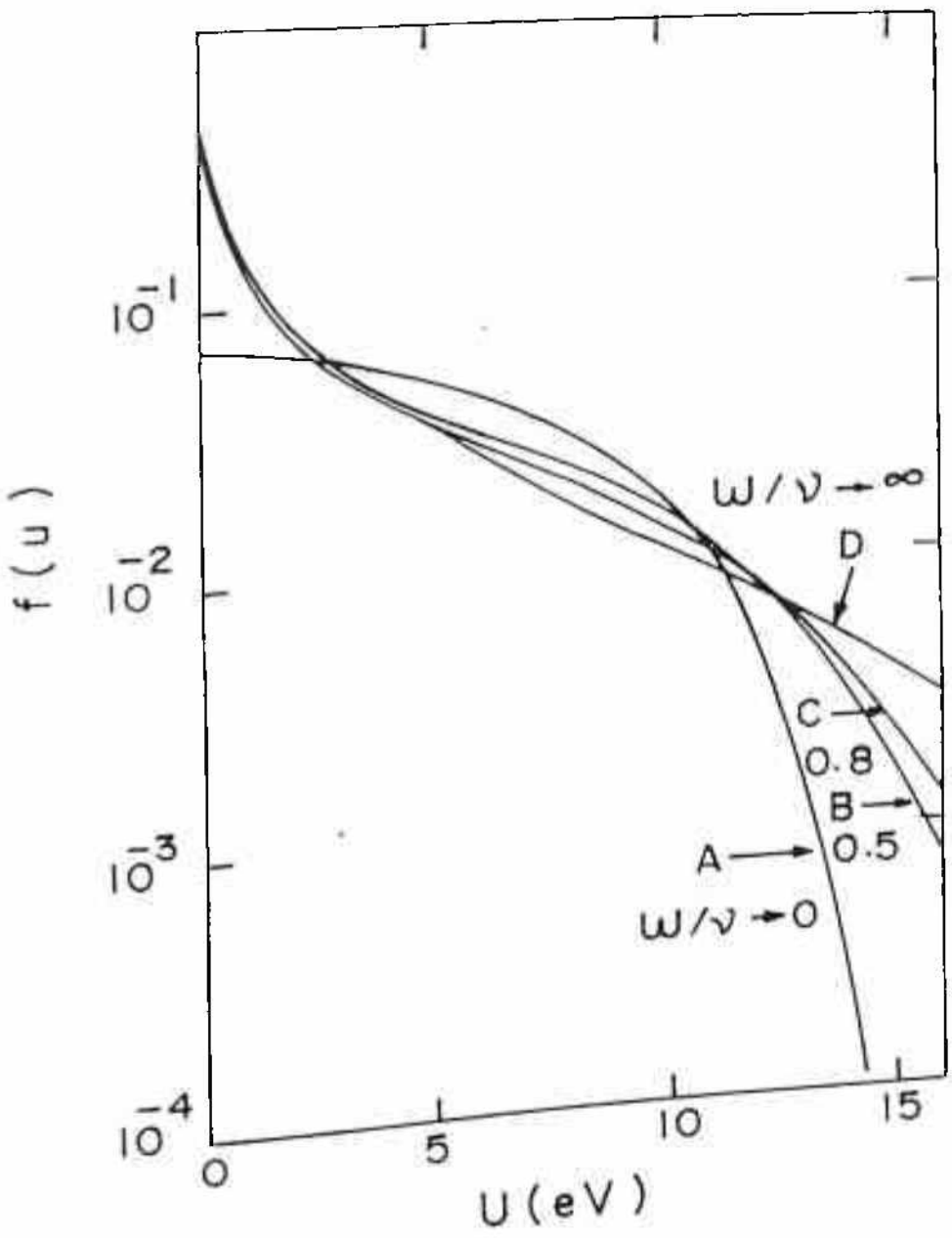

Fig.4.1 Electron energy distribution function at different excitation frequency.

3 $A°s^{-1}$ in a conventional RF deposition system while maintaining almost comparable optoelectronic properties as at 13.56 MHz. These authors explained the observed increase of deposition rate largely based on the hypothesis of increase in the population of high energy electrons due to increasing ω. This will cause higher ionisation, a large total electron density, more efficient dissociation and hence higher r_d. They also observed that the extremely well contained plasma glow at VHF in the interelectrode space contributes in a way to the enhancement of growth rate.

It will be contextual to mention that before Curtins et al.'s[4] discovery it was believed that a further increase of excitation frequency (beyond 13.56 MHz) would not have a major influence on the growth and properties of a-Si:H because one is already above the ion plasma frequency regime. Above this frequency, ions are considered to remain stationary in the alternating electric field and, thus, a further increase of excitation frequency was originally assumed to have no direct beneficial effect on process performance. Despite this, the Neuchatel group[4] obtained a considerable increase in the deposition rate of device quality material upto 20 $A°s^{-1}$ at a frequency of about 70 MHz as compared to typical growth rate of 2 - 3 $A°s^{-1}$ for a 13.56 MHz discharge.

After two years of this discovery by Neuchatel group[4], Glasstech Solar Inc., USA[5] came up for the first time with a solar cell having an efficiency ≈ 10% over 1 cm^2 area grown at 20 $A°s^{-1}$ using 110 MHz discharge in one of their research reactor. However, they used a low a pressure (≈ 50 to 80 mTorr) disilane discharge. Their main idea for working at low pressure was to reduce gas phase reactions which otherwise leads to polymerisation. Recently Neuchatel[6] group has reported deposition of a-Si:H/a-Si:H stacked cells grown in a singlezone reactor using VHF-GD and obtained an initial efficiency of 9.8% and a stabilised 9% efficiency. For these cells i-layers were grown at 4.0 $A°s^{-1}$.

Oda et al.[7] have reported a comparative study of 13.56 and 144 MHz discharge grown a-Si:H. They concluded with the help of Langmuire probe, optical emission and electrode potential measurements that VHF plasma decomposition leads to a large population of high energy electrons compared to RF plasma. Although they correlated increase of deposition rate with the increase in OES signals and EEDF, they did not mention any exact nature of these correlations. They found that for the VHF discharge, the excitation frequencies happen to be larger than ion-neutral collision frequency but close to the plasma frequency. In fact, plasma

frequency discriminates whether the electron can follow the alternating electric field or not. Within an year the same group demonstrated[8] thin film transistors with a mobility of 1.5 $cm^2V^{-1}s^{-1}$ and a current on/off ratio of 10^7 for films grown in discharges maintained at 144 MHz.

In another pioneering study Matsuda et al.[9] showed that internal stresses in a-Si:H films, prepared by the glow discharge decomposition of SiH_4 to be high in films grown at frequencies lower than 500 KHz, and to be low for those films deposited at higher frequencies (≈ 50 MHz). They attributed the low stress in films grown at higher frequencies to the low energy ion bombardment of the deposition surface. In this connection it is to be noted that Favre et al.[10] have been able to deposit 100 μm thick a-Si:H film using 70 MHz discharge. This is in contrast to the tendency of 13.56 MHz discharge grown films to peel off at comparable thicknesses. Therefore, it becomes absolutely clear that intrinsic stress in a-Si:H films decreases with increasing discharge frequency.

It is known that a space charge layer called sheath always forms at the surface exposed to the plasma due to the difference in mobilities of ions and electrons. At frequencies lower than 100 MHz the ion transit time (τ_i) across the sheath becomes shorter than the negative RF half cycle and so ion energies get time modulated. At $\omega > 13$ MHz ($1/\tau_i < \omega$), ions are accelerated to an energy equal to the average potential drop across the sheaths. Therefore, one assumes that further increase of excitation frequency above 13.56 MHz would have no direct influence on the ions in the bulk plasma volume.

Looking closely one finds the following to be the likely situation associated with higher excitation frequency: first, the energy transfer mechanism from the electric field to the electrons in the plasma bulk has a frequency dependence (e.g. a resonance at the electron momentum exchange frequency) and second, the excitation frequency strongly effects the plasma electrode sheath characteristics and, in particular, the sheath potential drop. This potential drop and the ratio of the ion transit frequency to the excitation frequency determines the ion impact energy distribution on the substrate.

A detailed Monte-carlo simulation study by Surendra et al.[11] revealed that upon transition from RF to VHF the fraction of energy given to the electrons in the plasma bulk increases steadily and also many sheath properties become frequency dependent. Specifically Monte-carlo simulation of an Ar plasma from 30 to 120 MHz has shown that for constant

power input plasma potential decreases with ω i.e. ion energy at the substrate decreases with ω. It was pointed out by Flamm et al.[12] that at higher ω electric field in the sheaths decreases with ω. Measurements of plasma impedance and peak to peak voltage show that the potential drop across the sheaths and the fraction of power dissipated in the sheath decreases with ω. Consequently, the ionisation process shifts from the sheath to the plasma bulk. In another study Surendra et al.[13] have mentioned that average ion energy available at the electrode increases due to the decrease in sheath thickness (in a VHF discharge, sheath thickness, $d_{sh} \propto \omega^{-0.87}$). Therefore, ions experience fewer collisions with neutrals in the sheath and therefore retain more energy before colliding with the electrode. They have also found that as pressure is lowered at constant electrode gap and frequency the following are the phenomena that take place in the discharge i) increase of sheath thickness ($d_{sh} \propto p^{-0.4}$), ii) sheath becomes less collisional, iii) increase of plasma potential, iv) increase of average ion energy at the electrode, average electron energy at the body of the glow, v) less pronounced charge exchange collisions between ions and neutrals in the sheath at lower pressure, vi) scaling of ion collisionality (d_{sh}/ion-neutral mean free path) in the sheath as $p^{1/2}\omega^{-1}$ and vii) increase of ion directionality. This is an additional advantage of VHF operation, that is, pressure can be lowered while maintaining a relatively high ion current.

Perrin et al.[14] have demonstrated that ion bombardment is necessary for enhanced surface species reactivity but can as well damage the film during deposition. The low energy ion bombardment appears as the key to understand the maintenance of optimal a-Si:H film microstructure and optoelectronic properties when increasing the deposition rate in VHF discharges, whereas these properties usually degrade in conventional 13.56 MHz RF discharges where the ion impact energy becomes too high as the RF power increases.

Recently Perrin has reviewed VHF discharges[15]. He has suggested that the observation of deposition rate maximum at 70 MHz by Curtins et al.[4] is basically related to the variation of power transfer efficiency from the generator to the discharge. He has mentioned that the apparent success of VHF discharges is however counter balanced by limitations in industrial applications. As ω increases, the problems of homogeneity of discharge power dissipation and a-Si:H deposition on large-area planar diode system, which are already encountered at 13.56 MHz, become more difficult to solve, especially because of the series

inductance in the electrode plates. For this he has suggested the use of guided-microwave applicators.

Schwarzenbach et al.[16] have found that mean energy of the ion flux almost doubles in Ar plasma while changing excitation frequency from 13.56 to 70 MHz. They attributed this to the lower probability of charge exchange collision in the thinner sheaths at the higher frequency.

Again measurement of ion flux (Φ_{ion}) and energy distribution at the substrate by Heintz et al.[17-20] for H_2 plasma shows that Φ_{ion} increases with frequency ($\Phi_{ion} \propto \omega$). Also, the maximum ion energy (E_{max}) decreases with increasing ω. A similar study carried out recently by the same group [21] using SiH_4, H_2 mixture has revealed the decrease in ion energy with a simultaneous increase in ion flux with increasing frequency.

Two dimensional analysis of VHF discharge by Meyyappan et al.[22] indicate the following:

i) high density plasmas can be generated in a capacitively coupled system at frequencies above the industry standard of 13.56 MHz

ii) total power absorbed per electron decreases with an increase in frequency

iii) at a given pressure, the power spent on accelerating the ions in the sheath decreases with an increase in frequency and an increasing fraction of the supplied power goes into generation of electron-ion pairs

iv) sheath thickness, ion energy, ion flux, rates of inelastic processes, all scale favorably with frequency

v) plasma and ion characteristics are uniform across even large area electrodes except near the edge.

In summary, the reduction in sheath impedance $1/\omega C$ at high frequency is responsible for a higher power factor, leading to higher ion fluxes and ion density for a given plasma potential. This in turn reduces the sheath width and increases the sheath capacitance; this accentuates the effectiveness of operational frequency by reducing sheath impedance still further. Advantages associated with thinner sheaths are improved flux uniformity, a shorter path length for reactive radicals from the plasma bulk to the substrate and improved ion directionality due to reduced scattering.

Another interesting feature associated with the VHF discharge is the behaviour of the particles in the VHF plasma. In all cases of capacitively coupled discharges negatively charged particles suspended in the plasma accumulate near the plasma sheath boundary. Besides electrostatic forces, the particles are subjected to thermophoresis forces in the presence of any gas temperature gradient as well as viscous forces in the gas flow. Bouchoule et al.[23] have found in isothermal plasma experiments that powder formation is suppressed if electrodes are sufficiently hot. Dorier et al.[24] also observed that when the deposition temperature is increased, the total scattered intensity is reduced and the powder profile is displaced towards the colder electrode. To explain these they considered the changes in the plasma chemistry which in turn influences powder formation in the plasma. One can assume that reaction rates of the radicals with the growing film surface depends on the surface temperature[25]. Thus radical sticking coefficients are temperature dependent. Therefore, the surface temperature could influence the relative concentration of different dissociative products in the vicinity of the electrodes. On the other hand a reduction in the electrostatic trapping of powders in the VHF discharge due to smaller sheath potential indicates that when substrate temperature is increased then the total scattered intensity (amount of powder) and the scattered intensity near the heated ground electrode will decrease because in VHF discharge thermophoresis forces can overcome electrostatic forces and displace the powder layer towards the powered electrode. In this regard Jellum et al.[26] have found that for a sufficiently high temperature gradient (80 $^{o}Ccm^{-1}$) thermophoresis force appears strong enough to overcome the electrostatic forces acting to hold particles at the substrate sheath plasma boundary. In another study on particles in high frequency SiH_4 discharge Kawasaki et al.[27] have demonstrated that as excitation frequency increases particles appear earlier after the discharge initiation but their subsequent growth rate decreases significantly. This indicates that many short life time neutral radicals such as SiH_2 produced at a high rate, principally contribute to the nucleation and initial growth of one particulate, at least, for a relatively high power density.

Based on the above observations discussed so far tentative explanations for the attainment of high deposition rate in VHF silane discharge can be the following.

i) in the past higher a-Si:H deposition rates have been attributed to the changes in the bulk plasma properties like increased plasma density and in particular the enhancement of high

energy tail of the EEDF with frequency. It was believed that only the species with low excitation threshold are enhanced in VHF discharges

ii) second possible mechanism for enhanced r_d was often thought to be higher SiH_4 decomposition as a result of higher electron density. However mass spectroscopic results of Heintz et al.[17-20] show that the dissociation rate is only marginally enhanced. Optical emission intensities also indicate little increase in electron density, n_e and do not agree with the results obtained in RF discharges where r_d was found to be proportional to the increased SiH^* (414 nm) emission intensity as RF power is increased.

iii) Beneking et al.[28] have attributed the enhancement of deposition rate to (a) higher permissible application of VHF power without undue increase in ion energy and (b) changes in the spatial distribution in the discharge so that deposition concentrates between the electrodes leading to a higher deposition rate without an increase in the total deposited material. The first result is in contradiction to the mass spectroscopic results of Heintz et al.[17] whereas, the second one was not reexamined by others. According to the present understanding, formation of reactive film precursors is only weakly enhanced with frequency. The other parameter left is the surface reactivity whose frequency dependence can be a predominant reason for high deposition rate at VHF. Earlier Veprek et al.[29] have demonstrated that ion induced surface dehydrogenation controls the deposition rate in plasma CVD. Again surface dehydrogenation by neutrals having energy $\approx$ 40 meV cannot explain the attainment of high r_d in VHF. Heintz et al.[17-20] have shown that ion flux increases strongly with frequency by a degree compatible to the change in film growth rate and may be the direct cause of enhanced growth rate at VHF.

iv) Very recently Keppner et al.[30] reviewed the present status in the understanding of VHF-GD. There they have introduced a new terminology named "breeding effect", which is basically the generation of radicals due to electron impact dissociation in the bulk plasma. According to Keppner et al.[30] there is an additional and alternative explanation for the increase in deposition rate, apart from the enhanced "breeding effect" of radicals. They have also mentioned that rate limiting mechanism as assumed by Heintz et al.[17] is not necessarily the breeding effect in the bulk but rather it is the ion induced "preparation" of the growing surface. Though in case of VHF-GD both the breeding and the ion flux are increased it is not possible to prove or disprove one of the two explanations by experimental facts. However, impedance measurements show that real and imaginary part of impedance decreases with the increasing frequency. Furthermore, the power dissipation ratio (P_{shear}/P_{n-n}) decreases as well. This

means that higher fraction of total RF plasma power is invested for radical generation in the bulk rather than being diverted into bombardment by ions being accelerated within the sheaths. Again, they suggested that the most efficient "breeding zone" within the bulk plasma is the sheath-edge region. The sheath thickness reduces at higher excitation frequency and as a consequence, the short life time radicals e.g. SiH_2 can now directly contribute to the growth of the film.

Thus, from the attempts so far been made to understand the growth of high quality a-Si:H films at high rates using VHF excitation, it becomes clear that VHF discharge provides an access to yet another process parameter i.e. excitation frequency to control ion flux and ion energy. The advantage of using VHF discharge over RF discharge is the attainment of very high growth rate. In addition to this, VHF discharge also provides an edge over RF so far as suppression of powder is concerned.

Therefore, keeping in view all the above advantages of VHF discharges, VHF MPPD (modified pulsed plasma discharge) has been experimented for the first time with the anticipation of achieving higher deposition rate of a-Si:H films with better optoelectronic properties as compared to the CW VHF grown films.

4.2 Experimental Details

The a-Si:H films were deposited in a capacitively coupled multichamber PECVD system (described in Chapter-II). The reactor geometry remained unchanged in switching from 13.56 to 100 MHz operation. Only the plasma excitation source and matching network were changed. A 100 MHz VHF generator that can operate in CW and pulsed modes was locally fabricated in collaboration with Nuclear Science Centre, New-Delhi. The details of the generator is given below.

The basic generator of VHF energy is of crystal oscillator type which oscillates at overtone mode. The generator in pulsed mode generates VHF energy modulated by low frequency rectangular pulses in predetermined frequency (2 Hz) and user controlled pulse width (ON TIME 5 to 100 msec). The amplitude control of the "ON TIME" power is done through power control settings. The output is further filtered to generate distortion free VHF energy at 100 MHz.

The power amplifier consists of three stages. In the first stage, the oscillator output is preamplified by a class A VHF amplifier module to generate 250 mW maximum and in the second stage it is amplified to a level of 10 Watts by another driver amplifier in class AB mode. Finally the output of this driver amplifier is further amplified by a power amplifier using RF Power MOSFET in push pull class AB mode upto 200 Watts at 50Ω impedance.

The online VHF power measurement is done through built-in 'THRU-LINE' sensors of Bird Corporation make and front panel power meter. The SWR protection is provided by controlling MOSFET gate voltage in case of higher SWR. The generator is forced air cooled. The regulated +28 volts high current DC power supply is built in.

The matching network used in CW and pulsed VHF discharge is a standard three element LC L-network with two variable air capacitors and one variable inductor. The network has variable phase and amplitude controls to match less than 50Ω complex impedance of the discharge. Components used were of high Q in order to minimise losses in the matching network itself. Matching network is connected to the powered electrode with shortest length of cable possible. At each applied power, the matching network was adjusted for minimum (almost zero) reflected power. The block diagram of the VHF generator is shown in **Fig. 4.2**.

Different deposition parameters were systematically varied for optimising a-Si:H film growth rate and optoelectronic properties. Discharge pressure, feed gas flow, hydrogen and helium dilution, dwell time (τ) and high power level (HPL) were systematically varied. For this study low power level (LPL) was maintained constant at 10 W as used in 13.56 MHz MPPD. At first pressure variation studies were carried out. Chamber pressure was varied from 0.7 Torr to 0.07 Torr in order to maximise r_d. Due to pumping speed limitation only 24 sccm of SiH_4 (100%) was used to get the lowest pressure. It is interesting to note that r_d shows a higher value at 0.3 Torr and it decreases on either increase or decrease of pressure. Typical r_d values are 6.1 $A^{\circ}s^{-1}$ at 0.4 Torr, 13.6 $A^{\circ}s^{-1}$ at 0.3 Torr and 8.0 $A^{\circ}s^{-1}$ at 0.10 Torr. Finally a systematic variation of dwell time and duty cycle was carried out using optimised pressure, flow and HPL. Deposition was also carried out using hydrogen and helium diluted silane with the discharge parameters as 0.3 Torr pressure, 24 sccm SiH_4 flow, 8 sccm H_2 / He flow and 60W HPL. In the end 0.1 Torr and 40 sccm undiluted SiH_4 discharge was studied.

Time resolved OES (TROES) was carried out at specific wavelengths corresponding to SiH^*, H^* and Si^* excited species using the procedure discussed in section 2.8.

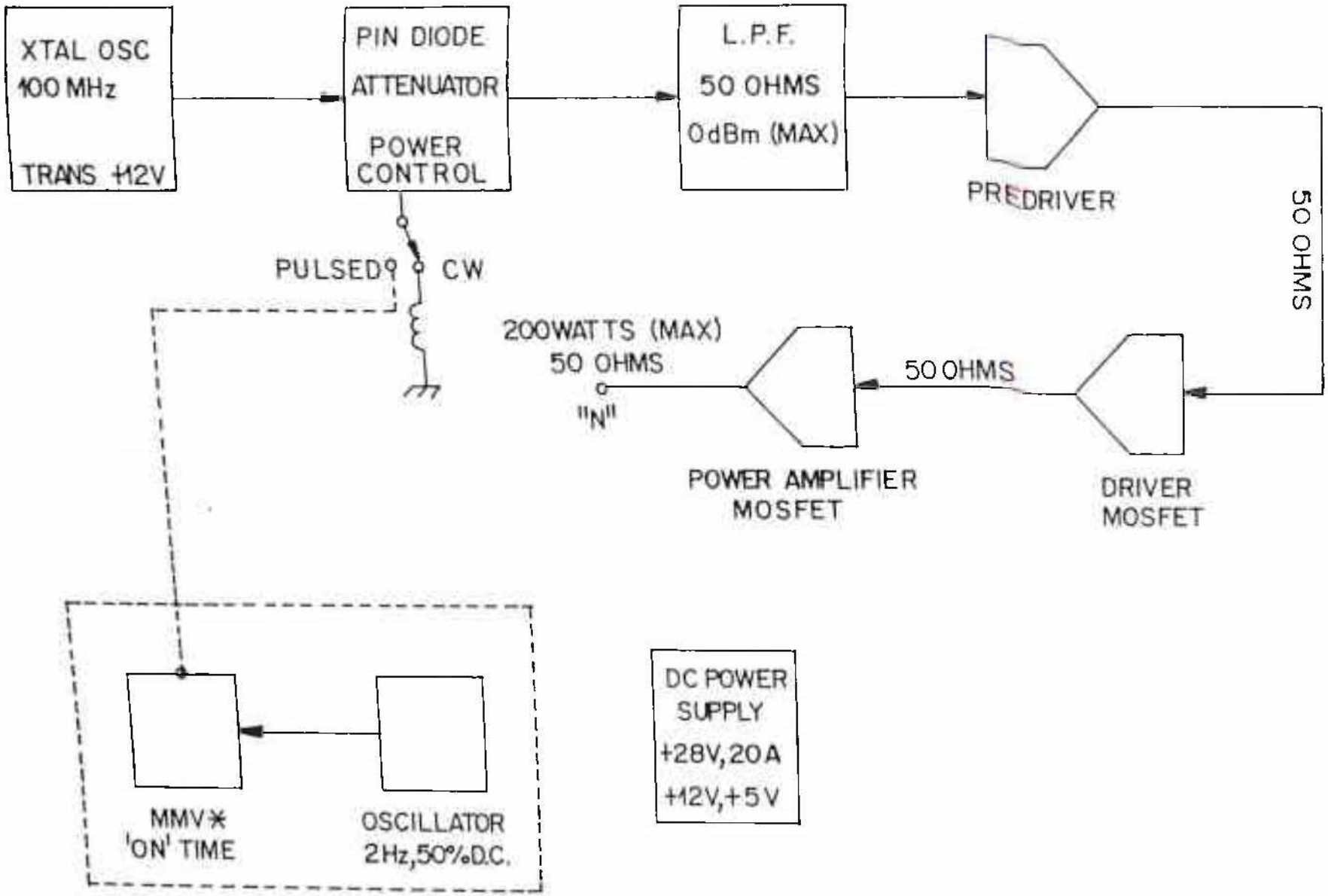

Fig.4.2 Block diagram of the VHF (100 MHz) generator used in the present study

Dark and photoconductivity, optical band gap, hydrogen content and its nature of bonding and defect density studies were carried out following the procedures discussed in Chapter-II.

4.3 Results

4.3.1 Dependence of growth rate on discharge parameters

Fig.4.3 shows the variation of r_d with τ for different deposition conditions like CW (represented by a horizontal line) and MPPD in undiluted SiH_4 discharge at 0.3 Torr and 0.1 Torr corresponding to 24 and 40 sccm flow rates respectively, and MPPD in 25% H_2 and 25% He dilution at 0.3 Torr. Similar to MPPD at 13.56 MHz (see chapter - III) it is evident from **Fig. 4.3** that r_d depends on τ for the two different HPLs used . Another similarity with 13.56 MHz MPPD is the lower deposition rate in VHF MPPD upto a certain τ as compared to the CW discharge at LPL. Around τ=40 msec, r_d for MPPD crosses r_d for CW discharge. Increasing HPL from 60 to 75W causes a noticeable increase in r_d at τ values higher than 40 msec. Although, higher HPL has marginal effect in r_d, it causes degradation of σ_{ph} (as discussed later) by substantial amount. From **Fig.4.3** it seems that the crossover point is dependent on HPL. For 75W HPL it occurs earlier than 60W HPL.

Effects of dilutions in VHF discharge seems to be similar to that at 13.56 MHz MPPD (section 3C.3.1). In 100 MHz MPPD, r_d increases by substantial amounts at lower dwell times either by H_2 or He dilution. It also appears that rate of increase of r_d with τ were different in H_2 and He diluted discharges. Variation of r_d with τ was also experimented at 0.1 Torr in order to understand the discharge kinetics away from discharge conditions which leads to maximum growth in a CW discharge. In order to avoid SiH_4 depletion flow rate was increased from 24 sccm to 40 sccm. CW (VHF) deposition rate dropped from 13.6 $A^{\circ}s^{-1}$ to 8.6 $A^{\circ}s^{-1}$ along with an increase in σ_{ph} by an order of magnitude. Though, the similarity between 0.1 and 0.3 Torr discharge is that r_d increases with τ, at higher τ, r_d is found to saturate at 0.1 Torr much earlier. It appears here that film forming reactions involved in 0.1 Torr MPPD and 25% H_2 diluted MPPD at 0.3 Torr are quiet similar. The only difference here is that the residence times of the gas molecules are three times higher in H_2 diluted case as compared to undiluted case. The striking difference between 0.1 Torr is the early

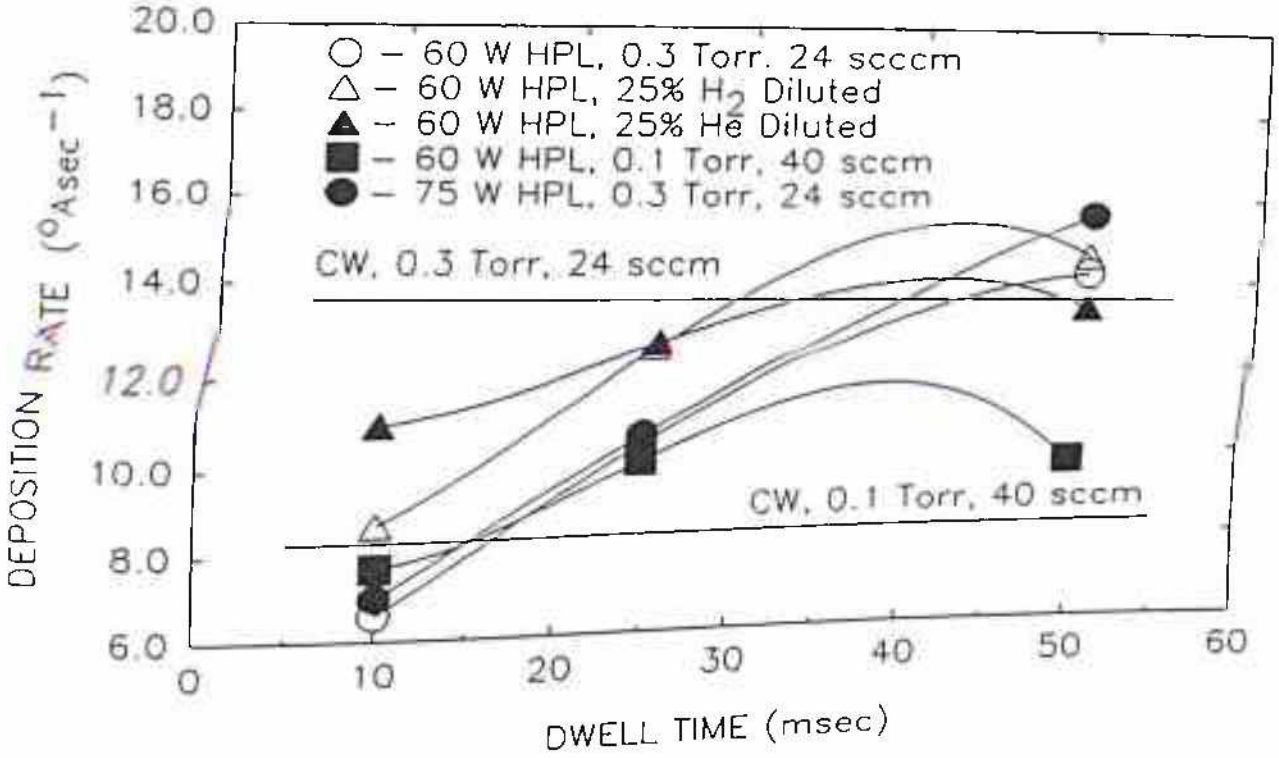

Fig.4.3 Variation of deposition rate with dwell time at different deposition conditions.

appearance of r_d cross over point (τ = 15 msec) compared to 0.3 Torr (τ = 40 msec) discharge

4.3.2 *Time resolved optical emission spectroscopy studies*

The TROES studies were carried out in 100 MHz MPPD using discharge conditions which were used in 13.56 MHz MPPD of H_2 diluted SiH_4 (see chapter - III). **Fig. 4.4** show the variation of (a) SiH^* (414 nm), (b) H^* (656 nm) and (c) Si^* (288 nm) intensities at different H_2 dilutions for both 13.56 and 100 MHz discharges. It is clear from **Fig. 4.4(a)** and **4.4(c)** that at 100 MHz MPPD, SiH^* and Si^* intensities increase with H_2 dilution upto 25% dilution and then decrease, whereas, in 13.56 MHz MPPD both the intensities increase upto 75% H_2 dilution and then decrease. In VHF discharge the rate of decrease of SiH^* beyond 50% H_2 dilution is very fast. **Fig.4.4(b)** shows the variation of H^* intensity for RF and VHF MPPD. In RF discharge H^* intensity increase slowly upto 50% H_2 dilution but thereafter it increases very fast. In VHF MPPD the variation in H^* intensity is small and shows a broad maxima around 50% H_2 dilution.

Fig. 4.5 shows the variation of the above three intensities at various VHF discharge conditions which were used for depositing a-Si:H films, in terms of a bar graph. An arbitrary scale is used for representing the intensities. If VHF MPPDs are compared at 0.3 Torr and 0.1 Torr then it is found that intensities of all the excited species are higher at 0.3 Torr compared to 0.1 Torr.

It is to be noted that for all the discharge conditions displayed in **Fig. 4.5**, τ was 25 msec and duty cycle was 5%. The main feature of **Fig. 4.5** is that H^* intensity is higher in 25% H_2 diluted discharge compared to 25% He diluted discharge. Two other important observations are lower r_d and higher σ_{ph} in H_2 diluted discharges.

Fig. 4.6 shows the variation of SiH^*, H^* and Si^* intensities with dwell time for 25% H_2 diluted VHF MPPD. It is clear from the figure that they all increase with τ linearly. This feature is in quiet contrast to RF MPPD where intensities of different excited species were found to be independent of dwell time as shown in **Fig. 4.6**. Although arbitrary scale is used for representing the intensities, all the intensities of different excited species are quiet high in VHF MPPD compared to RF MPPD.

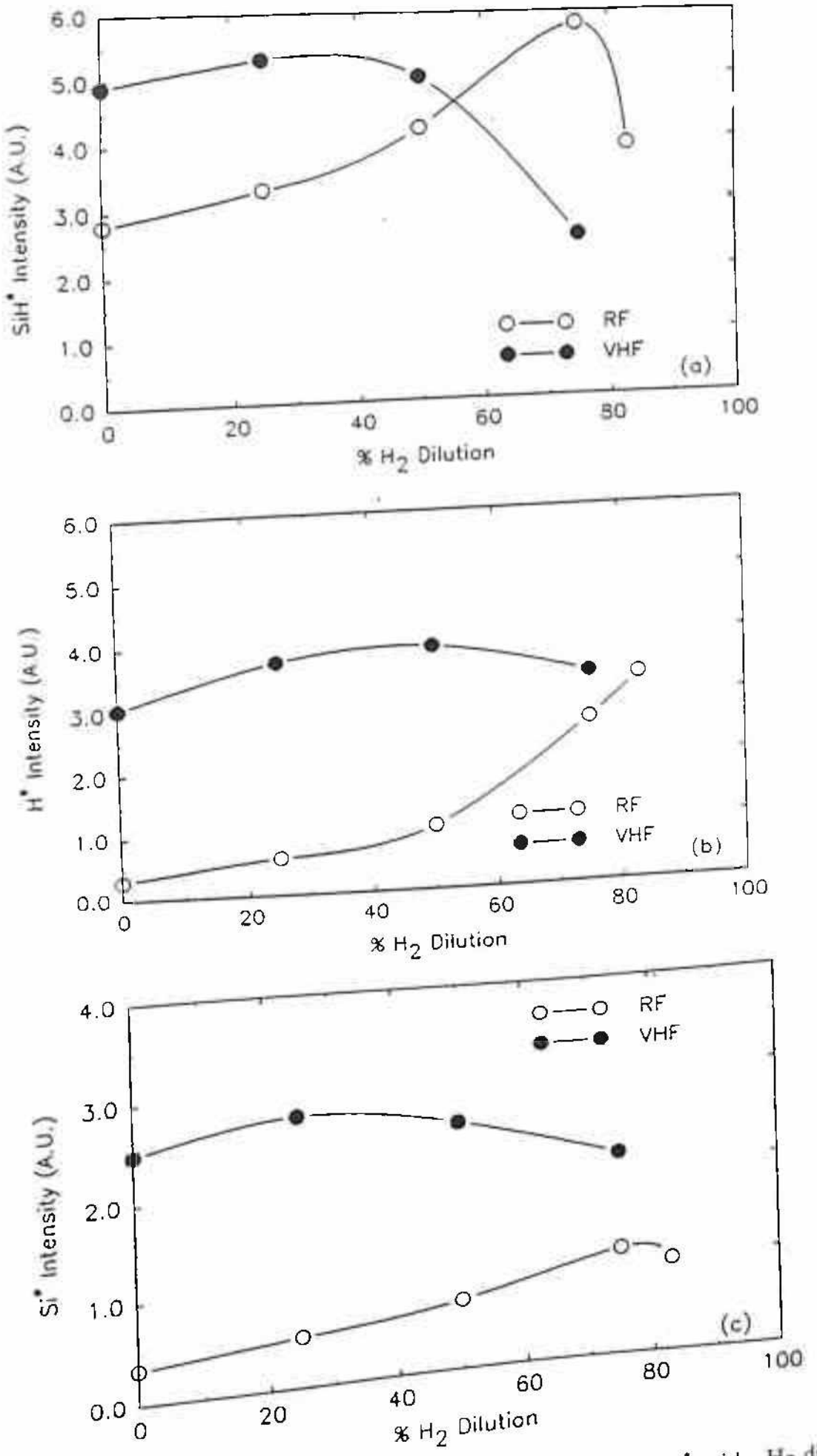

Fig.4.4 Variation of emission intensities of (a) SiH^* (b) H^* and (c) Si^* with H_2 dilution for both 13.56 and 100 MHz discharges

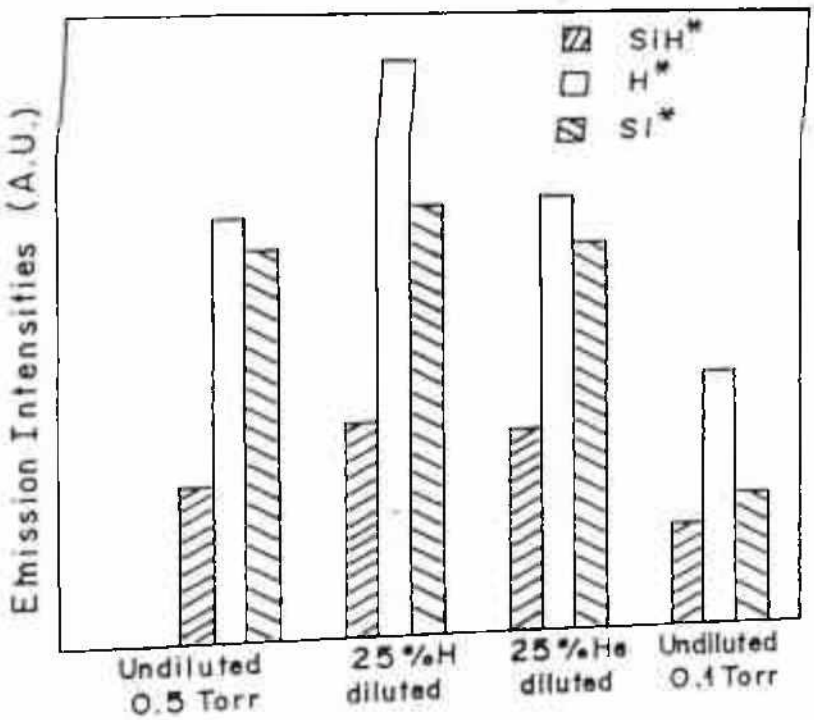

Fig.4.5 Bar graph representation of emission intensitiesfrom SiH^*, H^* and Si^* species at different dilution conditions.

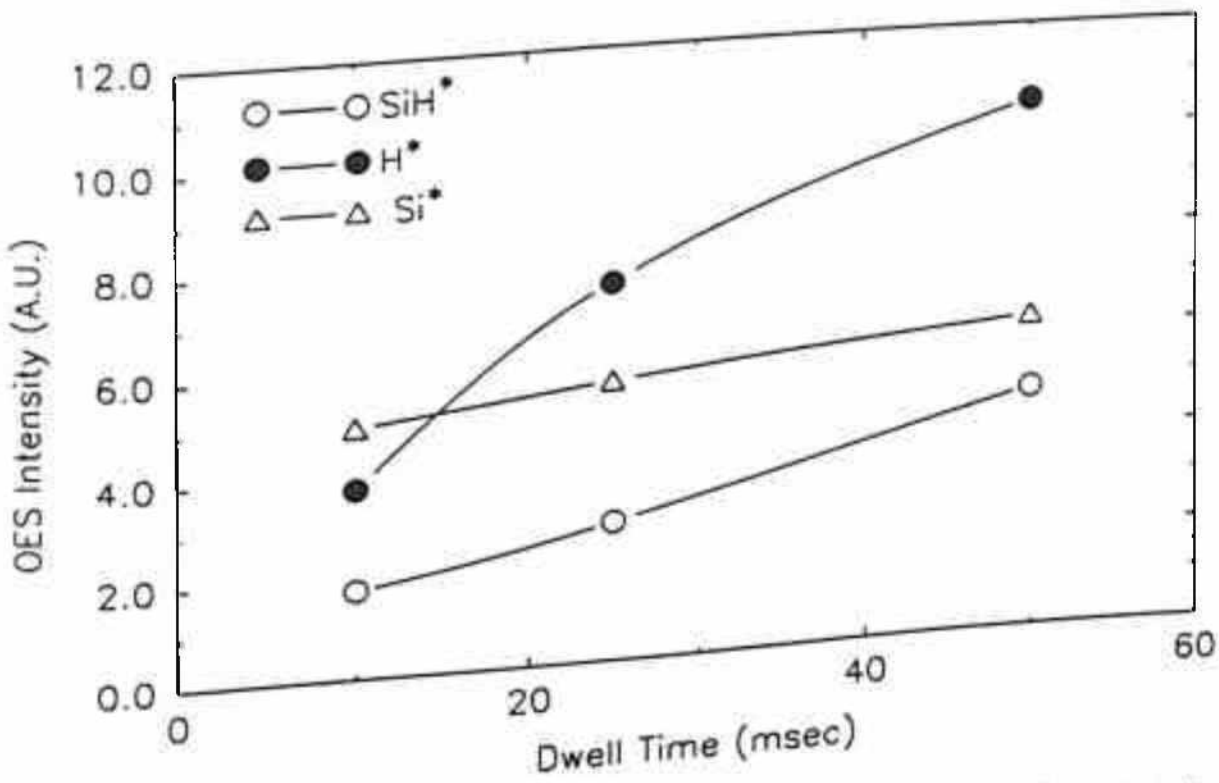

Fig.4.6 Variation of emission intensities of (a) SiH^*, (b) H^* and (c) Si^* with dwell time or 25% H_2 dilution.

4.3.3 Optical band gap

Fig. 4.7 represents the optical band gap, E_g of films grown at different deposition rates. The most interesting feature in this figure is that the optical band gapdoes not change (1.75 eV) for the deposition conditions shown in figure. The variation in E_g values lie within a very narrow energy range (±0.03 eV). The main idea of plotting E_g versus r_d was to show that E_g is insensitive to variations in deposition conditions and more significantly deposition rate. Further E_g hardly changes even if the composition of the diluent gases used is changed over a wide range. Such high degree of insensitivity of E_g on variations in deposition conditions seen in VHF MPPD suggests that short time fluctuations in discharge conditions during long hours of deposition to grow thicker films will have negligible effect on device performance. This is particularly useful for devices such as radiation detectors, position sensors and so on.

4.3.4 Dark conductivity and photoconductivity measurements

Variation of dark conductivity, σ_D with dwell time is shown in **Fig.4.8**. For CW discharges σ_D values are shown as horizontal lines. Same symbols are used for both σ_{ph} and σ_D. For H_2 and He diluted films σ_D values are higher than CW values by at least one order of magnitude. For 60W HPL discharge in 100% silane σ_D is almost independent of dwell time, but for 75W HPL σ_D values are quiet low beyond $\tau = 25$ msec.

Variation of σ_{ph} with τ is plotted in **Fig. 4.9** for different deposition conditions. Again for CW discharges σ_{ph} values are shown by horizontal lines. σ_{ph} has been measured in a coplanar geometry at 100 $mWcm^{-2}$ intensity having AM 1.5 spectrum. The main observation from **Fig.4.9** are the following:

i) For CW discharge at 100 MHz, σ_{ph} for films grown at 0.3 Torr is lower than 0.1 Torr discharge grown film by almost an order of magnitude.

ii) Pulsing the VHF discharge at 0.3 Torr pressure improves σ_{ph} over the CW VHF discharge. This happens when 60W HPL is used. For 75W HPL and for 0.1 Torr discharge this improvement in σ_{ph} is observed only in the lowest τ value used.

iii) For all the parameters studied (VHF MPPD) σ_{ph} decreases with increasing τ.

iv) It was found during studies relating to the variation of pressure (for deposition rate maximisation) that as pressure decrease σ_{ph} improves steadily from 0.7 Torr to 0.07 Torr.

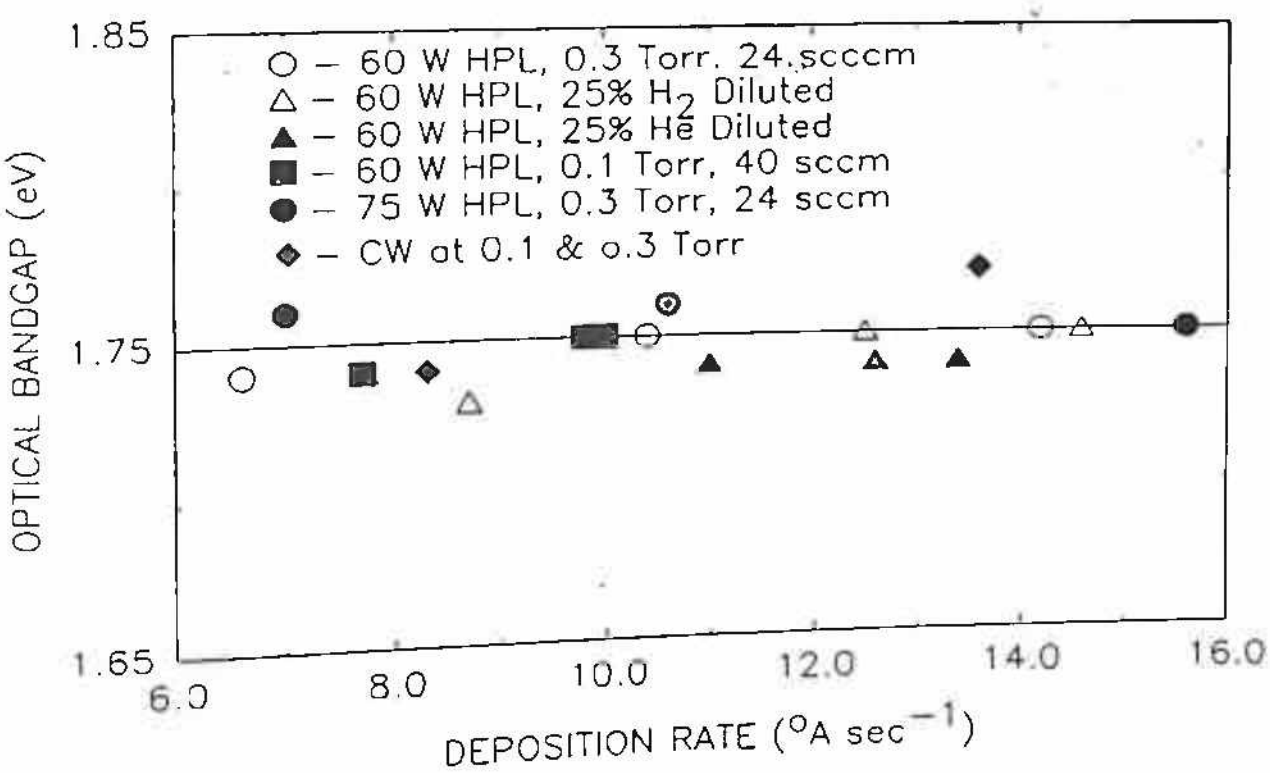

Fig.4.7 Variation of optical bandgap with deposition rate.

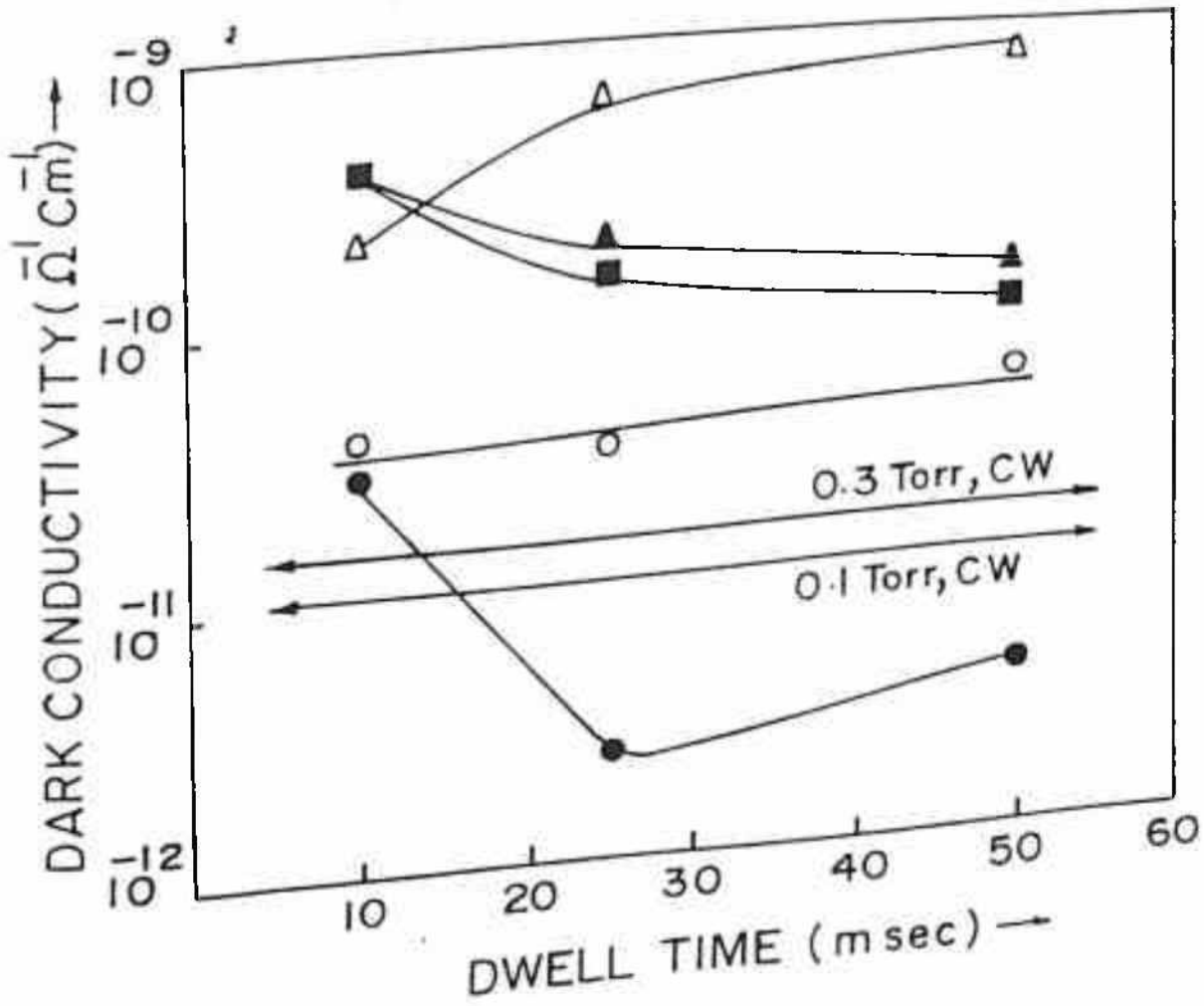

Fig.4.8 Variation of σ_d with dwell time.

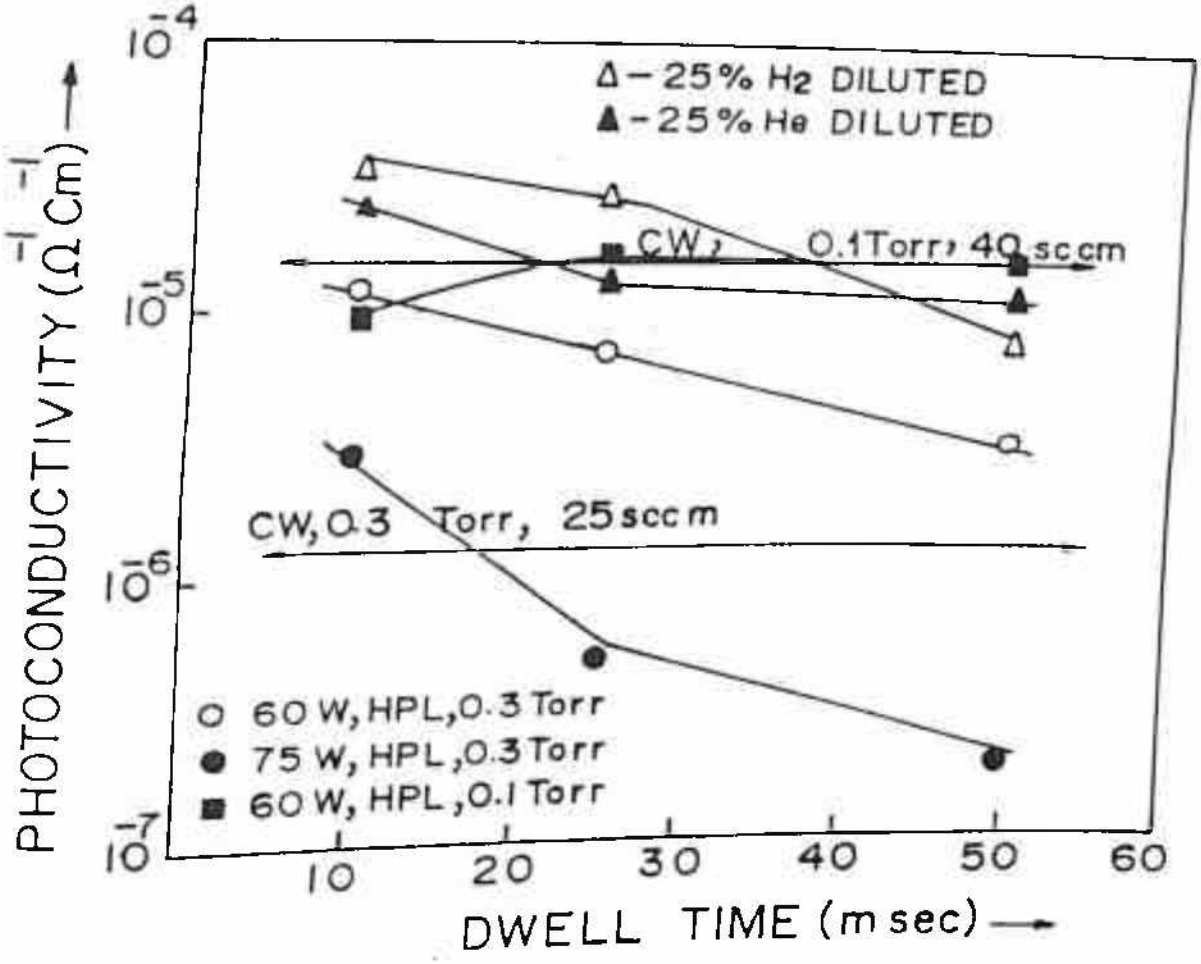

Fig.4.9 Variation of σ_{ph} with dwell time

v) Comparing the σ_{ph} values as shown in **Fig. 4.9** with the σ_{ph} values for 13.56 MHz MPPD grown films as described in chapter-III it is found that σ_{ph} value ($7x10^{-5}\Omega^{-1}cm^{-1}$) for films grown by RF CW discharge at 0.5 Torr is much higher than VHF CW discharge grown films at 0.3 Torr ($10^{-6}\Omega^{-1}cm^{-1}$) and σ_{ph} for VHF discharge produced films only becomes comparable to RF discharge grown films (0.5 Torr) if it is deposited at lower pressures ($P \leq$ 0.1 Torr) or by moderate H_2 or He dilution (25%) at 0.3 Torr.

vi) Both H_2 and He dilution improves σ_{ph} by substantial amounts over undiluted VHF MPPD films. The most encouraging feature is that this increase in σ_{ph} is associated with a substantial increase in r_d over undiluted MPPD. This is quiet in contrast to the a-Si:H films deposited at standard conditions.

Often in the literature the product $\eta\mu\tau$ is mentioned as a figure of merit for comparing materials of different band gap. Here in VHF MPPD since optical band gapis almost constant with respect to parametric variations, therefore σ_{ph} can be used as a measure of quality of materials being grown without any difficulty.

4.3.5 Hydrogen content and microstructure factor

Hydrogen content, C_H and microstructure factor R estimated as discussed in chapter - II are shown in **Fig. 4.10 (a) & (b)** respectively for different discharge conditions. FTIR traces in the energy range 2300 to 500 cm^{-1} for H_2 and He diluted discharge grown films are shown in **Fig. 4.11 (a) & (b)** respectively. From the analysis of all these following observations are made.

i) For CW discharges R factor is 0.4 for 0.3 Torr discharge grown films, which is higher as compared to 0.1 Torr grown film where R is 0.17 only. Hydrogen content in these two films are close to 9 at%.

ii) As 0.3 Torr VHF discharge is either modulated using 60W or 75W HPL, R factor sharply increases and it is found to be 0.7 for 75W HPL grown film. C_H for 60W HPL varies with τ between 7 to 10 at% whereas, for 75W HPL hydrogen contents are quiet high and lie within 13 to 16 at%.

iii) Once either H_2 or He is added to SiH_4, R factors and hydrogen contents both decrease and even go below the CW discharge for 25% H_2 diluted case. R factor increases from 0.25 to 0.45 as τ increases from 10 to 50 msec but C_H remains within 6 to 7 at%. For

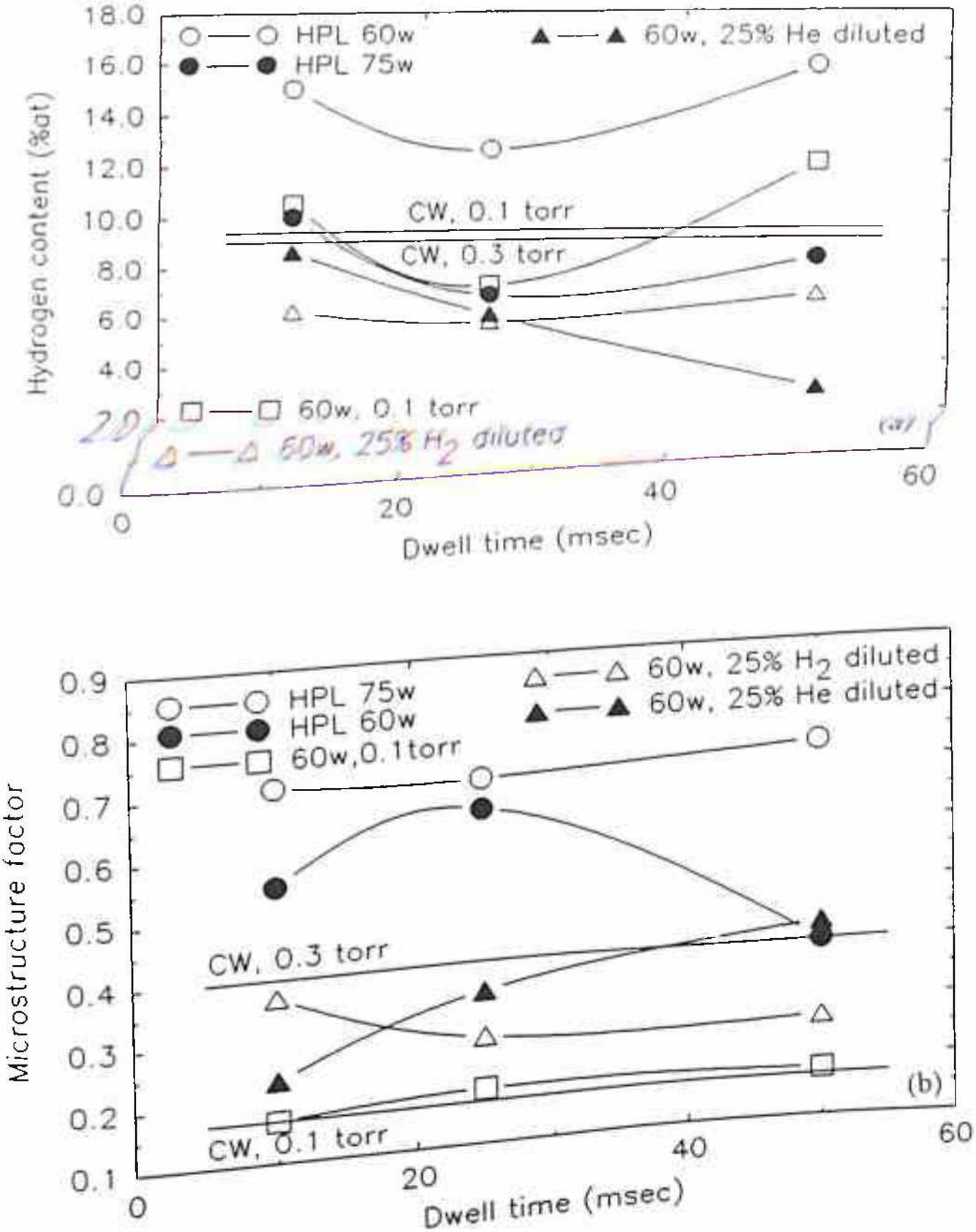

Fig.4.10 Variation of (a) C_H and (b) R factor with dwell time.

25% He diluted VHF MPPD R factor and C_H both decrease with increase of τ R factor remain within 0.37 to 0.27 and C_H varies from 9 at% to 3 at%.

iv) At 0.1 Torr, CW and MPPD R factors are low (0.17) and independent of τ but C_H lies within 6 to 11 at%

v) FTIR traces in **Fig.4.11(a) & (b)** all show predominant SiH bonding in these films. In H_2 diluted films, as τ increases, SiH_2 stretching mode becomes more and more prominent. **Fig.4.11(c)** shows the same behaviour for CW discharge grown films, at two different deposition pressures

4.3.6 Defect density studies

Fig. 4.12 shows PDS spectra in the energy range 0.9 to 2.1 eV of some selected films. Deposition conditions for these films are also mentioned in the figure. PDS spectra of CW VHF films are shown in **Fig.4.13**. E_o and N_D values of the films are shown in **Table 4.1**. For all the MPPD grown films, as given in table 4.1, τ=25 msec and duty cycle = 5% were used. **Fig.4.13** shows PDS spectra of CW films grown at different pressures and it appears that at lower pressure better quality films are produced. It was found that E_o and N_D values are almost same for undiluted CW and undiluted MPPD films. However, both H_2 and He dilution have some beneficial influence on the photoconductivity of the films. The best defect parameters obtained were E_o = 50 meV and N_D = 1.5 x 10^{17} cm^{-3}. This particular film has a growth rate of 11.1 $A^o s^{-1}$ and σ_{ph} = 2.3 x 10^{-5} $\Omega^{-1}cm^{-1}$. It is important to mention at this point that the best film grown using 13.56 MHz MPPD has E_o = 48.6 meV, N_D = 9.5 x 10^{16} cm^{-3} and σ_{ph} = 5 x 10^{-5} $\Omega^{-1}cm^{-1}$ however the corresponding deposition rate was only 1.35 $A^o s^{-1}$. Thus it is quiet clear that VHF discharge can produce films having optoelectronic properties comparable to 13.56 MHz discharge grown films with much higher (almost an order of magnitude) deposition rate.

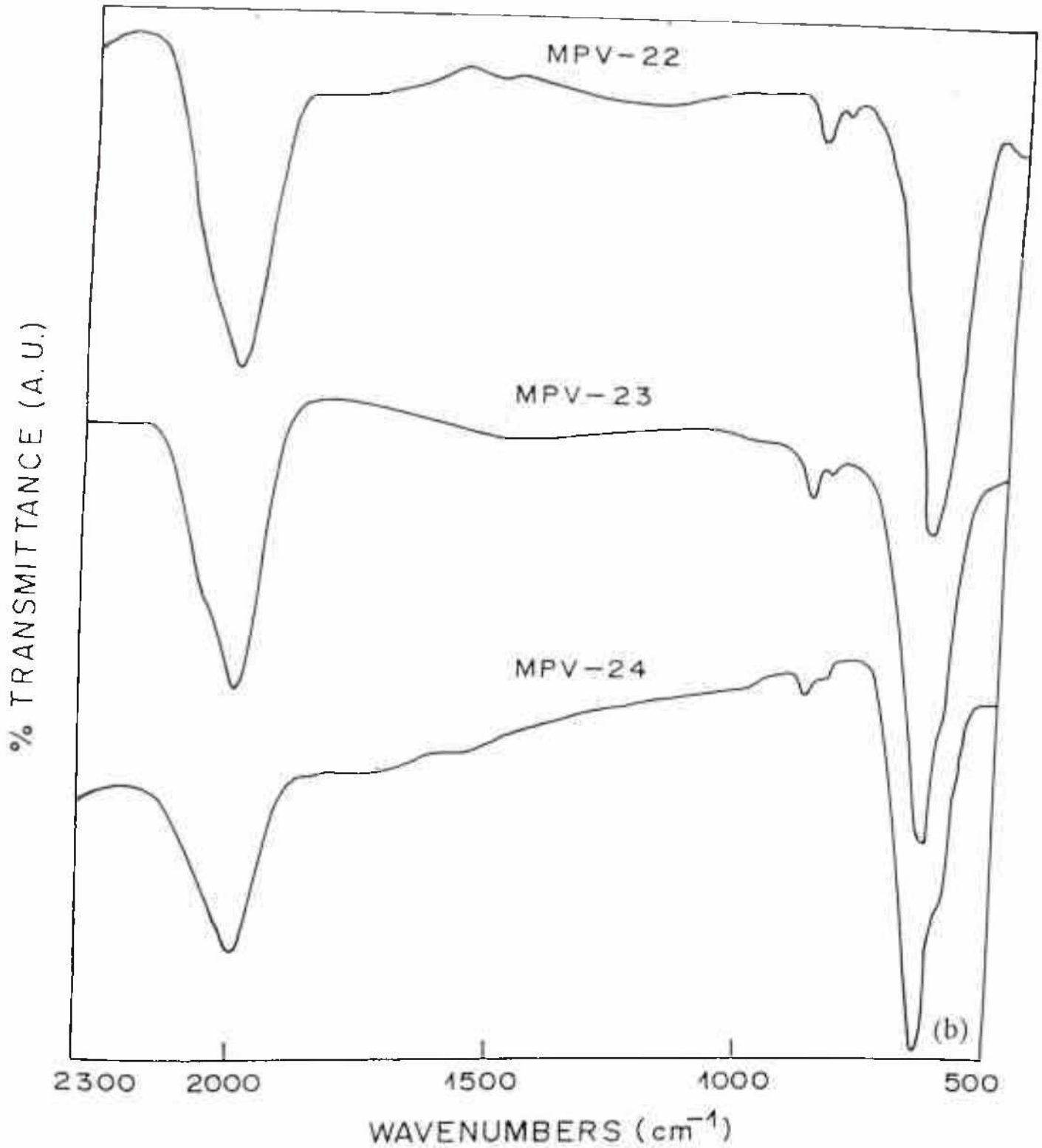

Fig.4.11 FTIR traces of (a) H_2 and (b) He diluted VHF MPPD grown films.

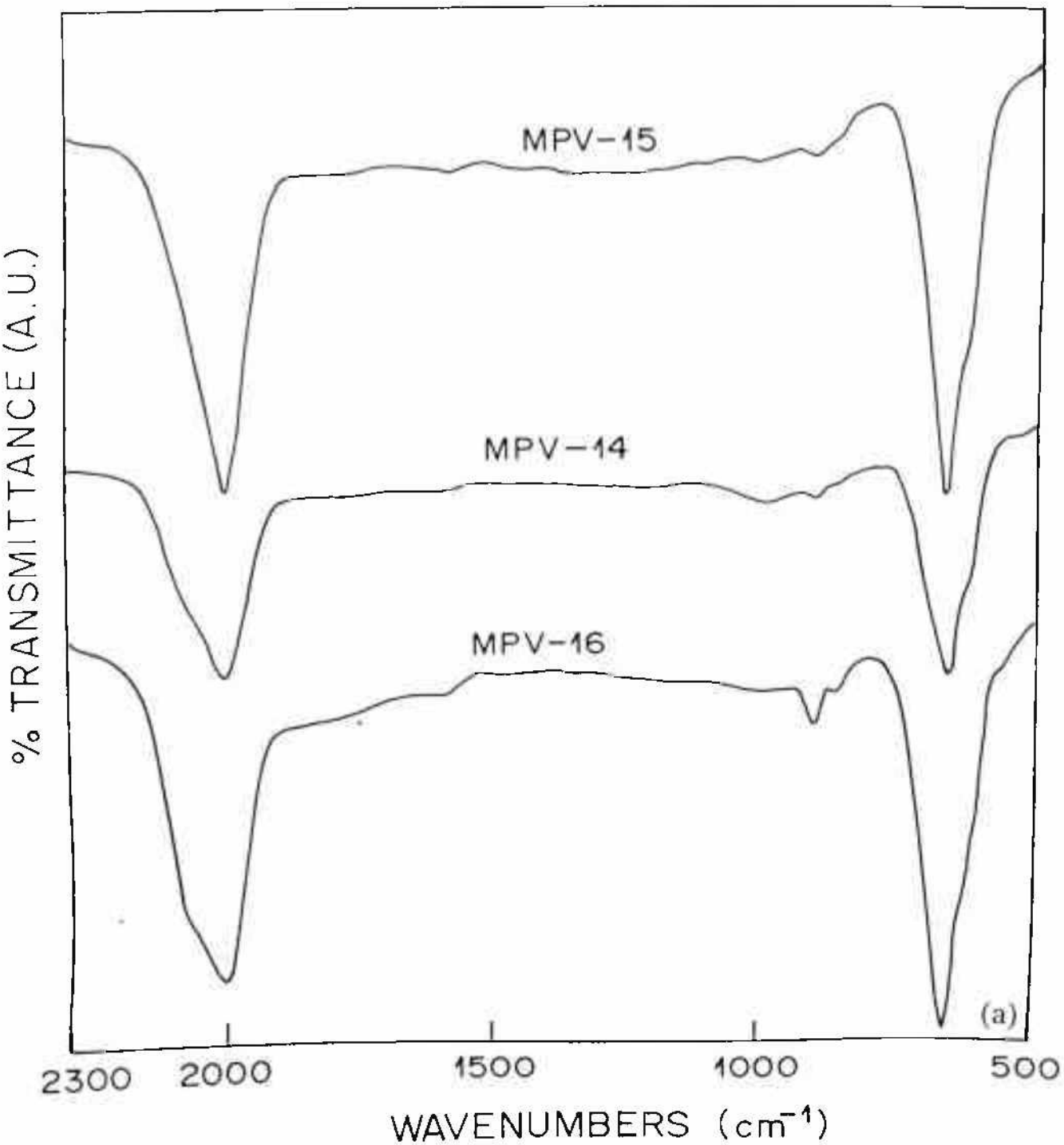
MPV-15
MPV-14
MPV-16
% TRANSMITTANCE (A.U.)
(a)
2300
2000
1500
1000
500
WAVENUMBERS (cm⁻¹)

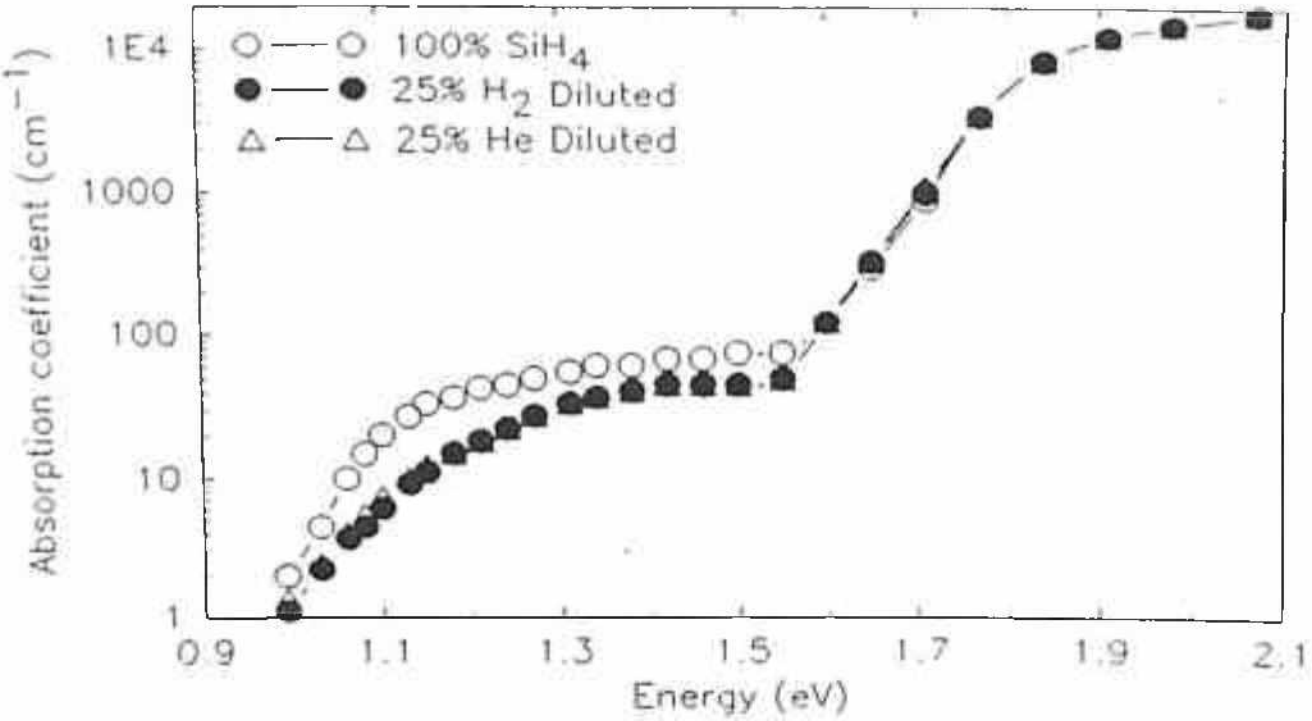

Fig.4.12 PDS spectra of undiluted, H_2 and He diluted VHF MPPD grown a-Si:H films.

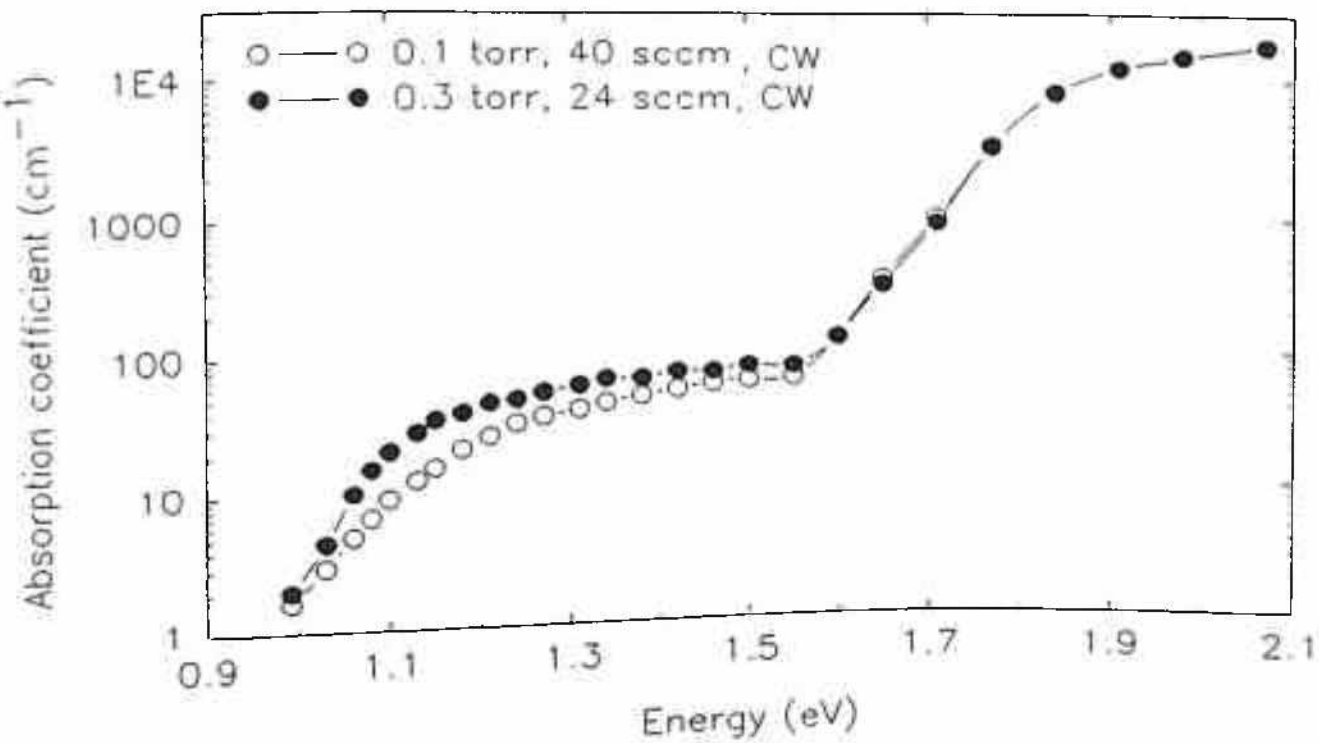

Fig.4.13 PDS spectra of VHF CW films grown at different pressures.

Table 4.1 Defect parameters (PDS) of some selected films

Film description	E_o(meV)	N_D (cm^{-3})
CW, 0.3 Torr	54.6	2.7×10^{17}
CW, 0.1 Torr	51.1	1.7×10^{17}
60W HPL, 0% Dilution	54.7	2.4×10^{17}
60W HPL, 25% H_2 Dilution	51.3	1.5×10^{17}
60W HPL, 25% He Dilution	50.0	1.4×10^{17}

It is to be noted that N_D values as shown in the above table are higher compared to the values reported for device quality material. It is well known that defect density as obtained by PDS technique is highly dependent on the thickness of the film. For thin films, contribution to the total defect density by the surface states may become comparable or even more than the bulk defect density ($N_D = N_b + N_{ss}/t$). The thicknesses of all the films grown for this study were around 1μm and it appears that surface state density as low as $N_{ss} \approx 10^{13}$ cm^{-2} would be enough to push N_D values in 10^{17} range. However, σ_{ph} and σ_{ph}/σ_D values indicate that bulk defect density (N_b) should be comparable to those obtained for device quality material.

4.4 Interpretation of results

The most important features of RF and VHF MPPD as observed during the present investigation are found to be the following:

i) Growth rates are found to increase with dwell time, however, it remains lower than their respective CW values below certain dwell time (dependent on high power levels).

ii) H_2 and He dilution have been found to be beneficial in both RF and VHF MPPD (enhancement of growth rate and optoelectronic properties).

iii) Photoconductivity values remain lower than the corresponding CW values for RF MPPD whereas in case of VHF MPPD it is found to improve over CW VHF value.

iv) close correlation between ion bombardment on the growing surface and film microstructure has been found for VHF MPPD produced a-Si:H films.

In the following an effort has been made to understand the effects of VHF discharges, VHF power modulation and dilution of feed stock by correlating various observations described in the previous section.

Enhancement of growth rate

First, the increase of growth rate while changing the deposition pressure from 0.7 to 0.3 Torr is discussed. It can be qualitatively correlated to the expansion of the discharge glow zone with the decrease of pressure as observed visually. At 0.7 Torr, discharge was very much confined over the powered electrode. As the pressure was reduced glow region expanded and at around 0.3 Torr it occupied the whole inter-electrode space. Similar expansion of glow zone from 1.0 Torr to 0.1 Torr was earlier reported by Oda et al.[7]. In glow-discharges as pressure is reduced glow regions expand. This phenomenon becomes readily observable in a 100 MHz SiH_4 discharge and in general not discernable in a 13.56 MHz discharge.

Present results for VHF CW discharges reveal that for a particular reactor geometry, i.e. for a constant inter-electrode separation and gas flow dynamics if the discharge frequency is increased from 13.56 MHz to 100 MHz then accordingly the chamber pressure should be reduced in order to maintain the device quality optoelectronic properties of a-Si:H films. In fact, Chatham et al.[5] have also found that higher frequency operation reduces the operating pressure. They have reported device quality films grown at 100 MHz and 0.08 Torr pressure in a deposition system similar to the one used in the present experiment. In view of the above result it appears that for similar reactor geometry, pressures, RF power etc. the onset of reactions which lead to the insertion of higher hydrides in a growing a-Si:H film appears to happen at a lower pressure in a VHF discharge compared to a RF discharge. This increase in gas phase reactions could be due to high concentration of reactive species such as neutrals, radicals, ions etc. available at VHF frequencies due essentially to thinner sheaths and increased power factor of a VHF discharge. In a related study Finger et al.[31] have shown how the frequency at which the maximum r_d is achieved for device quality films depends on the reactor geometry.

It will be contextual to refer to some simulation studies at this point. Numerical simulations by Surendra et al.[13] show that as the pressure is lowered at constant electrode gap and constant excitation frequency, the sheath becomes less collisional and the plasma potential increases. Thus, the charge exchange collisions between ions and neutrals in the sheath becomes less pronounced at lower pressure. Therefore, sheath collisionality decreases since it

is proportional to $p^{1/2}\omega^{-1}$. Average ion energy at the electrode, average electron energy in the bulk of the glow region, sheath thickness and plasma potential all increase as chamber pressure is lowered. Thus, an additional advantage of VHF operation is that working pressure can be lowered (maintaining a relatively high current), while increasing ion directionality.

Thus the basic aim of opting for VHF discharges for material processing in the present study has been to increase the radical generation by essentially producing higher plasma density. In addition to this, the effect of modulating the VHF discharge needs also to be considered. The idea behind modulating the VHF discharge was to further increase deposition rate by applying additional power and also to improve the optoelectronic properties by controlling the right degree of ion bombardment on the growth surface (this aspect will be discussed later).

MPPD can be thought of as a discharge where sheath electric field never vanishes, rather switches between a high and low value almost in a similar fashion as the applied power. It is to be remembered that sheath field and thicknesses are low in 100 MHz discharge as compared to a 13.56 MHz discharge. Now the negatively charged ions or particles that are formed in the inter-electrode space have a low probability to reach the growth zone i.e near the substrate surface, in MPPD. These large number of negative ions can influence the discharge and/growth kinetics so that the ultimate result is a restricted growth rate. Again if it is assumed that the generation of negative ions attain saturation at low τ discharges ($\tau \approx 10$ msec) then the above negative influence on growth rate decreases with the increase of dwell time. As a result, r_d can be expected to increase with τ and ultimately may cross the CW value. Obviously, at higher power, the formation of negative ions will be higher and hence crossover will take place at proportionately lower τ.

Effects of dilution in VHF MPPD environment

In the present study while finding a plausible explanations of different observations variation of plasma parameters namely n_e and τ_e are utilised and referred at many places. In the present study OES has been extensively utilised for understanding the growth process. It is to be noted that above plasma parameters are indirectly related to OES intensities and this fact has very well been documented in existing literature. Therefore no additional attempt has been made to measure these parameters separately.

The use of H_2 or He dilution to enhance optoelectronic properties of a-Si:H films is a well known technique at 13.56 MHz[32]. Reports of increase of growth rate by H_2 dilution are also available. It is expected that this trend may continue at VHF frequencies as well. The magnitude of change may be different as the discharge kinetics is obviously different in this case. Again, the increase of r_d on dilution could be due to either enhancement of electron density (n_e) or electron decay time constant (τ_e) or both as discussed in Chapter-III and in reference no. 33.

Cabarrocas et al.[34] have demonstrated that electrode geometry, gas flow condition, residence time of the growth precursors, pressure, dilution, etc. need to be optimised carefully so that primary dissociation process is predominant as any deviation from this leads to secondary plasma reactions leading to the formation of clusters, polymers and powders. Since polyhydride formation is inhibited after dilution in the gas phase, more number of film forming precursors become available and can reach the growth surface. That gas phase reactions do not contribute to film growth has been shown by Schmitt et al.[35]. They have also found that films grown under secondary plasma reaction conditions possess inferior optoelectronic properties. Also the suppression of gas phase secondary plasma reaction[34] due to dilution of the feed stock is expected to decrease incorporation of polyhydrides in the growth surface. Therefore, the mechanism namely the suppression of polyhydride incorporation may contribute to the enhancement of σ_{ph} by substantial amount after dilution. Photoconductivity in a-Si:H, as in any semiconductor, depends on absorption of light, generation of electron - hole pair and finally collection of carriers which can escape recombination before reaching the electrodes. As defect density increases light absorption increases however at the same time carriers get lost in the defect states leading to the loss of photoconductivity. For material of comparable band gapand defect density if the energy gap (ΔE_D) between Fermi level and conduction band edge decreases then σ_{ph} increases. In the present investigation it has been found that ΔE_D decreases on H_2/He dilution by almost 0.2 eV and thereby increases σ_{ph} substantially. As supporting evidences improvements in both E_o and N_D values can be mentioned (**Table 4.1**). It may however be noted that under certain situations as reported by Fortmann[36] σ_{ph} is not entirely controlled by midgap defects.

In diluted silane discharges, as the dwell time increases r_d shows saturation effect for both H_2 and He dilution. It could possibly be due to the saturation of hydrogen abstraction

sites on the growth surface. Higher r_d in He dilution compared to H_2 dilution at τ=10 msec may be due to the higher n_e and τ_e in He diluted SiH_4 discharge compared to H_2 diluted SiH_4 discharge[33]. Therefore, it appears that the different rates of increase of r_d with τ reflects that discharge kinetics are quiet different in H_2 and He diluted MPPDs. The advantage of using He dilution (higher rate) vanishes at high τ values since the saturation effect in r_d coupled with the decreasing trend in σ_{ph} values suggest that for higher τ values, discharge is entering into secondary plasma reaction regime. This is also supported by IR studies (increasing R factor, **Fig.4.10(b)**). In case of He diluted discharges the lower concentration of hydrogen atoms does not affect the film properties as in the case of H_2 dilution at higher τ. At this point if one looks into the variation of σ_{ph} with τ (***Fig.4.9***) in He diluted discharges, it can be inferred that higher n_e and τ_e, available at τ=50 msec and He dilution, is an added advantage (deterioration in σ_{ph} from τ=25 msec to τ=50 msec in He diluted case is negligible) over the ability to suppress gas phase secondary plasma reactions by H_2 dilution. This is evident from the comparison of R factors (**Fig. 4.10(b)**).

Further support for the above mechanisms comes from the study of TROES results presented in section 4.3.2. Higher intensity of SiH^* in 0.3 Torr as compared to 0.1 Torr discharge correlates well with the higher r_d at 0.3 Torr since SiH^* is considered as a growth rate indicator. In 25% H_2 diluted and 25% He diluted silane discharges, SiH^* intensities are higher than undiluted 0.3 Torr MPPD and so explains higher r_d in the former case. Comparable deposition rates obtained in H_2 and He diluted discharges can be correlated to the SiH^* intensities in these two cases. Also, these intensities are much higher compared to undiluted discharges. Lower r_d and higher σ_{ph} in H_2 diluted SiH_4 discharge as compared to He diluted discharge can be attributed to the higher H^* intensity in H_2 diluted SiH_4 which can lead to etching by energetic hydrogen atoms as discussed in Chapter-III.

Even though the increased emission intensities at VHF offers a plausible explanation for the enhanced growth rates, this do not give an exact functional dependence of r_d on emission intensities. The increase of emission intensities of different species with the increase of discharge frequency was earlier reported by Oda et al. [7] and Heintz et al.[17]. Heintz et al.[17] have found that increase in SiH^* intensity with increasing ω is not at par with the increase in r_d. In the present investigation case r_d increase by 5 - 6 times as compared to RF discharge whereas SiH^* intensity increase only by nearly 1.5 times. Therefore, the increase in emission

intensities in 100 MHz discharge gives an indication of an increase in electron density above the emission thresholds i.e. an increase in higher energy tail of EEDF. This manifold increase in r_d shows that the overall growth rate is influenced by other film forming reactions as well which may, perhaps, involve ion-neutral reactions. In fact, electron temperature (τ_e) calculations at different excitation frequencies by Heintz et al.[17] from the intensity ratio of $H_\alpha/H_{2(fulcher)}$ in a H_2 plasma and He I (667.8 nm)/Ar I (667.7 nm) in a-Si:H deposition plasma also show no significant increase in high energy electron population. Further $H_\alpha/H_{2\ (fulcher)}$ ratio in a-Si:H deposition plasma in their study show a decreasing trend with ω, indicating a lower degree of dissociation at higher ω. Also their mass spectroscopic results show low SiH_4 depletion (30-40%) and only marginal increase in the dissociation rate. Therefore, all the above studies indicate inadequacy of explaining the high r_d in VHF discharge based on higher n_e alone.

Ion bombardment in VHF MPPD

would increase and this would cause higher diffusion of the precursors on the growth surface (as per Surface diffusion model by Matsuda & Tanaka[41]). This in turn allows the growth precursors to find the lowest energy (minimum defect) position and accordingly σ_{ph} and σ_{ph}/σ_{D} both increase by an order of magnitude. At this point if it is considered that increase in the ion flux causes more surface dehydrogenation, as suggested by Perrin et al.[14] then r_d should also increase but in the present study r_d is found to decrease as the pressure is changed from 0.3 to 0.1 Torr. This may, perhaps, be due to less overall dissociation of the gas molecules available at the reduced pressure, as evidenced from lower TROES intensities. Also films grown at 0.3 Torr CW VHF discharge show lower σ_{ph} values as compared to 0.5 Torr grown RF films ($\sigma_{ph} \approx 3 \times 10^{-5}\Omega^{-1}cm^{-1}$ [42]). Therefore, a straight forward comparison of RF and VHF grown films may be misleading. This is because at VHF frequencies a number of changes take place like ionisation process shifts towards the bulk plasma, the breeding effect becomes more prominent, the ion induced preparation of the growing surface and overall power factor increases. Further, detailed pressure optimisation study in CW VHF discharges yielded $\sigma_{ph} \sim 5 \times 10^{-5}\Omega^{-1}cm^{-1}$ at 0.08 Torr which is comparable to RF films grown at 0.5 Torr and 25 sccm SiH_4 flow.

Now the interesting point is that as the CW VHF discharge is modulated in the modified way then significant improvement in σ_{ph} is observed. In MPPD, in addition to the ions produced during LPL, ions are also produced during HPL and reach the substrate with much higher energy which may help obtaining a better network along with an increase in σ_{ph} as observed in low τ discharges[14]. Again if HPL is increased further, then beyond a critical energy, these higher energy ion along with providing higher surface diffusion, can cause damage to the growth surface as well, as seen in 75W HPL discharge. Regarding this critical energy Cabarrocas et al.[43] have showed that microstructural modifications in film are accompanied by an improvement of σ_{ph} and a reduction of N_d as long as the ion energy does not exceed 75 eV. This puts an upper energy limit to the beneficial effect of ion bombardment. Similarly, it is quiet plausible that if the duration of HPL (dwell time) is increased, longer periods of ion bombardment may also increase surface damage. Thus either increase of ion energy by increasing HPL or by the increase of the duration of HPL i.e. τ, increases ion induced damage on the growing surface causing drop in σ_{ph}. When 0.1 Torr VHF discharge is modulated a different picture emerges. Pulsing deteriorates optoelectronic

properties. This may be, perhaps, due to the following. In 0.1 Torr CW VHF discharge ion flux and average ion energy both are higher compared to 0.3 Torr VHF discharge and these ion parameters may be sufficient for providing adequate surface diffusion (as per surface diffusion model by Matsuda & Tanaka[41]). Additional ion flux of higher energy even for very small duration (25 msec) may cause damage on the growth surface resulting in a drop in optoelectronic quality. Therefore, it seems that it is very important to optimise the discharge for proper ion energy and duration of ion bombardment on the growing surface otherwise, film properties will reflect the resulting surface damage due to improper selection of pulse parameters. The best compromise is therefore to combine large ion flux and moderate ion energy (20 - 50 eV)[15] for maintaining a-Si:H film quality while increasing the deposition rate. Either H_2 or He dilution of 0.3 Torr VHF MPPD improves both σ_{ph} and σ_{ph}/σ_D by substantial amounts. For H_2 dilution a typical result of VHF MPPD is r_d=12.5 $A^o s^{-1}$, $\sigma_{ph}=1.2\times10^{-5}\Omega^{-1}cm^{-1}$ $\sigma_{ph}/\sigma_D = 4\times10^5$, and for He dilution it is r_d=12.6 $A^o s^{-1}$, $\sigma_{ph} = 1.2\times10^{-5}\Omega^{-1}cm^{-1}$ $\sigma_{ph}/\sigma_D = 6.6 \times 10^4$. This improvement in film properties has earlier been discussed in section 3B.4 (etching by H atoms).

[illegible] of a-Si:H grown by VHF MPPD

intensities in 100 MHz discharge gives an indication of an increase in electron density above the emission thresholds i e an increase in higher energy tail of EEDF. This manifold increase in r_d shows that the overall growth rate is influenced by other film forming reactions as well which may, perhaps, involve ion-neutral reactions. In fact, electron temperature (τ_e) calculations at different excitation frequencies by Heintz et al.[17] from the intensity ratio of $H_\alpha/H_{2(Fulcher)}$ in a H_2 plasma and He I (667.8 nm)/Ar I (667.7 nm) in a-Si:H deposition plasma also show no significant increase in high energy electron population. Further $H_\alpha/H_{2\ (fulcher)}$ ratio in a-Si:H deposition plasma in their study show a decreasing trend with ω, indicating a lower degree of dissociation at higher ω. Also their mass spectroscopic results show low SiH_3 depletion (30-40%) and only marginal increase in the dissociation rate. Therefore, all the above studies indicate inadequacy of explaining the high r_d in VHF discharge based on higher n_e alone.

Ion bombardment in VHF MPPD

Regarding the role of ion bombardment on the growing surface in influencing the growth rate and optoelectronic properties of VHF CW and MPPD grown films correlations are given below.

Numerical simulations of VHF discharges show higher r_d and improved uniformity[37], reduced stress of the deposited films[38], thinner sheaths[39] with low energy[21] and high flux[22] ion bombardment at the substrate. Perrin et al.[14] have demonstrated that certain degree of ion bombardment is necessary for enhanced reactivity of the film forming species at the growing surface but this can also damage the film during deposition. In view of all the above simulation studies, discussed in detail in section 4.1 and also in view of the available results of different measurements, one can say that reactivity at the growth surface is enhanced a great deal due to the presence of high ion flux in VHF discharge, which in turn enhances surface dehydrogenation and, thus, a high growth rate is achieved. This enhanced surface reactivity at VHF has recently been stressed by Keppner[10] and perhaps can be explained by the a-Si:H growth model (chemisorption based growth mechanism) proposed by Bruno et al.[40]. All the same a quantitative correlation of the enhancement of surface reactivity and achievement of high r_d is still lacking.

In the present study, when pressure is dropped from 0.3 Torr to 0.1 Torr sheath collisionality should have decreased. As a result ion flux towards the grounded electrode

would increase and this would cause higher diffusion of the precursors on the growth surface (as per Surface diffusion model by Matsuda & Tanaka[41]). This in turn allows the growth precursors to find the lowest energy (minimum defect) position and accordingly σ_{ph} and σ_{ph}/σ_D both increase by an order of magnitude. At this point if it is considered that increase in the ion flux causes more surface dehydrogenation, as suggested by Perrin et al.[14] then r_d should also increase but in the present study r_d is found to decrease as the pressure is changed from 0.3 to 0.1 Torr. This may, perhaps, be due to less overall dissociation of the gas molecules available at the reduced pressure, as evidenced from lower TROES intensities. Also films grown at 0.3 Torr CW VHF discharge show lower σ_{ph} values as compared to 0.5 Torr grown RF films ($\sigma_{ph} \approx 3 \times 10^{-5}\Omega^{-1}cm^{-1}$ [42]). Therefore, a straight forward comparison of RF and VHF grown films may be misleading. This is because at VHF frequencies a number of changes take place like ionisation process shifts towards the bulk plasma, the breeding effect becomes more prominent, the ion induced preparation of the growing surface and overall power factor increases. Further, detailed pressure optimisation study in CW VHF discharges yielded $\sigma_{ph} \sim 5 \times 10^{-5}\Omega^{-1}cm^{-1}$ at 0.08 Torr which is comparable to RF films grown at 0.5 Torr and 25 sccm SiH_4 flow.

Now the interesting point is that as the CW VHF discharge is modulated in the modified way then significant improvement in σ_{ph} is observed. In MPPD, in addition to the ions produced during LPL, ions are also produced during HPL and reach the substrate with much higher energy which may help obtaining a better network along with an increase in σ_{ph} as observed in low τ discharges[14]. Again if HPL is increased further, then beyond a critical energy, these higher energy ion along with providing higher surface diffusion, can cause damage to the growth surface as well, as seen in 75W HPL discharge. Regarding this critical energy Cabarrocas et al.[43] have showed that microstructural modifications in film are accompanied by an improvement of σ_{ph} and a reduction of N_d as long as the ion energy does not exceed 75 eV. This puts an upper energy limit to the beneficial effect of ion bombardment. Similarly, it is quiet plausible that if the duration of HPL (dwell time) is increased, longer periods of ion bombardment may also increase surface damage. Thus either increase of ion energy by increasing HPL or by the increase of the duration of HPL i.e. τ, increases ion induced damage on the growing surface causing drop in σ_{ph}. When 0.1 Torr VHF discharge is modulated a different picture emerges. Pulsing deteriorates optoelectronic

properties. This may be, perhaps, due to the following. In 0.1 Torr CW VHF discharge ion flux and average ion energy both are higher compared to 0.3 Torr VHF discharge and these ion parameters may be sufficient for providing adequate surface diffusion (as per surface diffusion model by Matsuda & Tanaka[41]). Additional ion flux of higher energy even for very small duration (25 msec) may cause damage on the growth surface resulting in a drop in optoelectronic quality. Therefore, it seems that it is very important to optimise the discharge for proper ion energy and duration of ion bombardment on the growing surface otherwise, film properties will reflect the resulting surface damage due to improper selection of pulse parameters. The best compromise is therefore to combine large ion flux and moderate ion energy (20 - 50 eV)[15] for maintaining a-Si:H film quality while increasing the deposition rate. Either H_2 or He dilution of 0.3 Torr VHF MPPD improves both σ_{ph} and σ_{ph}/σ_D by substantial amounts. For H_2 dilution a typical result of VHF MPPD is r_d=12.5 $A^{\circ}s^{-1}$, σ_{ph}=1.2x$10^{-5}\Omega^{-1}cm^{-1}$ σ_{ph}/σ_D = 4x10^5, and for He dilution it is r_d=12.6 $A^{\circ}s^{-1}$, σ_{ph} = 1.2x$10^{-5}\Omega^{-1}cm^{-1}$ σ_{ph}/σ_D = 6.6 x 10^4. This improvement in film properties has earlier been discussed in section 3B.4 (etching by H atoms).

Microstructure of a-Si:H grown by VHF MPPD

It can be visualised that higher ion bombardment by ions of higher average energy reduces dihydride bonding in the film. But similar C_H values (Fig.4.10(a)) indicate that this increase of ion bombardment is not sufficient for enhancing surface dehydrogenation and as a result r_d does not change. As VHF discharge is modulated in the modified way then C_H and R factor increase with higher and higher HPL i.e. higher HPL causes more polyhydride formation. But at the same time it is to be noted that the band gap does not open up further rather it remains at 1.75 eV as shown in **Fig.4.7**. Thus at 75W HPL the positive role of ion bombardment that was seen in 60W HPL vanishes because of higher polyhydride incorporation in the film as can be seen in **Fig. 4.10(b)**. In line with this it is very easy to understand the reduction of R and C_H after H_2 or He dilution. Infact some amount of etching by hydrogen (as discussed in section 3B.4) atom may also be responsible for improvements in σ_{ph} values. The increase of R factor with τ in H_2 dilution is quiet expected. Again, For He dilution the decrease of R & C_H with τ is quiet interesting. Taking a clue from Mashima et al's.[44] observation it seems that this decreasing trend in C_H is plausible. This is because excited He atoms, during the deexcitation process release energy to the growing film surface which can help the relaxation of a-Si:H

network during deposition in a manner that leads to decrease of C_H. But the decrease of R with τ can be possible only when excited He atoms can also suppress the polydydride formation / incorporation into the film.

The encouraging picture is that films with C_H as low as 3 at% can be grown at 13.0 $A^{\circ}s^{-1}$ with $\sigma_{ph} = 10^{-5}\ \Omega^{-1}cm^{-1}$ and $\sigma_{ph}/\sigma_D = 10^5$ in He diluted VHF MPPD. In H_2 dilution also films with C_H = 6 at%, r_d =12.5 $A^{\circ}s^{-1}$, $\sigma_{ph} = 2 \times 10^{-5}\ \Omega^{-1}cm^{-1}$ and $\sigma_{ph}/\sigma_D = 4 \times 10^5$ can be obtained. From the above VHF MPPD study, it seems that low R factor is correlated to the high ion flux having high average energy. In fact, in RF MPPD there were distinct advantages of using He dilution over H_2 dilution. In VHF MPPD although dilution is advantageous but choice of a particular diluent is not that much important.

4.5 Conclusions

In the present investigation a novel pulsed plasma growth of a-Si:H was carried out in which VHF (100 MHz) power was modulated between high and low power limits. Discharges in 100% SiH_4, H_2 and He diluted silane were studied. It has been found that films grown at rates upto 13.0 $A^{\circ}s^{-1}$ to be of sufficiently good quality (for some device applications).

Pressure variation studies for rate maximisation reveal that for a fixed reactor geometry and gas flow dynamics use of higher frequency discharge requires lower pressure to get device quality films. In the present case pressure was reduced to 0.3 Torr in VHF as compared to that of 0.5 Torr at 13.56 MHz operated discharge.

Similar to RF MPPD deposition rate in VHF MPPD is lower than VHF CW discharge upto a critical dwell time and its crossover to CW value occurs at high dwell times. This crossover point depends on the HPL and the operating pressure. Higher the HPL lower the crossover point.

Optoelectronic properties seem to be very much sensitive to the high power level. The beneficial effects of ion bombardment are only realised when it is optimised for right energy (dependent on HPL), right duration (dependent on dwell time) and right flux (dependent on pressure). Further the optoelectronic properties obtained under VHF MPPD are better than VHF CW films grown at similar conditions. This success was not obtained in case of RF MPPD grown films.

Thus, pulsing the VHF discharge provides some additional advantages over the CW VHF discharge. It provides much better control on ion flux, ion energy, duration of ion

4.5 References

1 C M Ferriera and J Loureirs, *J. Phys. D: Appl. Phys.* **1**, 1175 (1984).

2 M R Wertheimer and M Moisan, *J. Vac. Sci. Tech.* **A3**, 2643 (1986)

3 M Moisan, C Barbeau, R Claudi, C.M Ferreira, J Magit, J Paraszczak, A.B Sa, G Saure and M.R Wertheimer, *J. Vac. Sci. Tech.* **B19**, 8 (1991).

4 H Curtins, N Wyrsch and A.V. Shah, *Elect. Lett.* **23**, 228 (1987).

5 H Chatham, P.K Bhat, A. Benson and C. Matovich, *J. Non-cryst. Solids* **115**, 201 (1989)

6 R Platz, D Fischer, S. Dubail & A. Shah, *Solar Energy Mat. & Solar Cells* **46**, 157 (1997)

7 S Oda, J Noda and M. Matsumara, *Jpn. J. Appl. Phys.* **29** 1889 (1990)

8 S Oda and M Yasukawa, *J. Non-cryst. Solids* **137 & 138**, 677 (1991).

9. A matsuda, T. kaga, H Tanaka and K. Tanaka, *Jpn. J. Appl. Phys.* **23,** 1567 (1984)

10. M. Favre, A. Shah, J. Hubin, E. Bustarret, M.A. Hachicha and S. Basrour, *J. Non-cryst. Solids* **137 & 138**, 335 (1991).

11. M. Surendra and D.B. Graves, *Appl. Phys. Lett.* **59**, 2091 (1991).

12 D.L Flamm, *J. Vac. Sci. & Tech.* **A4**, 729 (1986).

13. M. Surendra and D.B. Graves, *IEEE Trans. Plasma Sci.* **19**, 144 (1991).

14. J. Perrin, Y. Takeda, N. Hirano, H. Matsuura and A. Matsuda, *Jap. J. Appl. Phys.* **28**, 5 (1989).

15. J. Perrin in *Plasma Deposition of Amorphous Silicon-Based Materials*, ed. by G. Bruno et al., Academic Press, 1995, p-218.

16. W. Schwarzenbach, A.A. Howling, M. Fivaz, S. Brunner and Ch. Hollenstein, *J. Vac. Sci. Tech.* **A14**, 132 (1996).

17 M. Heintze, R. Zedlitz and G.H. Bauer, *J. Phys. D: Appl. Phys* **26**, 1781 (1993).

18. M. Heintz and R. Zedlitz, In *Proc. ICAS-15*, 1993, Cambridge, U.K.

19 M Heintz and R. Zedlitz, in *Progress in Photovoltaics: Research and Applications*, Vol. 1 (John Wiley and Sons, Ltd., 1993) p-213.

20 R Zedlitz, M. Heintz and G.H. Bauer, in *MRS Spring Meeting 1992*, San Fransisco.

21 M Heintze and R. Zedlitz, *J. Non-cryst. Solids* **198-200**, 1038 (1996).

22. M Meyyappan and M.J. Colgan, *J. Vac. Sci. & Tech.* **A14**, 2790 (1996).

Thus, pulsing the VHF discharge provides some additional advantages over the CW VHF discharge. It provides much better control on ion flux, ion energy, duration of ion bombardment and powder suppression by suitably changing the pulse parameters. Although in RF pulsed discharges these pulse parameters were also found to play as independent deposition parameters but the favourable sheath characteristics of VHF discharge provides an edge to VHF pulsing over RF pulsing.

Both H_2 and He dilution improves deposition rate and optoelectronic properties substantially from CW VHF and undiluted VHF MPPD films. Device quality films could be grown at deposition rates above 12.0 $A^{o}s^{-1}$ using both He and H_2 dilutions. Specifically low hydrogen content (3 at%) films could be grown in He diluted VHF MPPD environment. Attainment of low C_H values would be interesting so far as light induced degradation is concerned. In VHF MPPD choice of a particular diluent (H_2/He) is not important whereas He dilution has distinct advantage in RF MPPD.

Thus it has been very clearly shown that the beneficial effects of operating at VHF frequencies i.e. attainment of high growth rate, can be combined with the additional advantage produced by pulsing the discharge to improve optoelectronic quality of the material. Again the method suggested in the present study is readily applicable to all existing PECVD reactors without requiring much change in hardware. Only the plasma excitation source need to be changed.

4.5 References

1 C M Ferriera and J Loureirs, *J. Phys. D: Appl. Phys.* **1**, 1175 (1984)

2 M R Wertheimer and M Moisan, *J. Vac. Sci. Tech.* **A3**, 2643 (1986)

3 M Moisan, C Barbeau, R Claudi, C M Ferreira, J. Magit, J Paraszczak, A.B. Sa, G. Saure and M R Wertheimer, *J. Vac. Sci. Tech.* **B19**, 8 (1991).

4 H Curtins, N Wyrsch and A.V. Shah, *Elect. Lett.* **23**, 228 (1987).

5 H Chatham, P K Bhat, A Benson and C. Matovich, *J. Non-cryst. Solids* **115**, 201 (1989).

6 R Platz, D Fischer, S. Dubail & A. Shah, *Solar Energy Mat. & Solar Cells* **46**, 157 (1997)

7 S Oda, J Noda and M. Matsumara, *Jpn. J. Appl. Phys.* **29** 1889 (1990).

8 S Oda and M Yasukawa, *J. Non-cryst. Solids* **137 & 138**, 677 (1991).

9. A matsuda, T. kaga, H. Tanaka and K. Tanaka, *Jpn. J. Appl. Phys.* **23,** 1567 (1984).

10. M. Favre, A. Shah, J. Hubin, E. Bustarret, M.A. Hachicha and S. Basrour, *J. Non-cryst. Solids* **137 & 138**, 335 (1991).

11. M. Surendra and D.B. Graves, *Appl. Phys. Lett.* **59**, 2091 (1991).

12. D L. Flamm, *J. Vac. Sci. & Tech.* **A4**, 729 (1986).

13. M. Surendra and D.B. Graves, *IEEE Trans. Plasma Sci.* **19**, 144 (1991).

14. J. Perrin, Y. Takeda, N. Hirano, H. Matsuura and A. Matsuda, *Jap. J. Appl. Phys.* **28**, 5 (1989).

15. J. Perrin in *Plasma Deposition of Amorphous Silicon-Based Materials*, ed. by G. Bruno et al., Academic Press, 1995, p-218.

16. W. Schwarzenbach, A.A. Howling, M. Fivaz, S. Brunner and Ch. Hollenstein, *J. Vac. Sci. Tech.* **A14**, 132 (1996).

17. M. Heintze, R. Zedlitz and G.H. Bauer, *J. Phys. D: Appl. Phys* **26**, 1781 (1993).

18. M. Heintz and R. Zedlitz, In *Proc. ICAS-15*, 1993, Cambridge, U.K.

19. M. Heintz and R. Zedlitz, in *Progress in Photovoltaics: Research and Applications*, Vol. 1 (John Wiley and Sons, Ltd., 1993) p-213.

20. R. Zedlitz, M. Heintz and G.H. Bauer, in *MRS Spring Meeting 1992*, San Fransisco.

21. M. Heintze and R. Zedlitz, *J. Non-cryst. Solids* **198-200**, 1038 (1996).

22. M. Meyyappan and M.J. Colgan, *J. Vac. Sci. & Tech.* **A14**, 2790 (1996).

23 A Bouchoule, A Plain, L. Boufendi, J. -ph. Blondeau and C Laure, *J. Appl. Phys.* **70**, 1991 (1991)

24 J -L Dorier, Ch Hollenstein, A A Howling and U. Kroll, *J. Vac. Sci. Tech.* **A10**, 1048 (1992)

25 J -L Andujar, E. Brartran, A. Cannillas, J. Campmany and J.L. Morenza, *J. Appl. Phys.* **69**, 3757 (1991)

26 G M Jellum, J E Daugherty and D.B. Graves, *J. Appl. Phys.* **69**, 6923 (1991).

27 H Kawasaki, Y Ueda, T Yoshioka, T Fukuzawa, M. Shiratani and Y Watanabe, *Appl. Phys. Lett* **67**, 3880 (1995).

28 C Beneking, F. Finger and H. Wagner, in *Proc. 11th E.C. PVSEC* (Montreux, Switzerland, 1992), p-586, Harwood Academic Publishers, Chur, 1993.

29 S Veprek and M. Heintze, "The mechanism of plasma induced deposition of amorphous silicon from silane", *Plasma Chem. Plasma Proc.* **10**, 3 (1991).

30. H Keppner, Abstract of thesis submitted to The faculty of Science, University of Neuchatel (Private communication).

31 F Finger, U Kroll, V. Viret, A. Shah, W. Bayer, X.-M. Tang, J. Weber, A. Howling and Ch Hollenstein, *J. Appl. Phys* **71**, 5665 (1992).

32. P.E Vanier, F.J. Kampas, R.R. Corderman & R. Rajeswaran, *J. Appl. Phys.* **56**, 1812 (1984).

33. C.B. Fleddermann, J.H. Beberman and J.T. Verdeyen, *J. Appl. Phys.* **58**, 1344 (1985).

34 P Roca i Cabarroacs, *J. Non-Cryst Solids* **162-164**, 37 (1993).

35 J.P.M. Schmitt, *Mat. Res. Soc. Symp.* Proc. 219, 631 (1991).

36 C M Fortmann in *Plasma Deposition of Amorphous Silicon-Based Materials*, ed. by G. Bruno et al., Academic Press, 1995, p-143.

37. A.A. Howling, J.-L. Dorier, Ch. Hollenstein, U. Kroll and F. Finger, *J. Vac. Sci. & Tech.* **A10**, 1080 (1992).

38. J. Dutta, U. Kroll, P. Chabloz, A. Shah, A.A. Howling, J.-L. Dorier and Ch. Hollenstein, *J. Appl. Phys.* **72**, 3220 (1992).

39. U. Kroll, Y. Ziegler, J. Meier, H. Keppner and A. Shah, *Mat. Res. Soc. Symp.* Proc. 336, 115 (1994).

40 G Bruno, P. Capezzuto and G. Cocala, *J. Appl. Phys.* **69**, 7256 (1991).

41 A Matsuda and K Tanaka, *J. Non-cryst. Solids* **97 & 98**, 1367 (1987).

42 Tanay Seth, Ph D thesis, Pnajab University, 1994

43 P Roca i Cabarrocas, P Morin, V Chu, J.P Conde, J.Z. Lin, H R. Park and S. Wagner, *J. Appl. Phys.* **69**, 2942 (1991).

44 S Mashima, G Ganguli and A Matsuda, *Plasma Sources Sci. & Tech.* **2**, 23 (1993).

CHAPTER - V

Conclusions

5.1 Important conclusions of the present study

For the present study hydrogenated amorphous silicon films (undoped) were deposited away from the so called standard deposition conditions. Films were deposited by a low frequency amplitude modulation of 13.56 and 100 MHz silane discharges separately. The basic aim of the study was to attain high deposition rates with acceptable optoelectronic properties of the a-Si:H films so produced. The other reasons behind choosing pulsed plasma discharge technique are that, it is believed, intermittent plasma produces higher thickness uniformity and inhibits growth of powder in the plasma and also in the films. These considerations are extremely important for successful fabrication of large area a-Si:H based devices. The main disadvantage of intermittence, as highlighted by the Sanyo group (under reference 2, Chapter-III), was avoided by modifying the pulsing scheme with a novel approach in which modulation depth was always kept below 100% and was varied between 85 to 90%, for both 13.56 and 100 MHz excitation frequencies. Thus, in this mode of discharge plasma power was switched between a high and a low level. The important conclusions that were drawn from a detailed parametric variation, of the process parameters are the following.

5.1.1 Modified pulsed plasma discharge (MPPD) at 13.56 MHz with undiluted silane and disilane

1) Growth rate, r_d of a-Si:H is found to be lower in the MPPD as compared to CW discharges upto certain dwell time, τ. Higher τ is required for lower HPL and vice versa to cross the CW deposition rate. The lack of proper plasma diagnostics data does not allow a proper picture regarding the mechanism for this lower growth rate to emerge. However, the electron density (n_e) measurement of Overzet et al.(under reference 6, Chapter-III) and the investigation of Helium dilution of silane in a pulsed discharge by Fleddermann et al. (under

reference 21, Chapter-III) suggest that the different degree of electron attachment could be the reason behind the lower r_d in MPPD.

2) It was found that undiluted Si_2H_6 formed films grown at rates upto 9 $A^{\circ}s^{-1}$ to be of sufficiently good quality. Highest photoconductivity, σ_{ph} and band gap, E_g values obtained are 4.4 x 10^{-4} $\Omega^{-1}cm^{-1}$ and 2.07 eV respectively. The above values are comparable to those reported for device quality a-Si:C:H. It also appears that for such type of pulsed plasma growth, use of disilane has a distinct advantage.

3) Dwell time has been identified as an additional process parameter to tailor the material properties.

4) It is also found that in all cases of pulsed discharge film uniformity is comparable to that of CW deposited films, implying that fast switching of plasma between LPL and HPL hardly has any effect on the film growth over a fairly large deposition area (100 cm^2).

5) For a given τ, E_g increases in all cases with an increase of HPL and E_g can be tailored over a fairly wide window from 1.75 to 2.1 eV by just varying τ. Further detailed optimisation of process parameters may prove this pulsed plasma discharge suitable for fabricating Tandem Solar Cells and even multilayers by tailoring the band gap of the a-Si:H material as found possible in our experiments.

6) Powder formation zone was identified. In undiluted MPPD as growth rate exceeds the CW value, onset of powder formation takes place.

5.1.2 H_2 diluted MPPD

1) Growth rates increased above the undiluted MPPD values after H_2 dilution of the feed gas. Similarly dwell time (τ) dependence of r_d could be increased by diluting silane. TROES study of to SiH^* emission supports such observation of higher r_d in diluted silane, increase of r_d with τ and also with H_2 dilution of the feed stock.

2) For a given set of pulse parameters, r_d attains a maximum value (1.83 $A^{\circ}s^{-1}$) at a particular H_2 dilution (25%) which is significantly different from those reported by other workers (for CW discharge). Thereafter, r_d slowly decreases to reach a seemingly steady state value ($r_d \approx 1.35$ $A^{\circ}s^{-1}$) at higher dilutions. By conducting experiments at two different flow conditions it is shown that the steady state r_d value is controlled by an atomic hydrogen assisted chemical etching process, irrespective of the number of silane molecules present in the

discharge. TROES results supports this view. Further, the possibility of an etching reaction, predominantly taking place under high hydrogen dilution conditions is further supported by the observation of gradual improvement in σ_{ph} values between 25% and 75% H_2 dilution range.

3) It is known that the reaction $e^- + SiH_4 \Rightarrow SiH^* + H_2 + H + e^-$ is responsible for the increase of SiH^* emission intensity. Under hydrogen dilution this reaction increases H_2 and H partial pressures and, thus, increases the reaction probability for $e^- + H_2 \Rightarrow H + H^* + e^-$ and this is supported by the observation of an increased H^* emission intensity. Presumably this high concentration of H atoms determines the film growth rate under high dilution.

4) Further, it is shown that r_d can be increased by hydrogen dilution beyond the CW value by varying τ and HPL without onset of powder formation while maintaining optoelectronic properties of the films as well.

5.1.3 He and He+H_2 diluted MPPD

Based on the observation made on He+H_2 dilution studies, the following conclusions can be drawn.

1) Deposition rate in an MPPD environment depends both on the partial pressures of the constituent gases and on the parameters of the modulating pulse.

2) In an modified pulsed plasma discharge presumably the higher n_e in He diluted plasma, as compared to that in H_2 diluted one, leads to higher r_d.

3) H_2 seems to play a dual role since its addition increases n_e even in He diluted plasma as also it is found to improve optoelectronic properties of the material so grown presumably by suitably removing the weaker bonds.

4) Intuitively it appears that a surface coverage or shading of the freshly grown top surface by He atoms may be the cause behind the lower etching rate by atomic hydrogen in He diluted environment. However, He dilution provides a different mixture of SiH_x ion and radicals compared to 100% SiH_4 discharge and this may as well explain this lower etching rate.

5) The results of He dilution studies seem to support the model proposed by Mashima et al. (under reference 43, Chapter-III) wherein they proposed that the excess energy released by the excited He atoms to the film growth surface and/or subsurface helps the relaxation of a-Si:H network resulting in a decrease of hydrogen content, C_H value.

6) The lower C_H values in the MPPD films, grown using He diluted silane, indicates that the idea of hydrogen accumulation in artificially generated interfaces in pulsed discharges, as proposed by Cabarrocas et al (under reference 41, Chapter-III) may be specific to their growth environments. This means that in the present investigation films of better bulk uniformity or less void density are grown.

7) It appears from the present investigations that in order to optimise both r_d and electronic quality of a-Si:H films grown by MPPD one has to judiciously choose a mixture of diluents rather than a single diluent.

5.1.4 MPPD at 100 MHz

In the present investigations a novel pulsed plasma growth of a-Si:H was carried out in which VHF power was modulated between high power and low power limits. Specifically, 100% SiH_4, 25% H_2 and 25% He diluted silane discharges were studied. It has been found that films grown at rates upto 13 $A^{\circ}s^{-1}$ to be of sufficiently good quality (σ_{ph} = 1.2 x 10^{-5} $\Omega^{-1}cm^{-1}$)for device applications.

1) Gas pressure variation studies for the deposition rate maximisation reveals that, for a fixed reactor geometry and gas flow dynamics, use of VHF discharge necessitates a lower operating pressure to deposit device quality films. It appears that the probability of secondary plasma reaction increases with the excitation frequency, for a given pressure and feed gas composition.

2) Similar to RF MPPD, deposition rate in VHF MPPD is found to be lower than VHF CW discharge for low τ discharges, and its cross over occurs only at high τ values. The crossover point depends on the HPL applied and the operating pressure. Higher the HPL lower the crossover point.

3) The most interesting feature is that optical band gap is almost constant (1.75 ± 0.03 eV) i.e. insensitive to the variation of deposition conditions and more significantly deposition rate. Also it hardly changes with the nature and fraction of diluent gases at optimised condition of growth.

4) Pulsing the VHF discharge at 0.3 Torr improves σ_{ph} (1.2 x 10^{-5} $\Omega^{-1}cm^{-1}$) over CW VHF discharge (σ_{ph} = 1.3 x 10^{-6} $\Omega^{-1}cm^{-1}$). Both H_2 and He dilution improves deposition rate and optoelectronic properties substantially as compared to those grown by CW VHF and

undiluted VHF MPPD. This higher σ_{ph} is achieved in films deposited at r_d = 12.5 $A^{o}s^{-1}$ (σ_{ph} = 2.6 x 10^{-5} $\Omega^{-1}cm^{-1}$). In contrast to RF MPPD, these benefits are independent of the diluent used in VHF MPPD whereas, He dilution was found to be advantageous in RF MPPD.

5) Optoelectronic properties of the a-Si:H films seem to be very much sensitive to the application of high power level. That is to say that the beneficial effects of ion bombardment are realised only when it is optimised for right energy (dependent on HPL) and flux (dependent on pressure). The optoelectronic properties thus obtained are even better than VHF CW films grown in similar conditions. This breakthrough was not achieved for RF MPPD grown films.

6) For VHF CW grown films C_H was estimated to be approximately 9 at% and for undiluted VHF MPPD (60W HPL) grown films C_H values are ≈ 15 at%. Dilution by either H_2 or He reduces C_H value to around 5 at%. The lowest value of C_H (2.9 at%) is obtained for 25% He dilution. 60W HPL and τ = 50 msec. Attainment of low C_H values would be interesting so far as counter of light induced degradation in these films and devices made thereof are concerned.

7) Pulsing the VHF discharge provides additional advantages over the CW VHF discharge. It provides much better control of ion flux, ion energy and powder suppression by suitably changing the pulse parameters. Although in RF pulsed discharges these pulse parameters were also found to play a significant role but the favourable sheath characteristics of VHF discharge provides an edge over RF pulsing.

8) It has also been very clearly shown that beneficial effects of operating at VHF frequencies is the attainment of high growth rate and this can be combined with the additional advantage produced by pulsing the discharge i.e. improvement of optoelectronic quality of the material. Again the method suggested in the present study is readily applicable to all existing PECVD reactors without requiring much change in hardware. Only the plasma excitation source needs to be changed.

5.2 Final remarks

The present investigation was taken up at a point when Cabarrocas et al. in an important paper (Reference no. 41, Chapter-III) have noted that pulsing did not provide any satisfactory

scaling to the problem of powder formation in a-Si:H reactors and, on the contrary, film properties were jeopardised. By changing the method of pulsing and use of diluents it was thought that working at 13.56 MHz these short comings will somehow be circumvented. Results however, did not show much improvement but all the same these experiments proved that 100% modulation depth, deemed so far an essential condition for the success of SQWM, may not afterall be necessary as MPPD experiment undertaken for the first time during this research proved otherwise. A close study of the problem reveals the following. Any successful technique of enhancing r_d, while preserving the excellent set of optoelectronic properties which are otherwise obtained at so called standard condition of growth, should have the following two features satisfactorily taken care of.

i) An increase of the ion/radical flux ratio at a low total applied power.

ii) Only finite extent of ion bombardment of the growing surface (say no more than 75 eV)

Obviously, operating at 13.56 MHz these two together can not be achieved satisfactorily. The solution that appears possible is perhaps DC multipole or ECR discharges. However combining VHF excitation and the pulsing of the source, the desired two features as stated above can easily be achieved, as has been shown in the present investigation. Moreover, setting of DC multipole or ECR plasmas in existing systems require extensive changes. Whereas, the present suggested technique can be readily implemented. Summary of the present investigation is shown in **Fig.5.1.**

Thus the usefulness of the present investigation can hardly be overemphasised and looking into this aspect a patent application has been filed.

5.3 Scope of further work

The existing controversies in the wide spread application of VHF for material processing are the following.

i) At this frequency there could be interference with the allowed radio broadcasting channels

ii) The persisting doubt that when operating at such high frequency, due to the appearance of nodes i.e. finite wavelength effects film uniformity may be adversely affected.

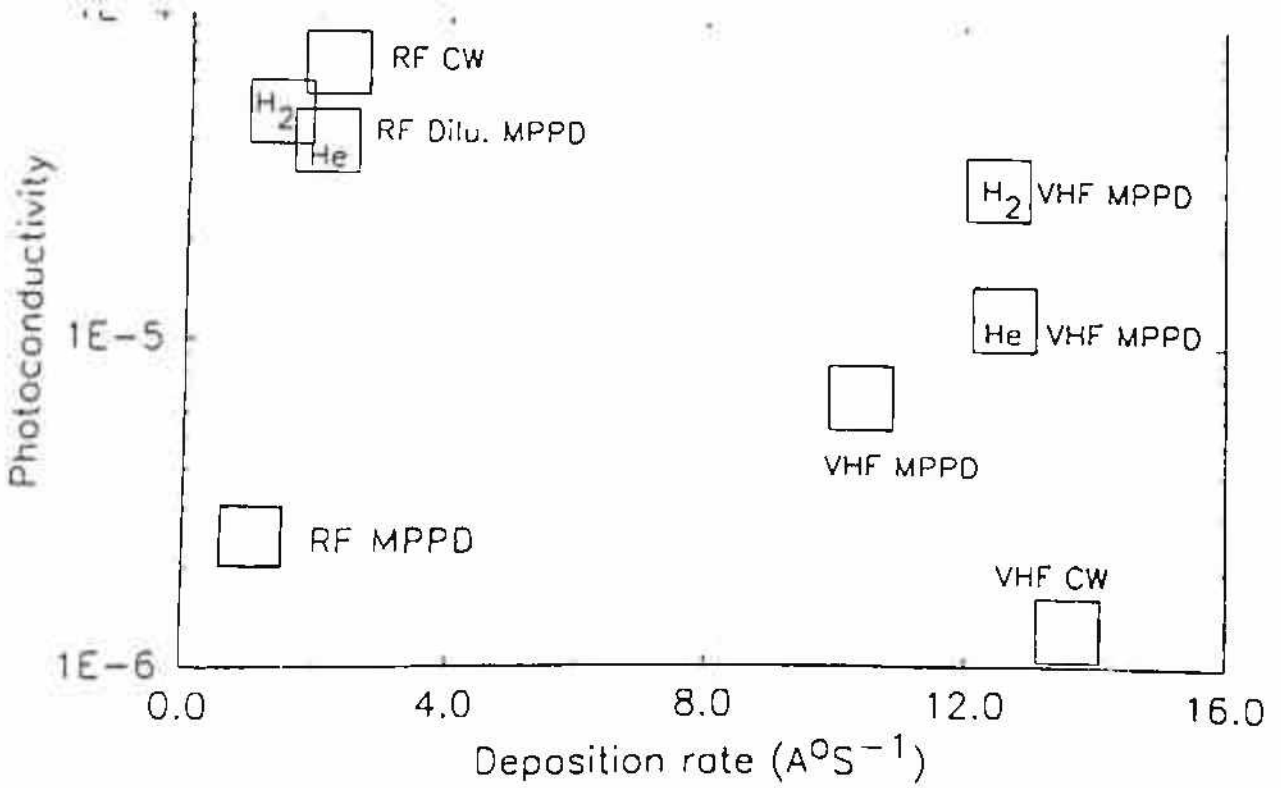

Fig.5.1 Summary of the thesis: attainment of high growth rate while preserving the optoelectronic quality of the material.

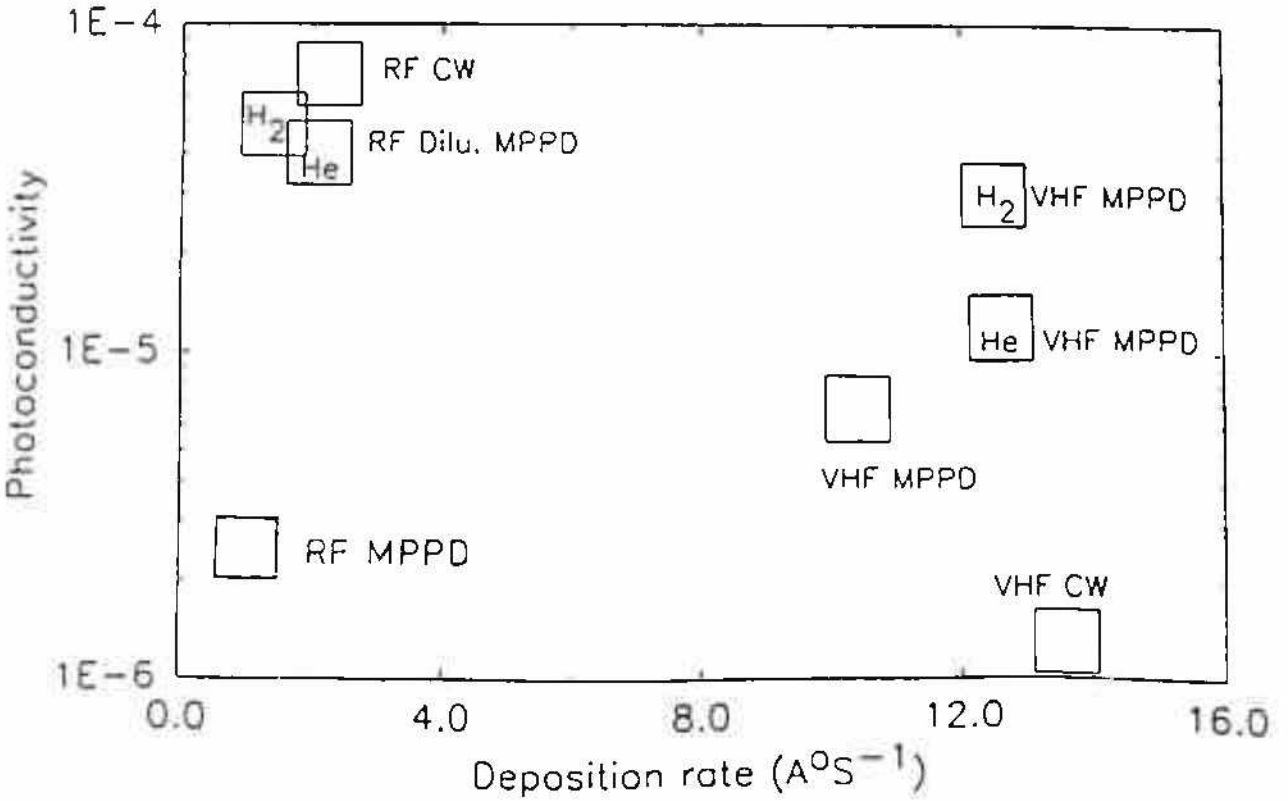

Fig.5.1 Summary of the thesis: attainment of high growth rate while preserving the optoelectronic quality of the material.

While for a widespread implementation of VHF material processing amendment of the existing laws may be necessary, it appears pulsing of VHF source may allow one to grow more uniform a-Si:H film even at these frequencies. Therefore, it is expected that VHF excitation and MPPE together on the whole should be capable of producing uniform coatings at high r_d, this together with the use of proper diluents will allow one to produce these films with superior optoelectronic properties. Scope of further work, therefore, is to prove this in a large area reactor. Fortunately a very large area multizone reactor with cassette to cassette transfer of substrate has been created, at NPL with MNES, Govt. of India support. It will, thus, be possible to prove the efficacy of this idea in the coming years.

iii) One should also look for the other subtle effects of VHF MPPD, for instance higher doping efficiency as also ease of inducing micro crystallisation.

List of publications

Papers published in Journals

1. Effect of pulse parameters on the deposition rate of hydrogenated amorphous silicon in a modified pulsed plasma discharge BY C. Anandan, **C. Mukherjee**, Tanay Seth, P.N. Dixit and R. Bhattacharyya IN **APPL. PHYS. LETT.** 66 (1994) 85.

2. Hydrogenated Amorphous Silicon Films Prepared At Low Substrate Temperature On Cathode Of An Asymmetric RF Plasma System BY Tanay Seth, P.N.Dixit, **C. Mukherjee**, C. Anandan & R. Bhattacharyya IN **THIN SOLID FILMS** 264 (1995) 11.

3. Optoelectronic properties of hydrogenated amorphous silicon films grown using a modified pulsed plasma discharge BY **C. Mukherjee**, C. Anandan, Tanay Seth, P.N. Dixit and R. Bhattacharyya IN **APPL. PHYS. LETT.**68 (1996) 194.

4. Effect of hydrogen dilution on the deposition rate of Hydrogenated amorphous silicon films in a modified pulsed plasma discharge BY **C. Mukherjee**, C. Anandan, Tanay Seth, P.N. Dixit and R. Bhattacharyya IN **APPL. PHYS. LETT.**68 (1996) 835.

5. High rate growth of Amorphous hydrogenated silicon films and their device applications BY Tanay Seth, **C. Mukherjee**, C. Anandan, P.N. Dixit, O.S. Panwar, S.S. Bawa and R. Bhattacharyya IN **IETE Journal of Research** 43 (1997) 131.

Conference papers presented

1) Subbandgap Absorption Studies On High Rate Deposited a-Si:H Films **IN 7th IWPSD**, New Delhi, Dec-1993 BY **C. Mukherjee**, Tanay Seth, C.Anandan, P.N.Dixit & R. Bhattacharyya.

2) Effect of high growth rate on the subgap absorption of a-Si:H IN **National Solar Energy Convention**, Vadodara, Dec-1993 BY **C. Mukherjee**, Tanay Seth, C.Anandan, P.N.Dixit & R.Bhattacharyya.

3) High Rate Deposited Hydrogenated Amorphous Silicon Films For Photovoltaic Applications **IN National Solar Energy Convention**, Vadodara, Dec-1993 BY Tanay Seth, C.Anandan, **C. Mukherjee**, P.N.Dixit & R.Bhattacharyya.

4) Deposition of Amorphous Silicon Films By Square Wave Modulated Discharge IN **Materials Research Society of India symposia**, Kharagpur, Feb-1995 **BY C. Mukherjee**, Tanay Seth, C. Anandan, P.N. Dixit and R. Bhattacharyya.

) Effect of Applied Power on Hydrogenated Amorphous Silicon Material Properties During 3.56 and 100 MHz (VHF) Glow Discharge Deposition IN **Materials Research Society of India symposia**, Kharagpur, Feb-1995 BY Tanay Seth, **C. Mukherjee**, C. Anandan, P.N.Dixit nd R. Bhattacharyya.

) Hydrogen evolution and surface morphology of unannealed and annealed hydrogenated morphous silicon films deposited in an asymmetric PECVD system at room temperature BY .S. Panwar, **C.Mukherjee**, C. Anandan, Tanay Seth, P.N. Dixit and R. Bhattacharyya IN **8th IWPSD** 11 to 16th Dec '95.

7) Deposition of Hydrogenated Amorphous Silicon films by square wave modulated RI PECVD of 100% and hydrogen diluted silane, **C. Mukherjee**, C. Anandan, Tanay Seth, P.N. Dixit and R.Bhattacharyya IN the proceedings of the national conference on Thin Film Characterisation and Application, Coimbatore, India, June 10 -12 1996, edited by K. Narayandass and D. Mangalaraj, published by Allied Publishers Ltd., New Delhi.

8. An account of amorphous silicon based photonic devices development work at NPL BY P.N. Dixit, C. Anandan, S.S. Bawa, **C. Mukherjee**, Tanay Seth, S. Qureshi and R. Bhattacharyya. IN **9th IWPSD** 15th to 21 Dec'97.